CECW-EH Engineer Manual 1110-2-1414	Department of the Army U.S. Army Corps of Engineers Washington, DC 20314-1000	EM 1110-2-1414 5 July 1989
	Engineering and Design WATER LEVELS AND WAVE HEIGHTS FOR COASTAL ENGINEERING DESIGN	
	Distribution Restriction Statement Approved for public release; distribution is unlimited.	

DEPARTMENT OF THE ARMY
U.S. ARMY CORPS of ENGINEERS
Washington, D.C. 20314-1000

EM 1110-2-1414

CECW-EH-D

Engineer Manual
No. 1110-2-1414

7 July 1989

Engineering and Design

WATER LEVELS AND WAVE HEIGHTS FOR COASTAL ENGINEERING DESIGN

1. Purpose. This manual provides guidelines for the engineering analysis of coastal water levels and waves.

2. Applicability. This manual is applicable to all HQUSACE elements and field operating activities (FOA) having responsibility for planning, design, construction, and operation and maintenance of civil works projects.

3. Discussion. Virtually every coastal and harbor project requires information about water levels and wave heights. This manual is concerned with procedures for obtaining, interpreting, and applying water level and wave information. The manual addresses projects located in the coastal zone and subject to attack by waves and currents of the oceans, bays, and Great Lakes. The guidance is primarily for planning and preliminary design stages of a project. The design engineer is expected to adapt the general guidance presented in this manual to site-specific projects.

FOR THE COMMANDER:

ALBERT J. GENETTI, JR.
Colonel, Corps of Engineers
Chief of Staff

DEPARTMENT OF THE ARMY
U.S. Army Corps of Engineers
Washington, D.C. 20314-1000

CECW-EH-D

Engineer Manual
No. 1110-2-1414

7 Jul 89

Engineering and Design
WATER LEVELS AND WAVE HEIGHTS FOR COASTAL ENGINEERING DESIGN

Table of Contents

CHAPTER 1

INTRODUCTION

1-1. Purpose. This manual provides guidelines for the engineering analysis of coastal water levels and waves. The guidance is primarily for the planning and preliminary design states of a project. The design engineer is expected to adapt the general guidance presented in this manual to site-specific projects. Deviations from this guidance are acceptable if adequately substantiated.

1-2. Applicability. This manual is applicable to all HQUSACE elements and field operating activities responsible for the planning, design, construction, and operation and maintenance of civil works projects.

1-3. References. The references listed below are needed to implement some of the guidance in this manual.

a. EM 1110-2-1412, Storm Surge Analysis and Design Water Level Determinations.

b. Harris, D. L. 1981 (Feb). "Tides and Tidal Datums in the United States," Special Report No. 7 (SR-7). Available from Library, US Army Engineer Waterways Experiment Station, Vicksburg, MS 39180-0631.

c. National Oceanic and Atmospheric Administration, "Tide Tables, High and Low Water Predictions, East Coast of North and South America Including Greenland." Available from National Ocean Service, Rockville, MD 20852 (published annually).

d. National Oceanic and Atmospheric Administration, "Tide Tables, High and Low Water Predictions, West Coast of North and South America Including the Hawaiian Islands." Available from National Ocean Service, Rockville, MD 20852 (published annually).

e. Shore Protection Manual (SPM). 1984. 4th ed., 2 Vols, US Army Engineer Waterways Experiment Station, Coastal Engineering Research Center. Available from Superintendent of Documents, US Government Printing Office, Washington, DC 20402.

1-4. Bibliography. Bibliographic items are cited in the text by numbers (items 1, 2, etc.) that correspond to items in Appendix A. Where any reference or bibliographic item contains information that conflicts with this manual, the provisions of this manual shall govern.

1-5. Background and Scope. Virtually every coastal and harbor project requires information about local water levels and wave heights. This manual is concerned with procedures for obtaining, interpreting, and applying water level and wave information. The manual addresses projects located in the coastal zone and subject to attack by waves and currents of the oceans, bays, and Great Lakes. Specific types of projects include shallow and deep draft coastal navigation; shore and beach restoration, protection, and nourishment; and coastal wave and flood protection projects.

1-6. Discussion.

a. Critical Conditions. In the selection of design water levels and design waves for a project, the critical conditions must be considered. The conditions represent critical threshold combinations of tide level, surge level, wave conditions, etc., which, if surpassed, will endanger the project and/or make the project nonfunctional during their occurrence.

(1) Water levels and waves cannot generally be considered independent of each other in determining critical conditions. Water levels have a direct impact on wave conditions in shallow water, particularly when the waves are near the point of depth-limited breaking. Also, waves can have some impact on water level, especially in the surf zone where wave-induced setup can raise the local water level by significant amounts.

(2) Three types of considerations relate to the design of a project. The first (structural integrity) relates to the structure's ability to withstand the effects of extreme storms without itself suffering significant damages. The second (functional performance) deals with the effectiveness of the structure at its intended function. The third (constructibility) relates to means, methods, materials, etc. involved in project construction.

(3) Structural integrity criteria determine the structure's life-cycle costs to the extent that a certain level of investment is necessary to prevent damages from an extreme event. There will always be a finite probability that any storm, no matter how extreme, will be exceeded in intensity; so this consideration also determines the expected repair costs during the project life. The most extreme sea state in which a particular structure design will suffer no damages cannot in practice be precisely defined. The statement of structural integrity should be phrased with this in mind. It should be stated in terms of the desired effect, such as prevention of breakwater damages (and associated repair costs). An example would be "damages to more than 5 percent of the breakwater armor will occur with less than 2 percent probability per year." There are numerous complications in achieving such a goal, including definition of the types of possible damages and determining the combined probability per year of the physical parameters (wave height, wave period, wave direction, water level, storm duration, and others) which could cause them. Nevertheless, this is a workable statement in terms of an objective, adaptable to more than one means of determining structural dimensions.

(4) Functional performance determines the incremental economic benefits of a project since it defines the structure's level of effectiveness. It also affects the cost since a certain additional increment of investment may be necessary to achieve a given level of effectiveness. For a breakwater, this level of effectiveness can usually be stated in terms of a maximum transmitted wave condition during a given extreme event. The probability of exceedance for this event can in turn be related to property damage and other economic losses. A workable statement of functional performance might be that 10 percent of transmitted waves can be related to some level of unacceptable property damage or operational disruption landward of the breakwater. An even more general statement might be that navigational delays and property damages from transmitted waves shall occur with less than 5 percent probability per year.

(5) Constructibility includes consideration of project construction requirements. The considerations may include requirements for low water access by land equipment, high water access by floating equipment, curing of cast-in-place concrete, etc.

b. Estimation of Water Levels and Waves. Probabilities of exceedance of critical conditions for structural integrity, functional performance, and constructibility design conditions are estimated using the information in this manual as shown by the flow diagram in Figure 1-1. Some branches of the flow diagram are inapplicable to certain design problems. For example, tsunamis are generally an important design consideration only in and around the Pacific Ocean basin.

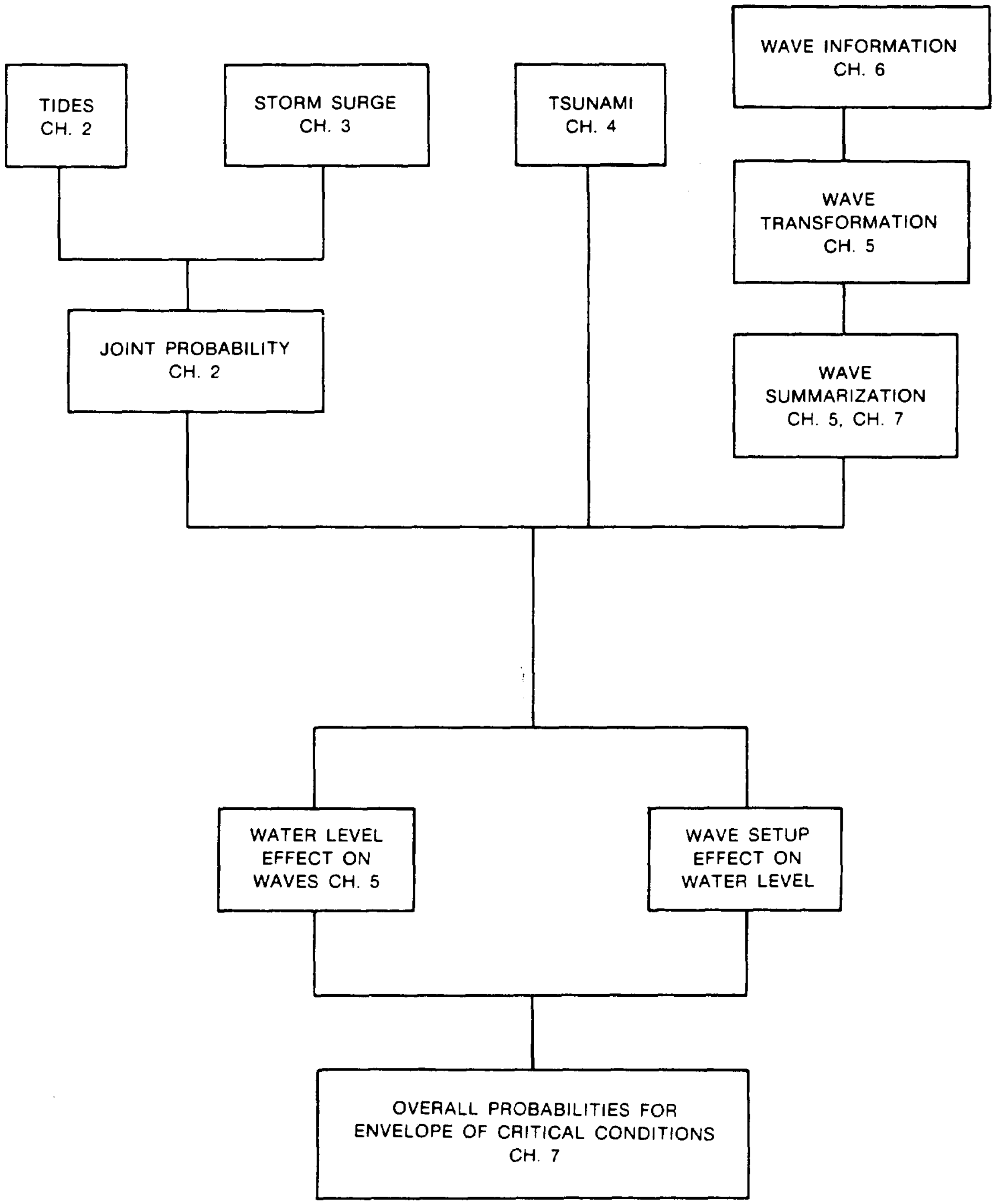

Figure 1-1. Flow diagram for the use of this manual

CHAPTER 2

TIDES AND TIDAL DATUMS

2-1. Description of Tide Records.

a. Astronomical Tides. Most of the material in this chapter was extracted from Special Report (SR)-7. Several important features of the astronomical tide are shown by the record in Figure 2-1. This record appears as a series of nearly sinusoidal oscillations with an average period near 12 hours and 25 minutes. The amplitude of these oscillations varies from one to the next, and the average range of any two successive tide waves rises and falls with a cycle of about 2 weeks. If a much longer period of record were shown, a cycle with a period near 29 days would also be discernible. The largest amplitudes (spring tides) coincide approximately with the time of a new moon and a full moon. The lowest (neap tides) amplitudes occur when the moon is in first or third quarter. There is an approximate repetition of the curve after periods of 14.5 and 29 days; i.e., periods of 1/2 and 1 full lunar month. Lines connecting alternate highs and lows have been drawn in the figure to show that the semidiurnal wave of greatest amplitude near the full moon has become the wave of least amplitude near the new moon. Both waves have nearly the same amplitude when the moon is in its first quarter.

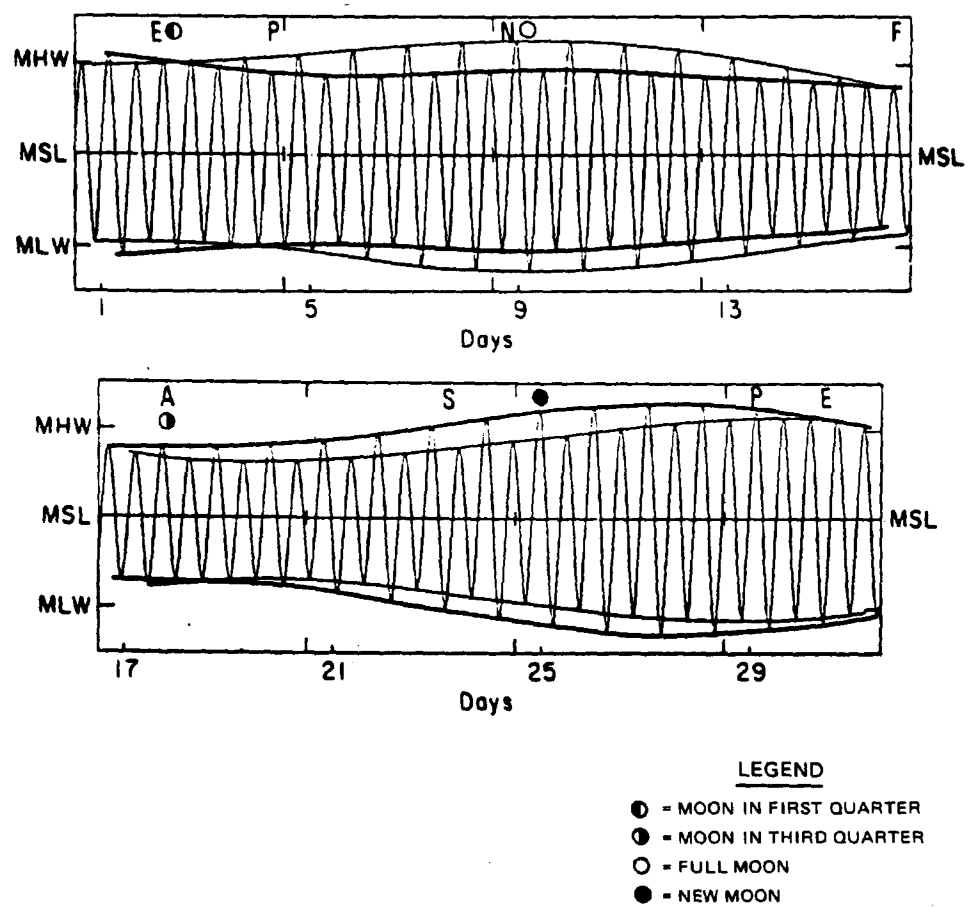

Figure 2-1. Tide predictions for Boston, Massachusetts, January 1963; predicted mean range 9.58 feet (2.92 meters)

(1) The tidal curve in Figure 2-1 (MHW = mean high water, MSL = mean sea level, MLW = mean low water) shows a classical semidiurnal tide. This tide behavior is the most common type along the US Atlantic coast. Tidal curves, however, may have many other shapes. Astronomical tides at five locations for January 1963 are shown in Figure 2-2. These curves have been normalized with respect to maximum range for each station to show the shape of the various curves rather than the relative range of the tide at each location. Curve A for New York, New York, is another example of a semidiurnal tide. The two highs and two lows of each tidal day (approximately 24 hours and 50 minutes) are more nearly equal than in curves B, C, and D. Curve E for Pensacola, Florida, is a typical example of a diurnal tide. Only one high and one low are clearly discernible for each lunar day. The other curves illustrate intermediate types of tide.

(2) Two highs and two lows during a tidal day can be recognized in curves B and C for Key West, Florida, and Port Townsend, Washington, respectively. The amplitudes of consecutive tide waves for these locations are very unequal, except for short periods near 15 and 30 January in curve B. Tidal curves of this type are called mixed tides. Curve D for St. Petersburg, Florida, is intermediate between the mixed and diurnal types. Two distinct, unequal lows and highs are recognized on most days, but there are several days when one tide wave vanishes. The tide appears to stand for a time at an intermediate value between the daily high and low, although only one distinct high and low can be identified. This phenomenon is often called a vanishing tide. The tidal range is generally low where these tides occur in the eastern United States, and there has been some confusion about a proper method for treating tidal datums where a vanishing tide occurs (discussed in Section 2-3).

b. Tide Observations and Tide Record Analysis. Tracings from several National Ocean Service (NOS, formerly US Coast and Geodetic Survey (USC&GS)) standard tide gage records are shown in Figure 2-3. The Portsmouth, Virginia, trace, obtained from a harbor well inland from the open sea, is relatively smooth, but a nontidal perturbation is indicated by an arrow above the curve near 0000, 13 August 1955. The trace from Atlantic City, New Jersey, was obtained as a tropical storm passed to the east of the station. The predicted tide is shown for comparison. The tide gage at Atlantic City is located near the end of the Steel Pier in the open ocean. Thus, with an exceptionally open exposure, and in spite of the use of a stilling well, wind waves make a significant contribution to the record. Several small oscillations with periods of 5 to 30 minutes also are clearly apparent. Similar short-period oscillations, but not the wind waves, are prominent in the trace obtained at Little Creek, Virginia.

(1) Tides, tsunamis, and storm surges cover similar ranges in amplitude. The periods of tsunamis are always much shorter than those of tidal periods. The periods of storm effects overlap those of both tsunamis and astronomical tides but are less regular.

(2) Most tide measurement devices are now digital gages. Both stilling wells and pressure gages are in common use. Stilling wells require a surface-piercing mounting structure, while pressure gages can be mounted on the bottom as well as on a structure. Data are usually recorded on either punched paper

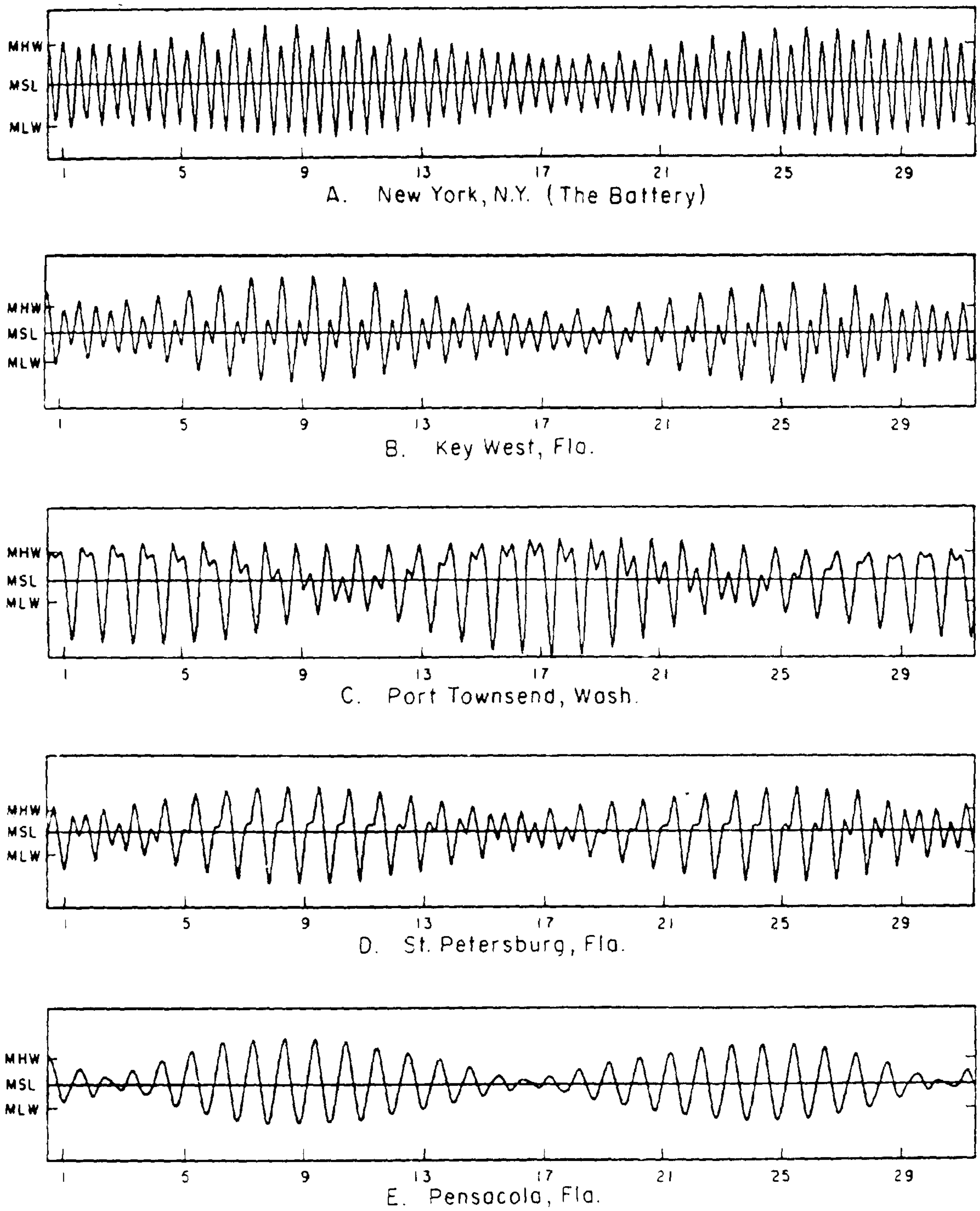

Figure 2-2. Predicted tidal curves showing various astronomical tides at five locations for January 1963

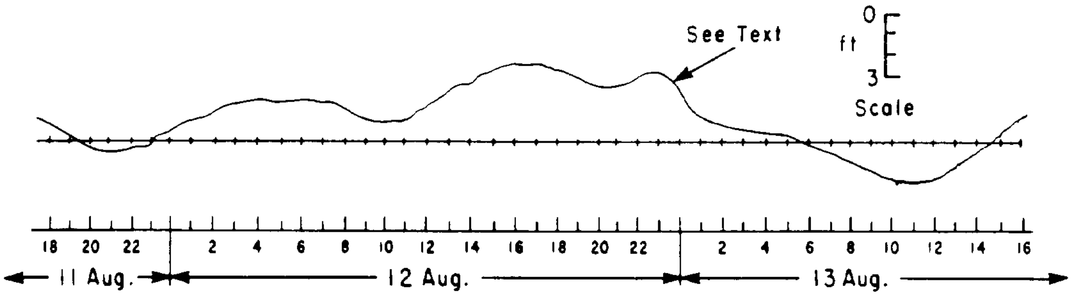

Portsmouth , Va.
12-13 Aug. 1955

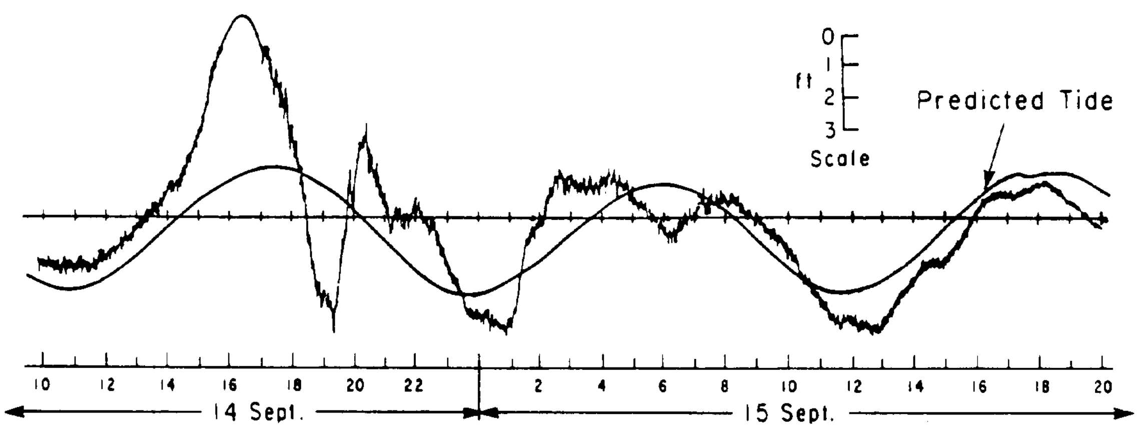

Atlantic City, N.J.
14-15 Sept. 1944

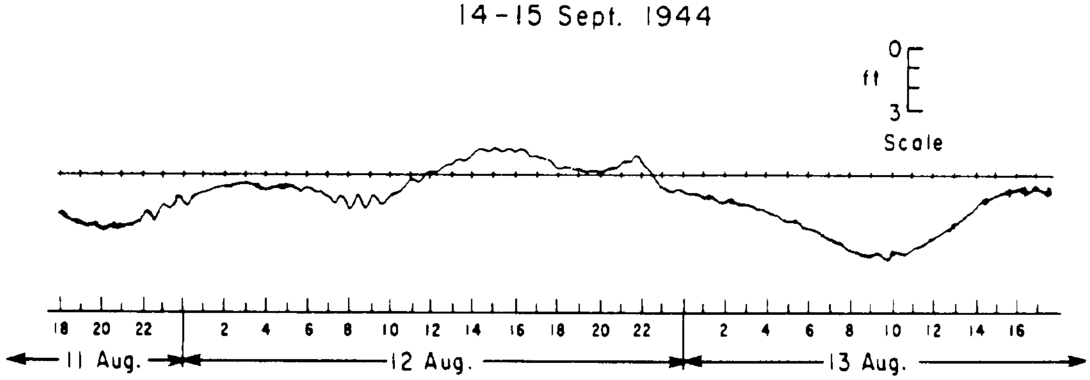

Little Creek , Va.
12-13 Aug. 1955

Figure 2-3. Tracings from tide gage records tape or a digital magnetic tape. The present standard NOS procedure is to collect 6-minute records on punched paper tape. This procedure is expected to be replaced with real-time collection of digital data by a central computer. Data will be available to users in near real-time and will be archived on magnetic tape.

(3) Standard tide records are routinely analyzed by tabulating the time and height of each high and low astronomical tide and each hourly value. Most tide records compiled by the NOS are used for defining tidal datums and the harmonic constants used for tide prediction. Thus, a systematic analysis procedure is used for all records. Detailed instructions for tide gage operation and data analysis are given in a manual published by the USC&GS (item 133). Perturbations with periods of 2 hours or less are smoothed in determining the high and low waters and hourly values. Perturbations with periods of several hours, such as those shown in the record for Atlantic City (Figure 2-3), are included in the tabulations. It is necessary to filter short-period oscillations with periods less than 2 hours from the hourly records to avoid errors in determining the harmonic constants used for tide prediction. Including storm surges with durations exceeding 2 hours in the records facilitates the determination of the extreme high and low water level; and because large storm surges are not common or very regular, it introduces very little error in the determination of harmonic constants.

(4) An average of all hourly tidal heights in a given month is taken as the average sea level for that month. A 12-month average is taken as the average sea level of the year.

c. Perturbations in Tide Records with Periods Much Longer Than the Tidal Period. Tide records include many perturbations with small amplitudes and periods much longer than those of the astronomical tide. The difference between the observed average daily sea level (average of the 24 hourly values) and the predicted daily mean at five tide stations is plotted in Figure 2-4 (item 44). Figure 2-5 (item 45) illustrates the annual cycle of sea level and the yearly variability in this cycle. Each plotted point represents the average tide departure from the established local sea level datum (in use in 1963) for a period of one month. The local sea level has been established for some earlier time periods, and the sea is rising, relative to the land, in this area. Thus, the mean of the observed record lies slightly above the established local MSL. The vertical bars plotted above the curves indicate months in which hurricanes passed near the tide gage. Perturbations in sea level with periods longer than one year are very important in coastal engineering. They are discussed in Section 2-4.

2-2. Tide Prediction.

a. The Tide Prediction Equation. The astronomical tide results primarily from the interaction of the gravitational fields of the Earth, Moon, and Sun. The gravitational tide-generating force can be expressed, with any desired accuracy, as the sum of a number of periodic terms determined from the astronomical parameters pertaining to the orbit of the Moon around the Earth and the orbits of Earth and Moon around the Sun.

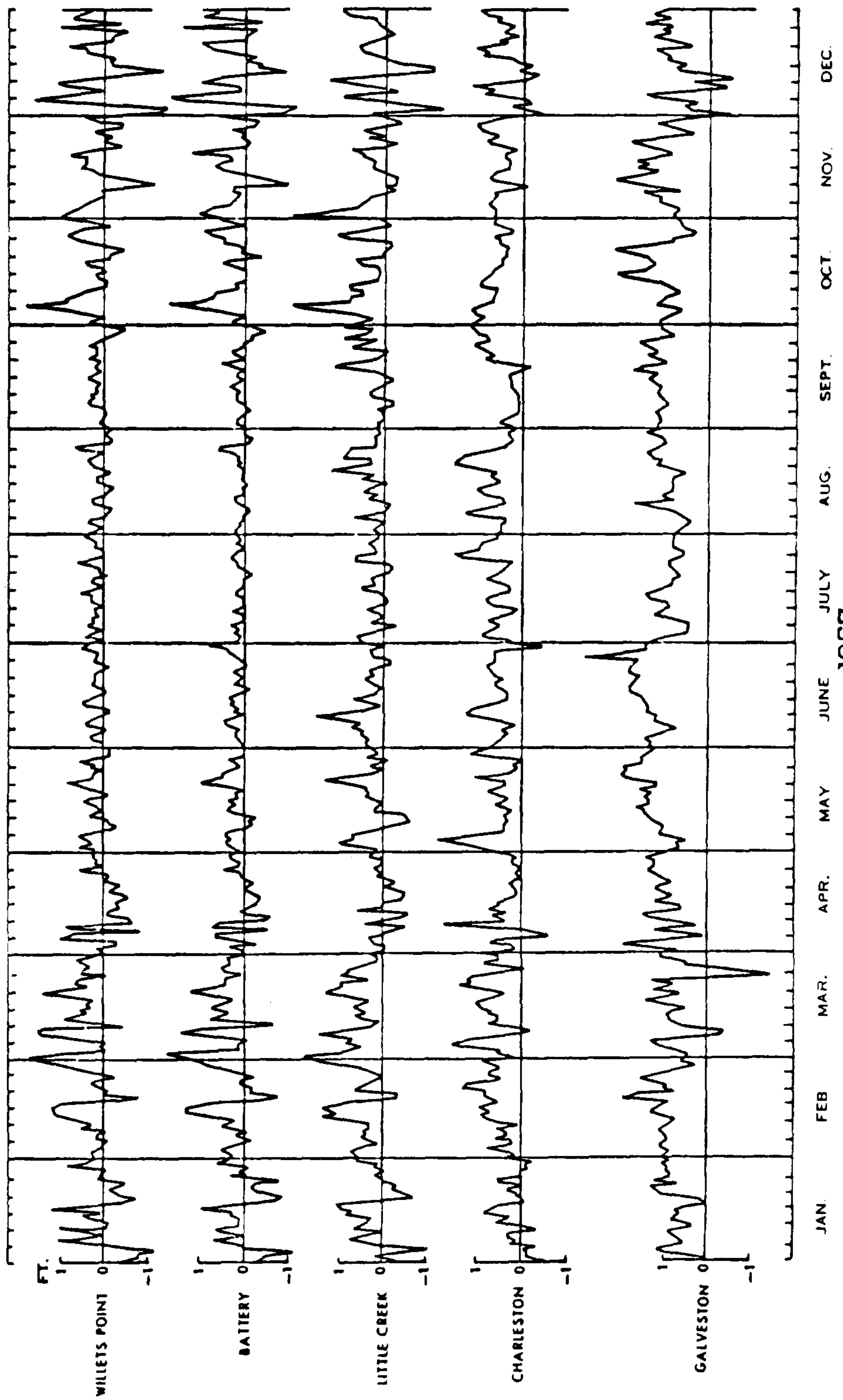

Figure 2-4. Departure of the observed daily MSL from the predicted value for selected NOS tide stations in 1957

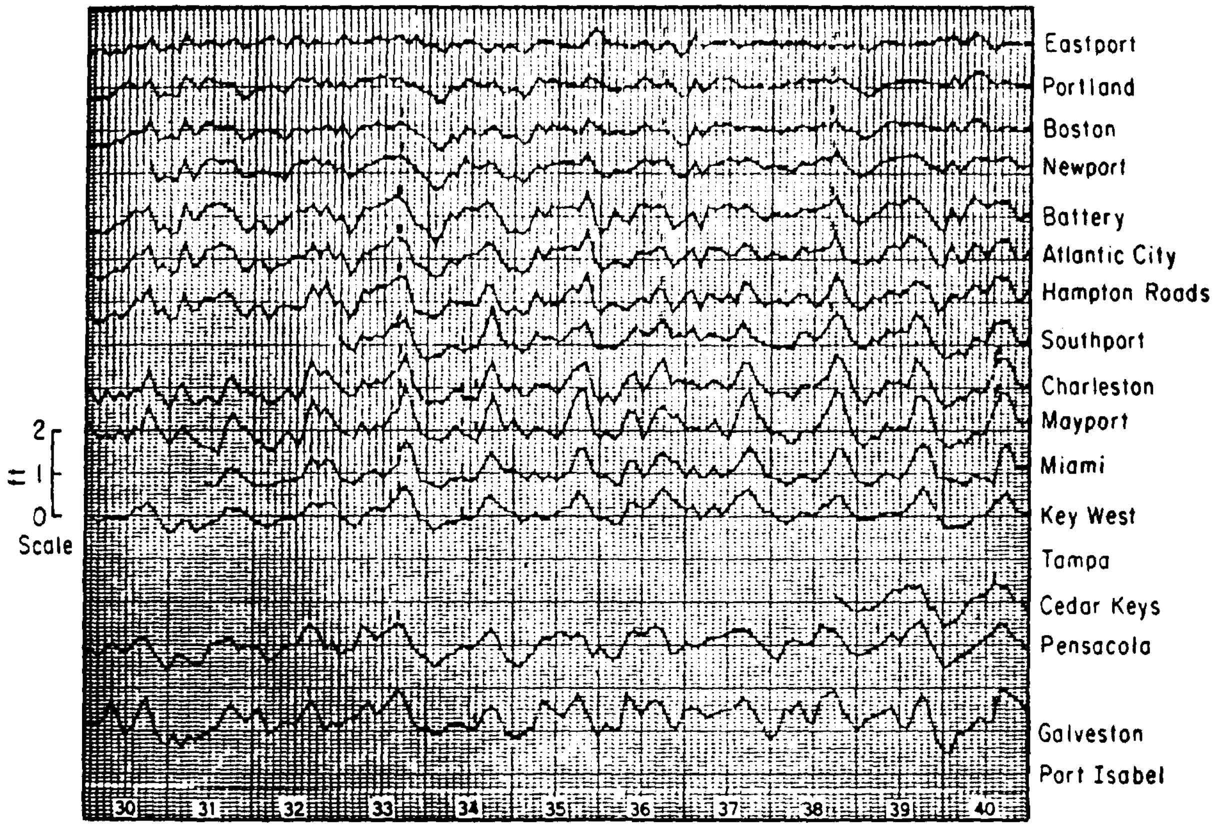

Figure 2-5. Observed monthly MSL at NOS Atlantic coast tide stations, 1930-1940

(1) The rotation of the Earth about the Sun and the Moon about the Earth gives rise to primary variations in the tide-generating force with periods near 1 day and near 12 hours. The amplitude of these oscillations is modulated by the variation in direction and distance of the selected point on the Earth's surface from the center of the Moon and the center of the Sun. The most prominent periods in the modulating terms are near one lunar month and one solar year. Interaction between these oscillations leads to other prominent periods near 2 weeks and near 19 years. Several of the more prominent astronomical periods, important for tide prediction, are listed in Table 2-1 (items 26 and 115). The periods of major importance in predicting tides at most locations are less than 30 days, but often non-negligible contributions are also present at longer periods.

(2) The tide prediction equation is expressed as:

$$h_{ys}(t) = h_o + \sum_{n=1}^{N} f_{ny} A_{ns} \cos (\sigma_n t - \nu_{ny} - \kappa_{ns}) \quad (2\text{-}1)$$

Table 2-1

Astronomical Periods Affecting the Tides

Phenomenon	Astronomical period d	yr
Sidereal day (with respect to fixed stars)	0.997270	
Lunar day (with respect to the Moon)	1.035050	
Nodical month (north-south cycle)	27.212220	
Tropical month (vernal equinox)	27.321582	
Anomalistic month (perigee to perigee, distance)	27.554550	
Synodical month (phase of the Moon)	29.530588	
Eclipse year (with respect to the lunar orbit)	346.620	
Tropical year (vernal equinox)	365.242	
Anomalistic year (distance)	365.259	
Revolution of lunar perigee		8.85
Revolution of Moon's node (ecliptic)		18.61
Saros cycle (recurrence of eclipses)		18.03
Metonic cycle (recurrence of lunar phases)		19.00
Revolution of solar perigee	209 centuries	

where $h_{ys}(t)$ = tide at station s during year y at time t *

h_o = height of the local MSL datum above the datum of reference

N = number of constituents

f_{ny} = node factor

A_{ns} = amplitude

σ_n = frequency, or angular speed

t = time reckoned from some initial epoch

ν_{ny} = equilibrium argument

κ_{ns} = phase lag, or epoch

The subscript y indicates the parameter may change yearly but is independent of location. The subscript s indicates the parameter depends on the location of the tide station. The parameters σ_n, f_{ny}, and ν_{ny} are

*Symbols and units of measurement are listed in the Notation (Appendix B).

determined from astronomical theory. The parameters f_{ny} and ν_{ny} represent the effect of periodicities longer than 1 year on the amplitude and phase, respectively. Tabulations of yearly values of f_{ny} and ν_{ny} for the years 1900 to 2000 are given in item 115. The parameters A_{ns} and κ_{ns} are standardized for a particular location based on past measurements at the site. A minimum record length of 29 days is needed, although a 369-day record is preferred. The parameters A_{ns} and κ_{ns} are estimated by removing the theoretically determined terms from the empirically determined amplitudes and phases. A procedure for making these computations, which has been computerized, is described in item 105.

(3) When the parameters of equation (2-1) are known, the equation can be used for tide prediction without additional consideration of the theory of tides. Additional description of the nature and origin of tidal generating forces is given by SR-7.

b. Shallow-Water Tides.

(1) The astronomical tides generated in the deep ocean act (in general) like progressive waves as they travel across shallow parts of the continental shelves and into estuaries where the tides are most important to man. Whenever the amplitude of the tide wave is of the same order of magnitude as the water depth, the crest of the wave travels more rapidly than the trough. As a result, the time interval from low water to high water in the upper reaches of an estuary is generally shorter than the time interval from high water to low water. The complete cycle, low water to high water to low water, however, remains unchanged. The resulting hydrograph can be described by introducing new trignometric functions whose frequencies are sums and differences of the frequencies used to describe the tide in the open sea.

(2) The number of trigonometric terms needed to describe the astronomical tide varies with the location. More terms are needed where the tide must travel a great distance through shallow water than when the tide station is near the open sea. Additional terms may be needed to obtain an adequate representation when the tidal range is large rather than small. In the United States, 37 standard constituents are found to be adequate for most tide stations (item 115), however 114 constituents are needed for Anchorage, Alaska (item 146).

(3) Because of the strong modification of tides in shallow water, tide measurements or predictions at one site should be transferred to other sites with great care. For nearby sites along the open coast, tide information may be transferred directly. When the site for which tide information is available is inland from the open coast, the information should not be directly transferred to other sheltered areas or the open coast. For example, tide measurements inside a sheltered bay should not be directly used as an estimate of instantaneous water levels for a dredge operating several miles offshore. Such cases should be treated by establishing a tide gage at a more appropriate location or conducting a numerical model study to determine the relationship between the existing tide station and the site of interest.

c. Harmonic Constituents of the Tide. The 37 tidal constituents regularly used by NOS are given in Table 2-2. The symbols represent normal usage. Frequencies are expressed as degrees per hour. The symbols may be used to identify the frequency, amplitude, or phase of the constituent. Symbols with subscripts 1, 2, 3, 4, 6, or 8 indicate the approximate number of cycles per tidal day; symbols without subscripts indicate periods much longer than 24 hours.

(1) A quantitative definition of the type of tide (diurnal, semidurnal, or mixed) may be expressed by

$$R = \frac{A(K_1) + A(O_1)}{A(M_2) + A(S_2)} \tag{2-2}$$

where $A(K_1)$, $A(O_1)$, etc., represent the amplitude of constituents, such as K_1, O_1. The type of tide is specified as

semidiurnal, if $R < 0.25$,

mixed, if $0.25 \leq R \leq 1.50$, and

diurnal, if $1.50 < R$

The constituents identified by K_1 and O_1 in equation (2-2) are generally the dominant components of the diurnal tide; constituents identified by M_2 and S_2 generally indicate the largest components of the semidurnal tide.

(2) The harmonic constants of the tide (the amplitudes A_{ns} and the phases κ_{ns} ,of equation (2-1)) are available for many US locations from NOS. Harmonic constants for a station may be altered when the character of the channel between the tide station and the open sea is changed by dredging, silting, or construction which modifies the free travel of waves from the open sea. The harmonic constants for Philadelphia, Pennsylvania, as determined from observations in 1946, 1952, and 1957 show that the amplitude of major constituents varies by about 4 to 8 percent of the minimum value, and phases vary by about 5° to 40°. Philadelphia has one of the longest, most constricted channels from the open sea of any US port. The variability of the harmonic constants at Philadelphia is believed to be near an upper limit for the United States.

d. Use of Tide Tables.

(1) Tide tables and tidal current tables are published annually by NOS in separate volumes for the Atlantic and Gulf coasts and for the Pacific coast of the US. The tide tables provide the predicted time and elevation for each high and low water at each reference station for the entire year. An example is given in Figure 2-6 for the reference station at Miami Harbor Entrance, Florida. Elevations are referred to the local datum which is presently MLW for the Atlantic and Gulf and mean lower low water (MLLW) for the Pacific.

Table 2-2

Tidal Constituents Commonly Used by NOS

Symbol	Frequency deg/hr	Symbol	Frequency deg/hr
M_2	28.984	Mm	0.544
S_2	30.000	Ssa	0.082
N_2	28.439	Sa	0.041
K_1	15.041	Ms_f	1.015
M_4	57.968	M_f	1.098
O_1	13.943	ρ_1	13.471
M_6	86.952	Q_1	13.398
$(MK)_3$	44.025	T_2	29.958
S_4	60.000	R_2	30.041
$(MN)_4$	57.423	$(2Q)_1$	12.854
ν_2	28.512	P_1	24.958
S_6	90.000	$(2SM)_2$	31.015
μ_2	27.968	M_3	43.476
$(2N)_2$	27.895	L_2	29.528
$(OO)_1$	16.139	$(2MK)_3$	42.927
λ_2	29.455	K_2	30.082
S_1	15.000	M_8	115.936
M_1	14.496	$(MS)_4$	58.984
J_1	15.585		

Times are given in local standard time. The times and tidal elevations at numerous secondary stations can be obtained by applying corrections to the reference station. The appropriate corrections are given in the tide tables as illustrated in Figure 2-7. Figure 2-7 also provides information on mean and spring tidal ranges and mean tide level for each secondary station. Example problem 2-1 illustrates the use of the tide table.

MIAMI HARBOR ENTRANCE, FLA., 1985

Times and Heights of High and Low Waters

JANUARY

Day	Time (h m)	Height (ft)	Height (m)
1	0347	2.0	0.6
Tu	0948	0.5	0.2
	1545	2.0	0.6
	2209	0.1	0.0
2	0441	2.1	0.6
W	1041	0.5	0.2
	1633	2.0	0.6
	2256	-0.1	0.0
3	0528	2.3	0.7
Th	1131	0.4	0.1
	1720	2.1	0.6
	2341	-0.2	-0.1
4	0613	2.4	0.7
F	1216	0.3	0.1
	1805	2.2	0.7
5	0024	-0.3	-0.1
Sa	0656	2.5	0.8
	1259	0.2	0.1
	1850	2.2	0.7
6	0108	-0.4	-0.1
Su	0736	2.6	0.8
	1341	0.1	0.0
	1934	2.3	0.7
7	0151	-0.5	-0.2
M	0819	2.6	0.8
	1425	0.0	0.0
	2020	2.4	0.7
8	0236	-0.6	-0.2
Tu	0902	2.6	0.8
	1509	-0.1	0.0
	2108	2.4	0.7
9	0323	-0.5	-0.2
W	0947	2.6	0.8
	1555	-0.2	-0.1
	2157	2.5	0.8
10	0413	-0.5	-0.2
Th	1032	2.6	0.8
	1643	-0.2	-0.1
	2250	2.4	0.7
11	0503	-0.4	-0.1
F	1119	2.5	0.8
	1735	-0.3	-0.1
	2346	2.4	0.7
12	0558	-0.2	-0.1
Sa	1210	2.4	0.7
	1830	-0.3	-0.1
13	0047	2.3	0.7
Su	0657	-0.1	0.0
	1308	2.3	0.7
	1929	-0.3	-0.1
14	0152	2.3	0.7
M	0801	0.0	0.0
	1407	2.2	0.7
	2032	-0.4	-0.1
15	0300	2.3	0.7
Tu	0909	0.1	0.0
	1508	2.2	0.7
	2135	-0.4	-0.1
16	0406	2.3	0.7
W	1014	0.1	0.0
	1610	2.2	0.7
	2236	-0.5	-0.2
17	0509	2.4	0.7
Th	1115	0.1	0.0
	1712	2.2	0.7
	2333	-0.5	-0.2
18	0605	2.5	0.8
F	1213	0.0	0.0
	1808	2.2	0.7
19	0027	-0.6	-0.2
Sa	0659	2.5	0.8
	1304	-0.1	0.0
	1859	2.3	0.7
20	0118	-0.6	-0.2
Su	0745	2.5	0.8
	1351	-0.1	0.0
	1946	2.3	0.7
21	0204	-0.6	-0.2
M	0828	2.5	0.8
	1437	-0.2	-0.1
	2034	2.3	0.7
22	0246	-0.5	-0.2
Tu	0908	2.5	0.8
	1519	-0.2	-0.1
	2117	2.2	0.7
23	0328	-0.4	-0.1
W	0947	2.4	0.7
	1559	-0.2	-0.1
	2200	2.2	0.7
24	0409	-0.3	-0.1
Th	1026	2.3	0.7
	1637	-0.2	-0.1
	2242	2.1	0.6
25	0450	-0.2	-0.1
F	1104	2.2	0.7
	1717	-0.1	0.0
	2327	2.0	0.6
26	0530	0.0	0.0
Sa	1142	2.1	0.6
	1800	-0.1	0.0
27	0012	1.9	0.6
Su	0615	0.1	0.0
	1223	1.9	0.6
	1844	0.0	0.0
28	0100	1.8	0.5
M	0702	0.3	0.1
	1306	1.8	0.5
	1931	0.0	0.0
29	0157	1.8	0.5
Tu	0757	0.4	0.1
	1355	1.8	0.5
	2022	0.0	0.0
30	0255	1.8	0.5
W	0857	0.4	0.1
	1449	1.7	0.5
	2118	-0.1	0.0
31	0354	1.9	0.6
Th	0957	0.4	0.1
	1545	1.7	0.5
	2212	-0.2	-0.1

FEBRUARY

Day	Time (h m)	Height (ft)	Height (m)
1	0449	2.0	0.6
F	1054	0.3	0.1
	1643	1.8	0.5
	2307	-0.3	-0.1
2	0541	2.1	0.6
Sa	1145	0.2	0.1
	1736	2.0	0.6
	2357	-0.5	-0.2
3	0630	2.3	0.7
Su	1234	0.0	0.0
	1827	2.1	0.6
4	0048	-0.6	-0.2
M	0713	2.4	0.7
	1319	-0.2	-0.1
	1917	2.3	0.7
5	0135	-0.7	-0.2
Tu	0758	2.5	0.8
	1404	-0.4	-0.1
	2007	2.4	0.7
6	0221	-0.8	-0.2
W	0840	2.6	0.8
	1448	-0.5	-0.2
	2054	2.5	0.8
7	0309	-0.8	-0.2
Th	0925	2.6	0.8
	1535	-0.6	-0.2
	2144	2.6	0.8
8	0358	-0.7	-0.2
F	1010	2.6	0.8
	1623	-0.7	-0.2
	2236	2.6	0.8
9	0447	-0.6	-0.2
Sa	1058	2.5	0.8
	1713	-0.7	-0.2
	2330	2.5	0.8
10	0540	-0.4	-0.1
Su	1148	2.4	0.7
	1806	-0.6	-0.2
11	0028	2.4	0.7
M	0636	-0.2	-0.1
	1241	2.2	0.7
	1905	-0.5	-0.2
12	0132	2.2	0.7
Tu	0739	0.0	0.0
	1342	2.1	0.6
	2007	-0.5	-0.2
13	0239	2.1	0.6
W	0848	0.1	0.0
	1447	2.0	0.6
	2115	-0.4	-0.1
14	0350	2.1	0.6
Th	0958	0.1	0.0
	1553	1.9	0.6
	2222	-0.4	-0.1
15	0456	2.1	0.6
F	1103	0.1	0.0
	1700	2.0	0.6
	2321	-0.4	-0.1
16	0553	2.2	0.7
Sa	1203	0.0	0.0
	1758	2.0	0.6
17	0017	-0.5	-0.2
Su	0645	2.3	0.7
	1253	-0.1	0.0
	1849	2.1	0.6
18	0106	-0.5	-0.2
M	0728	2.3	0.7
	1335	-0.2	-0.1
	1935	2.2	0.7
19	0148	-0.5	-0.2
Tu	0807	2.3	0.7
	1416	-0.3	-0.1
	2017	2.2	0.7
20	0228	-0.5	-0.2
W	0844	2.3	0.7
	1453	-0.3	-0.1
	2057	2.2	0.7
21	0306	-0.4	-0.1
Th	0916	2.3	0.7
	1528	-0.3	-0.1
	2135	2.2	0.7
22	0342	-0.3	-0.1
F	0951	2.2	0.7
	1602	-0.3	-0.1
	2212	2.2	0.7
23	0418	-0.2	-0.1
Sa	1024	2.2	0.7
	1637	-0.3	-0.1
	2250	2.1	0.6
24	0455	-0.1	0.0
Su	1058	2.0	0.6
	1714	-0.2	-0.1
	2332	2.0	0.6
25	0534	0.1	0.0
M	1135	1.9	0.6
	1754	-0.2	-0.1
26	0015	1.9	0.6
Tu	0617	0.2	0.1
	1214	1.8	0.5
	1836	-0.1	0.0
27	0104	1.8	0.5
W	0708	0.4	0.1
	1303	1.7	0.5
	1928	0.0	0.0
28	0204	1.8	0.5
Th	0806	0.4	0.1
	1359	1.7	0.5
	2029	0.0	0.0

MARCH

Day	Time (h m)	Height (ft)	Height (m)
1	0309	1.8	0.5
F	0913	0.4	0.1
	1504	1.7	0.5
	2134	-0.1	0.0
2	0411	1.9	0.6
Sa	1017	0.3	0.1
	1611	1.8	0.5
	2235	-0.2	-0.1
3	0507	2.1	0.6
Su	1115	0.1	0.0
	1712	2.0	0.6
	2333	-0.4	-0.1
4	0600	2.3	0.7
M	1206	-0.1	0.0
	1808	2.3	0.7
5	0026	-0.5	-0.2
Tu	0646	2.5	0.8
	1253	-0.3	-0.1
	1900	2.5	0.8
6	0116	-0.7	-0.2
W	0732	2.6	0.8
	1342	-0.6	-0.2
	1951	2.7	0.8
7	0205	-0.8	-0.2
Th	0817	2.7	0.8
	1426	-0.8	-0.2
	2039	2.8	0.9
8	0251	-0.8	-0.2
F	0901	2.8	0.9
	1513	-0.9	-0.3
	2128	2.9	0.9
9	0339	-0.7	-0.2
Sa	0947	2.7	0.8
	1600	-0.9	-0.3
	2218	2.8	0.9
10	0429	-0.6	-0.2
Su	1034	2.6	0.8
	1650	-0.8	-0.2
	2311	2.7	0.8
11	0521	-0.4	-0.1
M	1125	2.5	0.8
	1742	-0.7	-0.2
12	0009	2.5	0.8
Tu	0617	-0.1	0.0
	1218	2.3	0.7
	1841	-0.5	-0.2
13	0110	2.3	0.7
W	0720	0.1	0.0
	1321	2.1	0.6
	1945	-0.3	-0.1
14	0219	2.2	0.7
Th	0831	0.2	0.1
	1430	2.0	0.6
	2055	-0.2	-0.1
15	0332	2.1	0.6
F	0945	0.3	0.1
	1542	1.9	0.6
	2207	-0.1	0.0
16	0439	2.1	0.6
Sa	1051	0.2	0.1
	1651	2.0	0.6
	2310	-0.1	0.0
17	0536	2.2	0.7
Su	1147	0.1	0.0
	1749	2.1	0.6
18	0001	-0.2	-0.1
M	0624	2.3	0.7
	1232	0.0	0.0
	1837	2.2	0.7
19	0047	-0.2	-0.1
Tu	0705	2.3	0.7
	1314	-0.1	0.0
	1919	2.3	0.7
20	0129	-0.2	-0.1
W	0739	2.4	0.7
	1349	-0.2	-0.1
	1958	2.4	0.7
21	0204	-0.2	-0.1
Th	0813	2.4	0.7
	1421	-0.3	-0.1
	2033	2.4	0.7
22	0239	-0.2	-0.1
F	0845	2.4	0.7
	1454	-0.3	-0.1
	2107	2.4	0.7
23	0314	-0.1	0.0
Sa	0915	2.3	0.7
	1526	-0.3	-0.1
	2143	2.4	0.7
24	0347	0.0	0.0
Su	0946	2.2	0.7
	1600	-0.3	-0.1
	2218	2.3	0.7
25	0421	0.1	0.0
M	1018	2.1	0.6
	1634	-0.2	-0.1
	2257	2.2	0.7
26	0458	0.2	0.1
Tu	1053	2.0	0.6
	1711	-0.1	0.0
	2338	2.1	0.6
27	0540	0.4	0.1
W	1132	1.9	0.6
	1754	0.0	0.0
28	0025	2.0	0.6
Th	0630	0.5	0.2
	1221	1.9	0.6
	1847	0.1	0.0
29	0121	2.0	0.6
F	0729	0.5	0.2
	1322	1.8	0.5
	1950	0.1	0.0
30	0228	2.0	0.6
Sa	0835	0.5	0.2
	1435	1.9	0.6
	2102	0.1	0.0
31	0332	2.1	0.6
Su	0944	0.4	0.1
	1545	2.0	0.6
	2207	0.0	0.0

Time meridian 75° W. 0000 is midnight. 1200 is noon.
Heights are referred to mean low water which is the chart datum of soundings.

Figure 2-6. Example tide table for the reference station at Miami Harbor Entrance, Florida

NO.	PLACE	POSITION Lat.	POSITION Long.	DIFFERENCES Time High water	DIFFERENCES Time Low water	DIFFERENCES Height High water	DIFFERENCES Height Low water	RANGES Mean	RANGES Spring	Mean Tide Level
		° ' N	° ' W	h. m.	h. m.	ft	ft	ft	ft	ft
	FLORIDA, St. Johns River Time meridian, 75°W			on MAYPORT, p.108						
2857	Pablo Creek bascule bridge	30 19	81 26	+1 39	+1 15	*0.64	*0.64	2.9	3.4	1.4
2859	Fulton	30 23	81 30	+0 29	+0 42	-1.1	0.0	3.4	4.0	1.7
2861	Dame Point	30 23	81 33	+0 46	+0 55	*0.67	*0.67	3.0	3.5	1.5
2863	Phoenix Park (Cummers Mill)	30 23	81 38	+0 58	+1 25	*0.44	*0.44	2.0	2.3	1.0
2865	Jacksonville (Dredge Depot)	30 21	81 37	+1 24	+1 50	*0.44	*0.44	2.0	2.3	1.0
2867	Jacksonville (RR. bridge)	30 19	81 40	+2 06	+2 13	*0.27	*0.27	1.2	1.4	0.6
2869	Ortega River entrance	30 17	81 42	+2 27	+2 50	*0.20	*0.20	0.9	1.1	0.5
2871	Orange Park	30 10	81 42	+3 49	+4 14	*0.16	*0.16	0.7	0.8	0.3
2873	Green Cove Springs	30 00	81 40	+5 26	+6 13	*0.18	*0.18	0.8	0.9	0.4
2875	East Tocoi	29 51	81 34	+6 47	+7 18	*0.22	*0.22	1.0	1.2	0.5
2877	Bridgeport	29 45	81 34	+6 58	+7 32	*0.24	*0.24	1.1	1.3	0.5
2879	Palatka	29 39	81 38	+7 26	+8 21	*0.27	*0.27	1.2	1.4	0.6
2881	Welaka	29 29	81 40	+7 46	+8 25	*0.11	*0.11	0.5	0.6	0.2
	FLORIDA, East Coast									
2883	Atlantic Beach	30 20	81 24	-0 25	-0 18	+0.7	0.0	5.2	6.0	2.6
2885	St. Augustine Inlet	29 53	81 17	-0 21	-0 01	0.0	0.0	4.5	5.3	2.2
2887	St. Augustine	29 54	81 18	+0 14	+0 43	-0.3	0.0	4.2	5.0	2.1
2889	Daytona Beach (ocean)	29 14	81 00	-0 33	-0 32	-0.4	0.0	4.1	4.9	2.0
				on MIAMI HARBOR ENT., p.112						
2891	Ponce de Leon Inlet	29 04	80 55	+0 06	+0 20	-0.2	0.0	2.3	2.7	1.2
2893	Cape Canaveral	28 26	80 34	-0 41	-0 41	+1.0	0.0	3.6	4.1	1.8
2894	Oak Hill, Mosquito Lagoon <21>	28 52	80 50	- - -	- - -	- -	- -	- -	- -	- -
	Indian River									
2895	Melbourne <22>	28 06	80 37	- - -	- - -	- -	- -	- -	- -	- -
2896	Palm Bay	28 02	80 35	+3 40	+4 19	*0.10	*0.10	0.2	0.2	0.1
2897	Wabasso	27 45	80 26	+2 48	+3 19	*0.16	*0.16	0.4	0.5	0.2
2898	Vero Beach	27 38	80 22	+3 21	+3 50	*0.32	*0.32	0.8	1.0	0.4
2900	Fort Pierce	27 27	80 19	+1 08	+1 01	*0.48	*0.48	1.2	1.4	0.6
2901	Jensen Beach	27 14	80 13	+2 40	+3 06	*0.40	*0.40	1.0	1.2	0.5
2902	Sebastian Inlet	27 52	80 27	-0 24	-0 20	-0.4	0.0	2.1	2.5	1.0
2903	Vero Beach (ocean)	27 40	80 22	-0 31	-0 25	+0.9	0.0	3.4	4.0	1.7
2905	Fort Pierce Inlet, south jetty	27 28	80 17	-0 09	-0 14	+0.1	0.0	2.6	3.1	1.3
	St. Lucie River									
2907	North Fork	27 15	80 19	+2 50	+3 29	*0.40	*0.40	1.0	1.2	0.5
2908	Stuart	27 12	80 16	+2 37	+3 33	*0.36	*0.36	0.9	1.1	0.4
2909	South Fork	27 10	80 15	+2 54	+3 34	*0.36	*0.36	0.9	1.1	0.4
2911	Sewall Point	27 10	80 11	+1 35	+2 11	*0.36	*0.36	0.9	1.1	0.4
2912	Seminole Shores	27 11	80 10	-0 30	-0 14	+0.5	0.0	3.0	3.6	1.5
2913	Great Pocket	27 09	80 10	+1 18	+1 51	*0.44	*0.44	1.1	1.3	0.6
2914	Gomez, South Jupiter Narrows	27 06	80 08	+1 56	+2 41	*0.52	*0.52	1.3	1.6	0.6
2916	Hobe Sound - State Park	27 02	80 06	+1 46	+2 22	-0.9	0.0	1.6	1.9	0.8
2917	Conch Bar, Jupiter Sound	26 59	80 06	+1 19	+1 38	-0.8	0.0	1.7	2.0	0.8
2918	Jupiter Sound, south end	26 57	80 05	+0 46	+0 49	-0.5	0.0	2.0	2.4	1.0
2919	Jupiter Inlet	26 57	80 04	+0 15	+0 01	0.0	0.0	2.5	3.0	1.2
	Loxahatchee River									
2921	Tequesta	26 57	80 06	+1 18	+2 02	-0.7	0.0	1.8	2.2	0.9
2922	North Fork	26 58	80 07	+1 27	+1 59	-0.6	0.0	1.9	2.3	1.0
2923	Southwest Fork (spillway)	26 56	80 09	+1 15	+1 49	-0.5	0.0	2.0	2.4	1.0
2924	Northwest Fork	26 59	80 08	+1 34	+2 10	-0.5	0.0	2.0	2.4	1.0
2926	Southwest Fork	26 57	80 07	+1 15	+1 47	-0.6	0.0	1.9	2.3	1.0
2927	Jupiter, Lake Worth Creek	26 56	80 05	+0 57	+1 16	-0.4	0.0	2.1	2.5	1.0
2928	Donald Ross Bridge	26 53	80 04	+0 43	+0 54	-0.2	0.0	2.3	2.8	1.2
2929	North Palm Beach, Lake Worth Creek	26 50	80 03	+0 05	+0 17	+0.4	0.0	2.9	3.4	1.4
2931	Port of Palm Beach, Lake Worth	26 46	80 03	0 00	+0 12	+0.1	0.0	2.6	3.1	1.3
2932	Palm Beach (ocean)	26 43	80 02	-0 21	-0 18	+0.3	0.0	2.8	3.3	1.4
2933	West Palm Beach Canal	26 39	80 03	+1 08	+1 36	0.0	0.0	2.5	2.8	1.2
2934	Lake Worth Pier (ocean)	26 37	80 02	-0 19	-0 17	+0.3	0.0	2.8	3.3	1.4
2936	Boynton Beach	26 33	80 03	+1 26	+2 09	0.0	0.0	2.5	2.8	1.2
2937	Delray Beach	26 28	80 04	+1 45	+2 09	0.0	0.0	2.5	2.9	1.2
2938	Yamato	26 24	80 04	+1 43	+1 59	-0.1	0.0	2.4	2.8	1.2
2939	Boca Raton	26 21	80 05	+0 47	+1 13	-0.3	0.0	2.2	2.5	1.1
2941	Deerfield Beach	26 19	80 05	+0 51	+1 07	-0.1	0.0	2.4	2.9	1.2
2942	Hillsboro Beach, Intracoastal waterway	26 16	80 05	+0 26	+0 38	+0.3	0.0	2.8	3.2	1.4
2943	Hillsboro Inlet (inside)	26 16	80 05	+0 08	+0 06	0.0	0.0	2.5	2.9	1.2
2944	Lauderdale-by-the-sea	26 11	80 06	-0 08	-0 08	+0.1	0.0	2.6	3.1	1.3
	Fort Lauderdale									
2946	Bahia Mar Yacht Club	26 07	80 06	+0 19	+0 38	-0.1	0.0	2.4	2.8	1.2
2947	Andrews Ave. bridge, New River	26 07	80 09	+0 39	+0 56	-0.4	0.0	2.1	2.4	1.0
2948	Port Everglades	26 06	80 07	-0 06	-0 06	+0.1	0.0	2.6	3.1	1.3
2949	South Port Everglades	26 05	80 07	0 00	+0 01	0.0	0.0	2.5	2.9	1.3
2951	Hollywood Beach	26 02	80 07	+1 00	+1 08	-0.4	0.0	2.1	2.4	1.0
2952	Golden Beach	25 58	80 08	+1 36	+2 04	-0.4	0.0	2.1	2.4	1.0
2953	Sunny Isles, Biscayne Creek	25 56	80 08	+2 23	+2 27	-0.7	0.0	1.8	2.2	0.9
2954	North Miami Beach	25 56	80 07	-0 04	0 00	0.0	0.0	2.5	3.0	1.2
2956	Bakers Haulover Inlet (inside)	25 54	80 08	+1 17	+1 35	-0.5	0.0	2.0	2.4	1.0
2957	Indian Creek	25 52	80 09	+1 36	+1 50	-0.4	0.0	2.1	2.5	1.1
2958	Miami Beach	25 46	80 08	0 00	0 00	0.0	0.0	2.5	3.0	1.3
2959	MIAMI HARBOR ENTRANCE	25 46	80 08	Daily predictions				2.5	3.0	1.3

Figure 2-7. Example of tidal differences, mean and spring tidal ranges, and mean tide level for secondary stations

* * * * * * * * * * * * * * EXAMPLE PROBLEM 2-1 * * * * * * * * * * * * * *

GIVEN: NOS Tide Tables

FIND: (a) Time difference between high water at Cape Canaveral and high water at Miami.

(b) Tide level at Cape Canaveral at 0900 EST, 31 January 1985.

SOLUTION:

(a) From Figure 2-7:
Time difference at high water = -41 minutes; i.e., high water occurs 41 minutes earlier at Cape Canaveral than at Miami.

(b) From Figure 2-7:
Time difference at low water = -41 minutes.
Height difference at low water = 0.0 ft.
Height difference at high water = +1.0 ft.

From Figure 2-6:
At 0957 EST on 31 January 1985,
Height at Miami = 0.4 ft (low water condition).

This means that the condition at 0916 EST at Cape Canaveral will correspond to the condition at 0957 at Miami. Assume that the tide level change at Cape Canaveral between 0900 and 0916 is negligible.

Finally, at 0900 EST on 31 January 1985,

Height at Cape Canaveral = 0.4 ft + 0.0 ft
= 0.4 ft above MLW.

* *

(2) Tidal current tables provide estimates of the times for slack water and maximum current and the velocity of maximum current for reference stations (Figure 2-8). The reference stations differ from those used for the tide tables. Estimates of currents can be made for numerous secondary stations by using corrections provided in the tidal current tables (Figure 2-9).

(3) Interactive personal computer programs for estimating tide elevation and current speed based on the published NOS tables are available under the Microcomputer Applications for Coastal Engineering (MACE) program (Appendix C).

F-Flood, Dir. 065° True E-Ebb, Dir. 245° True

JULY

Day	Slack Water Time h.m.	Maximum Current Time h.m.	Maximum Current Vel. knots	Day	Slack Water Time h.m.	Maximum Current Time h.m.	Maximum Current Vel. knots
1	0152	0526	5.5E	16	0235	0554	4.5E
Su	0919	1223	4.2F	M	0950	1250	3.4F
	1558	1808	2.4E		1615	1830	2.3E
	2107				2150		
2		0003	2.6F	17		0033	2.2F
M	0242	0615	5.3E	Tu	0318	0636	4.0E
	1005	1309	4.0F		1027	1327	3.1F
	1643	1858	2.6E		1651	1911	2.3E
	2207				2240		
3		0058	2.5F	18		0118	1.9F
Tu	0339	0704	4.8E	W	0405	0717	3.5E
	1052	1400	3.8F		1103	1404	2.8F
	1728	1950	2.7E		1727	1954	2.4E
	2316				2338		
4		0159	2.3F	19		0213	1.7F
W	0444	0800	4.1E	Th	0500	0804	2.9E
	1143	1449	3.5F		1140	1445	2.5F
	1813	2047	3.0E		1804	2044	2.6E
5	0031	0308	2.3F	20	0042	0313	1.6F
Th	0601	0859	3.4E	F	0607	0855	2.3E
	1236	1542	3.2F		1221	1528	2.2F
	1900	2147	3.3E		1844	2137	2.7E
6	0145	0426	2.3F	21	0149	0418	1.6F
F	0725	1002	2.7E	Sa	0725	0950	1.9E
	1334	1639	2.9F		1310	1617	2.0F
	1947	2247	3.7E		1926	2232	3.0E
7	0254	0546	2.6F	22	0252	0534	1.8F
Sa	0848	1112	2.2E	Su	0845	1052	1.5E
	1435	1738	2.8F		1409	1714	1.8F
	2036	2350	4.1E		2012	2326	3.3E
8	0356	0701	3.1F	23	0348	0646	2.2F
Su	1004	1222	1.9E	M	0957	1153	1.4E
	1537	1834	2.7F		1511	1810	1.9F
	2125				2101		
9		0047	4.5E	24		0021	3.8E
M	0452	0803	3.5F	Tu	0439	0745	2.7F
	1111	1335	1.8E		1059	1257	1.5E
	1635	1929	2.6F		1610	1859	2.0F
	2214				2149		
10		0139	4.8E	25		0113	4.3E
Tu	0543	0856	3.9F	W	0526	0832	3.2F
	1208	1433	1.9E		1152	1353	1.7E
	1728	2019	2.7F		1701	1952	2.3F
	2302				2237		
11		0230	5.0E	26		0205	4.8E
W	0630	0941	4.0F	Th	0610	0916	3.7F
	1257	1520	2.0E		1240	1442	1.9E
	1816	2105	2.7F		1748	2041	2.6F
	2348				2325		
12		0314	5.1E	27		0252	5.3E
Th	0714	1024	4.1F	F	0653	0959	4.1F
	1341	1559	2.0E		1323	1530	2.3E
	1900	2149	2.7F		1833	2126	2.9F
13	0032	0355	5.1E	28	0012	0338	5.6E
F	0756	1105	4.0F	Sa	0735	1041	4.3F
	1422	1638	2.1E		1404	1617	2.6E
	1942	2229	2.7F		1919	2214	3.1F
14	0114	0436	5.0E	29	0100	0424	5.8E
Sa	0836	1142	3.9F	Su	0817	1119	4.5F
	1501	1712	2.2E		1444	1700	2.9E
	2023	2309	2.5F		2007	2303	3.3F
15	0155	0513	4.8E	30	0150	0512	5.6E
Su	0914	1216	3.6F	M	0859	1200	4.4F
	1538	1749	2.2E		1524	1747	3.2E
	2105	2348	2.4F		2059	2352	3.3F
				31	0244	0559	5.3E
				Tu	0942	1242	4.2F
					1603	1836	3.5E
					2156		

AUGUST

Day	Slack Water Time h.m.	Maximum Current Time h.m.	Maximum Current Vel. knots	Day	Slack Water Time h.m.	Maximum Current Time h.m.	Maximum Current Vel. knots
1		0045	3.2F	16		0053	2.4F
W	0342	0648	4.6E	Th	0349	0646	3.3E
	1026	1327	3.9F		1015	1317	2.7F
	1643	1924	3.7E		1625	1914	3.1E
	2258				2251		
2		0146	3.0F	17		0139	2.2F
Th	0446	0741	3.8E	F	0440	0730	2.7E
	1112	1412	3.4F		1045	1354	2.4F
	1726	2017	3.8E		1657	2001	3.1E
					2347		
3	0006	0252	2.8F	18		0230	2.0F
F	0559	0836	2.9E	Sa	0541	0818	2.2E
	1203	1503	2.9F		1120	1435	2.0F
	1812	2113	3.9E		1733	2047	3.1E
4	0118	0410	2.6F	19	0050	0333	1.8F
Sa	0720	0939	2.2E	Su	0655	0912	1.7E
	1303	1603	2.5F		1205	1524	1.7F
	1903	2213	3.9E		1818	2143	3.2E
5	0230	0534	2.7F	20	0159	0447	1.9F
Su	0842	1051	1.6E	M	0814	1015	1.3E
	1411	1707	2.2F		1309	1626	1.6F
	1959	2322	4.0E		1912	2243	3.4E
6	0337	0651	3.0F	21	0305	0604	2.2F
M	0958	1215	1.4E	Tu	0929	1122	1.2E
	1521	1815	2.1F		1430	1729	1.6F
	2058				2014	2344	3.7E
7		0027	4.2E	22	0403	0710	2.6F
Tu	0437	0752	3.3F	W	1032	1228	1.4E
	1103	1341	1.5E		1541	1831	1.9F
	1625	1917	2.2F		2116		
	2156						
8		0128	4.4E	23		0044	4.2E
W	0530	0846	3.6F	Th	0456	0807	3.2F
	1156	1440	1.7E		1124	1327	1.7E
	1719	2011	2.4F		1640	1929	2.3F
	2249				2214		
9		0221	4.6E	24		0140	4.7E
Th	0617	0933	3.8F	F	0543	0850	3.7F
	1239	1521	1.9E		1210	1421	2.2E
	1807	2058	2.6F		1730	2022	2.8F
	2338				2309		
10		0305	4.7E	25		0230	5.2E
F	0659	1010	3.9F	Sa	0628	0931	4.1F
	1318	1550	2.1E		1250	1509	2.7E
	1849	2140	2.7F		1818	2112	3.2F
11	0022	0342	4.7E	26	0002	0319	5.5E
Sa	0737	1045	3.8F	Su	0710	1011	4.4F
	1353	1619	2.3E		1328	1554	3.3E
	1928	2218	2.8F		1906	2201	3.6F
12	0104	0418	4.6E	27	0055	0406	5.5E
Su	0813	1115	3.7F	M	0752	1050	4.5F
	1426	1648	2.5E		1405	1636	3.7E
	2006	2252	2.8F		1955	2250	3.9F
13	0144	0453	4.5E	28	0149	0455	5.3E
M	0846	1144	3.5F	Tu	0833	1131	4.4F
	1457	1720	2.7E		1441	1723	4.1E
	2043	2331	2.7F		2046	2341	3.9F
14	0223	0528	4.2E	29	0244	0542	4.8E
Tu	0917	1213	3.3F	W	0915	1211	4.1F
	1527	1757	2.9E		1519	1807	4.4E
	2122				2140		
15		0010	2.6F	30		0036	3.8F
W	0305	0605	3.8E	Th	0343	0629	4.1E
	0946	1242	3.0F		0958	1252	3.6F
	1556	1833	3.0E		1557	1855	4.5E
	2204				2238		
				31		0133	3.5F
				F	0447	0721	3.2E
					1044	1340	3.1F
					1640	1946	4.4E
					2342		

Time meridian 120° W. 0000 is midnight. 1200 is noon.

Figure 2-8. Example of tidal current table for the reference station at San Francisco Bay Entrance, California

CURRENT DIFFERENCES AND OTHER CONSTANTS, 1984

NO.	PLACE	METER DEPTH	POSITION Lat.	POSITION Long.	TIME DIFFERENCES Min. before Flood	Flood	Min. before Ebb	Ebb	SPEED RATIOS Flood	Ebb	AVERAGE SPEEDS AND DIRECTIONS Minimum before Flood	Maximum Flood	Minimum before Ebb	Maximum Ebb
		ft	° ' N	° ' W	h. m.	h. m.	h. m.	h. m.			knots deg.	knots deg.	knots deg.	knots deg.
	BAY of PANAMA Time meridian, 75°W				on SAN FRANCISCO BAY ENT., p.10									
1	Bayoneta I., 1.5 miles W of, Perlas Is..		8 30	79 05	+1 17	+2 02	+2 21	+1 22	0.6	0.4	0.0 - -	1.6 005	0.0 - -	1.5 200
5	Chame Bay Entrance, near Chame Point....		8 39	79 43	+2 10	+2 31	+2 10	+2 45	0.6	0.4	0.0 - -	1.8 210	0.0 - -	1.4 065
	COSTA RICA Time meridian, 90°W													
10	Puntarenas, Gulf of Nicoya.............		9 58	84 49	+0 01	- - -	+0 44	- - -	- -	- -	0.0 - -	- - 300	0.0 - -	- - - -
	LOWER CALIFORINA Time meridian, 105°W													
15	Magdalena Bay entrance.................		24 32	112 02	-4 43	-3 52	-3 46	-3 45	0.4	0.3	0.0 - -	1.3 035	0.0 - -	1.0 - -
	SAN CLEMENTE ISLAND Time meridian, 120°W				on SAN DEIGO BAY ENT., p.4									
20	China Point Light, 20 miles SSW of......		32 29	118 32	- - -	- - -	- - -	- - -	0.3	0.1	0.0 - -	0.4 315	0.0 - -	0.2 115
	SAN DIEGO BAY													
25	SAN DIEGO BAY ENTRANCE.................		32 41	117 14	Daily Predictions						0.0 - -	1.2 355	0.0 - -	1.5 173
30	Ballast Point, 100 yards north of.......		32 41	117 14	-0 27	-0 24	-0 23	-0 02	1.0	0.9	0.0 - -	1.2 325	0.0 - -	1.4 133
35	Quarantine Station, La Playa...........		32 42	117 14	-0 03	+0 15	+0 10	+0 20	0.8	0.8	0.0 - -	1.0 021	0.0 - -	1.2 200
40	San Diego, 0.5 mile west of............		32 43	117 11	-0 16	-0 08	-0 12	-0 12	0.6	0.5	0.0 - -	0.7 121	0.0 - -	0.7 304
45	Pier No. 1, San Diego <1>..............		32 43	117 11	- - -	- - -	- - -	- - -	- -	- -	- - - -	0.2 - -	- - - -	0.2 - -
50	Coronado, off northeast end............		32 42	117 10	-0 21	+0 03	-0 16	+0 04	0.7	0.5	0.0 - -	0.8 130	0.0 - -	0.8 343
55	National City..........................		32 39	117 07	+0 23	0 00	-0 02	+0 50	0.4	0.4	0.0 - -	0.5 166	0.0 - -	0.6 002
	California Coast				on SAN FRANCISCO BAY ENT., p.10									
60	San Pedro Channel <2>..................		33 36	118 16	- - -	- - -	- - -	- - -	- -	- -	- - - -	- - - -	- - - -	- - - -
65	Los Angeles and Long Beach Harbors <3>..		- - -	- - -	- - -	- - -	- - -	- - -	- -	- -	- - - -	- - - -	- - - -	- - - -
70	El Segundo, Santa Monica Bay <4>........		33 54	118 26	- - -	- - -	- - -	- - -	- -	- -	0.0 - -	0.6 330	0.0 - -	- - - -
75	Point Arguello.........................		34 34	120 40	-2 20	-2 20	-2 20	-2 20	0.2	0.2	0.0 - -	0.5 005	0.0 - -	0.5 185
80	Point San Luis.........................		35 09	120 46	-2 00	-2 00	-2 00	-2 00	0.2	0.2	0.0 - -	0.5 305	0.0 - -	0.5 125
85	Point Piedras Blancas..................		35 40	121 18	-1 30	-1 30	-1 30	-1 30	0.2	0.2	0.0 - -	0.5 315	0.0 - -	0.5 135
90	Point Sur..............................		36 18	121 55	-1 10	-1 10	-1 10	-1 10	0.2	0.2	0.0 - -	0.5 325	0.0 - -	0.5 145
	Monterey Bay													
95	Point Pinos............................		36 38	121 57	Current weak and variable									
100	Point Santa Cruz, 2 miles south of......		36 55	122 01	Current weak and variable									
	California Coast-continued													
105	Ano Nuevo Island, 2 miles SW of.........		37 05	122 22	Current weak and variable									
110	Point Montara, 2 miles west of..........		37 32	122 34	Current weak and variable .									

Endnotes can be found at the end of Table 2.

Figure 2-9. Example of tidal current differences for secondary stations

2-3. Tidal Datums.

a. Definitions of Tidal Datums.

(1) MSL was widely adopted as a primary datum many years ago on the assumption that it could be determined accurately and simply from the records of any reasonably well-exposed tide gage. MSL determinations are based on the average of the hourly determinations of tide level.

(2) The length of record considered is 19 years, partly to account for the cycles of 18 to 19 years in tidal amplitude and phase, but mostly to average out the more important meteorological effects. The existence of trends in the elevation of the sea relative to the land for periods longer than 19 years is not explicitly recognized in selecting a period of 19 years. The existence of long-period trends, however, is a major factor in requiring revisions of the official datums at intervals of about 25 years. These relative long-period trends are neither uniform in rate from station to station nor linear in form. Therefore, to fix the datum in time at any station and to assist in meaningful comparisons among stations, a particular and common 19-year series is used. This specific 19 years is called the National Tidal Datum Epoch. The present Epoch is 1960 to 1978. The MSL must often be estimated when less than 19 years of data are available. An integral number of years should be used, if possible. If less than 1 year of data must be used, the preferred period is 29 days or a multiple of 29 days. Methods for minimizing the errors in short-period determinations of sea level are provided in items 90 and 122. Briefly, their technique compares the available record for MSL or mean tide level with the same period of record at nearby stations with similar tide forms with a record duration of 19 years or longer to identify any long period anomaly and to assume that any anomaly in the short record is the same as that at a station with long records.

(3) If it is impractical to consider hourly values, a good approximation is provided by the half-tide level, sometimes called mean tide level (MTL). The half-tide level is a tidal datum midway between MHW and MLW. The MTL may be above or below MSL by an amount which depends on the relative importance of the diurnal components of the tide.

(4) Several other datums are defined with respect to the tides such as mean high water springs (MHWS), National Geodetic Vertical Datum of 1929 (NGVD), and mean low water springs (MLWS) (Figure 2-10). Formal definitions of standard tidal datums (not specialized US Army Corps of Engineers (USACE) harbor datums necessarily) for the US are officially promulgated in item 50. Each datum is more suitable than MSL for a restricted class of problems, and all depend on the tidal range and the characteristic shape of the tidal curve. Corrections may be necessary to the observed data when the datums are determined from less than 19 years of record.

(5) The most important of these datums for most navigation-related activities are MLW for the Atlantic coast and MLLW for the Pacific coast (defined as the average height of the tide at low water or lower low water when all tides for a 19-year period are considered). MLLW is being adopted as the standard datum for all locations as NOS charts are revised.

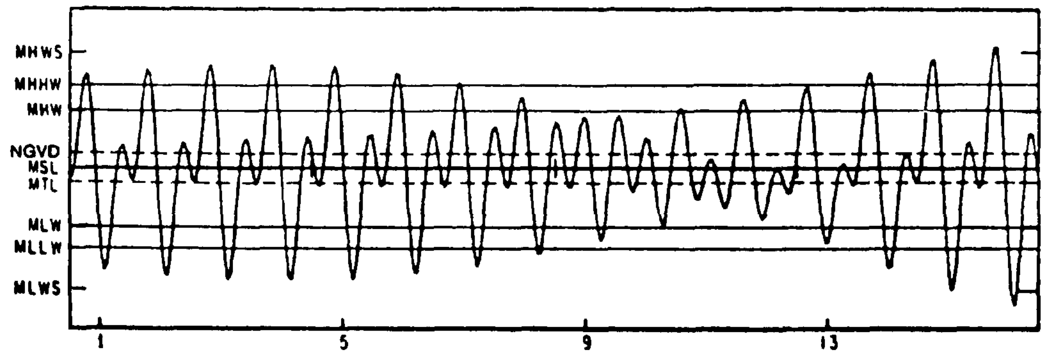

Figure 2-10. Illustration of tidal datums (Los Angeles, California (Outer Harbor), January 1973 (mean range = 3.78 feet or 1.15 meters)

(6) When planning the development of land above MSL, the datums MHW and mean higher high water (MHHW) may be more useful than the low water datums. They are defined in a manner analogous to that used for MLW and MLLW and require similar corrections when based on short series of observations. The MHW or MHHW datum is often used to define the limit of private property and beach recreational area for Corps of Engineers (Corps) projects.

(7) The difference between MHW and MLW is called the mean range of the tide. The difference between MHHW and MLLW is called the diurnal range of the tide. The diurnal range is identical with the mean range for diurnal tides. The range of the tide may change drastically within short distances, as shown in Figure 2-11 (item 122). This is not an extreme example. Because the tide range, and, consequently, the high and low water datums may vary greatly with short distances, measurements referred to these datums are not suitable for comparing elevations at different locations unless both comparisons are based on the same benchmark.

b. NGVD. NGVD should be used as the primary datum for engineering design. Local tide gage records and benchmarks should be related to NGVD. NGVD has the important advantage of being a national fixed datum; whereas MSL, MTL, and other tidal datums apply only locally and change slowly with time. NGVD was originally established out of a need for comparing land elevations for locations near the coast where no tide observations are available and at interior locations where tide observations are impossible. By the mid-1920's, several first-order leveling lines connecting the Atlantic and Pacific coasts, and many tide gages on both coasts, had been surveyed. These surveys consistently show sea level to be higher on the Pacific coast than on the Atlantic coast and higher in the north than in the south on both coasts. It seemed desirable to have the zero of the geodetic leveling net coincide with local MSL wherever both quantities were known. Thus, a general adjustment was made in 1929 in which it was assumed that the geodetic and local sea levels were equal to zero at 26 selected tide gages in the United States and Canada. The differences previously computed were treated as errors and were distributed over the network of observation points. The locations of the tide gages used are shown in Figure 2-12. The period of the observations from US tide stations used in defining the reference datum and the height of MSL at all

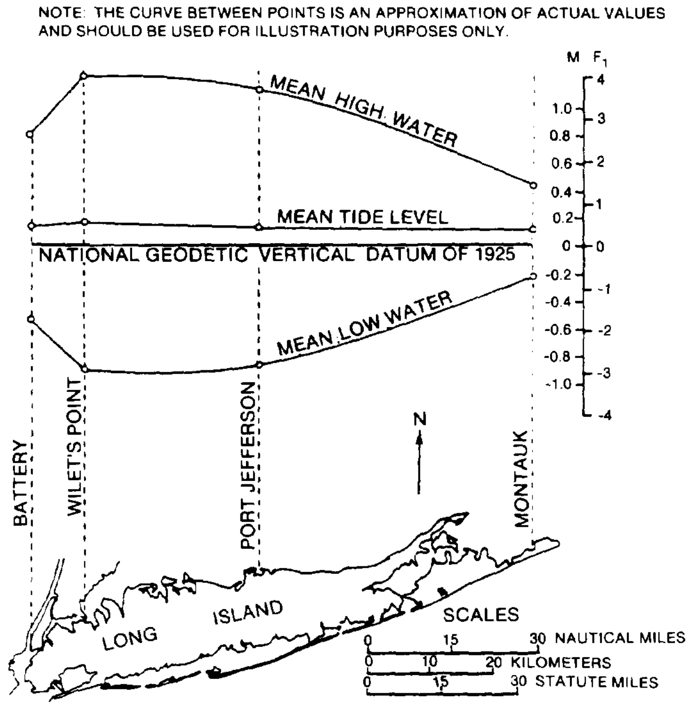

Figure 2-11. Relationship between NGVD and several tidal datums between Montauk and The Battery

stations relative to Galveston, Texas, is given in Table 2-3 (items 46 and 109). The reference datum defined in this manner is called the NGVD of 1929.

(1) Before 1963, NGVD was termed the Sea Level Datum of 1929. Sometimes it was also called Mean Sea Level of 1929. The use of different terms for the same datum can lead to considerable confusion. The terms Sea Level Datum of 1929 and Mean Sea Level of 1929 are used on many older Corps documents and US Geological Survey (USGS) charts. Mean Sea Level of 1929 is an entirely different datum from the statistically derived datum, mean sea level, which represents the average of hourly observations (Section 2-3.a.1). Because of the potential for confusion, datum information used in project studies must be carefully interpreted.

(2) It has been well established since 1929 that the elevation of the mean water level with respect to the land varies with time as a consequence of land subsidence and emergence and a slow redistribution of the waters of the earth. In 1963 a new determination of a geodetic datum of national scope based only on stations for which a series of 19 years of tide data was available was published (item 7). The variations in sea level revealed by this survey are shown in Figure 2-13 (item 7). Some leveling lines in regions of known subsidence and suspected subsidence have been resurveyed many times since 1929. New surveys of this type are based on elevations assigned to the more stable parts of the continent by the 1929 adjustment, and they lead to new determination of the elevations of benchmarks in the subsiding or emerging

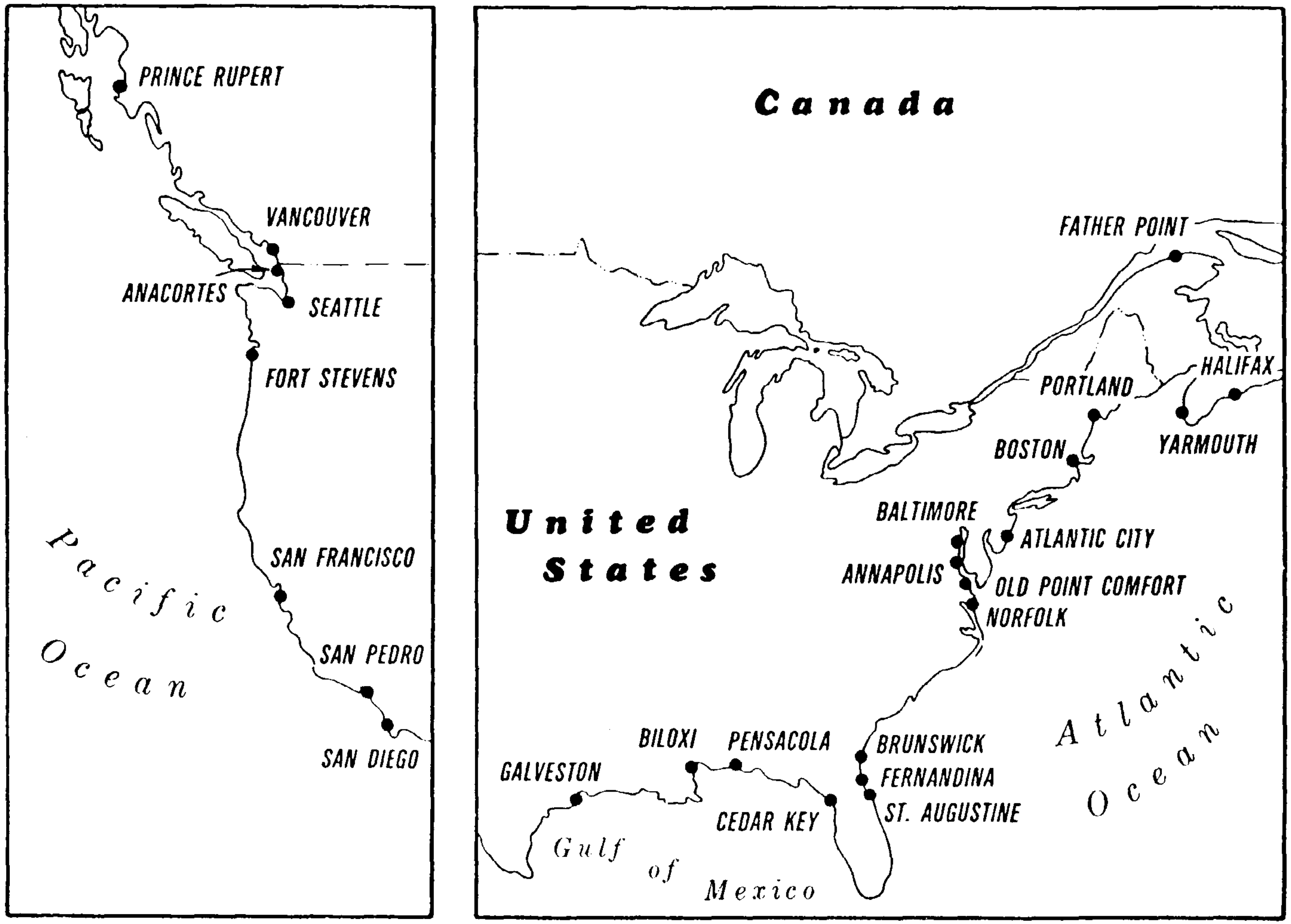

Figure 2-12. Location of tide stations used in establishing the NGVD of 1929

Table 2-3

Tide Data Used in Establishing NGVD of 1929

Station	Period of record used	Elevation of local MSL[1]	
		m	ft
Galveston, Tex.	1 Dec. 1903 to 29 Nov. 1906	0.00	0.00
Biloxi, Miss.	1882; 1884; 1896-98	-0.09	-0.30
Pensacola, Fla.	1924-26 (compared with Key West)	-0.05	-0.16
Cedar Key, Fla.	1892-93	-0.08	-0.26
St. Augustine, Fla.	1892-93	-0.27	-0.89
Fernandina, Fla.	1898-1923 (25 mo)	-0.20	-0.66
Brunswick, Ga.	1904-05, 1908-09	-0.16	-0.52
Norfolk, Va.	1908-1915	-0.14	-0.46
Old Point Comfort, Va.	1853-1878	-0.28	-0.92
Annapolis, Md.	Two 1-month series 1875, 1888	-0.17	-0.56
Baltimore, Md.	1903-1921	+0.18	-0.59
Atlantic City, N.J.	1912-26	+0.03	+0.10
Perth Amboy[2]		+0.01	+0.03
Boston, Mass.	Aug. 1921 to July 1923	+0.07	+0.23
Portland, Maine	1915-25	+0.12	+0.39
Yarmouth, Nova Scotia	----------[3]	+0.05	+0.16
Halifax, Nova Scotia	----------	+0.08	+0.26
Father Point, Quebec[4]	----------	+0.20	+0.66
San Diego, Calif.	1906-08	+0.33	+1.08
San Pedro, Calif.	1924-25; 1927-28	+0.31	+1.02
San Francisco, Calif.	1898-1913	+0.34	+1.12
Fort Stevens, Oreg.	1925-26	+0.59	+1.94
Seattle, Wash.	1899-1917	+0.48	+1.57
Anacortes, Wash.	1 June 1921 to 31 May 1924	+0.45	+1.48
Vancouver, British Columbia	----------	+0.50	+1.64
Prince Rupert, British Columbia	----------	+0.58	+1.90

[1] Relative to Galveston, Texas.

[2] No tide gage located on Perth Amboy; a bench-mark elevation was held as determined by leveling from the tide gage at Sandy Hook, New Jersey.

[3] Dates for the Canadian tide gage are unavailable.

[4] Pointe Au Pere.

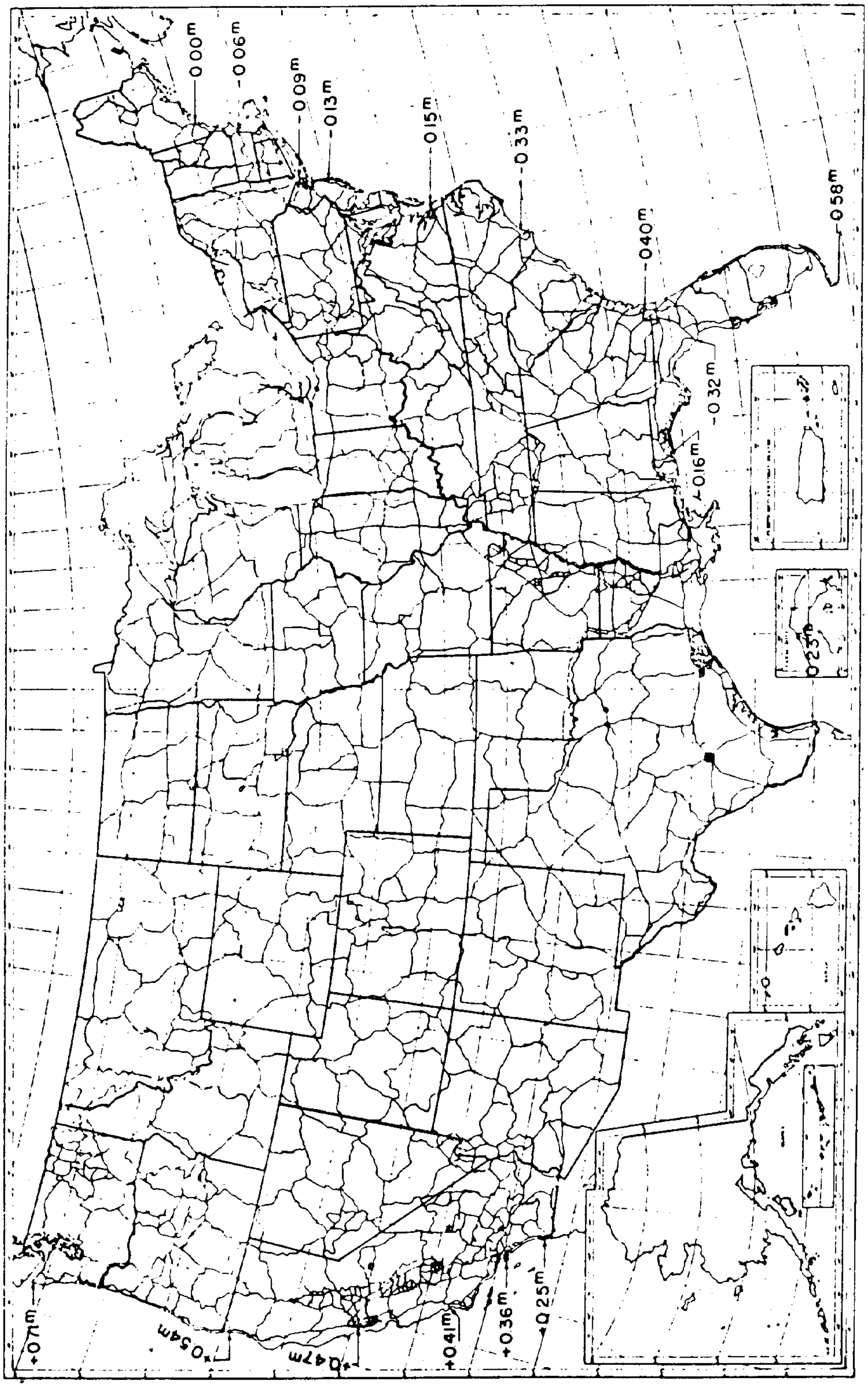

Figure 2-13. First-order level net (1963) showing MSL variations (plus variation shows that local MSL plane from tide observations higher than geoid surface determined by leveling, assuming equality at Portland, Maine)

areas. Thus, the elevation assigned to a specified benchmark may vary over a period of many years because of changes in the elevation of the solid surface of the earth or changes in the mean elevation of the nearby surface of the sea.

c. North American Vertical Datum. A major effort is under way by NOS to relevel first order leveling lines and to establish a single, more accurate datum for North America. The datum will be called the North American Vertical Datum (NAVD) of 1988. Results from this effort are scheduled to be available by 1989.

d. Tidal Datum Benchmarks. Index maps of tidal datum benchmarks and lists of the established references between the NGVD of 1929 and other datums are available for each state from the Tidal Datum Quality Assurance Section, N/OMA1230, 6th Floor, WSC-1, National Ocean Service, NOAA, 6001 Executive Blvd., Rockville, MD 20852. Several maps are required for states with long coastlines. A sample index map and related index map numbers are shown in Figure 2-14 (a and b). Individual benchmark sheets, describing two or more benchmarks established near each tide observation point and the relation between the various tidal datums, are reported for each tide observation station. A sample of an NOS tidal benchmark sheet is shown in Figure 2-15. The MSL datum is not included in the sample. It can easily be added and should be requested whenever tidal benchmark sheets are obtained. The tidal benchmark sheets are updated periodically as new data become available.

(1) A general trend toward rising sea levels, relative to the land, is evident along all of the US coastline except for southeast Alaska. As a result of this trend, the MSL datum changes with each new epoch used for defining tidal datums. The NGVD, however, is a fixed surface whose elevation does not vary with time, although elevations of fixed points (as referred to NGVD) may change.

(2) The NGVD of 1929 is defined or definable everywhere by first-order leveling. The other tidal datums are defined with respect to a specific tide gage location. Thus, when a low water datum, half-tide level datum, or any tidal datum other than the NGVD of 1929 is used, the location at which the datum applies should be specified. In areas where subsidence or emergence is known to be in progress, the date of the survey used should also be given. Reference datums have also been established by many states and local jurisdictions.

(3) The relation between the various datums discussed in this section at the reference tide stations (where NOS publishes daily tide predictions) are presented in Table 2-4. The station locations are shown in Figure 2-16. The same information for these and other stations can be obtained from the NOS tidal benchmark sheets.

(4) In 1977, a new regional datum called the Gulf Coast Low Water Datum (GCLWD) was adopted by the National Oceanic and Atmospheric Administration (items 99 and 100). This datum is defined as the MLLW where the tide is mixed and MLW in regions with diurnal tides. This datum, which became the chart datum for the Gulf of Mexico, is desirable because of the frequent shifts in the type of tide along the Gulf coast (Figure 2-17) ending numerous

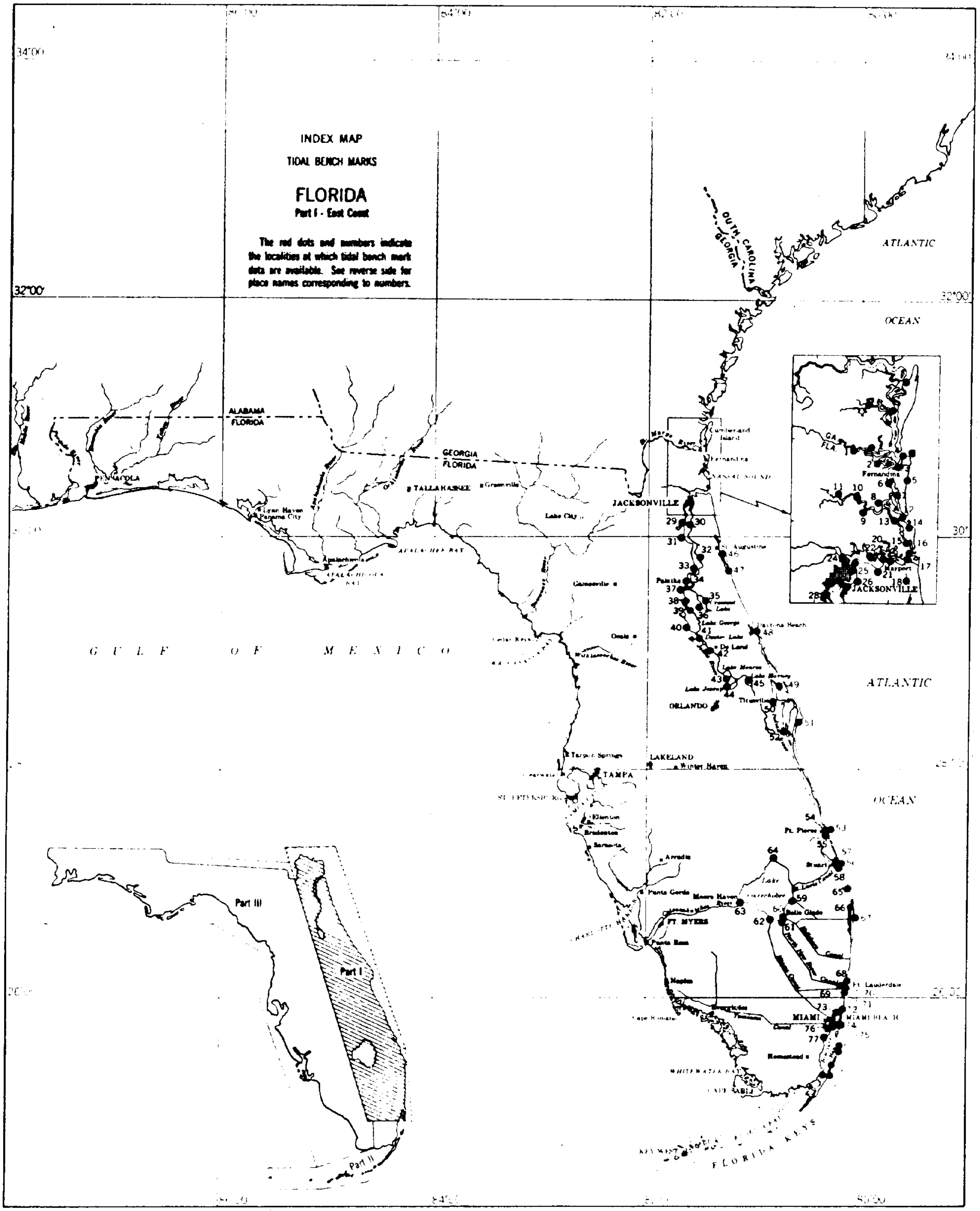

a. Tidal benchmark locations

Figure 2-14. Sample NOS index map and map numbers (Continued)

INDEX MAP NUMBER (See reverse side)	NAME
1.	Crandall, St. Marys River
2.	Chester, Bell River
3.	Fernandina Beach, Amelia River
4.	Fort Clinch, Amelia Island
5.	Fernandina Beach, Atlantic Ocean
6.	Kingsley Creek (S.A.L. R.R. BR.)
7.	Amelia, South Amelia River
8.	Nassauville, Nassau River
9.	Mink Creek Entr., Nassau River
10.	Half Moon Island, Nassau River
11.	Boggy Creek, Upper Nassau River
12.	Sawpit Creek Entr., Nassau Sd.
13.	Sawpit Creek
14.	Simpson Creek Entr., Nassau Sd.
15.	Fort George ~~[illegible]~~ Ft. George River
~~16.~~	~~Pilot Town, St. Johns River~~ Island
17.	Mayport, St. Johns River
18.	Pablo Creek
~~19.~~	~~St. Johns Bluff, St. Johns River~~
20.	Fulton, St. Johns River
21.	Mill Cove, St. Johns River
22.	Dame Point, St. Johns River
23.	Chaseville, St. Johns River
24.	Trout River, St. Johns River
25.	Jacksonville (Corp of Engineers Dredge Depot)
26.	Little Pottsburg Creek, Arlington R., St. Johns R.
27.	Jacksonville ~~(McGiffin Terminal Co.~~), St. Johns R.
28.	Ortega River Entrance Acosta Bridge
29.	Orange Park, St. Johns River
30.	Mandarin, St. Johns River
31.	Green Cove Springs, St. Johns River
32.	East Tocoi, St. Johns River
33.	Palmetto Bluff, St. Johns River
34.	Palatka, St. Johns River
35.	Shell Bluff, Crescent Lake
36.	Crescent City, Crescent Lake
37.	Buffalo Bluff, St. Johns River
38.	Welaka, St. Johns River
39.	Georgetown, St. Johns River

25A Piney Point

INDEX MAP NUMBER (See reverse side)	NAME
40.	Juniper Club, Lake George, St. Johns River
41.	Astor and Volusia, St. Johns River
42.	De Land Landing, St. Johns River
43.	Sanford, Lake Monroe, St. Johns R.
44.	Lake Jessup, St. Johns R.
45.	Lake Harney Outlet, St. Johns River
46.	St. Augustine
47.	Summer Haven, Mantanzas Inlet
48.	Daytona Beach
49.	Allenhurst, Indian River
50.	Titusville, Indian River
51.	~~Cape~~ Canaveral Harbor Entrance
52.	Cocoa, Indian River
53.	Ft. Pierce Breakwater
54.	Binney Dock, Ft. Pierce Inlet
55.	Ft. Pierce (Municipal Docks)
56.	North Jetty, St. Lucie Inlet
57.	Sewall Point, St. Lucie River
58.	Great Pocket, St. Lucie Inlet
59.	Canal Pt., West Palm Beach Canal
60.	Belle Glade, Hillsboro Canal Entr. Locks, L. Okeechobee
61.	South Bay, North New River Canal Entr. Locks
62.	Lake Harbor, Miami Canal Entr. Locks, L. Okeechobee
63.	Moore Haven, Old Locks in Caloosahatchee Canal
64.	Taylors Creek, L. Okeechobee
65.	Jupiter Inlet
66.	Port of Palm Beach
67.	Palm Beach (Rainbo Pier)
~~68.~~	~~New River Sound~~
69.	Fort Lauderdale, New River
70.	Port Everglades, Lake Mabel
71.	Intracoastal Canal, L. Mabel
72.	Indian Creek Golf Club, Biscayne Bay
73.	Miami (79th Street Causeway)
74.	Miami Beach (City Pier)
~~75.~~	~~Miami Beach (East End of McArthur Causeway~~)
76.	Miami, Biscayne Bay
~~77.~~	~~Cutler, Biscayne Bay~~

51A Patrick Air Force Base
51B Sebastian Inlet

NOTE: Unnumbered red dots on the index map on the reverse side indicate nearest tidal bench mark locations in the State of Florida, Part II (Florida Keys) and in the State of Georgia.

Tidal bench mark locations in the State of Florida are shown on three index maps as follows:

Part I. East Coast
Part II. Florida Keys
Part III. West Coast

Tidal bench mark data are available for the above locations and may be obtained by writing to the Director, Coast and Geodetic Survey, Washington 25, D. C. In requesting these data, please refer to both the index map numbers and the names of the particular localities in which you are interested

b. Index map numbers

Figure 2-14. (Concluded)

FLORIDA - I - 74

U.S. DEPARTMENT OF COMMERCE
NATIONAL OCEANIC AND ATMOSPHERIC ADMINISTRATION
NATIONAL OCEAN SURVEY

TIDAL BENCH MARKS

Miami Beach (City Pier)
Lat. 25° 46'.1; Long. 80° 07'.9

BENCH MARK 4 (1928) is a standard disk, stamped "NO 4 1928", set vertically in the south face of the south post in the north-south fence line around a large city water tank. It is about 66 feet north of the extended centerline of Commerce Street, 36 feet west of the centerline of Jefferson Avenue, and 1/2 foot above ground level. Elevation: 5.62 feet above mean low water.

BENCH MARK 6 (1931) is a standard Corps of Engineers disk, stamped "BM NO 6," set in top of a 2-inch pipe surrounded at top with a 12-inch by 18-inch manhole frame with a removable cast iron cover, directly in centerline of a blacktop driveway which parallels Government Cut. It is at the U.S. Government Reservation on the north side of Government Cut, about 186 feet east of U.S. Engineers flagpole and 13 1/2 feet west of the center of a road junction. Elevation: 7.13 feet above mean low water.

BENCH MARK 7 (1937) is a standard disk, stamped "7 1937," set in the top of the northwest side of the concrete base to the east post of entrance gate to drive to the Corps of Engineers Office Building. It is about 100 yards south of intersection of Washington Avenue and Biscayne Street, 8 feet east of the extended centerline of the Avenue and 1/2 foot above ground level. Elevation: 5.03 feet above mean low water.

BENCH MARK 9 (1955) is a standard disk, stamped "9 1955," set in top of concrete deck along northedge of City Pier near the east end of Biscayne Street. It is about 122 yards east of the west end of pier, 39 feet northwest of the northeast corner of the ladies rest room and 1/2 foot south of south face of north guardrail. Elevation: 11.29 feet above mean low water.

BENCH MARK 10 (1956) is a standard disk, stamped "NO 10 1956," set on top of the northwest corner of the concrete base of light pole No. 166D6 about 68 yards west of the junction of Biscayne Street and Alton Road. It is near the northwest corner of the South Shore Recreation Park about 62 feet east of the west edge of the bulkhead on the water front and 9 1/2 feet northeast of the east edge of the north entrance to the Recreation Building. Elevation: 5.23 feet above mean low water.

BENCH MARK 11 (1956) is a standard disk, stamped "NO 11 1956," set in top of north corner of a concrete base which supports a 6 inch metal post near the City of Miami Beach Warehouse. It is near the intersection of Alton Road and First Street about 21 1/2 feet southwest of the southwest curb of Alton Road and 9 feet northwest of the northwest corner of the warehouse building. Elevation: 4.92 feet above mean low water.

Mean low water at Miami Beach is based on 19 years of records, 1941-1959. Elevations of other tide planes referred to this datum are as follows:

	Feet
Highest tide (observed) September 8, 1965	6.4
Mean high water	2.50
Mean tide level	1.25
NGVD, 1929	0.96
Mean low water	0.00
Lowest tide observed (March 24, 1936)	-1.6

Figure 2-15. Sample NOS sheet describing tidal benchmarks

Table 2-4

Datums for Reference Tide Stations[1]

Station	Normalizing factor[2]	MSL	MTL	NGVD	MLLW	MLW	MLLW	MHHW	Extremes of Record		Interval for Establishment of datum
									Highest	Lowest	
Atlantic and Gulf Coasts											
Eastport, Maine	M	9.2	9.10	9.00	-----[3]	0.00	18.20	-----[3]	23.0	-4.4	1941-61
Portland, Maine	M	4.5	4.50	4.28		0.00	9.00		13.9	-3.7	1941-59
Boston, Mass.	M	5.2	5.05	4.89		0.30[4]	9.80		14.2	-3.5	1941-59
Newport, R.I.	M	1.6	1.75	1.37		0.00	3.50		13.5	-2.9	1941.59
New London, Conn.	M	1.4	1.30	0.97		0.00	2.60		10.7[5]	-3.4	1941-59
Bridgeport, Conn.	M	3.4	3.35	2.86		0.00	6.70		12.4	-3.5[5]	1967 (1 yr)
Willets Point, N.Y.	M	3.6	3.55	3.02		0.00	7.10		16.7	-4.1	1941-59
New York, N.Y. (The Battery)	M	2.3	2.25	1.81		0.00	4.50		10.2	-4.2	1941-59
Albany, N.Y.	M	2.5	2.5	----[6]		0.00	4.60		----[6]	----[6]	1941-59
Sandy Hook, N.J.	M	2.3	2.30	1.79		0.00	4.60		10.3	-4.4	1941-59
Breakwater Harbor, Del.	M	2.1	2.05	1.69		0.00	4.10		9.5	-3.9	1953-61
Reedy Point, Del.	M	2.8	2.75	2.45		0.00	5.50		10.0[5]	-6.3	1957-61
Philadelphia, Pa.	M	3.2	3.10	2.14		0.00	6.19[7]		10.7	-6.6	1941-59
Baltimore, Md.	M	1.0	0.97	0.57		0.42[8]	1.52		8.3	-4.5	1941-59
Washington, D.C.	M	1.97	1.97	1.43		0.52[9]	3.42		11.9	-4.2	1941-59
Hampton Roads, Va. (Sewalla Point)	M	1.3	1.25	1.28		0.00	2.50		8.5	-3.1	1941-59
Wilmington, N.C.	M	1.9	2.10	1.52		0.00	4.20		8.2	-1.7	Jan. 1969 to Nov. 1973
Charleston, S.C.	M	2.7	2.91	2.65		0.31[10]	5.51		10.7	-3.3	1941-59
Savannah River Entrance, Ga. (Ft. Palaski)	M	3.6	3.45	3.32		0.00	6.90		11.1	-4.4	1941-59
Savannah, Ga.	M	4.0	3.7	----[6]		0.00	7.40		----[6]	----[6]	1941-59
Mayport, Fla.	M	2.3	2.25	2.00		0.00	4.50		7.4	-3.2	1941-59
Miami Harbor Entrance, Fla.	M	1.3	1.25	0.96		0.00	2.50		6.4	-1.6	1941-59
Key West, Fla.	M	0.6	0.65	0.42		0.00	1.30		3.8	-1.6	1941-59
St. Petersburg, Fla.	D	1.2	1.15	0.83		0.00	2.30		5.3	-2.5[5]	1948-59
St. Marks River Entrance, Fla.	D	1.8	1.8	----[6]		0.00	2.40		8.0	-3.5[5]	1941-59
Pensacola, Fla.	D	0.6	0.65	0.33		0.00	1.30		8.9	-2.2	1941-59
Mobile, Ala.	D	0.8	0.75	----[6]		0.00	1.50		9.0[5]	-30.0[5]	1941-59
Galveston, Tex. (Ship channel)	D	0.8	0.70	0.70		0.00	1.40		11.4	-5.3	1941-59
San Juan, P.R.	M	0.6	0.55	----[6]		0.00	1.10		2.4	-1.1	Apr. 1962 to Dec. 1963
Pacific Coast											
San Diego, Calif.	D	3.0	2.95	2.79	0.00	0.90	5.00	5.70	8.3	-2.8	1941-59
Los Angeles, Calif. (Outer Harbor)	D	2.8	2.80	2.72	0.00	0.90	4.70	5.40	7.8	-2.6	1941-59
San Francisco, Calif. (Golden Gate)	D	3.0	3.30	3.06	0.20[11]	1.30	5.30	5.90	8.6	-2.5	1941-59
Humboldt Bav. Calif	D	3.4	3.75	----	0.00	1.20	5.70	6.40	9.5[5]	-3.0[5]	1962
Astoria, Oreg. (Tongue Point)[9]	D	4.3	4.35	3.05	0.00	1.10	7.60	8.30	12.1	-2.8	1941-59
Aberdeen, Wash.	D	5.5	5.45	----	0.00	1.50	9.40	10.10	14.9	-2.9	1955, 1956
Port Townsend, Wash.	D	4.8	5.10	----	0.00	2.50	7.70	8.40	12.0[5]	-4.5[5]	1972-74
Seattle, Wash.	D	6.6	6.60	6.25	0.00	2.80	10.40	11.30	14.8	-4.7	1941-59
Ketchukan, Alaska	D	8.0	7.95	----	0.00	1.50	14.40	15.30	21.2	-5.2	1941-59
Juneau, Alaska	D	8.6	8.50	----	0.00	1.60	15.40	16.40	23.20	-5.20	1966-72
Sitka, Alaska	D	5.2	5.30	----	0.00	1.40	9.10	9.90	14.6	-3.8	1941-59
Cordova, Alaska	D	6.6	6.45	----	0.00	1.40	11.50	12.40	16.8	-4.9	1965-74
Seldovia, Alaska	D	9.4	9.35	----	0.00	1.60	17.00	17.80	24.3	-6.2	1971-74
Anchorage, Alaska	D	16.8	15.25	----	0.00	2.20	28.30	29.00	35.5[5]	-6.5[5]	1964-68
Kodiak, Alaska	D	4.3	4.30	----	0.00	1.00	7.60	8.50	13.0[5]	-4.0[5]	1935-36
Dutch Harbor, Alaska	D	2.2	1.30	----	0.00	1.20	3.40	3.70	6.6	-2.7	1935-38
Sweeper Cove, Alaska (Adak Island)	D	2.1	1.85	----	0.00	----	----	3.70	7.0[5]	-3.3	1958-60, 1944, 1949
Masacre Bay, Alaska (Attu Island)	D	1.9	1.65	----	0.00	----	----	3.30	7.0[5]	-3.0[5]	1950, 1952, 1960
Nashagak Bay, Alaska (Clarks Pt)	D	10.3	10.15	----	0.00	2.50	17.80	19.50	24.5	-5.0	1958
St. Michael, Alaska	D	2.0	-----	----	----	----	-----	-----	----	----	------------------
Honolulu, Hawaii	D	0.8	0.80	----	0.00	0.20	1.40	1.90	3.5	-1.3	1941-59

[1] Except as footnoted, chart datum is MLW for the Atlantic and gulf coasts and MLLW for the Pacific coast; numbers are in feet.
[2] D = diurnal; M = mean.
[3] MLLW and MHHW were not routinely derived for Atlantic and gulf coast stations for the 1941-59 epoch used for establishing most of the datums.
[4] Boston Low Water Datum (adopted about 1927).
[5] Estimated value.
[6] Data unavailable at the time of compilation.
[7] Datums and the mean range for Philadelphia were revised in July 1979 based on observations for the period 1969-77.
[8] Baltimore Low Water Datum (adopted 1922 by NOS and COE based on observations 1903-1921).
[9] Mean River Level.
[10] Charleston Low Water Datum (used since 1905 by NOS, and by COE in May 1929).
[11] Low Water Datum at the Presidio, Golden Gate, San Francisco, is based on miscellaneous observations before 1907.

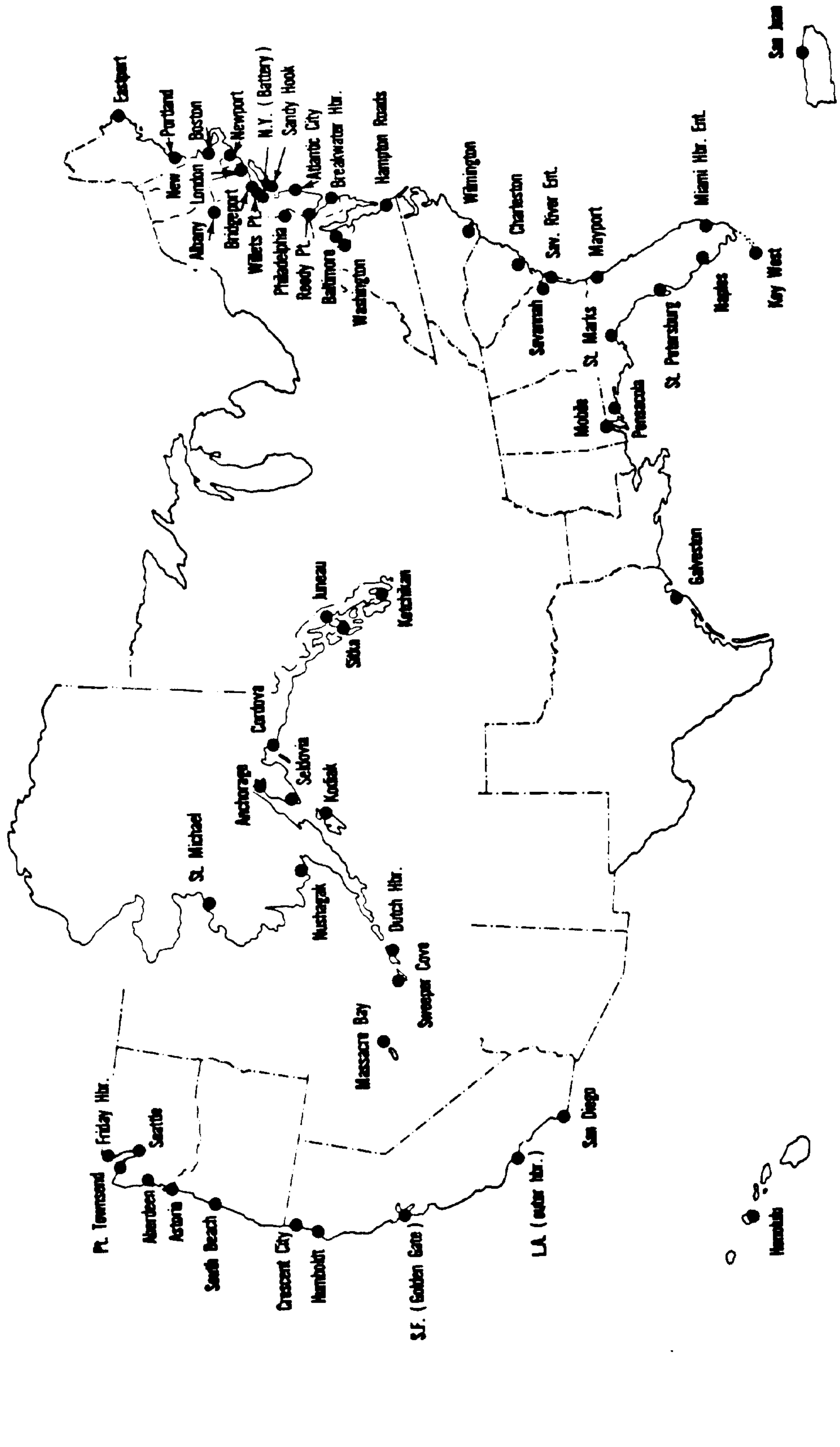

Figure 2-16. Location of reference and comparative tide stations for Atlantic, Gulf, and Pacific coasts

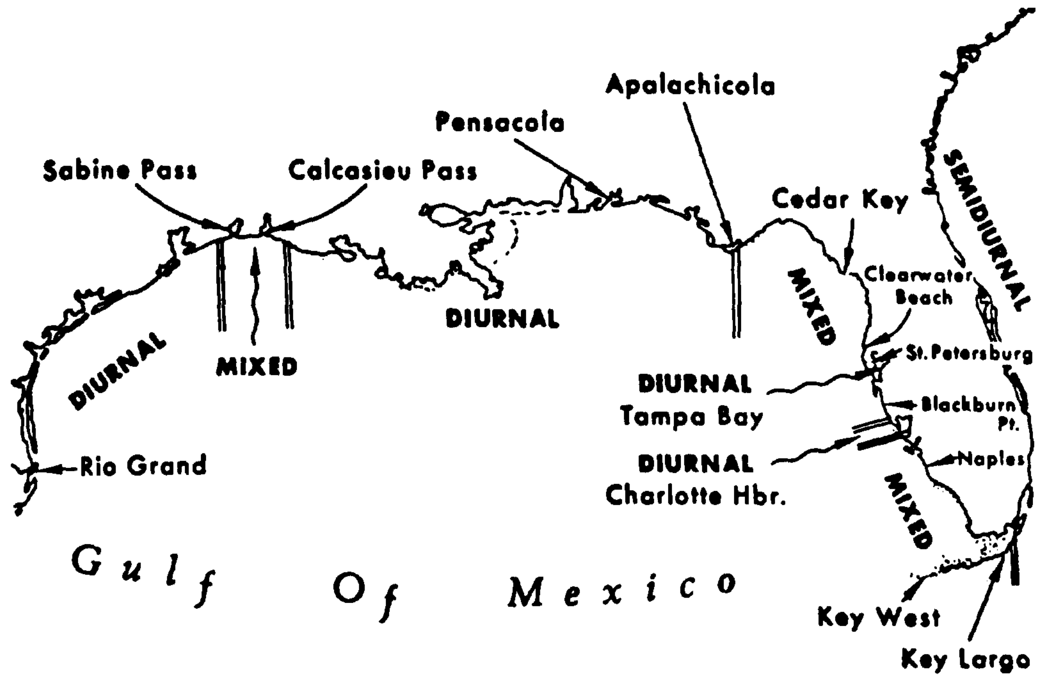

Figure 2-17. Areal extent of tidal types and locations of stations with illustrated tidal curves

discontinuities in the chart datum along the Gulf coast. Subsequently, GCLWD was changed to MLLW in name but not in elevation or purpose.

e. Special Datum Planes. Special datums for the Great Lakes region, based on the assumption that the mean water level in each lake defines a level surface, have been in use for more than a century. The most widely accepted in both the US and Canada is the International Great Lakes Datum (IGLD) of 1955.

(1) The Great Lakes Basin and St. Lawrence River were treated as an integral system in defining the IGLD. The zero of the system was established as the average of all hourly water level readings at Father Point (Point Au Pere), Quebec, for 11 years of available records between 1941 and 1956. Although additional records were available, this period was selected as representing the most reliable data. First-order level lines were run from Father Point to Kingston to establish the elevation of Lake Ontario.

(2) It was assumed that the mean water level of Lake Ontario in the ice-free period during the years 1952-1958 defined a level surface. First-order leveling was run from western Lake Ontario to eastern Lake Erie to define the elevation of Lake Erie. The mean water level of Lake Erie from June to September (1952-1958) was assumed to define a level surface. First-order levels were run from western Lake Erie to southern Lake Huron to establish the level of Lakes Michigan and Huron. Lakes Michigan and Huron are assumed to have the same level because of the wide and deep connection of both lakes at the Straits of Mackinac. First-order leveling was run from northern Lake Huron to

eastern lakes at the Strait of Mackinac. First-order leveling was run from northern Lake Huron to eastern Lake Superior to establish the level of Lake Superior. As with Lakes Ontario and Erie, the mean water level from June to September (1952-58) was used to establish the datum for the entire shoreline of each lake. All calculations were made to a resolution of 0.001 ft. Elevations assigned in the IGLD of 1955 do not, in general, agree exactly with elevations assigned to the same benchmarks in the NGVD system based on orthometric leveling. The differences, however, have never exceeded 2 ft. The different systems are discussed in SR-7.

2-4. Variation in Mean Sea Level

a. Explanation of Sea Level Trends. Although MSL with respect to the land is a relatively stable reference surface, it varies irregularly with time and location. In general, the sea level is either rising with respect to the land or shows no discernible trend at low latitudes and is falling with respect to the land at northern latitudes. The variability in sea level during this century, as revealed by many tide gage records in the United States, is clearly shown in Table 2-5. Data from the entire series should be used for the best values at each station, and data from 1940-80 should be used for comparing stations. All but two stations south of Alaska show a trend of rising sea level when the full period of record is considered. The Alaska stations in this table, other than Ketchikan, show a trend toward falling sea level over the same period.

(1) A worldwide increase in sea level occurred between 16,000 and 6,000 years ago. It is generally attributed to the melting of the ice sheet from the last glacial stage and is generally referred to as the glacioeustatic rise. The trend toward falling sea levels, relative to high latitude landmasses, is generally explained as a regional glacioeustatic adjustment of the earth's crust to the removal of the ice overburden. As the ice sheet accumulated, its increased weight caused a downward deformation of the earth's crust in the glaciated area and a compensatory rise in peripheral zones. With the removal of the excess weight, the glaciated areas are gradually rebounding toward their former shape, leading to emergence of these land surfaces relative to the water.

(2) Other factors must also be considered. Earthquakes and volcanic eruptions can cause tectonic adjustments. Continued slow increase in sea level during the last few thousand years may be partially attributable to delayed isostatic reponse to the loading on continental shelves by higher sea levels. Some of this rise in sea level may also be due to retreat of coastal glaciers.

(3) An important factor affecting modern sea level relative to the land, in certain cases, is subsidence of the earth's surface, often as a result of the withdrawal of subsurface water, petroleum, gas, minerals, or the imposition of excessively heavy loads, such as buildings, dams, and occasionally water. Except for subsidence due to the removal of subsurface fluids and other minerals, there appears to be little reason for believing that future predictions of sea level variation can be made with great confidence. The optimum procedure to use for any essential extrapolation depends on the reason for extrapolation. For structure design, extrapolation of observed trends for

Table 2-5

Trends and Variability of Yearly MSL Through 1980

Location	Date series began	Dates of Missing	Entire Series Trend	Entire Series Standard error of trend[2]	Variability	1940-80 Trend[1]	1940-80 Standard error of trend[2]	Variability
			mm/yr	mm/yr	mm	mm/yr	mm/yr	mm
Eastport, ME	1930	1957, 58, 76-78, 80	3.1	0.3	26.2	3.2	0.4	28.6
Portland, ME	1912		2.3	0.2	29.2	2.3	0.4	29.7
Portsmouth, NH	1927	1935-39, 73,78	2.0	0.2	24.2	1.3	0.3	22.6
Boston, MA	1922		2.3	0.2	28.1	0.9	0.3	23.5
Woods Hole, MA	1933	1965, 1967-69	2.7	0.2	23.1	2.3	0.3	22.0
Newport, RI	1931		2.6	0.2	23.1	2.0	0.3	22.1
Providence, RI	1939	1947-56, 1967	1.8	0.4	25.7	1.8	0.4	26.1
New London, CT	1939	1978-80	2.2	0.3	23.5	2.2	0.3	23.7
Willets Pt., NY	1932		2.2	0.4	42.9	1.6	0.6	44.5
New York, NY 1893			2.8	0.1	28.0	2.5	0.3	25.3
Sandy Hook, NJ	1933		4.2	0.3	28.4	4.0	0.4	29.3
Atlantic City, NJ	1912	1921-22, 1970-71, 79	4.0	0.2	30.7	3.9	0.4	32.3
Lewes, DE	1921	1923-36, 1940-47, 1950-52	3.0	0.4	37.9	2.0	1.8	39.1
Philadelphia, PA	1901	1921-22, 1959-60	2.6	0.2	39.5	2.3	0.5	41.3
Baltimore, MD	1903		3.2	0.1	27.7	2.5	0.4	28.0
Annapolis, MD	1929	1976	3.7	0.3	28.1	3.0	0.4	26.9
Washington, DC	1932	1980	3.0	0.4	35.8	2.8	0.5	37.1
Solomons, MD	1938		3.3	0.3	28.1	3.2	0.4	28.7
Hampton Roads, VA	1928		4.3	0.3	32.6	3.6	0.4	32.1
Portsmouth, VA	1936		3.6	0.3	29.5	3.6	0.4	30.7
Charleston, SC	1922		3.4	0.3	35.6	2.4	0.5	36.1
Fort Pulaski, GA	1936		2.7	0.4	33.2	2.5	0.4	33.8
Fernandina, FL	1898	1924-38	1.7	0.4	34.7	1.6	0.5	34.6
Mayport, FL	1929		2.3	0.3	34.9	1.5	0.5	34.7
Miami Beach, FL	1932	1979	2.3	0.2	23.8	1.9	0.3	24.0
			Gulf Coast					
Key West, FL	1913		2.2	0.2	25.9	1.6	0.4	27.2
Cedar Key, FL	1915	1926-38	2.0	0.2	30.2	1.2	0.4	31.2
Pensacola, FL	1924		2.4	0.3	37.2	1.6	0.5	37.1
Galveston, TX (Pier 21)	1909	1979	6.3	0.3	48.2	6.2	0.7	48.1
			Pacific Coast					
San Diego, CA	1906		1.9	0.1	25.2	1.6	0.4	27.5
LaJolla, CA	1925	1954-55, 78, 79	1.7	0.2	26.4	1.5	0.4	28.4
Los Angeles, CA	1924	1979	0.6	0.2	26.5	-0.1	0.4	26.3
Alameda, CA	1940		0.1	0.5	34.6	0.1	0.5	34.6
San Francisco, CA	1855		1.2	0.1	39.8	1.5	0.4	33.2
Crescent City, CA	1933		-0.9	0.3	30.0	-1.6	0.4	28.7
Astoria, OR	1925		-0.5	0.3	41.0	-1.3	0.5	38.8
Seattle, WA	1899		1.9	0.1	29.6	2.1	0.4	27.2
Neah Bay, WA	1935		-1.3	0.3	29.4	-1.8	0.4	29.0
Friday Harbor, WA	1934		0.9	0.3	28.3	0.5	0.4	28.4
Ketchikan, AL	1919		-0.1	0.2	34.8	-0.4	0.5	38.6
Sitka, AL	1938		-2.4	0.3	28.2	-2.4	0.4	28.9
Juneau, AL	1936		-12.9	0.4	36.8	-12.8	0.5	38.3
Yakutat, AL	1940		-4.6	0.4	33.0	4.6	0.4	33.6
Honolulu, HA	1905		1.6	0.2	35.0	0.7	0.4	30.7

[1] Slope of a least squares line of regression:

$$b = \frac{Sxy - (Sx)(Sy)/m}{Sx^2 - (Sx)2/m}$$

where
x = height of yearly MSL
y = date
n = number of yearly MSL values

[2] Standard error of estimate (standard deviation from line of regression):

the next 100 years is perhaps the most conservative policy. Extrapolation should always be based on the best available data.

(4) Recent studies have predicted an accelerated rate of sea level rise in coming years. They attribute the rise to warming of the atmosphere induced by increasing concentrations of carbon dioxide and other gases. Increases of between 20 and 60 inches by the year 2100 have been suggested (item 101).

b. Data Sources for Detailed Studies.

(1) NOS maintains a running summary of monthly MSL, mean and extreme high and low waters of the month, and many other tidal statistics. Photocopies of these records may be obtained upon request from the Tidal Data and Quality Assurance Section, N/OMA1230, 6th Floor, WSC-1, National Ocean Service, NOAA, 6001 Executive Blvd., Rockville, MD 20852. A sample NOS summary of tide level and sea level is provided in Figure 2-18. This particular sample was selected because it shows several realistic characteristics of the records. For example, a complete or nearly complete data set is needed each month to provide a meaningful estimate of the tabulated quantity. In cases where sufficient data were not available, the estimate is shown in parentheses. Erroneous data may be entered in the record and not immediately detected; e.g., repairs to a gage may cause a small shift in gage zero that is not measured until the next visit of a survey party. In these cases, the incorrect data are ruled out and corrected values entered. Because tide level and sea level are entered on the same sheet in this sample, it is readily seen that although MSL and MTL are highly correlated, they are different. Even where annual means are considered, MTL may be above MSL in some years and below MSL in others.

(2) The National Geodetic Survey (NGS) (part of NOS) continually relevels various survey lines throughout the United States. Elevation changes between surveys may be used to map the extent of vertical crustal movement. If information on vertical changes for a particular problem area is needed, the request to NGS should specify uncorrected data to compute vertical change. Adjusted level surveys should be compared only if the nature of the adjustments is fully understood.

2-5. Tide Height Probabilities

a. Introduction. A computer program which uses equation (2-1) for the prediction of hourly tidal heights and the times and heights of high and low waters has been used to develop tide height probabilities (SR-7). The hourly tides for one month are predicted first, then the time and height of high and low tides are determined by refining the calculations near the extreme hourly values to obtain the required accuracy in time and height. Times of high and low water are calculated to the nearest minute. The local MSL is used as the mean water level; thus, the mean value of the predicted tide is zero. Calculations are made for each of the 50 NOS reference stations listed in Table 2-4. The information needed to compute the tides is available for all reference stations but only a few nonreference stations. The nonreference stations for which calculations were made are listed in Table 2-6.

b. Description of the Graphs. Graphs for one tide station are shown in

Form 172a
DEPARTMENT OF COMMERCE
COAST AND GEODETIC SURVEY
Ed. August 1913

TIDES: MONTHLY MEANS OF TL + SL

Station: Alamitos Bay Entrance, Calif. Latitude Longitude

Observations begin July 6, 1953 Observations end

Datum is which is 14.88 feet below B. M. [illegible]

Linear quantities in feet Time in hours

		Year	Jan.	Feb.	Mar.	Apr.	May	June	July	Aug.	Sept.	Oct.	Nov.	Dec.	For Year Sum	For Year Mean	Total Sum	Total Mean
		1953								4.49	4.59	4.53	4.50	4.38				
TL	(1)	1954	4.36	4.34	4.19	4.12	4.48	4.68	4.66	4.62	4.64	4.40	4.48	4.40	53.37	4.45	4.45	4.46
	(2)	1955	4.29	4.24	4.32	4.14	4.32	4.42	4.45	4.60	4.60	4.30	4.33	4.18	52.19	4.35	8.80	4.40
	(3)	1956	4.18	4.24	4.14	4.24	4.28	4.54	4.58	4.71	4.63	4.50	4.52	4.50	53.06	4.42	13.22	4.41
	(4)	1957	4.38	4.36	4.24	4.27	4.45	4.66	4.86	4.87	4.76	4.81	4.76	4.86	55.28	4.61	17.83	4.46
	(5)	1958	4.70	4.62	4.51	4.52	4.50	4.55	4.68	4.88	5.00	5.08	4.88	4.76	56.68	4.72	22.55	4.51
	(6)	1959	4.75	4.68	4.50	4.50	4.48	4.66	4.78	4.92	5.01	5.07	4.72	4.94	57.01	4.75	27.30	4.55
	(7)	1960	4.57	4.28	4.44	4.38	4.44	4.56	4.72	4.76	4.86	4.69	4.61	4.66	54.97	4.58	31.88	4.55
	(8)	1961	4.66	4.56	4.37	4.38	4.36	4.56	4.74	4.78	4.86	4.68	4.58	4.64	55.17	4.60	36.48	4.56
	(9)	1962	4.61	4.63	4.23	4.36	4.43	4.51	4.61	4.78	4.89	4.89	4.61	4.62	55.17	4.60	41.08	4.56
	(10)	1963	4.56	4.55	4.37	4.30	4.47	4.75	4.89	4.99	5.15	4.91	4.84	4.83	56.61	4.72	45.80	4.58
	(11)	[illegible]	[illegible]	[illegible]	[illegible]	[illegible]	[illegible]	[illegible]	[illegible]	[illegible]	[illegible]	[illegible]	[illegible]	[illegible]	[illegible]	[illegible]	[illegible]	[illegible]
	(12)	1964	4.74	4.42	4.40	4.28	4.26	4.44	4.64	4.86	4.85	(4.74)	4.58	4.58	54.81	4.57	50.37	4.58
	(13)	1965	4.52	4.68	4.64	(4.66)	4.47	4.66	4.79	5.07	5.16	4.97	4.96	(5.08)	57.66	4.80	55.17	4.60
	(14)	1966	4.89															
	(15)	1953								4.49	4.57	4.49	4.45	4.33				
SL	(16)	1954	4.36	4.29	4.19	4.09	4.43	4.62	4.62	4.61	4.60	4.34	4.44	4.37	52.96	4.41	4.41	4.41
	(17)	1955	4.27	4.23	4.28	4.12	4.28	4.40	4.44	4.58	4.57	4.28	4.29	4.14	51.88	4.32	8.73	4.36
	(18)	1956	4.17	4.22	4.13	4.21	4.25	4.52	4.59	4.69	4.61	4.49	(4.49)	(4.47)	52.86	4.40	13.13	4.38
	(19)	1957	4.36	4.35	4.21	4.25	4.41	4.63	4.83	4.87	4.74	4.78	4.75	4.85	55.03	4.59	17.72	4.43
	(20)	1958	4.71	4.60	4.49	4.51	4.46	4.53	4.65	4.85	4.99	5.04	4.84	4.72	56.39	4.70	22.42	4.48
	(21)	1959	4.74	4.68	4.49	4.48	4.48	4.64	4.78	4.94	5.00	5.04	4.71	4.92	56.90	4.74	27.16	4.53
	(22)	1960	4.52	4.28	4.37	4.37	4.43	4.58	4.71	4.69	4.84	4.65	4.58	4.64	54.66	4.55	31.71	4.53
	(23)	1961	4.66	4.57	4.38	4.42	4.38	4.52	4.76	4.79	4.84	4.69	4.57	4.69	55.27	4.61	36.32	4.54
	(24)	1962	4.60	4.62	4.22	4.34	4.40	4.47	4.60	4.78	4.93	4.86	4.57	4.59	54.78	4.58	40.90	4.54
	(25)	1963	4.56	4.56	4.37	4.30	4.48	4.74	4.88	4.97	5.09	4.89	4.85	4.81	56.50	4.71	45.61	4.56
	(26)	[illegible]	[illegible]	[illegible]	[illegible]	[illegible]	[illegible]	[illegible]	[illegible]	[illegible]	[illegible]	[illegible]	[illegible]	[illegible]	[illegible]	[illegible]	[illegible]	[illegible]
	(27)	1964	4.72	4.40	4.41	4.24	4.21	4.41	4.63	4.83	4.83	(4.71)	4.51	4.54	54.44	4.54	50.15	4.56
	(28)	1965	4.50	4.66	4.59	(4.62)	4.41	4.63	4.75	5.06	5.14	4.94	4.92	(5.04)	57.26	4.77	54.92	4.58
	(29)	1966	4.86															
	(30)																	

Figure 2-18. Sample of an NOS tabulation of tide parameters

Table 2-6

Comparative Tide Stations[1]

Station	Reference Station	Normalizing Factor[2]	MTL	NGVD	MLLW	MLW	MHW	MHHW	Record Highest	Record Lowest	Interval for Establishing Datums
Atlantic City, N.J.	Sandy Hook	M	2.05	1.70	--[3]	0.00[4]	1.10	--	8.9	-3.7	1941 to 1959
Naples, Fla.	St. Marks	D	1.05	0.57	-0.50	0.00[4]	2.10	2.30	12.2	-2.5[5]	1966 to 1968
Crescent City, Calif.	Humboldt Bay	D	3.75	3.63	0.00[6]	1.20	6.30	6.90	10.0	-2.9	1934 to 1941
Southbeach, Oreg.	Humboldt Bay	D	4.50	4.01	0.00[6]	1.30	7.60	8.30	--	--	1968 to 1973
Friday Harbor, Wash.	Port Townsend	D	4.75	4.42	0.00[6]	2.50	7.00	7.70	10.9	-3.9	1941 to 1959

[1] Measurements are in feet.
[2] M = mean tidal range; D = diurnal tidal range.
[3] Missing data.
[4] Local datum is MLW.
[5] Estimated record.
[6] Local datum is MLLW.

Figure 2-19. The predicted tides for each tide station are plotted to display characteristics of the monthly and annual cycles at each location. The scale for each plot is adjusted to allow the extreme range of the 19-year epoch to occupy the full vertical expanse of the graph. The graph shows the variable wave forms of the astronomical tide but does not provide quantitative data. In general, the changes in tide hydrographs with distance along the shore are slow and continuous from Eastport, Maine, to Galveston, Texas, and from San Diego, California, to Alaska.

(1) Explanations of each graph are as follows:

(a) Plot A shows the predicted annual cycle of mean water levels in feet as defined by the monthly mean of the predicted tides averaged over the 19-year period.

(b) Plot B shows the predicted MSL for each year in the metonic (19-year) cycle. The variability in annual MSL cannot be predicted by any established procedure; therefore, the annual MSL has been held at zero in these calculations. This constant plot is included only to emphasize that long-term changes in sea level have not been considered in these calculations.

(c) Plot C is the annual cycle in tidal range. Three measures of the range have been used: the standard deviation of all computed hourly values, the mean tidal range, and the mean diurnal tidal range. The data are normalized with respect to the computed mean range for each Atlantic coast station and the computed diurnal range for Gulf and Pacific coast stations. In general, the standard deviation shows the least variability with season, and the diurnal range shows the most. Calculations were first made for each month, and the monthly values were averaged for 19 years.

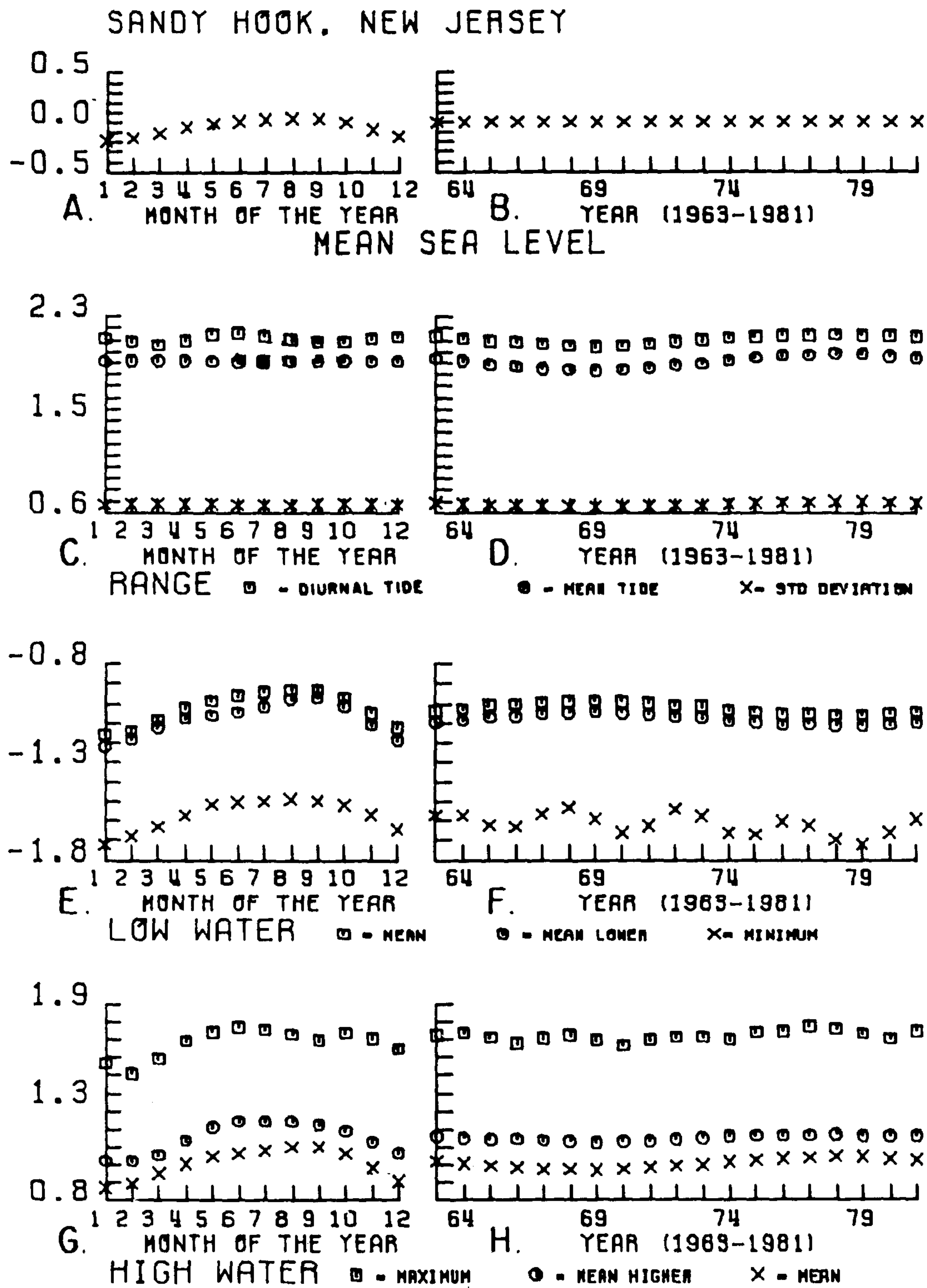

Figure 2-19. Annual and 19-year cyclical distribution of tide parameters (in feet)

(d) Plot D shows the variability of each measure of range for the metonic cycle. The anticipated 19-year cycle is apparent for each measure. These data also are normalized with respect to the computed mean daily range.

(e) Plot E gives the annual cycle of calculated low water parameters. The lowest point for each month represents the lowest predicted tide for that month in any year of the metonic cycle. The upper point represents the mean predicted low water for that month, when all predicted low waters of the 19-year period are considered. The intermediate point represents the mean of the lower low water for each calendar day averaged for each month. All data are normalized as indicated in (c) above. Note that the MLW and MLLW plots represent a combination of the annual cycle in MSL and the annual cycles in the tidal range. In nearly all cases, the annual cycle in MSL is dominant.

(f) Plot F is similar to plot E and normalized in the same manner but presents data for the metonic cycle. The MLW and MLLW graphs show the expected 19-year cycle.

(g) Plots G and H are similar to plots E and F and are normalized as indicated in (c) above. The annual cycles follow approximately the same patterns as the mean sea levels. The 19-year cycle is apparent in the MHW and MHHW data. A period of approximately 6 years appears in the extreme predicted high waters as well as the predicted low waters.

(2) Values of MHHW, MHW, MLW, MLLW, standard deviation, mean range, and the mean diurnal range based on these calculations are given in Table 2-7. Observed values of the mean and diurnal ranges obtained from NOS benchmark sheets are also shown in the table. All of the calculations are based on the period 1963 to 1981; no storm effects are included. The NOS values are based on observations, generally for the period 1941 to 1959 and include minor storm effects. Thus, exact agreement is not to be expected.

(3) The definitions used in the computer program to derive the high and low water datums differ slightly from those used by NOS for dealing with observations. In the computer program, the definitions used for HHW, HW, LW, LLW, and the mean and diurnal ranges are identical on all stations. Each identifiable high or low water is used in defining MHW and MLW provided the difference between adjacent high and low waters is 0.1 foot or greater. The definition of MHW and MLW and mean range agrees with NOS practice at locations with semidiurnal or mixed tides. NOS is now introducing MLLW as the primary datum for all nautical charts; the diurnal range will be used as the principal measure of tidal range. A complete changeover will require several years. The classifications in the 1979 NOAA NOS Tide Tables are used in these summaries. Where the type of tide is classified as diurnal, NOS neglects all secondary high and low waters, and the highest and lowest values are considered high and low water. Thus, for stations with diurnal tides the MHW and MLW given by NOS correspond to the MHHW and MLLW in these summaries; the mean range given by NOS for diurnal tides corresponds to the diurnal range. When determining the HHW or LLW for days with a single high or low water, NOS accepts the single tide as a HHW only if it is larger than the preceding or following high tides, and as a LLW only if it is lower than the preceding or following low tides.

Table 2-7

Computed Datums, Ranges, and Standard Deviations Referred to MSL[1]

Station	Standard Deviation	MHHW	MHW	MLW	MLLW	Mean Range[2] Observed	Mean Range[2] Computed	Diurnal Range[2] Observed	Diurnal Range[2] Computed
Eastport	6.32	9.32	8.88	-9.01	-9.41	18.20	17.89		18.73
Portland	3.24	4.87	4.45	-4.46	-4.80	9.00	8.91		9.68
Boston	3.40	5.16	4.72	-4.86	-5.19	9.50	9.58		10.35
Newport	1.33	2.18	1.93	-1.69	-1.75	3.50	3.62		3.93
New London	0.94	1.48	1.22	-1.34	-1.45	2.60	2.56		2.93
Bridgeport	2.41	3.61	3.31	-3.36	-3.52	6.70	6.67		7.13
Willets Point	2.68	3.85	3.59	-3.58	-3.78	7.10	7.17		7.65
New York (The Battery)	1.65	2.51	2.19	-2.29	-2.42	4.50	4.48		4.94
Albany	1.70	2.76	2.32	-2.51	-2.65	4.60	4.83		5.40
Sandy Hook	1.70	2.66	2.33	-2.34	-2.47	4.60	4.67		5.13
Atlantic City	1.52	2.41	2.01	-2.07	-2.18	4.10	4.08		4.59
Breakwater Harbor	1.53	2.46	2.04	-2.08	-2.15	4.10	4.20		4.60
Reedy Point	1.96	3.07	2.73	-2.77	-2.85	5.50	5.51		5.92
Philadelphia	2.04	3.15	2.82	-3.09	-3.17	5.90	5.91		6.33
Baltimore	0.51	0.74	0.51	-0.52	-0.64	1.10	1.03		1.38
Washington	1.02	1.54	1.39	-1.37	-1.42	2.90	2.76		2.96
Hampton Roads	0.92	1.41	1.22	-1.22	-1.26	2.50	2.44		2.67
Wilmington	1.51	2.26	2.02	-2.24	-2.33	4.20	4.26		4.59
Charleston	1.88	2.87	2.50	-2.67	-2.81	5.20	5.17		5.69
Savannah River Entrance	2.52	3.77	3.38	-3.56	-3.70	6.90	6.94		7.48
Savannah	2.73	4.07	3.65	-3.96	-4.12	7.40	7.61		8.19
Mayport	1.66	2.49	2.20	-2.27	-2.38	4.50	4.46		4.87
Miami Harbor Entrance	0.95	1.33	1.26	-1.26	-1.40	2.50	2.52		2.74
Key West	0.58	0.92	0.63	-0.64	-0.88	1.30	1.26		1.80
Naples	0.94	1.30	1.03	-1.07	-1.69	2.10	2.10	2.80	2.99
St. Petersburg	0.71	1.04	0.72	-0.70	-1.14		1.42	2.30	2.19
St. Marks River Entrance	1.09	1.51	1.23	-1.18	-1.86	2.40	2.41	3.30	3.37
Pensacola	0.54	0.67	0.61	-0.57	-0.63		1.18	1.30	1.30
Mobile	0.58	0.73	0.65	-0.62	-0.70		1.27	1.50	1.44
Galveston (ship channel)	0.53	0.57	0.47	-0.44	-0.85		0.91	1.40	1.42
San Juan	0.54	0.87	0.57	-0.58	-0.79	1.10	1.15		1.66
San Diego	1.81	2.90	2.11	-2.09	-3.06	4.10	4.20	5.70	5.96
Los Angeles (Outer Harbor	1.66	2.63	1.91	-1.87	-2.82	3.80	3.78	5.40	5.45
San Francisco (Golden Gate)	1.75	2.59	2.04	-1.93	-3.14	4.00	3.97	5.70	5.73
Humboldt	1.93	2.97	2.26	-2.24	-3.44	4.50	4.50	6.40	6.40
Crescent City	2.12	3.22	2.56	-2.49	-3.75	5.10	5.04	6.90	6.97
South Beach	2.57	3.88	3.17	-3.09	-4.48	6.30	6.26	8.30	8.36
Astoria	2.53	3.98	3.28	-3.19	-4.38	6.50	6.47	8.20	8.37
Aberdeen	2.99	4.54	3.74	-4.03	-5.35	7.90	7.77	10.10	9.89
Pt. Townsend	2.66	3.40	2.74	-2.31	-4.80	5.10	5.04	8.30	8.20
Seattle	3.50	4.83	3.94	-3.75	-6.48	7.60	7.69	11.30	11.31
Friday Harbor	2.55	3.23	2.51	-2.17	-4.55	4.50	4.68	7.70	7.78
Ketchikan	4.91	7.36	6.46	-6.47	-8.02	13.00	12.92	15.40	15.38
Juneau	5.31	7.82	6.93	-7.10	-8.72	13.80	14.03	16.40	16.54
Sitka	3.11	4.69	3.92	-3.86	-5.32	7.70	7.77	9.90	10.01
Cordova	3.85	5.81	4.88	-5.03	-6.51	10.10	9.90	12.40	12.31
Seldovia	5.89	8.48	7.70	-7.81	-9.55	15.40	15.51	17.80	18.04
Anchorage	9.01	12.73	11.99	-13.90	-16.18	26.10	25.88	29.00	28.90
Kodiak	2.71	4.29	3.40	-3.39	-4.54	6.60	6.80	8.50	8.83
Dutch Harbor	1.24	1.52	1.21	-1.07	-2.17	2.20	2.28	3.70	3.69
Sweeper Cove	1.40	1.63	1.29	-1.40	-2.26		2.69	3.70	3.89
Massacre Bay	1.19	1.40	1.10	-1.02	-2.01		2.12	3.30	3.41
Nushagak	5.94	9.42	7.46	-7.78	-10.26	15.30	15.24	19.50	19.68
St. Michael	1.24	1.94	1.39	-1.29	-1.64		2.68	3.90	3.58
Honolulu	0.60	1.08	0.58	-0.65	-0.81	1.20	1.23	1.90	1.89

[1] Numbers are in feet.
[2] Observed values for both mean and diurnal range are not available for all stations.

(4) Table 2-7 shows that the net differences between observed and computed values are generally much less than 0.1 foot for mean ranges and slightly less than 0.1 foot for diurnal ranges. Differences up to 0.4 foot which occur at a few locations result from the necessity of basing the tide calculations on a shorter or earlier period of record than that currently used by NOS in defining the tidal datums on benchmark sheets. The differences between the working definition of HHW and LLW used in the computed summaries and the definition used by NOS account for a part of this difference. The effect of these differences can be reduced by using range determinations based on the latest benchmark sheets in obtaining dimensional values from the tabulated data.

(5) Probability density distribution graphs and tables have been developed for seven tide parameters:

(a) The highest predicted tide for each calendar month.
(b) The predicted HHW of each solar day.
(c) All predicted high waters of the 19-year period.
(d) Predicted hourly tidal heights.
(e) All predicted low waters of the 19-year period.
(f) The predicted LLW of each solar day.
(g) The lowest predicted tide level of each calendar month.

(6) Wherever the amplitude of each tide wave is a large fraction of the mean range, the distribution of hourly tidal heights will be distinctly bimodal (Figure 2-20). A Gaussian distribution function with the same total area is plotted in the figure for comparison. This is the most prominent form of the distribution function for hourly tides along the US Atlantic coast.

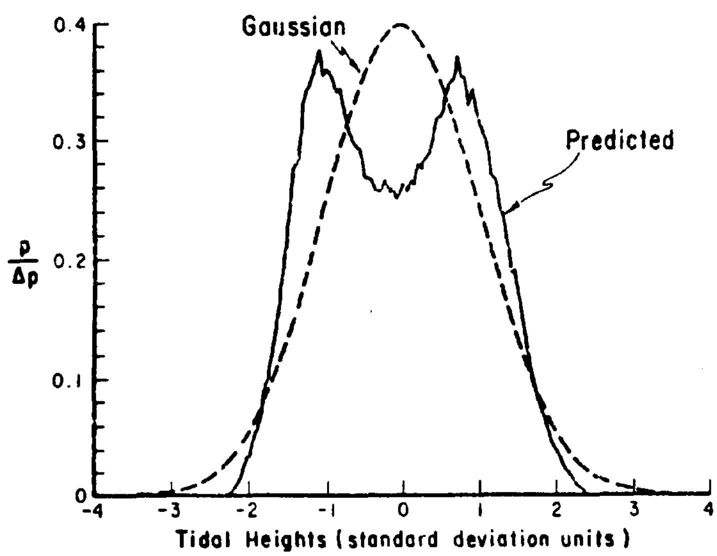

Figure 2-20. Probability density graph for predicted hourly tidal heights at Atlantic City, New Jersey (graph of the Gaussian probability density function (symmetric curve) superimposed)

(7) At some locations, such as Pensacola, Florida, and Mobile, Alabama, the range of spring tides is several times as large as the range of neap tides. This variability in the amplitude of the tide wave yields a distribution function that is nearly unimodal with a peak near MSL (Figure 2-21).

(8) Galveston, Texas, and San Francisco, California, show another common type of tide where the water level remains above MSL much longer than below MSL. The lowest predicted tide levels for these locations are farther below MSL than the maximum tide levels are above MSL. In these cases, the distribution function for hourly tidal heights is skewed, as shown in Figure 2-22.

(9) The seven curves shown in Figure 2-23 and similar graphs in SR-7 correspond to the seven tide parameters. The abscissa of these graphs gives the probability that each parameter will exceed the values indicated by the ordinate. All data have been scaled so that 98 percent of the ordinate scale corresponds to the height difference between the maximum and minimum predicted tidal heights within the metonic period of 19 years. The positions of MSL, MHW, MHHW, MLW, and MLLW have been indicated on the ordinate scale. The cumulative form of a Gaussian distribution function with the same standard deviation as the computed hourly tides has been superimposed as a straight line in all graphs.

(10) Graphs of the distribution of computed tide parameters (as in Figure 2-23) are presented only to show the character of the distribution function. Numerical values for quantitative work should be taken from the tables described in the following section.

c. Description of the Tables. The curves in Figure 2-23 are based on data as presented in Tables 2-8 and 2-9. The maximum and minimum values of each parameter were used to determine the range of variability for that parameter. Each range is divided into 101 intervals to provide 50 intervals above and 50 below the middle interval. The lowest computed value for each parameter was taken as the lower limit of the lowest interval for that parameter. The highest computed value was taken as the lower limit of the highest interval. Distribution functions were computed for each parameter by counting the number of times a computed value fell into each interval and were then converted into probability densities by dividing the number of values in each cell by the total number of values for that parameter. The cumulative probability that a given parameter will exceed a particular value is obtained as the sum of the probability that the parameter will have that value or a higher value. The maximum value of the cumulative probability is unity (1.0000).

(1) Calculations were made for each of the stations listed in Table 2-7. The relationships between tidal datum planes at each NOS reference station are given in Table 2-4. The locations of the stations are shown in Figure 2-16. Estimates of tidal height probabilities are needed for many locations for which primary tide predictions are not available. It is assumed that estimates at these stations can be determined with enough accuracy by adjusting the probability density distribution function derived for the reference station by the ratio of the tidal ranges at the two locations. To facilitate this estimate, the computed tidal heights in Tables 2-8 and 2-9 are expressed as fractions of one-half the mean tidal range or the diurnal range. An M in Tables 2-4 and 2-6 indicates that the mean range is used for normalization;

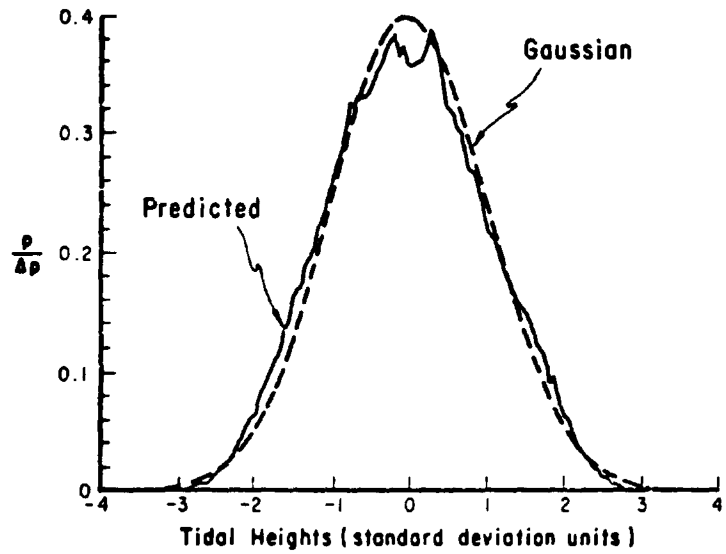

Figure 2-21. Probability density graph for predicted hourly tidal heights at Pensacola, Florida (graph of the Gaussian probability density function (symmetric curve) superimposed)

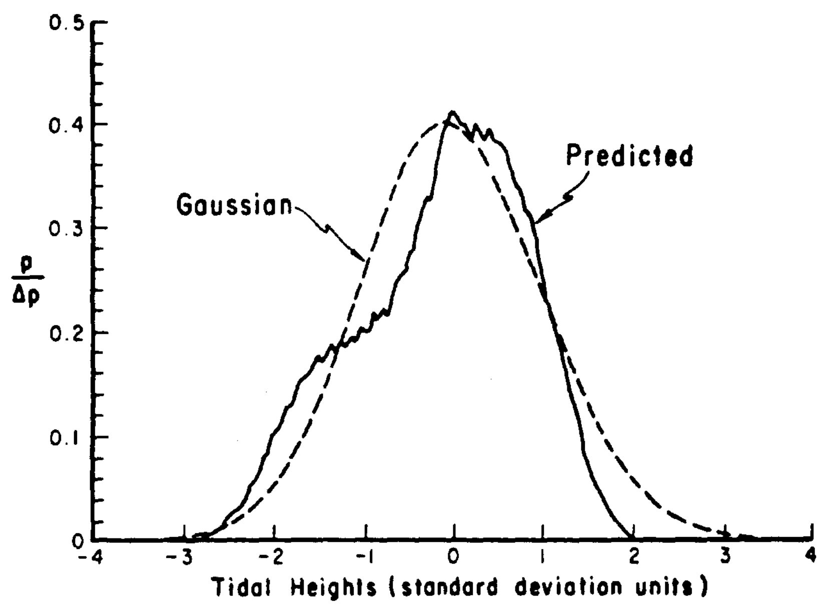

Figure 2-22. Probability density graph for predicted hourly tidal heights at San Francisco, California (graph of Gaussian probability density function (symmetric curve) superimposed)

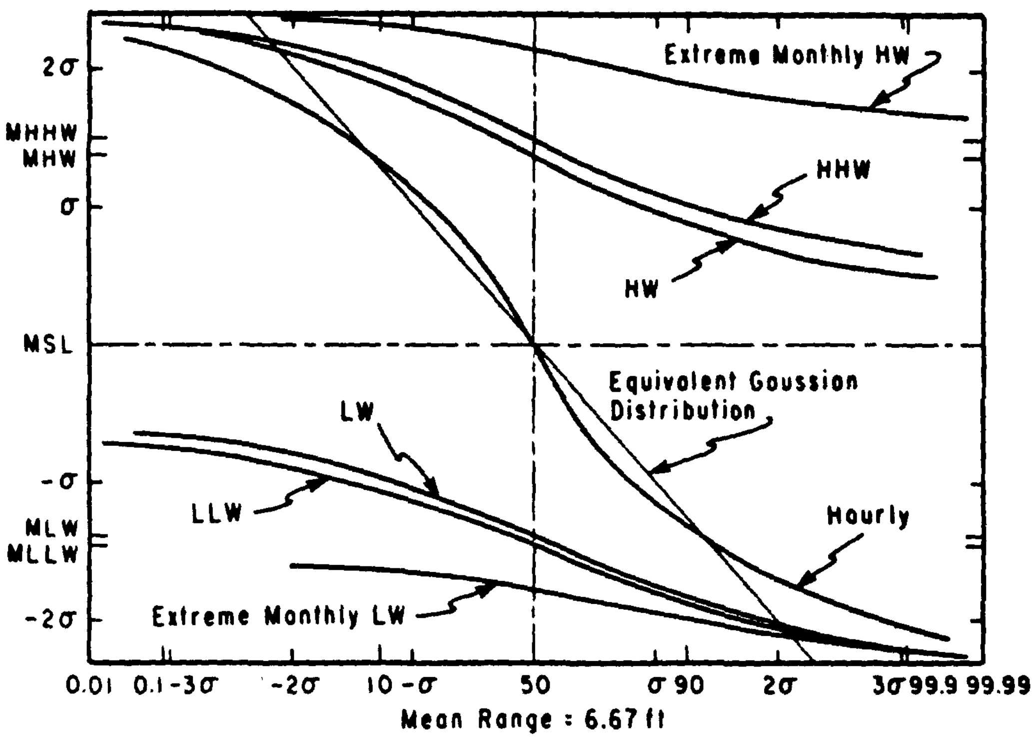

Figure 2-23. Cumulative frequency density curve for tide parameters, Bridgeport, Connecticut, 1963-1981

Table 2-8

Distribution Functions for Monthly High and Low Waters at New York (The Battery), New York

Class	Extreme Monthly HW			Extreme Monthly LW		
No.	Lower Limit	Freq.	Cum. Freq.	Lower Limit	Freq.	Cum. Freq.
101	1.6908	0.0044	0.0044	-1.1784	0.0044	0.0044
100	1.6856	0.0088	0.0132	-1.1838	0.0000	0.0044
99	1.6803	0.0044	0.0175	-1.1892	0.0000	0.0044
98	1.6751	0.0044	0.0219	-1.1947	0.0000	0.0044
97	1.6699	0.0088	0.0307	-1.2001	0.0000	0.0044
96	1.6646	0.0175	0.0482	-1.2055	0.0000	0.0044
95	1.6594	0.0175	0.0658	-1.2110	0.0000	0.0044
94	1.6542	0.0175	0.0833	-1.2164	0.0000	0.0044
93	1.6489	0.0088	0.0921	-1.2218	0.0088	0.0132
92	1.6437	0.0132	0.1053	-1.2273	0.0000	0.0132
91	1.6385	0.0088	0.1140	-1.2327	0.0088	0.0219
90	1.6332	0.0395	0.1535	-1.2381	0.0000	0.0219
89	1.6280	0.0219	0.1754	-1.2435	0.0000	0.0219
88	1.6228	0.0219	0.1974	-1.2490	0.0044	0.0263
87	1.6175	0.0088	0.2061	-1.2544	0.0088	0.0351
86	1.6123	0.0132	0.2193	-1.2598	0.0044	0.0395
85	1.6071	0.0307	0.2500	-1.2653	0.0088	0.0482
84	1.6018	0.0132	0.2632	-1.2707	0.0044	0.0526
83	1.5966	0.0088	0.2719	-1.2761	0.0132	0.0658
82	1.5914	0.0263	0.2982	-1.2816	0.0044	0.0702
81	1.5861	0.0175	0.3158	-1.2870	0.0000	0.0702
80	1.5809	0.0219	0.3377	-1.2924	0.0088	0.0789
79	1.5756	0.0132	0.3509	-1.2979	0.0088	0.0877
78	1.5704	0.0132	0.3640	-1.3033	0.0000	0.0877
77	1.5652	0.0263	0.3904	-1.3087	0.0088	0.0965
76	1.5599	0.0132	0.4035	-1.3141	0.0044	0.1009
75	1.5547	0.0175	0.4211	-1.3196	0.0219	0.1228
74	1.5495	0.0088	0.4298	-1.3250	0.0132	0.1360
73	1.5442	0.0000	0.4298	-1.3304	0.0088	0.1447
72	1.5390	0.0219	0.4518	-1.3359	0.0175	0.1623
71	1.5338	0.0044	0.4561	-1.3413	0.0132	0.1754
70	1.5285	0.0044	0.4605	-1.3467	0.0132	0.1886
69	1.5233	0.0088	0.4693	-1.3522	0.0088	0.1974
68	1.5181	0.0132	0.4825	-1.3576	0.0088	0.2061
67	1.5128	0.0263	0.5088	-1.3630	0.0175	0.2237
66	1.5076	0.0132	0.5219	-1.3684	0.0132	0.2368
65	1.5024	0.0219	0.5439	-1.3739	0.0132	0.2500
64	1.4971	0.0044	0.5482	-1.3793	0.0088	0.2588
63	1.4919	0.0132	0.5614	-1.3847	0.0175	0.2763
62	1.4867	0.0307	0.5921	-1.3902	0.0219	0.2982
61	1.4814	0.0263	0.6184	-1.3956	0.0132	0.3114
60	1.4762	0.0088	0.6272	-1.4010	0.0219	0.3333
59	1.4710	0.0088	0.6360	-1.4065	0.0132	0.3465
58	1.4657	0.0175	0.6535	-1.4119	0.0263	0.3728
57	1.4605	0.0175	0.6711	-1.4173	0.0219	0.3947
56	1.4553	0.0132	0.6842	-1.4228	0.0175	0.4123
55	1.4500	0.0132	0.6974	-1.4282	0.0175	0.4298
54	1.4448	0.0088	0.7061	-1.4336	0.0088	0.4386
53	1.4396	0.0132	0.7193	-1.4390	0.0175	0.4561
52	1.4343	0.0088	0.7281	-1.4445	0.0088	0.4649
51	1.4291	0.0088	0.7368	-1.4499	0.0263	0.4912
50	1.4239	0.0044	0.7412	-1.4553	0.0219	0.5132
49	1.4186	0.0175	0.7588	-1.4608	0.0263	0.5395
48	1.4134	0.0044	0.7632	-1.4662	0.0263	0.5658
47	1.4082	0.0132	0.7763	-1.4716	0.0219	0.5877
46	1.4029	0.0088	0.7851	-1.4771	0.0219	0.6096
45	1.3977	0.0088	0.7939	-1.4825	0.0088	0.6184
44	1.3925	0.0219	0.8158	-1.4879	0.0219	0.6404
43	1.3872	0.0175	0.8333	-1.4933	0.0263	0.6667
42	1.3820	0.0044	0.8377	-1.4988	0.0132	0.6798
41	1.3768	0.0044	0.8421	-1.5042	0.0044	0.6842
40	1.3715	0.0088	0.8509	-1.5096	0.0132	0.6974
39	1.3663	0.0000	0.8509	-1.5151	0.0088	0.7061
38	1.3611	0.0044	0.8553	-1.5205	0.0175	0.7237
37	1.3558	0.0088	0.8640	-1.5259	0.0000	0.7237
36	1.3506	0.0088	0.8728	-1.5314	0.0219	0.7456
35	1.3454	0.0044	0.8772	-1.5368	0.0175	0.7632
34	1.3401	0.0000	0.8772	-1.5422	0.0000	0.7632
33	1.3349	0.0044	0.8816	-1.5477	0.0088	0.7719
32	1.3297	0.0088	0.8904	-1.5531	0.0088	0.7807
31	1.3244	0.0132	0.9035	-1.5585	0.0088	0.7895
30	1.3192	0.0044	0.9079	-1.5639	0.0175	0.8070
29	1.3140	0.0088	0.9167	-1.5694	0.0132	0.8202
28	1.3087	0.0219	0.9386	-1.5748	0.0219	0.8421
27	1.3035	0.0088	0.9474	-1.5802	0.0044	0.8465
26	1.2983	0.0000	0.9474	-1.5857	0.0044	0.8509
25	1.2930	0.0000	0.9474	-1.5911	0.0219	0.8728
24	1.2878	0.0044	0.9518	-1.5965	0.0044	0.8772
23	1.2826	0.0044	0.9561	-1.6020	0.0088	0.8860
22	1.2773	0.0000	0.9561	-1.6074	0.0175	0.9035
21	1.2721	0.0000	0.9561	-1.6128	0.0088	0.9123
20	1.2668	0.0044	0.9605	-1.6182	0.0132	0.9254
19	1.2616	0.0000	0.9605	-1.6237	0.0088	0.9342
18	1.2564	0.0044	0.9649	-1.6291	0.0044	0.9386
17	1.2511	0.0088	0.9737	-1.6345	0.0044	0.9430
16	1.2459	0.0000	0.9737	-1.6400	0.0044	0.9474
15	1.2407	0.0000	0.9737	-1.6454	0.0044	0.9518
14	1.2354	0.0044	0.9781	-1.6508	0.0044	0.9561
13	1.2302	0.0044	0.9825	-1.6563	0.0000	0.9561
12	1.2250	0.0000	0.9825	-1.6617	0.0044	0.9605
11	1.2197	0.0044	0.9868	-1.6671	0.0044	0.9649
10	1.2145	0.0088	0.9956	-1.6726	0.0088	0.9737
9	1.2093	0.0000	0.9956	-1.6780	0.0000	0.9737
8	1.2040	0.0000	0.9956	-1.6834	0.0088	0.9825
7	1.1988	0.0000	0.9956	-1.6888	0.0044	0.9868
6	1.1936	0.0000	0.9956	-1.6943	0.0044	0.9912
5	1.1683	0.0000	0.9956	-1.6997	0.0000	0.9912
4	1.1831	0.0000	0.9956	-1.7051	0.0044	0.9956
3	1.1779	0.0000	0.9956	-1.7106	0.0000	0.9956
2	1.1726	0.0000	0.9956	-1.7160	0.0000	0.9956
1	1.1674	0.0044	1.0000	-1.7214	0.0044	1.0000

Note: Lower limit of class interval shown; all heights are normalized with respect to one-half the mean range 2,238 feet.

Table 2-9

Distribution Functions for Higher High, High, Hourly, Low, and Lower Low Waters at Atlantic City, New Jersey

Class No.	HHW Lower Limit	HHW Freq.	HHW Cum. Freq.	HW Lower Limit	HW Freq.	HW Cum. Freq.	Hourly Lower Limit	Hourly Freq.	Hourly Cum. Freq.	LW Lower Limit	LW Freq.	LW Cum. Freq.	LLW Lower Limit	LLW Freq.	LLW Cum. Freq.
101	1.6908	0.0002	0.0002	1.6908	0.0001	0.0001	1.6908	0.0000	0.0000	-0.3605	0.0001	0.0001	-0.4257	0.0001	0.0001
100	1.6793	0.0008	0.0009	1.6765	0.0004	0.0005	1.6567	0.0001	0.0001	-0.3741	0.0002	0.0003	-0.4387	0.0000	0.0001
99	1.6678	0.0014	0.0023	1.6621	0.0010	0.0014	1.6225	0.0003	0.0004	-0.3877	0.0002	0.0005	-0.4516	0.0004	0.0006
98	1.6563	0.0018	0.0041	1.6478	0.0011	0.0026	1.5884	0.0006	0.0010	-0.4013	0.0004	0.0008	-0.4646	0.0001	0.0007
97	1.6448	0.0018	0.0059	1.6335	0.0017	0.0042	1.5543	0.0007	0.0017	-0.4149	0.0006	0.0014	-0.4775	0.0003	0.0010
96	1.6333	0.0030	0.0089	1.6191	0.0017	0.0060	1.5202	0.0010	0.0027	-0.4285	0.0005	0.0020	-0.4905	0.0007	0.0018
95	1.6219	0.0033	0.0122	1.6048	0.0029	0.0088	1.4861	0.0013	0.0040	-0.4422	0.0012	0.0032	-0.5035	0.0009	0.0027
94	1.6104	0.0038	0.0159	1.5904	0.0026	0.0114	1.4519	0.0015	0.0056	-0.4558	0.0017	0.0049	-0.5164	0.0010	0.0037
93	1.5989	0.0041	0.0200	1.5761	0.0031	0.0145	1.4178	0.0020	0.0076	-0.4694	0.0019	0.0068	-0.5294	0.0015	0.0052
92	1.5874	0.0051	0.0251	1.5618	0.0031	0.0176	1.3837	0.0026	0.0102	-0.4830	0.0027	0.0095	-0.5423	0.0019	0.0072
91	1.5759	0.0050	0.0300	1.5474	0.0032	0.0207	1.3496	0.0026	0.0128	-0.4966	0.0037	0.0132	-0.5553	0.0012	0.0084
90	1.5644	0.0050	0.0350	1.5331	0.0037	0.0244	1.3154	0.0035	0.0163	-0.5102	0.0034	0.0166	-0.5682	0.0012	0.0096
89	1.5529	0.0050	0.0399	1.5188	0.0029	0.0273	1.2813	0.0043	0.0206	-0.5238	0.0033	0.0199	-0.5812	0.0013	0.0109
88	1.5414	0.0057	0.0456	1.5044	0.0053	0.0325	1.2472	0.0049	0.0255	-0.5374	0.0047	0.0246	-0.5942	0.0024	0.0133
87	1.5299	0.0051	0.0507	1.4901	0.0031	0.0356	1.2131	0.0058	0.0313	-0.5510	0.0033	0.0274	-0.6071	0.0024	0.0157
86	1.5185	0.0047	0.0554	1.4758	0.0050	0.0406	1.1790	0.0066	0.0379	-0.5646	0.0041	0.0320	-0.6201	0.0027	0.0184
85	1.5070	0.0080	0.0634	1.4614	0.0041	0.0447	1.1448	0.0074	0.0453	-0.5782	0.0045	0.0365	-0.6330	0.0033	0.0217
84	1.4955	0.0062	0.0695	1.4471	0.0060	0.0506	1.1107	0.0085	0.0538	-0.5919	0.0050	0.0416	-0.6460	0.0037	0.0254
83	1.4840	0.0062	0.0757	1.4327	0.0058	0.0564	1.0766	0.0095	0.0633	-0.6055	0.0049	0.0465	-0.6589	0.0037	0.0292
82	1.4725	0.0063	0.0820	1.4184	0.0066	0.0630	1.0425	0.0098	0.0731	-0.6191	0.0059	0.0524	-0.6719	0.0058	0.0350
81	1.4610	0.0062	0.0881	1.4041	0.0057	0.0687	1.0083	0.0111	0.0842	-0.6327	0.0062	0.0585	-0.6849	0.0061	0.0411
80	1.4495	0.0084	0.0465	1.3897	0.0072	0.0759	0.9742	0.0123	0.0965	-0.6463	0.0071	0.0656	-0.6978	0.0054	0.0465
79	1.4380	0.0092	0.1057	1.3754	0.0069	0.0828	0.9401	0.0131	0.1097	-0.6599	0.0066	0.0722	-0.7108	0.0079	0.0544
78	1.4265	0.0090	0.1147	1.3611	0.0062	0.0890	0.9060	0.0143	0.1240	-0.6735	0.0086	0.0808	-0.7237	0.0066	0.0610
77	1.4150	0.0090	0.1237	1.3467	0.0077	0.0966	0.8719	0.0149	0.1389	-0.6871	0.0108	0.0916	-0.7367	0.0075	0.0685
76	1.4036	0.0096	0.1333	1.3324	0.0087	0.1054	0.8377	0.0153	0.1541	-0.7007	0.0096	0.1012	-0.7496	0.0091	0.0776
75	1.3421	0.0093	0.1426	1.3181	0.0103	0.1157	0.8036	0.0158	0.1700	-0.7143	0.0116	0.1128	-0.7626	0.0085	0.0861
74	1.3806	0.0108	0.1534	1.3037	0.0102	0.1259	0.7695	0.0160	0.1859	-0.7279	0.0099	0.1228	-0.7756	0.0082	0.0943
73	1.3691	0.0084	0.1618	1.2894	0.0095	0.1354	0.7354	0.0171	0.2030	-0.7416	0.0114	0.1342	-0.7885	0.0120	0.1063
72	1.3576	0.0086	0.1704	1.2751	0.0113	0.1467	0.7012	0.0172	0.2202	-0.7552	0.0138	0.1480	-0.8015	0.0123	0.1186
71	1.3461	0.0110	0.1814	1.2607	0.0122	0.1594	0.6671	0.0168	0.2370	-0.7688	0.0119	0.1599	-0.8144	0.0108	0.1293
70	1.3346	0.0122	0.1935	1.2464	0.0135	0.1723	0.6330	0.0176	0.2546	-0.7824	0.0142	0.1741	-0.8274	0.0138	0.1431
69	1.3231	0.0125	0.2060	1.2320	0.0139	0.1863	0.5989	0.0172	0.2719	-0.7960	0.0149	0.1890	-0.8403	0.0126	0.1556
68	1.3116	0.0155	0.2214	1.2177	0.0122	0.1985	0.5648	0.0159	0.2878	-0.8096	0.0156	0.2086	-0.8533	0.0139	0.1695
67	1.3001	0.0119	0.2333	1.2034	0.0130	0.2115	0.5306	0.0168	0.3045	-0.8232	0.0165	0.2211	-0.8663	0.0141	0.1836
66	1.2887	0.0132	0.2465	1.1890	0.0157	0.2273	0.4965	0.0162	0.3207	-0.8368	0.0158	0.2369	-0.8792	0.0151	0.1987
65	1.2772	0.0147	0.2612	1.1747	0.0148	0.2420	0.4624	0.0149	0.3356	-0.8504	0.0179	0.2548	-0.8922	0.0157	0.2144
64	1.2657	0.0153	0.2765	1.1604	0.0154	0.2575	0.4283	0.0148	0.3504	-0.8640	0.0174	0.2722	-0.9051	0.0149	0.2293
63	1.2542	0.0171	0.2936	1.1460	0.0165	0.2740	0.3941	0.0143	0.3647	-0.8777	0.0178	0.2900	-0.9181	0.0144	0.2437
62	1.2427	0.0197	0.3133	1.1317	0.0160	0.2899	0.3600	0.0135	0.3782	-0.8913	0.0187	0.3087	-0.9310	0.0163	0.2600
61	1.2312	0.0162	0.3295	1.1174	0.0167	0.3066	0.3259	0.0131	0.3913	-0.9049	0.0182	0.3268	-0.9440	0.0173	0.2773
60	1.2197	0.0156	0.3451	1.1030	0.0146	0.3213	0.2918	0.0126	0.4039	-0.9185	0.0179	0.3447	-0.9570	0.0181	0.2954
59	1.2082	0.0170	0.3621	1.0887	0.0153	0.3365	0.2577	0.0125	0.4164	-0.9321	0.0179	0.3626	-0.9694	0.0193	0.3147
58	1.1967	0.0165	0.3786	1.0743	0.0184	0.3549	0.2235	0.0125	0.4289	-0.9457	0.0188	0.3814	-0.9829	0.0178	0.3325
57	1.1853	0.0201	0.3987	1.0600	0.0160	0.3709	0.1894	0.0118	0.4407	-0.9593	0.0193	0.4007	-0.9958	0.0176	0.3501
56	1.1738	0.0167	0.4154	1.0457	0.0186	0.3895	0.1553	0.0119	0.4526	-0.9729	0.0198	0.4205	-0.0088	0.0224	0.3730
55	1.1623	0.0188	0.4342	1.0313	0.0182	0.4077	0.1212	0.0115	0.4641	-0.9865	0.0186	0.4391	-1.0217	0.0202	0.3932
54	1.1508	0.0188	0.4529	1.0170	0.0201	0.4278	0.0870	0.0112	0.4753	-1.0001	0.0204	0.4596	-1.0347	0.0248	0.4180
53	1.1393	0.0192	0.4722	1.0027	0.0200	0.4477	0.0529	0.0114	0.4866	-1.0137	0.0218	0.4814	-1.0477	0.0239	0.4419
52	1.1278	0.0171	0.4893	0.9883	0.0187	0.4664	0.0188	0.0116	0.4982	-1.0274	0.0227	0.5041	-1.0606	0.0260	0.4679
51	1.1163	0.0161	0.5053	0.9740	0.0218	0.4882	-0.0153	0.0112	0.5095	-1.0410	0.0214	0.5255	-1.0736	0.0230	0.4910
50	1.1048	0.0153	0.5206	0.9597	0.0215	0.5097	-0.0494	0.0113	0.5208	-1.0546	0.0218	0.5473	-1.0865	0.0235	0.5144
49	1.0933	0.0159	0.5366	0.9453	0.0173	0.5270	-0.0836	0.0113	0.5320	-1.0682	0.0250	0.5723	-1.0995	0.0226	0.5370
48	1.0818	0.0183	0.5544	0.9310	0.0215	0.5486	-0.1177	0.0112	0.5432	-1.0818	0.0226	0.5949	-1.1124	0.0226	0.5596
47	1.0704	0.0179	0.5727	0.9167	0.0230	0.5716	-0.1518	0.0118	0.5550	-1.0954	0.0206	0.6155	-1.1254	0.0217	0.5813
46	1.0589	0.0141	0.5868	0.9023	0.0201	0.5917	-0.1859	0.0113	0.5664	-1.1090	0.0209	0.6364	-1.1384	0.0205	0.6017
45	1.0474	0.0183	0.6052	0.8880	0.0191	0.6109	-0.2201	0.0116	0.5779	-1.1226	0.0214	0.6578	-1.1513	0.0215	0.6233
44	1.0359	0.0171	0.6223	0.8736	0.0191	0.6300	-0.2542	0.0120	0.5899	-1.1362	0.0185	0.6763	-1.1643	0.0190	0.6422
43	1.0244	0.0197	0.6419	0.8593	0.0195	0.6495	-0.2883	0.0117	0.6017	-1.1498	0.0187	0.6950	-1.1772	0.0208	0.6630
42	1.0129	0.0188	0.6607	0.8450	0.0191	0.6687	-0.3224	0.0120	0.6137	-1.1634	0.0176	0.7126	-1.1902	0.0206	0.6837
41	1.0014	0.0171	0.6778	0.8306	0.0174	0.6861	-0.3565	0.0125	0.6262	-1.1771	0.0186	0.7312	-1.2031	0.0179	0.7016
40	0.9899	0.0158	0.6936	0.8163	0.0180	0.7041	-0.3907	0.0129	0.6391	-1.1907	0.0185	0.7497	-1.2161	0.0181	0.7197
39	0.9784	0.0189	0.7125	0.8020	0.0174	0.7215	-0.4248	0.0135	0.6526	-1.2043	0.0172	0.7669	-1.2291	0.0169	0.7366
38	0.9670	0.0191	0.7316	0.7876	0.0154	0.7369	-0.4589	0.0139	0.6665	-1.2179	0.0160	0.7830	-1.2420	0.0188	0.7554
37	0.9555	0.0182	0.7497	0.7733	0.0188	0.7557	-0.4930	0.0143	0.6807	-1.2315	0.0142	0.7972	-1.2550	0.0160	0.7714
36	0.9440	0.0123	0.7620	0.7590	0.0186	0.7743	-0.5271	0.0146	0.6954	-1.2451	0.0160	0.8133	-1.2679	0.0130	0.7844
35	0.9325	0.0159	0.7780	0.7446	0.0158	0.7901	-0.5613	0.0154	0.7108	-1.2587	0.0125	0.8258	-1.2809	0.0135	0.7979
34	0.9210	0.0173	0.7952	0.7303	0.0168	0.8069	-0.5954	0.0157	0.7265	-1.2723	0.0123	0.8381	-1.2938	0.0132	0.8110
33	0.9095	0.0147	0.8099	0.7159	0.0148	0.8217	-0.6295	0.0156	0.7421	-1.2859	0.0119	0.8500	-1.3068	0.0138	0.8248
32	0.8980	0.0158	0.8257	0.7016	0.0141	0.8358	-0.6636	0.0158	0.7578	-1.2995	0.0111	0.8611	-1.3198	0.0147	0.8394
31	0.8865	0.0119	0.8376	0.6873	0.0131	0.8489	-0.6978	0.0164	0.7742	-1.3131	0.0114	0.8726	-1.3327	0.0136	0.8530
30	0.8750	0.0132	0.8508	0.6729	0.0152	0.8641	-0.7319	0.0168	0.7910	-1.3268	0.0124	0.8850	-1.3457	0.0129	0.8659
29	0.8635	0.0107	0.8614	0.6586	0.0134	0.8775	-0.7660	0.0168	0.8078	-1.3404	0.0105	0.8955	-1.3586	0.0097	0.8756
28	0.8521	0.0108	0.8722	0.6443	0.0129	0.8904	-0.8001	0.0167	0.8245	-1.3540	0.0088	0.9045	-1.3716	0.0109	0.8865
27	0.8406	0.0077	0.8794	0.6299	0.0134	0.9038	-0.8342	0.0159	0.8408	-1.3676	0.0094	0.9137	-1.3845	0.0105	0.8970
26	0.8291	0.0093	0.8892	0.6156	0.0109	0.9147	-0.8684	0.0157	0.8560	-1.3812	0.0086	0.9223	-1.3975	0.0082	0.9052
25	0.8176	0.0093	0.8985	0.6013	0.0098	0.9245	-0.9025	0.0152	0.8712	-1.3948	0.0073	0.9296	-1.4105	0.0100	0.9152
24	0.8061	0.0084	0.9069	0.5869	0.0081	0.9326	-0.9366	0.0147	0.8859	-1.4084	0.0091	0.9387	-1.4234	0.0094	0.9247
23	0.7946	0.0068	0.9137	0.5726	0.0086	0.9412	-0.9707	0.0137	0.8996	-1.4220	0.0068	0.9455	-1.4364	0.0087	0.9333
22	0.7831	0.0080	0.9216	0.5583	0.0077	0.9489	-1.0049	0.0133	0.9129	-1.4356	0.0068	0.9522	-1.4493	0.0061	0.9395
21	0.7710	0.0080	0.9296	0.5439	0.0075	0.9563	-1.0390	0.0129	0.9259	-1.4492	0.0049	0.9571	-1.4623	0.0087	0.9481
20	0.7601	0.0077	0.9372	0.5296	0.0064	0.9627	-1.0731	0.0115	0.9373	-1.4629	0.0063	0.9634	-1.4752	0.0072	0.9653
19	0.7480	0.0056	0.9428	0.5152	0.0049	0.9676	-1.1072	0.0099	0.9472	-1.4765	0.0055	0.9689	-1.4882	0.0055	0.9608
18	0.7372	0.0063	0.9491	0.5009	0.0051	0.9727	-1.1413	0.0093	0.9565	-1.4901	0.0047	0.9736	-1.5012	0.0048	0.9656
17	0.7257	0.0062	0.9553	0.4866	0.0043	0.9770	-1.1755	0.0077	0.9642	-1.5037	0.0038	0.9774	-1.5141	0.0042	0.9698
16	0.7142	0.0053	0.9605	0.4722	0.0040	0.9810	-1.2090	0.0069	0.9712	-1.5173	0.0033	0.9807	-1.5271	0.0042	0.9740
15	0.7027	0.0047	0.9652	0.4579	0.0034	0.9844	-1.2437	0.0057	0.9768	-1.5309	0.0029	0.9837	-1.5400	0.0039	0.9779
14	0.6912	0.0039	0.9691	0.4436	0.0031	0.9875	-1.2778	0.0051	0.9819	-1.5445	0.0025	0.9861	-1.5530	0.0019	0.9798
13	0.0797	0.0042	0.9733	0.4292	0.0029	0.9904	-1.3120	0.0042	0.9861	-1.5581	0.0024	0.9886	-1.5659	0.0034	0.9833
12	0.0682	0.0050	0.9782	0.4149	0.0016	0.9920	-1.3461	0.0035	0.9896	-1.5717	0.0026	0.9911	-1.5789	0.0043	0.9876
11	0.0567	0.0036	0.9818	0.4006	0.0008	0.9928	-1.3802	0.0027	0.9923	-1.5853	0.0017	0.9928	-1.5919	0.0021	0.9897
10	0.0452	0.0044	0.9862	0.3862	0.0014	0.9943	-1.4143	0.0023	0.9947	-1.5989	0.0023	0.9950	-1.6048	0.0024	0.9421
9	0.0338	0.0038	0.9899	0.3719	0.0020	0.9962	-1.4484	0.0016	0.9963	-1.6126	0.0015	0.9965	-1.6178	0.0027	0.9948
8	0.6223	0.0036	0.9935	0.3575	0.0009	0.9971	-1.4826	0.0014	0.9977	-1.6262	0.0009	0.9974	-1.6307	0.0013	0.9961
7	0.6108	0.0021	0.9956	0.3432	0.0005	0.9977	-1.5167	0.0009	0.9986	-1.6398	0.0007	0.9981	-1.6437	0.0006	0.9967
6	0.5993	0.0015	0.9971	0.3284	0.0008	0.9984	-1.5508	0.0006	0.9992	-1.6534	0.0006	0.9987	-1.6566	0.0007	0.9975
5	0.5878	0.0003	0.9974	0.3145	0.0005	0.9989	-1.5849	0.0004	0.9996	-1.6670	0.0002	0.9989	-1.6696	0.0007	0.9982
4	0.5763	0.0014	0.9988	0.3002	0.0006	0.9995	-1.6191	0.0002	0.9998	-1.6806	0.0006	0.9995	-1.6826	0.0010	0.9993
3	0.5648	0.0005	0.9992	0.2859	0.0002	0.9948	-1.6532	0.0001	0.9999	-1.6942	0.0004	0.9998	-1.6955	0.0004	0.9997
2	0.5533	0.0006	0.9998	0.2915	0.0002	0.9998	-1.6873	0.0001	1.0000	-1.7078	0.0001	0.9999	-1.7085	0.0001	0.9999
1	0.5418	0.0002	1.0000	0.2572	0.0002	1.0000	-1.7214	0.0000	1.0000	-1.7214	0.0001	1.0000	-1.7214	0.0001	1.0000

Note: Lower limit of class interval shown; all heights are normalized with respect to one-half the mean range of 2.041 feet.

a D indicates that the diurnal range is used for normalization. Thus, absolute values for any location can be obtained by multiplying the value tabulated for the appropriate reference station in the form of Tables 2-8 and 2-9 by one-half the appropriate mean tidal range or diurnal tidal range.

(2) Table 2-8 presents the frequency distribution functions for the extreme high and low tides of each month. Similar tables for all stations are given in Appendix B of SR-7. The column on the left in Table 2-8 gives the class interval number. Three columns present each of the variables: the first gives the lower limit of each class interval (expressed in units of one-half the mean tidal range or one-half the diurnal range); the second gives the frequency with which the variable fell within the indicated class during the 19-year epoch; and the third gives the cumulative frequency (i.e., the frequency with which the variable was equal to or exceeded the lower limit of the class interval). Data from the first and third (variable) columns are plotted in Figure 2-23.

(3) Table 2-9 is similar to Table 2-8 and gives the distribution functions for higher high waters, all high waters, hourly tides, all low waters, and lower low waters. Figures 2-20, 2-21, and 2-22 are based on data of the type shown in the column for hourlies. Figure 2-23 is based on data from column 3 of the respective parameters.

d. Joint Probability Analysis. Actual tide levels near the coast are affected by both meteorological and gravitational forces. The effects of the two forces on coastal water levels are usually assumed to be independent of each other, although this assumption is not strictly correct (SR-7).

(1) When the probability distribution functions are determined empirically, the permissible values of the independent variables may be the integers 1, 2, 3, ... indicating the class numbers of the distribution table. The probability function for the sum of two independent variables is computed by the following approach. In the following discussion, lowercase p represents probability density and uppercase P represents cumulative probability. Let $p_1(k)$ be the probability that one variable is assigned to class k and $P_1(k)$ be the cumulative probability that the variable is not greater than k. Thus

$$P_1(k) = \sum_{j=1}^{k} p_1(j) \qquad (2\text{-}3)$$

(2) Let $p_2(m)$ and $P_2(m)$ be defined in a similar manner for a second variable. Let $p_3(n)$ and $P_3(n)$ have similar definitions for the sum of the first and second variables. The probability a given k will combine with a given m is given by

$$p_3\ (k + m) = p_1(k)\ p_2(m) \qquad (2\text{-}4)$$

(3) The probability of obtaining a specific value n is the sum of the probabilities of all sums of k and m which yield n. Thus,

$$p_3(n) = \sum_{m}^{n} p_1(n - m + 1)\ p_2(m) \qquad (2\text{-}5)$$

(4) The cumulative probability $P_3(n)$ can be expressed as

$$P_3(n) = \sum_{m=1}^{n} p_2(m)\ P_1(n + 1 - m) \qquad (2\text{-}6)$$

(5) An analogous expression for continuous distribution functions is given by

$$P_3(x) = \int_{-\infty}^{\infty} P_1(x - z)\ p_2(z)\ dz \qquad (2\text{-}7)$$

where P_1 is cumulative distribution function for one variable y , p_2 the distribution function for a second independent variable z , and $x = y + z$. The integral on the right is often called a convolution of P_1 and p_2 .

(6) When P_1 and p_2 are given as analytic functions and the integral in equation (2-7) can be solved easily, this formula can greatly simplify the computations. When either function is available only in tabular form and the calculations are made on a computer, equation (2-7) does not appear to offer any computational advantage over equations (2-3) and (2-4) which seem to provide more insight for the processes involved.

2-6. Application of the Tide Probability Tables. The astronomical tidal height probabilities for a nonreference location can be estimated by multiplying the values tabulated in Appendix B of SR-7 for the appropriate reference station by the appropriate tidal range parameters as obtained from Appendix C of SR-7, from the NOS tide tables, or from the latest benchmark sheets. The diurnal range might be more suitable than the mean range for some Gulf coast locations where the mean range has been indicated and vice versa. If this is the case, the height values can be converted by the ratios of the mean and diurnal ranges from Table 2-7. The computed probabilities will not be affected.

a. Tide Probability. Applications of the tide probability tables are demonstrated by example problem 2-2.

* * * * * * * * * * * * * * * * EXAMPLE PROBLEM 2-2 * * * * * * * * * * * * * *

GIVEN: Tide probability tables for Atlantic City, New Jersey (SR-7).

FIND: (a) Fraction of high tides and hourly tide levels above 2.0 ft MSL.

(b) Fraction of low tides and hourly tide levels below - 2.0 ft MSL.

SOLUTION: (a) Assume meteorological events can be neglected in estimating the frequencies of water levels between MLW and MHW.

Mean tidal range at Atlantic City = 4.08 ft (SR-7, Appendix C).

$$\begin{aligned}\text{Scaling factor} &= (0.5)\ (\text{mean tidal range}) \\ &= (0.5)\ (4.08) \\ &= 2.04 \text{ ft}\end{aligned}$$

Normalize the desired level (2.0 ft) with the scaling factor

h_c = 2.00/2.04 = 0.9804 normalized units.

The probability that the water level will be above the specified level h_c can be estimated by linear interpolation according to the following equation

$$P(h > h_c) = P_- + \frac{h_c - h_-}{h_+ - h_-}(P_+ - P_-) \qquad (2\text{-}8)$$

where

h_+ = tabulated limit immediately above h_c
h_- = tabulated limit immediately below h_c
P_+ = tabulated cumulative probability immediately above h_c
P_- = tabulated cumulative probability immediately below h_c

For high tides, using Table 2-9,

$$\begin{aligned}P(h > 0.9804) &= 0.5049 + \frac{0.9804 - 0.9669}{0.9835 - 0.9669}(0.4841 - 0.5049) \\ &= 0.4880\end{aligned}$$

For hourly tides, using Table 2-9,

$$\begin{aligned}P(h > 0.9804) &= 0.1073 + \frac{0.9804 - 0.9657}{1.0015 - 0.9675}(0.0955 - 0.1073) \\ &= 0.1025\end{aligned}$$

Thus the tide level will be above 2.0 feet an average of about 898 hours per year (0.1025 × 365 × 24). This estimate is based only on tides and does not include other effects on water level such as storm surge and wave setup.

SR-7 includes probability tables for Atlantic City, although it is not a reference tide station. Tables are not included for most secondary stations. The general procedure for a secondary station is illustrated below by recomputing the Atlantic City probability from the Sandy Hook, New Jersey, reference station tables. As before, h_c = 0.9804 . The appropriate section of the Sandy Hook tables for hourly tide levels is given in Table 2-10. Substitution into equation (2-8) gives

$$P(h > 0.9804) = 0.1004 + \frac{0.9804 - 0.9618}{0.9961 - 0.9618}(0.0883 - 0.1004)$$

$$= 0.0938$$

Thus the error committed in basing the estimate for Atlantic City on tabulated probabilities for the reference station, Sandy Hook, is 0.0087, or 9 percent.

(b) For low tides, $h_c = -0.9804$.

$$P(h < -0.9804) = 1 - P(h > -0.9804)$$

$$= 1 - 0.4765 + \frac{-0.9804 + 0.9904}{-0.9766 + 0.9904}(0.4569 - 0.4765)$$

(from Table 2-9 and equation (2-8))

$$= 1 - [0.4623]$$

$$= 0.5377$$

For hourly tides,

$$P(h < -0.9804) = 1 - P(h > -0.9804)$$

$$= 1 - 0.9143 + \frac{-0.9804 + 1.0048}{-0.9690 + 1.0048}(0.9007 - 0.9143)$$

(from Table 2-9 and equation (2-8))

$$= 1 - [0.9050]$$
$$= 0.0950$$

* *

Table 2-10
Part of Cumulative Distribution Table for Hourly Tide Levels at Sandy Hook, New Jersey

Class No.	Lower Limit of Height	Cumulative Frequency
79	0.9961	0.0883
	(0.9804)	
78	0.9618	0.1004

b. Water Level Probability from Tides, Storm Surge, and Wave Setup. The tide probability tables can also be used when determining design water level due to the combined effect of storm surge and tides. The tables provide the essential input on tides to be used in the joint probability approach.

CHAPTER 3

STORM SURGES

3-1. Storm Surge Generation. Storms are atmospheric disturbances characterized by one or more low pressure centers and high winds, frequently accompanied by precipitation of varying intensity. An important distinction is made in classifying storms: a storm originating in the tropics is called a "tropical storm;" a storm resulting from the interaction of a warm and a cold front is called an "extratropical storm;" and a severe tropical storm is referred to as a "hurricane" or "tropical cyclone" when the maximum sustained winds equal or exceed 75 miles per hour. Unlike extratropical storms and less severe tropical storms, hurricanes are well organized with respect to the wind patterns. The spatial scale of hurricanes is typically small in comparison to major extratropical storms. Both hurricanes and extratropical storms are capable of causing a significant rise or possible fall in the normal water level in coastal waters. A brief overview of procedures for estimating and predicting these abnormal water levels is provided in this chapter.

a. Tropical Storms and Hurricanes. Pronounced water level changes due to tropical storms may occur anywhere along the Gulf coast and anywhere from Cape Cod to the southern tip of Florida on the east coast of the United States. Occasionally, the southern coast of California on the west coast experiences changes in water level as a result of a tropical storm, but these are usually small due to the narrow continental shelf in that region.

(1) Many dangerous and destructive tropical storms have occurred along the Atlantic and Gulf coast areas of the United States. In many coastal areas, a severe storm causes the water level to rise in excess of 15 ft above the normal level on the open coast and even higher in estuaries and other inland areas. The elevated coastal waters due to surges provide a higher level in which short-period surface waves can propagate, thus subjecting beaches and structures to wave forces not ordinarily experienced. Surges coupled with the action of surface waves are responsible for the greatest damage to coastal areas. They can destroy or severely damage dwellings, business establishments, commercial properties, and docking facilities, erode beaches, displace stones or concrete armor units on jetties, groins, or breakwaters, undermine structures via scouring, cut new inlets through barrier beaches, and shoal navigational channels. The latter shoaling problem can result in hazards to navigation which impede vessel traffic and hamper harbor operations. The duration of the surge as well as the elevation is important for beach erosion and channel shoaling considerations.

(2) The wind pattern of a hurricane is more or less circular, with winds revolving counterclockwise in the northern hemisphere about the storm center or eye (not necessarily the geometric center). Winds in hurricanes blow spirally inward and not along a circle concentric with the storm center. Wind isovel patterns and wind directions are illustrated in Figure 3-1(a). The eye is characterized as an area of low atmospheric pressure and light winds. Atmospheric pressure increases with distance from the eye to the periphery or outskirts of the hurricane. Highest wind speeds usually occur in the right quadrants of the hurricane at a distance varying from about 4 to 70 nautical miles from the center. In all directions outward from the eye of the

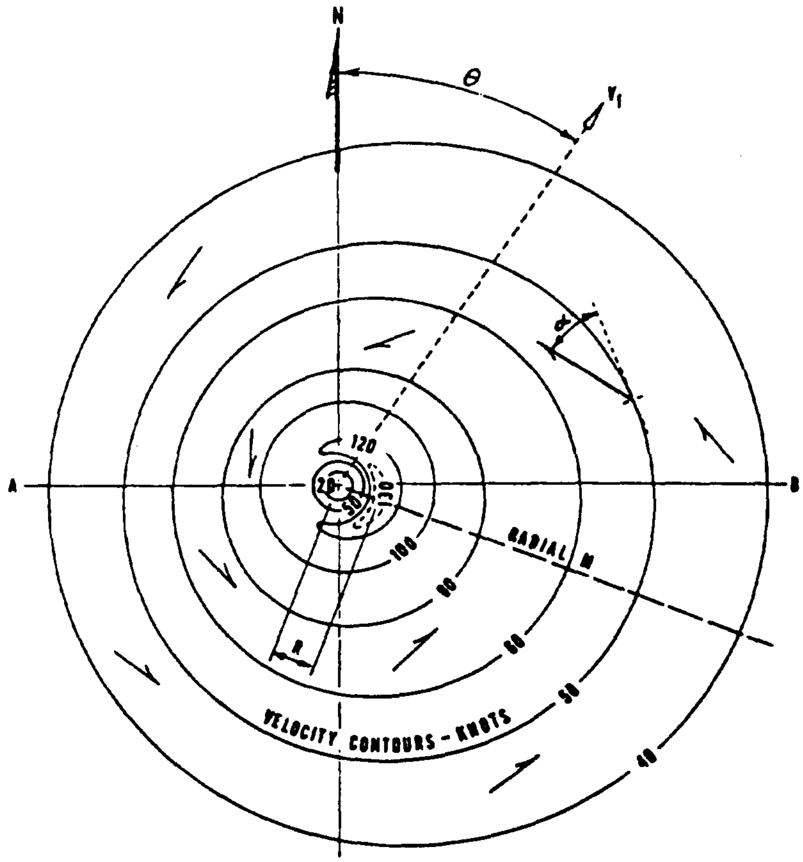

a. Wind isovel pattern and pertinent parameters

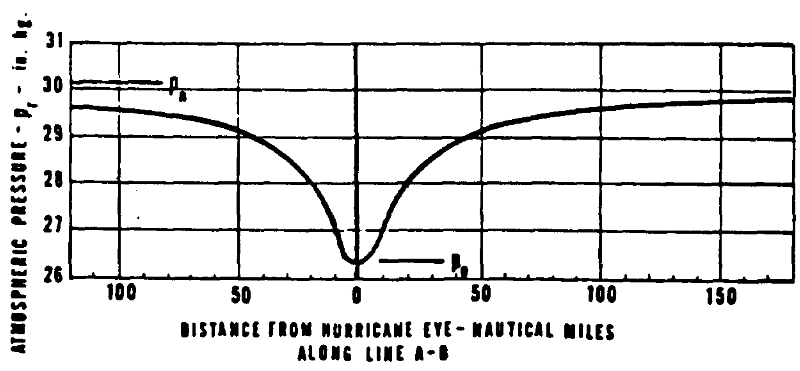

b. Pressure profile

Figure 3-1. Sketch showing hurricane parameters hurricane, wind speed increases rapidly to a maximum and then decreases with distance to the outskirts of the storm. The best single index for estimating the surge potential of a hurricane is the atmospheric pressure within the eye and is referred to as the central pressure index (CPI). In general, the lower the CPI, the higher the wind speeds. Other important parameters of a hurricane with regard to the surge potential are the radius of maximum winds R which is an index of the size of storm, the speed of forward motion of the storm system V_F, and the track direction θ in which a hurricane moves (measured clockwise from north).

(3) In engineering studies hypothetical hurricanes are frequently used to assess the levels of flooding for a predetermined degree of severity. These storms are derived based on the specification of meteorological parameters R, V_f, P_o, P_n, θ, and α in which P_o is the central pressure, P_n is the peripheral pressure, and α is the inflow angle (see Figure 3-1). It has been general practice to use invariant meteorological parameters for any given hypothetical hurricane prior to the storm making landfall. Thus, such storms are classified as constant valued hurricanes. Particular hypothetical hurricanes which have been used in some engineering investigations are referred to as the Standard Project Hurricane (SPH) and the Probable Maximum Hurricane (PMH). The SPH is defined as a hurricane having a severe combination of values of meteorological parameters that will give high sustained wind speeds reasonably characteristic of a specified coastal location. A PMH, on the other hand, is defined as a hurricane having a combination of values of meteorological parameters that will give the highest sustained wind speed that can probably occur at a specified coastal location. Recurrence intervals for the SPH and PMH are not assigned due to the uncertainties involved in establishing the frequencies. The SPH is used in the design of coastal works where a rather high degree of protection is required. The PMH was developed in connection with the design of nuclear power generation plants sited in coastal areas.

(4) Hypothetical hurricanes with more frequent recurrence intervals than the SPH are also used to estimate the frequency and levels of flooding. The flood frequencies are established by calculating the water levels produced by numerous hypothetical hurricanes and assessing the recurrence intervals by application of the joint probability method

b. Extratropical Storms. Large changes in water level may occur along the northern part of the east coast of the United States as a result of extratropical storms in which strong winds blow from a northeasterly direction. These storms are commonly referred to as "northeasters." Northeasters are important from the standpoint of design considerations on the east coast. However, an acceptable technique for specifying the wind fields for design storms is not presently available.

3-2. Prediction Models.

a. Numerical Prediction Models. Storm surge prediction for design is usually based on a theoretical approach, although in some cases sufficient data may be available at a site to warrant the historical approach discussed in Section 3-2.b. In the use of the theoretical approach, a number of mathematical or numerical models have been developed for simulating the storm wind fields and the storm-induced water motions. Computer programs are used in conjunction with the models to perform the necessary calculations. The models are formulated based on the governing hydrodynamic equations.

(1) The approach is also applicable to problems involving the SPH and PMH. In all studies concerned with water level determinations in coastal areas as a result of hurricanes the SPH is to be a part of the analysis except in the case that the design is to be based on the PMH.

(2) The magnitude and frequency of occurrence of storm-induced water levels coupled with the effects of astronomical tide is established by synthetic methods. The methods consist of an indirect approach in which water level data are generated from a rather large ensemble of synthetic storms via numerical computations, and flood frequencies are established based on an analysis of the computed water level data. A large variety of synthetic storms may be derived by utilizing various combinations of storm parameter probabilities that are characteristic of a given coastal location. Historical data of the individual storm parameters are used in the determination of the statistical distribution of the parameters. The statistical concept referred to as the joint probability method is used to determine the magnitude and frequency of occurrence of water levels when using the synthetic approach.

(3) The primary advantage of this method is that a rather large data base can be generated based on various combinations of the storm parameters. Also, the storm parameters are reasonably well defined due to the availability of regional historical data and the present technology available for describing meteorological aspects of storms, particularly hurricanes. In addition, computational hydrodynamics have advanced to the state that water levels can be computed with a reasonable degree of accuracy.

b. Historical Prediction Models. An accumulation of water level data from past storms over a span of many years at a given location may provide sufficient information for predicting design water level at that location. Rather long-period records of water level data are required to confidently predict the frequency and magnitude of flood levels by the historical data approach since the underlying assumption for this method is that past events are representative of future events.

(1) A subjective decision must be made with regard to whether the historical method should be used or not used for a given engineering study. This decision depends on the quantity and quality of data that are available as well as confidence that the sample data are representative of future events. With regard to the quantity of data, item 5 indicates that as a rule of thumb, at least N/2 years of data are required to confidently predict the annual percent chance of occurrence of an event with an average return interval of N years. This implies that data recorded over a period of 50 years would be required to confidently predict the elevation of the water surface with a 1 percent chance of occurrence.

(2) The historical method is considered applicable to various sites along the New England coast and other coastal areas where relatively long-term water level records exist. In general this method has limited usage due to the lack of sufficient historical data.

(3) From a statistical point of view, historical flood levels are not all from the same population. This is due to the observed levels that can be produced from either extratropical storms, tropical storms, or severe tropical storms (hurricanes) coincident with fluctuations caused by the astronomical tide. Consequently, mixed populations are always involved. As an approximation, however, it is generally considered appropriate to treat the entire water level record as a single population provided that the record is of sufficient length. In the event that a relatively short-term record, 20 years or less, is analyzed, the predicted astronomical tide should be extracted from the observed water levels and replaced with the mean high tide. The latter modification is recommended for the purpose of ensuring that the tide component is of sufficient magnitude.

c. Simplified Prediction Methods.

(1) Storm surge in an enclosed basin. The tilting of the water surface is an enclosed basin (e.g., lakes and reservoirs) caused by wind shear stress is known as wind setup. The water surface is above the normal still-water level (SWL) on the leeward side of the basin and below the SWL on the windward side. Wind setup can be reasonably estimated for basins of simple shape and long compared to their width, assuming motion in the long axis only. Wind setup, the rise in the water level at the leeward end relative to the SWL, may be estimated by

$$S = \frac{U^2 F}{1400 d} \qquad (3\text{-}1)$$

where

S = setup relative to the SWL (ft)

U = wind speed (mph)

F = fetch (miles)

d = average water depth over fetch (ft)

Wind speed is assumed by default to represent an elevation of 33 feet (10 meters). The coefficient in equation 3-1 is an average value based on previous investigations. The coefficient may vary for different basins. Advection of momentum, atmospheric pressure variation, astronomical effects, and precipitation are neglected. Also, a steady state is assumed to exist. Setup cannot be estimated satisfactorily by this method if natural barriers, such as islands, affect the horizontal water motions.

(2) Wave setup. Wave setup and setdown are the change in the mean water level due to the excess onshore momentum of the waves. At the shoreline there is normally a setup of the water surface relative to the SWL; whereas at the breaker line there is a setdown relative to the SWL (Figure 3-2).

(a) For monochomatic waves, the setdown at the breaker line S_b can be estimated

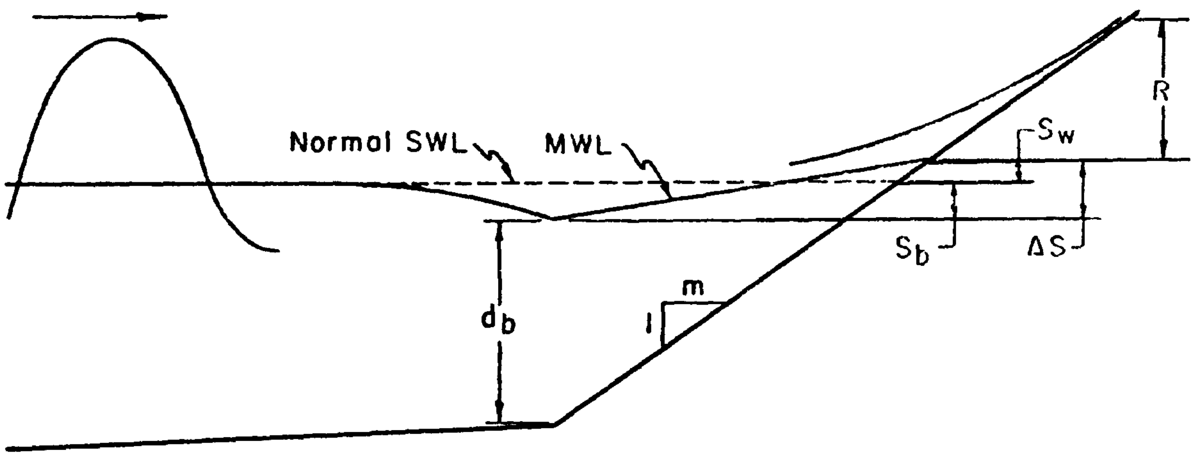

a. On a beach

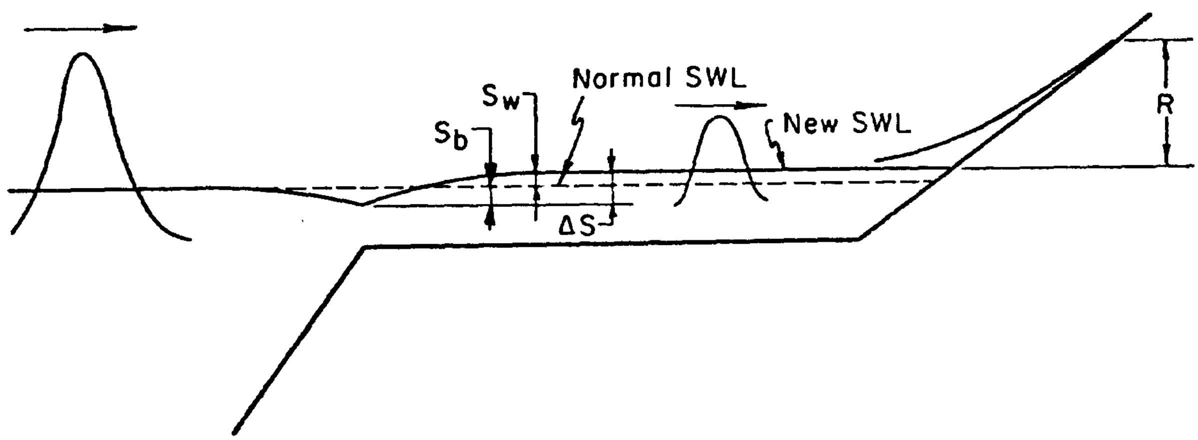

b. On a berm or reef

Figure 3-2. Definition sketch of wave setup

$$S_b = -\frac{g^{1/2}\left(H_o'\right)^2 T}{64\pi\, d_b^{3/2}} \qquad (3\text{-}2)$$

where

S_b = setdown at the breaker line relative to the SWL (ft)

T = wave period (sec)

H = equivalent unrefracted deepwater significant wave height (ft)

d_b = water depth at the breaker line (ft)

g = acceleration of gravity (ft/sec^2)

An approximation of the total difference in water surface elevation between the breaker line and the mean shoreline s , setup plus setdown, is expressed as

$$s = 0.15\, d_b \qquad (3\text{-}3)$$

based on laboratory data of item 113. Combining equations (3-2) and (3-3) yields an expression for the wave setup at the mean shoreline S_w as follows:

$$S_w = 0.15\, d_b - \frac{g^{1/2}\left(H_o'\right)^2 T}{64\pi\, d_b^{3/2}} \qquad (3\text{-}4)$$

where the water depth of breaking is given by the expression

$$d_b = \frac{H_b}{\dfrac{1.56}{1 + e^{-19.5m}} - \dfrac{43.75\,(1 - e)^{-19m}\, H_b}{gT^2}} \qquad (3\text{-}5)$$

with m equal to beach slope. Care must be taken to use consistent units for d_b , H_b , g , and T . The wave setup and setdown represent equilibrium conditions which require sufficient time to be established. The exact time to establish equilibrium is unknown, but the Shore Protection Manual (SPM) suggests a minimum duration of 1 hour.

(b) Wave setup should not be confused with wave runup. Runup is the greatest elevation above the SWL reached by the uprush of waves breaking on the shore. Measurements of wa/e runup include the effect of setup.

(3) Atmospheric pressure effect on water level. Table 3-1 gives the water level rise due to atmospheric pressure variation produced by a storm. The water level rise due to the atmospheric pressure can be linearly added to the water level rise due to other factors (eg., wind setup and wave setup).

3-3. Sources of Data for More Detail. Water level data recorded during storm periods may be obtained from a variety of sources. The principal source of

Table 3-1

Atmospheric Pressure Effect on Water Level

Storm Central Pressure mb	in. of Hg	Water Level Rise* ft
900	26.58	3.78
910	26.87	3.45
920	27.17	3.11
930	27.46	2.78
940	27.76	2.44
950	28.05	2.11
960	28.35	1.77
970	28.64	1.44
980	28.94	1.10
990	29.23	0.77
1000	29.53	0.43

*Relative to water level for atmospheric pressure of 1013 millibars = 29.91 inches of Hg.

recorded data is tide records of the NOS. Other sources of recorded data are gages operated by the Corps, USGS, and a few other organizations. High-water marks also provide a means for obtaining maximum water levels. They are, in general, inherently less reliable than measurements obtained from recording gages. Many sources are available for obtaining high-water marks such as those obtained by various government agencies, newspaper accounts, and private organizations. A principal source of high-water marks is poststorm reports prepared by district offices in the Corps. Maximum water levels from high-water marks are usually established from such effects as debris accumulation and mudline discoloration. In open areas these marks generally reflect both the water level rise and the maximum amplitude of short-period surface waves and possibly wave runup. There are no reliable techniques for establishing the true water level rise when surface wave effects are involved. The most preferable high-water marks are those for which surface waves are filtered out, such as pipe gages designed specifically for recording the maximum water level, within buildings, and other sheltered sites.

a. Transposing Data. Unfortunately, water level data are seldom available at the site for which the data are needed in connection with engineering studies. In the event there are sufficient and reliable water level data in the vicinity of the site, it may be possible to estimate the site data based on an adjustment to the existing data at nearby locations. Considerable care must be exercised in transposing the adjusted observed data to a nearby site.

b. More Information. Much more detailed information is given in Engineer Manual (EM) 1110-2-1412.

CHAPTER 4

TSUNAMI

4-1. Generation. Tsunami waves can be generated from a number of sources, including shallow-focus submarine earthquakes, volcanic eruptions, landslides and submarine slumps, and explosions. Each of these sources has its own generating mechanism, and the characteristics of the generated waves are dependent on the generating mechanism. The tsunami waves which travel long, transoceanic distances are normally generated by the tectonic activity associated with shallow-focus earthquakes. However, large waves can be generated locally by the other generating mechanisms. A comprehensive discussion of all aspects of tsunami engineering is given in item 11. Item 56 presents an assessment of state-of-the-art methods to establish tsunami, seich, and landslide-induced water wave hazards in the United States. Tsunami flood level predictions (100- and 500-year levels) have been made for the Hawaiian Islands in item 60, for the west coast of the continental United States in item 63, for southern California in item 57, for San Francisco Bay and Puget Sound in item 35, for American Samoa in item 58, and for Kodiak Island to Ketchikan, Alaska, in item 21. Additional information on tsunamis is also given in item 95.

a. Submarine Earthquakes. Tsunamis are generated by shallow-focus earthquakes of a dip-slip fault type; i.e., vertical motion upward on one side of the fault and downward on the other side (Figure 4-1). Laboratory and numerical studies indicate that where there is a positive net change in volume (e.g., a unipolar uplifting of the seafloor), waves of stable form (solitons) evolve, followed by a dispersive train of oscillatory waves. The number and amplitude of the solitons depends on the initial generating mechanism. The wave record for the 1964 tsunami at Wake Island (Figure 4-2, item 136) illustrates this type of wave generation.

(1) Horizontal motion of the seafloor does not appear to generate large tsunamis. However, large "local" tsunamis may be generated by horizontal motion (Fig. 4-3). A general expression for the lower limit of the earthquake magnitude M of tsunamigenic earthquakes is given in item 71 as

$$M = 6.3 + 0.005\ D_f \qquad (4\text{-}1)$$

based on tsunamigenic earthquakes in Japan, where D_f is the the focal depth in kilometers and M the magnitude on the Richter scale. Tsunamis usually do not occur for earthquake magnitudes less than those given by equation (4-1), although a small number of tsunamis of lesser magnitude have been associated with lesser magnitude earthquakes. Equation (4-1) does not consider the location of the earthquake with respect to the coastline, the configuration of the coastline, and possible local resonance effects. The Richter scale is given by

$$M = \frac{(\log E - 11.8)}{1.5} \qquad (4\text{-}2)$$

where E is the earthquake energy in ergs.

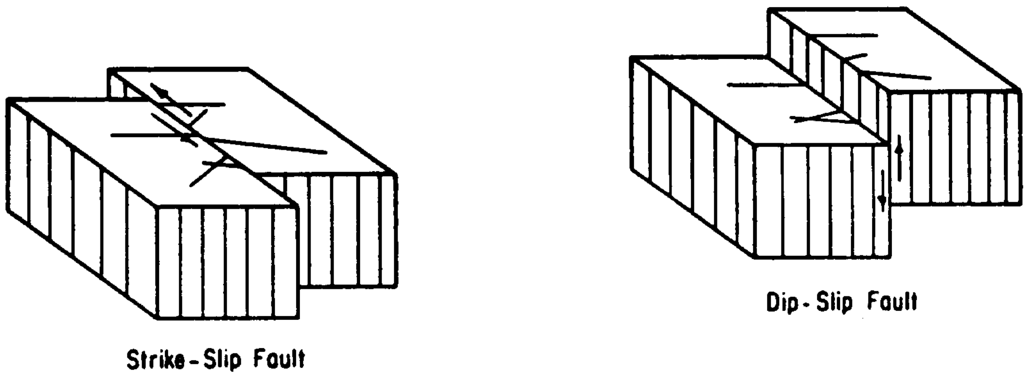

Figure 4-1. Movement along fault lines

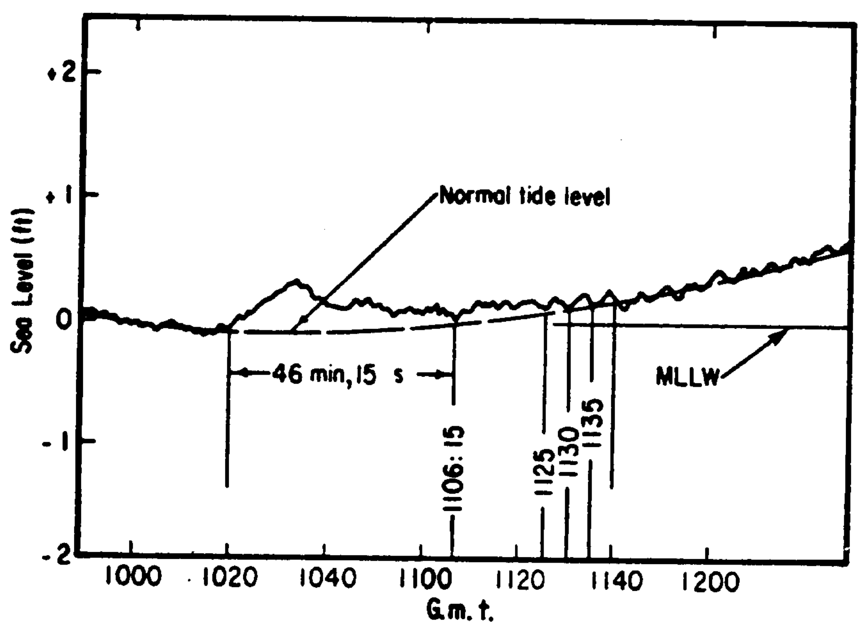

Figure 4-2. Wave record from Wake Island, showing arrival of tsunami (initial motion is positive and remains above normal tide curve for more than an hour) (from item 136)

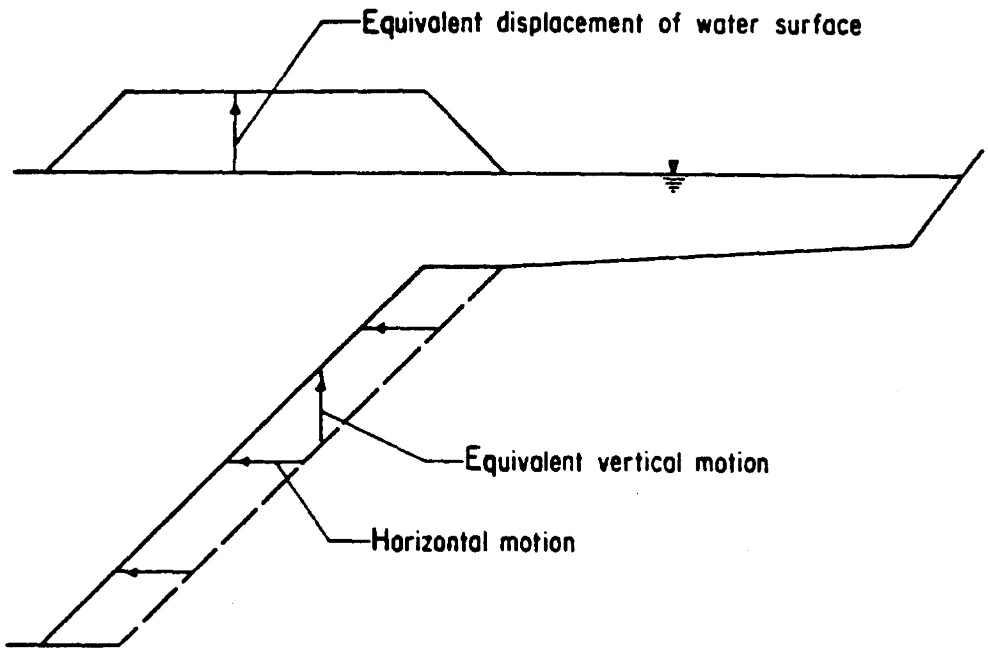

Figure 4-3. Horizontal motion normal to continental slope (scale exaggerated)

(2) Area and Height of Uplifting. An uplifting of the sea bottom will produce a vertical uplifting of the overlying water. Item 42 has shown for uplifts covering large spatial areas it may be assumed that the uplifting of the water surface equals the uplifting of the sea bottom and that the total uplifting occurs essentially instantaneously. The potential energy of the uplifted water is then given as

$$E = \sum_{i=1}^{n} \rho g \; A_i h_i \frac{h_i}{2} \tag{4-3}$$

where

E = energy in foot-pounds

ρ = density of the seawater, assumed to equal 1.989 slugs per cubic foot

g = gravitational acceleration, equal to 32.174 feet per second squared

A_i = an incremental area of uplifting

h_i = height of uplifting over the incremental area A_i

If the incremental areas are equal, i.e., $A_1 = A_2 = . . . = A_n$, then equation (4-3) can be rewritten as

$$E = \rho g A \frac{(h^2)_{avg}}{2} \tag{4-4}$$

where A is the total area and $(h^2)_{avg}$ is the average value of the square of the uplifted heights.

(a) For the 1964 Alaskan earthquake the height of uplifting varied considerably over the area of uplifting and had a maximum in excess of 49 feet at a point near Montague Island (item 89). The average value of h^2 was estimated as 44.1 square feet. The tsunami had a calculated potential energy of 1.67×10^{15} foot-pounds.

(b) When using equation (4-4) note that the average of the squared heights $(h^2)_{avg}$ is not equal to the average height squared $(h_{avg})^2$.

(3) Initial Wave Formation. Because of the long periods and corresponding long wavelengths of tsunamis, item 43 has shown the train of waves forming a tsunami can be taken to be shallow-water waves at its origin and propagated across the ocean as shallow-water waves. The actual form of the wave train is determined by the initial generating mechanism, i.e., the area of the uplifted sea bottom, the height and variation of the uplift within the area of uplift, and the depth of water and coastal characteristics in the generating area. While ordinary sea waves are assumed to have cnoidal shape as they approach a shore (i.e., high crests and shallow troughs), the waves in a tsunami may have various combinations of forms. The first noticeable wave may be a crest or trough depending on whether there is an uplift or drop in the ocean bottom at the source. The first crest is often not noticed visually because of its small height. Tsunamis may sometimes produce waves with narrow, deep troughs and low, wide crests at the shoreline, the opposite of the cnoidal waveform.

(a) Wave records from Wake Island for the March 1964 tsunami (item 136) show a positive surge with a period of 80 minutes (see Figure 4-2). There was a series of positive wave crests with the elevations of the intervening troughs above the normal expected tide level. This series was followed by a series of crests and troughs with the elevations of the troughs below the normal tide level. Using a shallow-water wave celerity at the source and an average depth of approximately 325 feet for the generating area, the period of the initial positive surge is approximately equivalent to the time required for the trailing edge of the initial uplifted water surface to travel completely across the area of generation. Thus, the uplifted water surface at the source appears to have formed a series of solitary waves. The multiple crest can be accounted for by initial instabilities in the waveform caused by the generating mechanism, and the effect of the varying bathymetry of the ocean basin through which the wave passes. The lower waves following the initial series of wave crests correspond to the expected oscillations from a disturbance in the water surface as the disturbance is damped out.

(b) The height of a tsunami at a coastal point near the source of generation can be given as a first approximation by the empirical equation

$$\log_{10} H = 0.75\ M - 5.07 \qquad (4\text{-}5)$$

where H is the height in meters and M the Richter magnitude (item 145). This empirical relationship does not completely account for the characteristics of the generating mechanism or the coastline. Determination of actual wave heights would require computation by numerical or empirical means.

(c) The fault length L_f in kilometers may be approximated (item 142) as

$$\log_{10} L_f = 0.87\ M - 4.44 \qquad (4\text{-}6)$$

This equation also approximates the length of the generating area, i.e., the length along the initial wave crest.

(d) The period T (in minutes) of the primary tsunami (carrying maximum energy) can be estimated (item 144) from

$$\log_{10} T = 0.625\ M - 3.31 \qquad (4\text{-}7)$$

The initial deformation of the water surface, for any tsunami, will collapse into some system of waves which must be defined. The simplest means of analysis is to assume the water surface has an initial displacement equal to the seabed displacement, and is not time dependent (item 42), and then propagate the initial displacement outward from the generating area using long-wave equations (items 8 and 62). Other means of establishing the initial waves, with varying degrees of complexity, are described by item 145 and other sources.

(e) Many of the mathematical representations of waves generated from bottom uplifting are based on circular source regions; however, item 86 presents one solution in terms of elliptic coordinates for a source region which is more elongated than circular (item 11). Uplifts for large tsunamis are typically elliptical, and the elliptical shape produces strong directionality in the radiated energy.

(f) Item 64 used an elliptical-shaped generating area, with an instantaneously displaced water surface, as input data for a standard design tsunami in a numerical solution. They define the surface displacement as a modified elliptic paraboloid, having a parabolic cross section parallel to the major axis of the ellipse, and a triangular cross section parallel to the minor axis of the ellipse. The numerical propagation of the wave uses the same procedure as used in item 8. The potential energy of the uplifted water surface for this type of surface displacement is given by

$$E = 4\left(\frac{\rho g}{6}\right) \frac{b}{a} \frac{c^2}{a^4} \int_0^a \left(a^2 - x^2\right)^{5/2} dx \qquad (4\text{-}8)$$

where

ρ = density of the seawater (taken as 1.99 slugs per cubic foot)

b = length of the semiminor axis

a = length of the semimajor axis

c = maximum uplifted elevation at coordinates (x=o, y=o, z=c)

x = measurement along the major axis of the ellipse

y = measurement along the minor axis of the ellipse

z = vertical direction upward from the undisturbed water surface

(g) The height of the wave in the direction perpendicular to the major axis of the ellipse is larger than the height of the wave perpendicular to the minor axis of the ellipse by the ratio of the major to minor axis lengths.

b. Volcanic Activity. Although most major tsunamis have been caused by shallow-focus earthquakes, a small percentage have been caused by volcanic activity which includes localized earthquakes, shoreline and submarine slumps, and volcanic explosions. Tsunamis with volcanic origins have the characteristics of waves generated from a small source area. These waves spread geometrically and do not cause large wave runup at locations distant from the source, but they may cause very large waves near the source. Also, there may be refraction effects which trap waves along the coastline, or standing edge waves may be generated along the coastline.

c. Landslides and Submarine Slumps. Landslides and submarine slumps can occur from various causes but are often associated with earthquakes. The waves generated by such events will spread geometrically as they propagate from their source in an open ocean, but they can be very high near their origin. Waves can be particularly high if they occur in a confined inlet or if resonant or refraction effects exist. Examples are cited in items 11 and 56.

d. Explosions. An explosion acts as an impulsive-generating mechanism which generates dispersive waves from a point source. Data from nuclear explosion Baker at Bikini Atoll in 1946 show that the wave height in shallow water is approximately inversely proportional to the radial distance from the point of origin; i.e., Hr = constant where H is the height of the wave, and r is the radial distance from the point source. At a radial distance equal to 35d, where d is the water depth, the relationship changes slightly, with the wave height decreasing less rapidly. A large number of tests conducted by the US Army Engineer Waterways Experiment Station (CEWES) have shown the inverse relationship between height and period to hold in deep water at any distance from the explosion. Item 141 discusses data on wave dispersion.

(1) The height of a wave generated by an explosion has been shown to be dependent on the depth of the explosion charge. Van Dorn, Le Mehaute, and item 137 show that two critical depths exist which will produce the highest waves for any given explosive charge. The critical depths are dependent on the charge yield (given in equivalent pounds of TNT).

(2) Extensive material is available on waves generated by explosions (item 121). Item 61 developed a numerical model that calculates explosion waves generated by conventional or nuclear detonations.

4-2. <u>Propagation</u>. After determining the initial disturbance of the water surface, as discussed in Section 4-1, the propagation of the tsunami to nearby or distant shorelines must be analyzed. Because tsunamis generated by large uplifts are long-period waves with long wavelengths in relation to both the water depth and the wave height, long-wave equations can be used (item 43). Dispersive equations may be required for tsunamis generated by uplift covering relatively small spatial areas. The importance of frequency dispersion is a function of the distance the waves must propagate. Item 43 presents criteria for determining when dispersion will be important.

a. Small-Amplitude Waves.

(1) The simplest means of analyzing the wave motion, where the ratio of the wave height to water depth H/d is small, is to use the small-amplitude solutions to the wave equations and the assumption that the ratio of wavelength L to water depth is very large. The wave celerity C is given by

$$C = (gd)^{1/2} \tag{4-9}$$

If the disturbed water surface elevation η at any point relative to its undisturbed location is given by

$$\eta = a \cos 2\pi\left(\frac{x}{L} - \frac{t}{T}\right) \tag{4-10}$$

where

a = amplitude of the wave above the undisturbed water level

x = distance measured in the direction of wave motion

t = time

T = wave period

then the horizontal velocity of a water particle in the direction of the wave motion u is

$$u = \frac{\eta}{d}(gd)^{1/2} = \frac{\eta g^{1/2}}{d^{1/2}} \tag{4-11}$$

The horizontal displacement of the water particle from its undisturbed position ξ is given by

$$\xi = -\frac{\eta L}{2\pi d} \tag{4-12}$$

Maximum values of u and ξ are given by

$$\left|u_{max}\right| = \frac{ag^{1/2}}{d^{1/2}} \tag{4-13}$$

$$\left|\xi_{max}\right| = \frac{aL}{2\pi d} \tag{4-14}$$

(2) A simple, first-order solution for the shoaling of an unrefracted, small-amplitude, shallow-water wave is given by

$$\frac{H_2}{H_1} = \left(\frac{d_1}{d_2}\right)^{1/4} \tag{4-15}$$

$$\frac{\left|u_{max_2}\right|}{\left|u_{max_1}\right|} = \left(\frac{d_1}{d_2}\right)^{3/4} \tag{4-16}$$

$$\frac{\left|\xi_{max_2}\right|}{\left|\xi_{max_1}\right|} = \left(\frac{d_1}{d_2}\right)^{3/4} \tag{4-17}$$

These equations do not account for wave refraction, diffraction, or dispersion. They cannot be used with any degree of accuracy when the ratio of H/d becomes large. Equation (4-15) does not account for wave reflection from bottom slopes and results in calculated wave amplitudes that are too high. When waves travel long distances, it is necessary to consider the curvature of the earth, discussed later in this section.

* * * * * * * * * * * * * * * EXAMPLE PROBLEM 4-1 * * * * * * * * * * * * * * *

GIVEN: A long wave with a period of 20 minutes and a height H of 1.31 foot passes from a 3,280-foot water depth into a 1,640-foot water depth. The wave is assumed to be nondispersive.

FIND:

(a) The unrefracted wave height in the 1,640-foot depth.

(b) The water particle velocity u_{max} in each water depth.

SOLUTION:

(a) $H_1 = 1.31$ ft, $d_1 = 3{,}280$ ft, $d_2 = 1{,}640$ ft

From equation (4-15),

$$\frac{H_2}{H_1} = \left(\frac{d_1}{d_2}\right)^{1/4}$$

$$\frac{H_{1,640}}{1.31} = \left(\frac{3{,}280}{1{,}640}\right)^{1/4} = 1.189$$

$$H_{1,640} = 1.31(1.189) = 1.56 \text{ ft}$$

(b) From equation (4-13),

$$u_{max} = \frac{ag^{1/2}}{d^{1/2}}$$

Assuming $a = \frac{H_1}{2} = 0.66$ ft, at $d_1 = 3{,}280$ ft,

$$u_{max\ 3,280} = \frac{0.66(32.174)^{1/2}}{(3{,}280)^{1/2}} = 0.065 \text{ ft/s}$$

From equation 4-16 where $d_2 = 1{,}640$ ft,

$$\frac{u_{max_2}}{u_{max_1}} = \left(\frac{d_1}{d_2}\right)^{3/4}$$

$$\frac{u_{max\ 1,640}}{u_{max\ 3,280}} = \left(\frac{3{,}280}{1{,}640}\right)^{3/4}$$

$$u_{max\ 1,640} = 0.065\left(\frac{3{,}280}{1{,}640}\right)^{3/4} = 0.11 \text{ ft/s}$$

* *

b. Long-Wave Equations. Since tsunamis have wavelengths much greater than water depths even in the deep ocean, long-wave equations govern their propagation. There have been questions concerning the importance of nonlinearities and dispersion on tsunami propagation, and these questions have been addressed by several investigators using both numerical models and laboratory measurements.

(1) Tuck (item 127) uses heuristic arguments based on the magnitudes of tsunami wavelengths and wave heights to water depths to conclude that, for large tsunamis such as the 1964 Alaskan tsunami, linear long-wave equations are adequate to describe most of the tsunami generation, propagation, and reflection processes. Hammack (item 42), in a series of detailed laboratory experiments and calculations employing the Korteweg and deVries (KdV) equation (includes frequency dispersion and nonlinear terms), concluded linear theory is applicable for determining tsunami generation for large tsunamis such as the 1964 Alaskan tsunami. In subsequent work using the KdV equation, Hammack (item 42) concluded the propagation of the lead wave of a two-dimensional tsunami is modeled by linear nondispersive theory for almost its entire trajectory. The KdV equation was found to be valid, but unnecessary, while linear dispersive theory was found never to apply. The trajectory was explained to extend from the source region to the vicinity of a beach. Nonlinearities were found to be negligible in the generation region and for deep ocean propagation. Frequency dispersion was shown to be negligible for the lead wave of the 1964 Alaskan tsunami until it propagated approximately

100 hours (equivalent to a propagation distance of approximately 50,000 miles). Carrier (items 12) and Kajiura (item 82) obtained similar results in separate analyses.

(2) The unimportance of nonlinearities and frequency dispersion for generation and deep ocean propagation of large tsunamis was confirmed by numerical simulations of the 1964 Alaskan tsunami and comparisons of results with a deepwater gage at Wake Island (item 69) and with tide gages in the Hawaiian Islands (item 60).

c. Distantly Generated Tsunamis. When a tsunami travels a long distance across the ocean, the sphericity of the Earth must be considered to determine the effects of the tsunami on a distant shoreline. Waves which diverge near their source will converge again at a point on the opposite side of the ocean. An example of this was the 1960 tsunami whose source was on the Chilean coastline. As a result of the convergence of unrefracted waves rays, the coast of Japan suffered substantial damage, and many deaths occurred. Figure 4-4 illustrates the convergence of the wave rays due to the Earth's sphericity. Items 35, 51, 60, 63 and 69 all solve linear long-wave equations in spherical coordinates to solve tsunami propagation over the deep ocean.

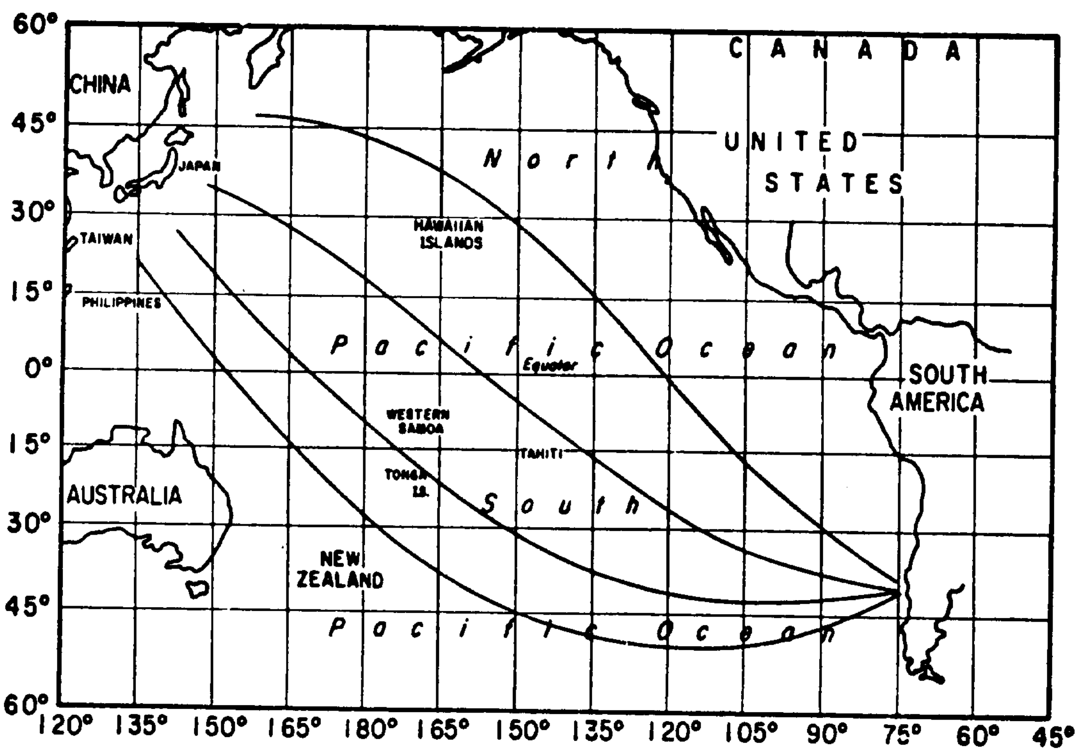

Figure 4-4. Convergence of wave rays

d. Nearshore Propagation. Hammack (item 42) considered tsunami propagation from the deep ocean to the nearshore area using the KdV equation and concluded linear nondispersive theory could be used until the lead wave propagates a distance of at least 200 miles across the continental shelf. Item 40 discusses laboratory experiments and calculations using Boussinesq equations (similar to the KdV equations, but allowing wave propagation in two directions) and concludes that the propagation of tsunamis from the deep ocean to the continental shelf break and for some distance onto the shelf could be predicted as well by linear nondispersive theory as by nonlinear theories. Items 35 and 57 discuss numerical simulations of the 1964 Alaskan tsunami demonstrating by comparisons with nine tide gages on the west coast of the continental United States that linear nondispersive equations are adequate to govern tsunami generation, propagation across the deep ocean, and propagation over the continental shelf to shore. Item 59 demonstrates nonlinear long-wave equations which are adequate to describe tsunami flooding over dry land (nonbore tsunamis).

e. Computer Model. Solutions of the equations for long water waves are obtained by numerical means. Notable approaches are described in items 21, 35, 57, 60, 62, 63, and 70.

(1) One difficulty in numerical modeling is the specification of boundary conditions for the computational area. All of these investigators use solid boundaries at coastlines and fictitious open boundaries at edges of the computational area where it is necessary to truncate the region of computation. At solid boundaries, complete reflection is assumed. At open boundaries, the wave is assumed to travel without change in form across the final space step. These assumptions introduce errors into the computations which limit the length of real-time records which can be simulated numerically. At a shoreline, some amount of wave energy may be trapped so that complete reflection does not occur. Wave trapping is discussed later in this chapter.

(2) For waves in the nearshore region, several notable numerical modeling approaches are available, including items 16, 57, 60, and 63. Listings of typical computer programs for solutions of long-wave equations can be found in item 8 for linear long-wave equations and item 59 for nonlinear long-wave equations.

f. Tsunamis Approaching the Shoreline. As a tsunami approaches a coastline, the waves are modified by the various offshore and coastal features. Submerged ridges and reefs, continental shelves, headlands, various shaped bays, and the steepness of the beach slope may modify the wave period and wave height, cause wave resonance, reflect wave energy, and cause the waves to form bores which surge onto the shoreline. Ocean ridges, however, provide very little protection to a coastline.

(1) Abrupt Depth Transitions. An ocean shelf along a coastline may cause greater modification to a tsunami than an ocean ridge. Waves may become higher and shorter, and dispersion may occur. The equations for a single nondispersive wave passing over an abrupt change in water depth (as shown in Figure 4-5) are given by

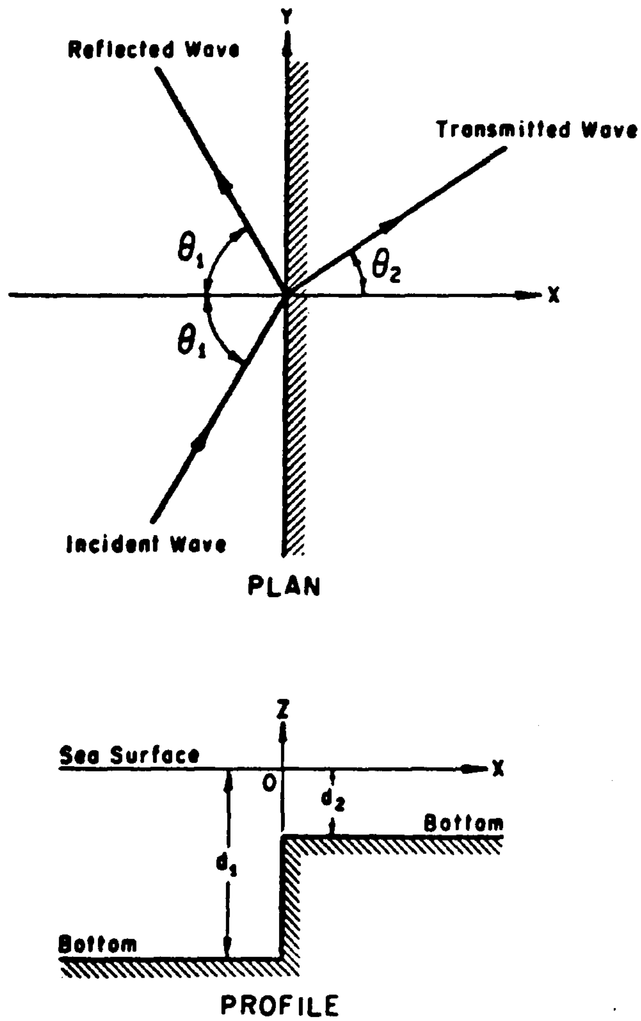

Figure 4-5. Wave passing onto shelf

$$\frac{H_r}{H_i} = \frac{\sqrt{d_1}\cos\theta_1 - \sqrt{d_2}\cos\theta_2}{\sqrt{d_1}\cos\theta_1 + \sqrt{d_2}\cos\theta_2} \tag{4-18}$$

$$\frac{H_t}{H_i} = \frac{2\sqrt{d_1}\cos\theta_1}{\sqrt{d_1}\cos\theta_1 + \sqrt{d_2}\cos\theta_2} \tag{4-19}$$

$$\frac{H_t}{H_i} = 1 + \frac{H_r}{H_i} \tag{4-20}$$

where

H_r = reflected wave height

H_i = incident wave height

d_1 = initial water depth

d_2 = water depth under the transmitted waves

H_t = transmitted wave height

θ_1 = incident wave angle

θ_2 = transmitted wave angle

For a given incident wave angle θ_1 , the value of θ_2 can be determined using Snell's Law (item 25) so that

$$\sin \theta_2 = (\sin \theta_1) \left(\frac{d_2}{d_1}\right)^{1/2} \tag{4-21}$$

(a) These equations, as written, apply to shallow-water waves; wave dispersion on the shelf is not considered. The solutions to the equation for reflected wave height are presented graphically in Figure 4-6. The equations predict that substantial reflection will occur when a wave passes from deep water to shallow water and when a wave passes from shallow water to deep water. It is assumed that no energy loss occurs and that a single incident wave splits into a single reflected wave and a single transmitted wave.

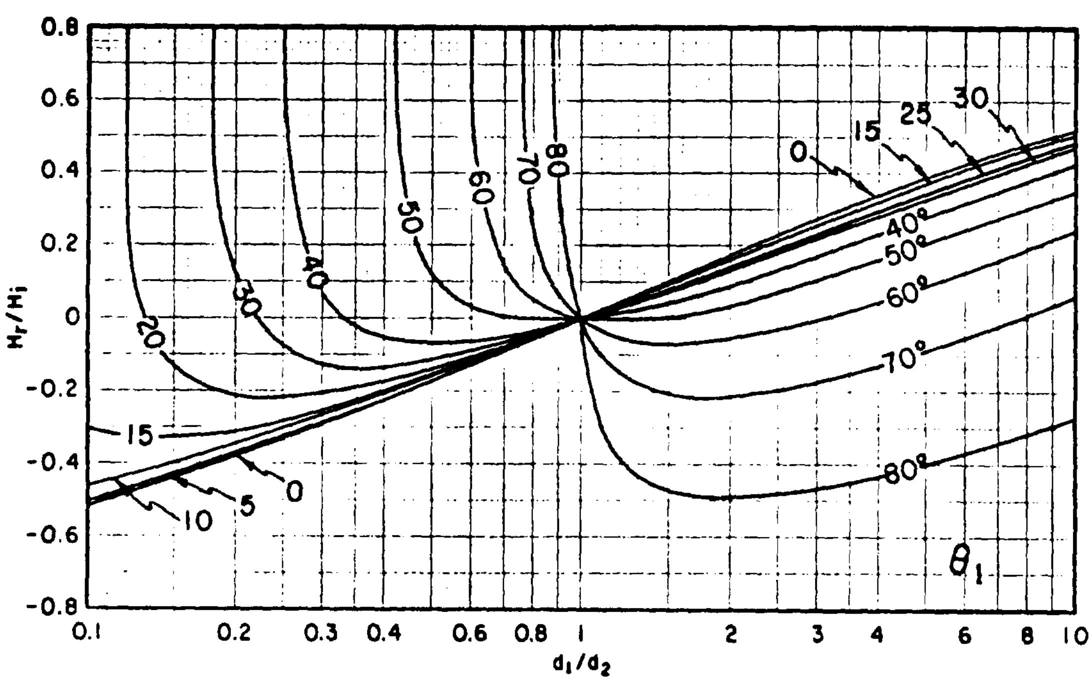

Figure 4-6. Wave reflection from a shelf (after item 20)

* * * * * * * * * * * * * * * EXAMPLE PROBLEM 4-2 * * * * * * * * * * * * * * *

GIVEN: An incident wave with a height of 3.28 feet and a period of 30 minutes approaches a coastline through water 8,200 feet deep and passes onto a shelf where the water depth is 328 feet, at an angle of incidence $\theta_1 = 30$ degrees.

FIND:

(a) The angle at which the transmitted wave propagates onto the shelf

(b) The height of the reflected wave.

(c) The height of the transmitted wave.

SOLUTION:

(a) From equation (4-21):

$$\sin \theta_2 = \left(\frac{d_2}{d_1}\right)^{1/2} \sin \theta_1$$

$$\theta_2 = \sin^{-1} \left[\left(\frac{328}{8,200}\right)^{1/2} \sin 30^\circ\right] = \sin^{-1} (0.1)$$

$$\theta_2 = 5.74^\circ$$

(b) From equation (4-18):

$$H_r = \frac{\sqrt{d_1} \cos \theta_1 - \sqrt{d_2} \cos \theta_2}{\sqrt{d_1} \cos \theta_1 + \sqrt{d_2} \cos \theta_2} (H_i)$$

$$H_r = \frac{\sqrt{8,200} \cos 30^\circ - \sqrt{328} \cos 5.74^\circ}{\sqrt{8,200} \cos 30^\circ + \sqrt{328} \cos 5.74^\circ} (3.28) = 2.05 \text{ ft}$$

(c) From equation (4-20):

$$H_t = H_i + H_r$$

$$H_t = 3.28 + 2.05 = 5.33 \text{ ft}$$

* *

(b) Reflected waves are normally of secondary, but not negligible, magnitude according to theory. At given stations, convergence may cause reflected waves to be of primary magnitude, but this occurs only in relatively few cases.

(2) Linear Depth Transitions. The case of a wave normally incident on a linear change in water depth is shown in Figure 4-7. Defining a parameter, Z_1, as

$$Z_1 = \frac{4\pi d_1}{L_1 S} \tag{4-22}$$

the transmission coefficient

$$K_t = \frac{H_t}{H_i} \tag{4-23}$$

and the reflection coefficient

$$K_r = \frac{H_r}{H_i} \tag{4-24}$$

Item 22 cites the results shown in Figure 4-8. When $d_1/d_2 < 1.0$, the value of the reflection coefficient K_r is negative. When $d_1/d_2 > 1.0$, the value of K_r is positive.

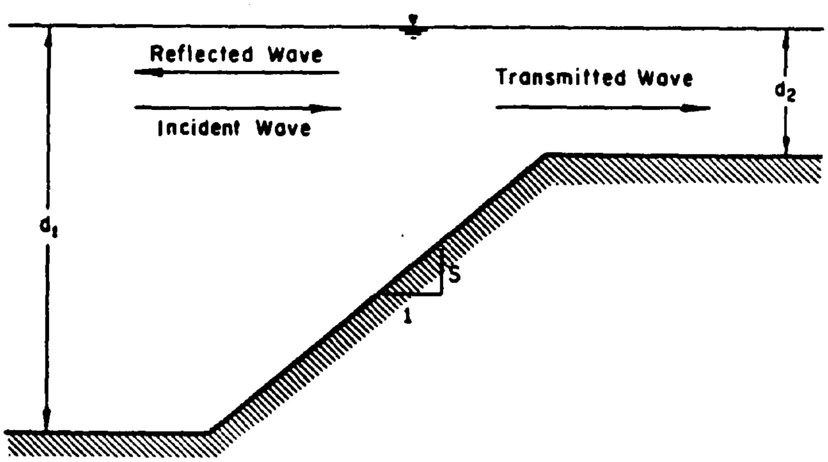

Figure 4-7. Linear slope and shelf

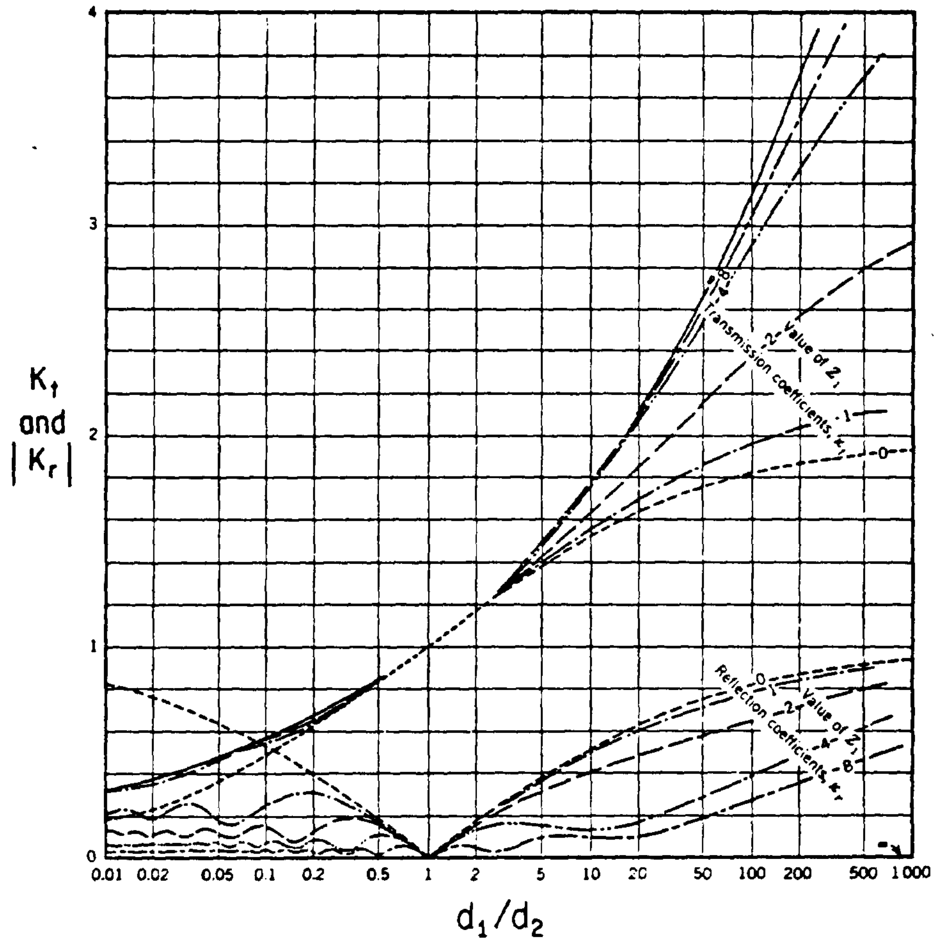

Figure 4-8. Reflection and transmission coefficients (item 22)

* * * * * * * * * * * * * * EXAMPLE PROBLEM 4-3 * * * * * * * * * * * * * * *

GIVEN: An incident wave, which is 1.64 feet high and has a period of 40 minutes, recedes from the coastline through water 328 feet deep and passes from the shallow water over a shelf into water 9,925 feet deep. The transition between the two water depths is a linear slope S = 0.1, and the wave is at a zero angle of incidence with the slope transition, i.e., $\theta_1 = 0$.

FIND:

(a) The height of the reflected wave.

(b) The height of the transmitted wave.

SOLUTION:

(a) $L_1 = C_1 \, T = \sqrt{gd_1} \, T$

$$L_1 = \sqrt{32.2 \times 328} \; (40 \times 60) = 247{,}000 \text{ ft}$$

From equation (4-22),

$$Z_1 = \frac{4\pi d_1}{L_1 S}$$

$$Z_1 = \frac{4\pi \times 328}{247{,}100 \times 0.1} = 0.167$$

From Figure 4-8, where

$$\frac{d_1}{d_2} = \frac{328}{9{,}925} = 0.033 \text{ and } Z_1 = 0.167$$

it is found that

$K_r \simeq -0.62$ (the negative sign indicates that the reflected wave is π radians out of phase with incident wave)

$H_r = 0.62\ H_i = 0.62(1.64) = 1.02$ ft

(b) From Figure 4-8,

$K_t \simeq 0.32$

$H_t = 0.32\ H_i = 0.32(1.64) = 0.52$ ft

* *

(3) Nonlinear Depth Transitions. Nondispersive waves passing from deep water to shallow water over the nonlinear slope profile shown in Figure 4-9 were investigated (item 81). The profile is defined by the equation

$$\frac{1}{d(x)} = \frac{1}{2}\left(\frac{1}{d_1} + \frac{1}{d_2}\right) - \frac{1}{2}\left(\frac{1}{d_2} - \frac{1}{d_1}\right) \tanh\left(\frac{nx}{2}\right) \qquad (4\text{-}25)$$

where the effective slope length ℓ is given by

$$\ell = \frac{2\pi}{n} \qquad (4\text{-}26)$$

where n is an arbitrary small number in equation (4-25) which fits the equation to the actual slope and determines the length of the slope in equation (4-26). The reflection coefficient obtained by item 81 is given by the equation

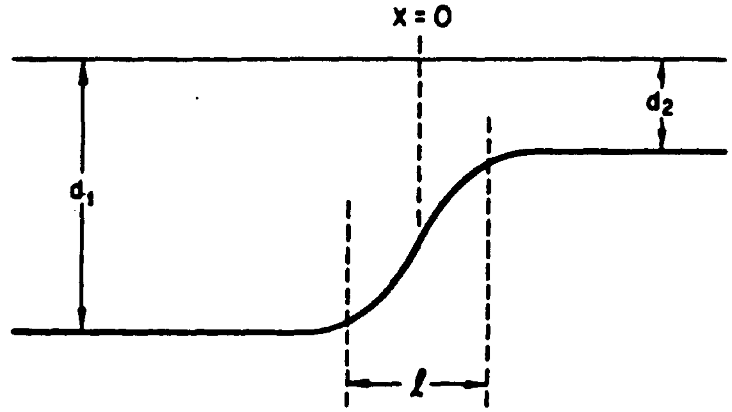

Figure 4-9. Slope and shelf

$$\frac{H_r}{H_i} = \frac{\sinh\left[\pi\left(\frac{\ell}{L_2} - \frac{\ell}{L_1}\right)\right]}{\sinh\left[\pi\left(\frac{\ell}{L_2} + \frac{\ell}{L_1}\right)\right]} \tag{4-27}$$

where

L_1 = wavelength at depth d_1

L_2 = wavelength at depth d_2

The solution is plotted in Figure 4-10. As shown in the figure, the reflection coefficient approaches zero as the slope length ℓ approaches the length of the incident wave L_1.

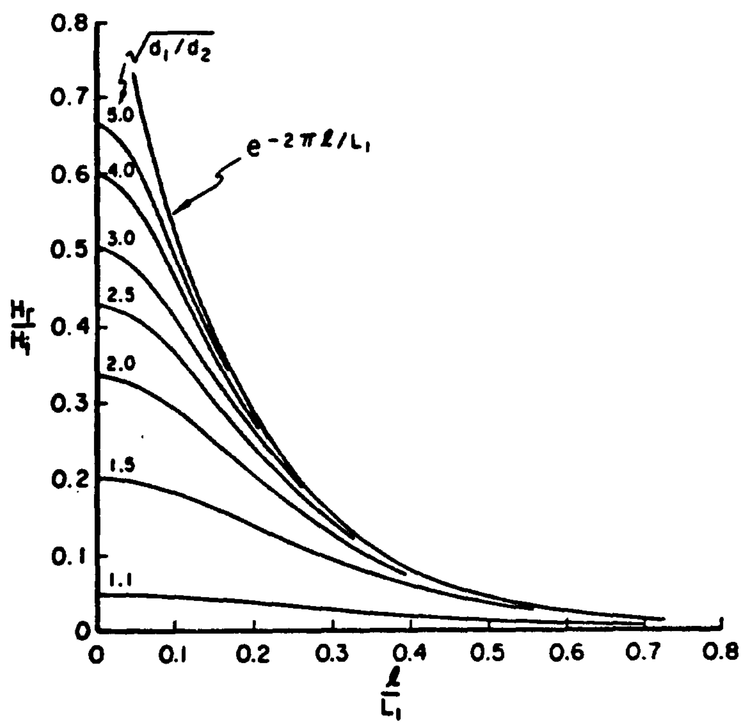

Figure 4-10. Reflection coefficients (from item 81)

4-3. Tsunami-Shoreline Interaction. In addition to the shoaling of waves on the nearshore slope, a tsunami may interact with a shoreline in a number of different ways, including standing wave resonance at the shoreline, the generation of edge waves by the impulse of the incident waves, the trapping of reflected incident waves by refraction, and, as the reflected wave from the shoreline propagates seaward, the reflection of wave energy from an abrupt change in water depth at the seaward edge of a shelf. Also, a wave arriving at an oblique angle to the shoreline may produce a Mach-stem along the shoreline. All of the above interactions depend on wave reflection at the shoreline. Tsunamis entering inlets and harbors may also produce resonant conditions within the inlets and harbors. Numerical models for tsunami-shoreline interaction are presented in items 57, 59, 60, and 63.

a. Wave Reflection. The reflection of an incident wave ray from a shoreline is illustrated in Figure 4-11. The angle α_1 between the wave ray and a line normal to a tangent to the shoreline will have the same value for the incident and the reflected wave rays. For a steep nearshore slope, the reflected wave will be in phase with the incident wave.

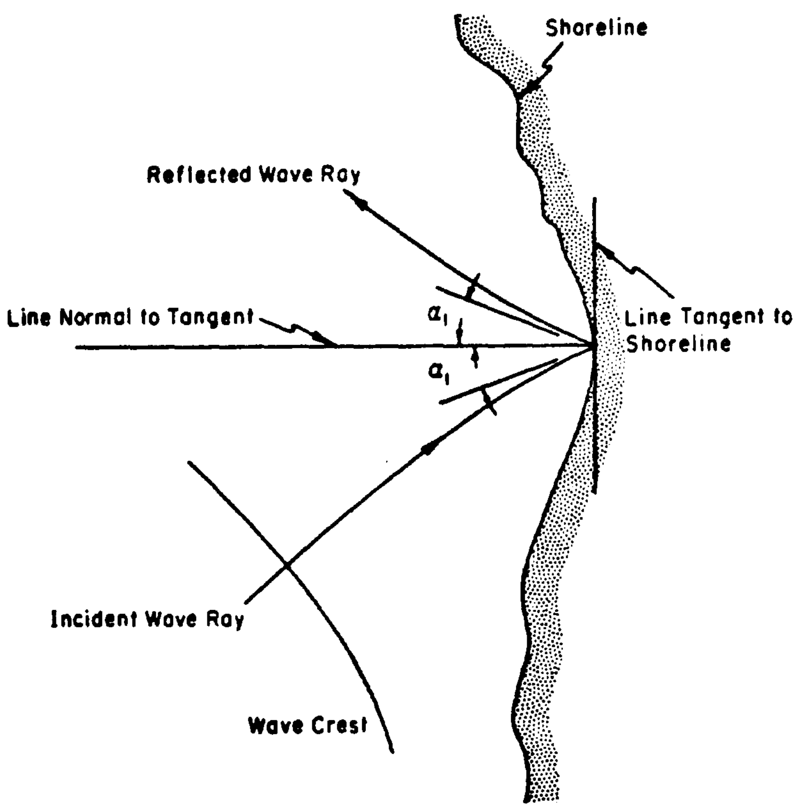

Figure 4-11. Wave reflection from a shoreline

(1) The wave reflection at a shoreline is defined in terms of a critical wave steepness $(H/L)_c$ which is given by

$$\left(\frac{H}{L}\right)_c = \left(\frac{2\beta}{\pi}\right)^{1/2} \frac{\sin^2 \beta}{\pi} \tag{4-28}$$

where β is the angle of the beach slope in radians. Complete reflection will occur if the wave steepness H/L in deeper water is given by

$$\frac{H}{L} \le \left(\frac{H}{L}\right)_c \tag{4-29}$$

* * * * * * * * * * * * * * * *EXAMPLE PROBLEM 4-4 * * * * * * * * * * * * * * * *

<u>GIVEN</u>: A tsunami has a height of 1.64 feet and a period of 20 minutes in a 3,280-foot water depth. The nearshore slope $S_3 = 0.1$ ($\beta = 0.0997$ radians).

<u>FIND</u>: If the wave is completely reflected at the shoreline.

<u>SOLUTION</u>: In the deeper water, the wave celerity C is

$$C = \sqrt{gd} = \sqrt{32.2 \times 3{,}280} = 325 \text{ ft/s}$$

$$L = CT = 325 \times 20 \times 60 = 390{,}000 \text{ ft}$$

$$\frac{H}{L} = \frac{1.64}{390{,}000} = 4.21 \times 10^{-6}$$

From equation (4-28)

$$\left(\frac{H}{L}\right)_c = \left(\frac{2\beta}{\pi}\right)^{1/2} \frac{\sin^2\beta}{\pi} = \left(\frac{2 \times 0.0997}{\pi}\right)^{1/2} \frac{\sin^2(0.0997)}{\pi}$$

$$\left(\frac{H}{L}\right)_c = 7.94 \times 10^{-4}$$

$$\frac{H}{L} < \left(\frac{H}{L}\right)_c$$

thus, the wave is completely reflected at the shoreline.

* *

(2) When

$$\frac{H}{L} > \left(\frac{H}{L}\right)_c \tag{4-30}$$

the reflection can be estimated by

$$\frac{H_r}{H_i} = c_R \frac{\left(\frac{H}{L}\right)_c}{\frac{H}{L}} \tag{4-31}$$

where c_R is a coefficient of roughness and permeability which has a value of $c_R = 0.8$ for a smooth, impervious beach. Various values of c_R have been defined for rough slopes for short-period waves (item 139). However, the effect of the slope roughness on longer period waves has not been adequately determined.

* * * * * * * * * * * * * * * EXAMPLE PROBLEM 4-5 * * * * * * * * * * * * * * *

GIVEN: A tsunami has a height of 1.64 feet and a period of 4 minutes in a 3,280-foot water depth. The nearshore slope $S_3 = 0.01$ ($\beta = 0.01$ radians), and the slope is smooth and impervious.

FIND: The coefficient of reflection H_r/H_i at the shoreline.

SOLUTION: In the deeper water, the wave celerity C is

$$C = \sqrt{gd} = \sqrt{32.2 \times 3,280} = 325 \text{ ft/s}$$

$$L = CT = 325 \times 4 \times 60 = 78,000 \text{ ft}$$

$$\frac{H}{L} = \frac{1.64}{78,800} = 2.10 \times 10^{-5}$$

From equation (4-28), where β is given in radians,

$$\left(\frac{H}{L}\right)_c = \left(\frac{2\beta}{\pi}\right)^{1/2} \frac{\sin^2\beta}{\pi} = \left(\frac{2 \times 0.01}{\pi}\right)^{1/2} \frac{\sin^2(0.01)}{\pi}$$

$$\left(\frac{H}{L}\right)_c = 2.54 \times 10^{-6}$$

$$\frac{H}{L} > \left(\frac{H}{L}\right)_c$$

$$\frac{H_r}{H_i} = c_R \frac{\left(\frac{H}{L}\right)_c}{\frac{H}{L}} = 0.8 \frac{2.54 \times 10^{-6}}{2.10 \times 10^{-5}} = 0.097$$

which indicates a low-reflected wave height where the shoreline has a very gradual slope.

* *

b. Shelf Resonance. Items 52 and 53 discuss a theoretical investigation of a vertical wall at the shoreline, where the water depth at the wall was d_s, and the sea bottom sloped seaward. The depth d at any arbitrary distance x from the shoreline is given by

$$d = d_s \left(1 + \frac{x^2}{a^2}\right)^{1/2} \tag{4-32}$$

where the horizontal distance x is positive measured seaward from the shoreline, $x = 0$ at the shoreline, and a is the distance from the shoreline to the depth $d = 2d_s$. The depth variation can be compared to a linear (constant) bottom slope S_2 between the toe of the nearshore slope (taken to be a vertical wall) and a point at the distance $x = a$ from the shoreline (Figure 4-12).

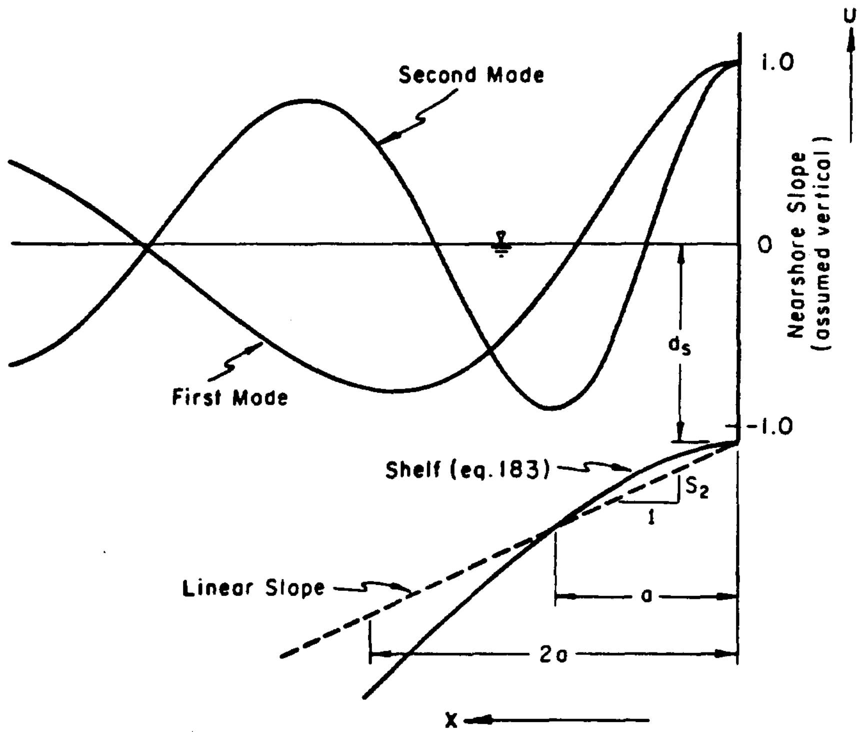

Figure 4-12. Shelf resonance

(1) Defining the wave by the equation

$$\frac{\partial^2 \eta}{\partial t^2} = g \frac{\partial}{\partial x}\left(d \frac{\partial \eta}{\partial x}\right) \tag{4-33}$$

Hidaka (items 52 and 53) defined the surface elevation η above the undisturbed water as

$$\eta = A \cos\left(\frac{2\pi t}{T}\right) \tag{4-34}$$

and A a dimensionless amplitude obtained by dividing the amplitude at any point by the amplitude A at the shoreline ($A = 1$ at the shoreline), the wave period, T, and time, t. Items 52 and 53 discuss a theoretical solution for wave resonance on the sloping shelf using Mathieu functions. The periods of the first and second modes of oscillation for the shelf denoted T_1 and T_2, respectively, are given by

$$T_1 = 3.2417 \frac{a}{\sqrt{gd_s}} \tag{4-35}$$

$$T_2 = 1.9254 \frac{a}{\sqrt{gd_s}} \tag{4-36}$$

The first and second modes are shown in Figure 4-12. The values obtained for resonant periods are for a shelf extending a long distance offshore; i.e., the shelf width $\ell_s \gg L$, where L is the wavelength of the incident wave.

(2) To determine the variation of wave amplitude with respect to distance from the shoreline, the equation for A is put in the form

$$\frac{d^2A}{d\rho^2} + \left[\frac{\frac{\theta}{2}}{(1+\rho^2)^{1/2}} + \frac{\frac{1}{4}}{(1+\rho^2)} + \frac{\frac{3}{4}}{(1+\rho^2)^2}\right] A = 0 \tag{4-37}$$

where $\rho = x/a$. The wave profile is defined in Table 4-1.

* * * * * * * * * * * * * * * EXAMPLE PROBLEM 4-6 * * * * * * * * * * * * * * *

GIVEN: Water depth d_s at the toe of a nearshore slope is 98 feet; the distance a = 40,770 feet (7.72 miles). Complete reflection occurs at the nearshore slope, and it can be assumed to behave as a vertical slope.

FIND:

(a) The primary and secondary periods of oscillation.

(b) The relative wave height of the wave at a distance one wavelength from the shoreline in relation to the wave height at the shoreline for the second mode.

SOLUTION:

(a) d_s = 98 ft and a = 40,770 ft.

From equation (4-35)

$$T_1 = 3.2417 \frac{a}{\sqrt{gd_s}}$$

$$T_1 = 3.2417 \frac{40,770}{\sqrt{32.2(98)}} = 2,350 \text{ s } (39.2 \text{ min})$$

From equation (4-36)

$$T_2 = 1.9254 \frac{a}{\sqrt{gd_s}}$$

$$T_2 = 1.9254 \frac{40,770}{\sqrt{32.2(98)}} = 1,395 \text{ s } (23.3 \text{ min})$$

(b) Both the first and second modes of oscillation are in the range of tsunami periods which are likely to occur. Taking h_s as the wave height at the shoreline, Table 4-1 gives, for the second mode, a height equal to 0.7818 h_s where x/a = 2.4 or where x = 2.4 (40,770) = 97,800 feet (18.5 miles). The values in Table 4-1 show that this is approximately the distance between second mode wave crests (one wavelength).

****

Table 4-1

Distribution of Amplitude A (from item 53)

First mode				Second Mode			
x/α	A	x/α	A	x/α	A	x/α	A
0.0	1.0000	2.0	-0.7985	0.0	1.0000	2.0	0.5600
0.1	0.9813	2.1	-0.7766	0.1	0.9474	2.1	0.6665
0.2	0.9265	2.2	-0.7432	0.2	0.7964	2.2	0.7392
0.3	0.8391	2.3	-0.6998	0.3	0.5668	2.3	0.7773
0.4	0.7244	2.4	-0.6476	0.4	0.2868	2.4	0.7818
0.5	0.5889	2.5	-0.5880	0.5	-0.0115	2.5	0.7548
0.6	0.4392	2.6	-0.5224	0.6	-0.2972	2.6	0.6995
0.7	0.2822	2.7	-0.4520	0.7	-0.5445	2.7	0.6197
0.8	0.1239	2.8	-0.3781	0.8	-0.7346	2.8	0.5200
0.9	-0.0305	2.9	-0.3018	0.9	-0.8566	2.9	0.4052
1.0	-0.1766	3.0	-0.2241	1.0	-0.9070	3.0	0.2800
1.1	-0.3110	3.1	-0.1462	1.1	-0.8887	3.1	0.1493
1.2	-0.4313	3.2	-0.0688	1.2	-0.8096	3.2	0.0176
1.3	-0.5357	3.3	0.0072	1.3	-0.6807	3.3	-0.1110
1.4	-0.6233	3.4	0.0810	1.4	-0.5149	3.4	-0.2327
1.5	-0.6936	3.5	0.1521	1.5	-0.3256	3.5	-0.3443
1.6	-0.7466	3.6	0.2197	1.6	-0.1261	3.6	-0.4430
1.7	-0.7827	3.7	0.2834	1.7	0.0716	3.7	-0.5267
1.8	-0.8028	3.8	0.3428	1.8	0.2572	3.8	-0.5940
1.9	-0.8076	3.9	0.3975	1.9	0.4221	3.9	-0.6436
		4.0	0.4473			4.0	-0.6754

(3) A different means of calculating the amplitude A, which will also account for refraction effects (i.e., the effect of a nonuniform offshore bathymetry), is suggested by item 143. These equations are

$$N_{j+1} = \frac{\left(B_j D_j - C\right) N_j - A_j}{C + B_j D_{j+1}}$$

$$A_{j+1} = A_j + 2C\left(N_{j+1} + N_j\right) \tag{4-38}$$

$$B_j = \frac{2}{\Delta(b_{j+1} + b_j)}$$

$$C = \frac{\Delta\omega^2}{(4g)}$$

$$D_j = b_j d_j$$

$$j = 1, 2, 3, \ldots$$

where

b_j , b_{j+1} = distance between refracted wave rays at stations j and $j+1$, respectively

N = horizontal displacement of a water particle

Δ = horizontal distance between stations j and $j+1$

For an unrefracted wave,

$$B_j D_j = \frac{d_j}{\Delta} \tag{4-39}$$

A_o = 1 at the shoreline (as in the case of Hidaka (items 52 and 53)), and N_o = 0 at the shoreline.

(4) The Wilson equations have been reformulated and compared with Hidaka's work in item 11. The two methods produced comparable results for the single comparison performed. Hidaka's method has the advantage of being a general solution. Wilson's method has the advantages of being much more readily used for a particular shelf slope and of including consideration of wave refraction.

c. Reflection from Seaward Edge of Shelf. Section 4-2 discussed the reflection of waves from an abrupt transition in water depth. It was shown that when a wave propagates seaward from the shoreline some of the wave energy is reflected shoreward from the transition in water depth at the seaward limit of the shelf. This is further illustrated in Figure 4-13 where d_s is the

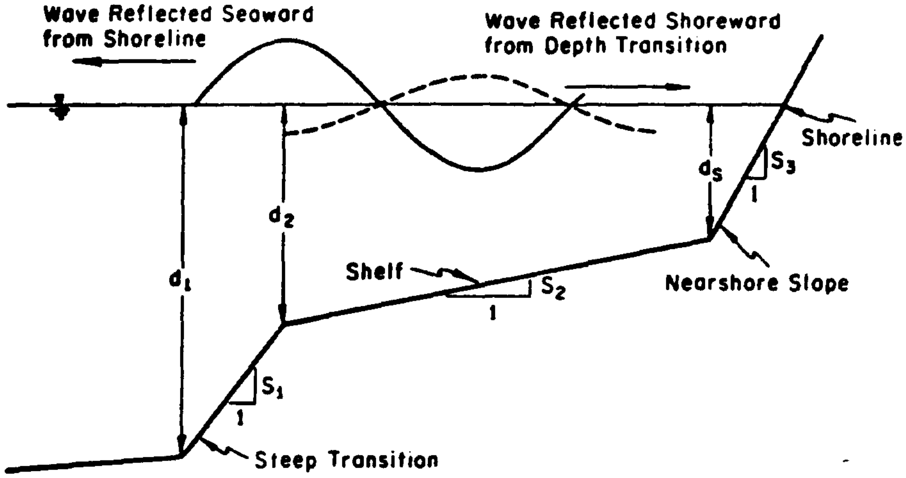

Figure 4-13. Reflected waves on a shelf

water depth at the toe of the nearshore slope, d_2 the water depth at the seaward limit of the shelf, d_1 the water depth at the seaward limit of the steep transition in water depth, S_1 the slope of the steep transition, S_2 the slope of the shelf, and S_3 the nearshore slope.

(1) The wave reflected shoreward from the steep transition may be π radians out of phase with the wave transmitted seaward across the transition. However, the actual phase difference will depend on the geometry of the shelf and transition and the water depth. For perfect reflection, the wave reflected from the shoreline will be in phase with the initial wave incident on the shoreline. The time t_s for the wave to travel the distance ℓ_s from the steep transition to the nearshore slope will be the same as the time required for the reflected wave from the nearshore slope to travel back to the steep transition in depth. Therefore, where the wave reflected from the transition is π radians out of phase with the incident wave, resonance will occur if

$$2t_s = \frac{nT}{2} \tag{4-40}$$

where T is the incident wave period, and n = 1, 2, 3, ... This leads to a first approximation for the resonant wave periods

$$T = \frac{8}{n} \frac{d_2^{1/2} - d_s^{1/2}}{S_2 \ g^{1/2}} \tag{4-41}$$

where T is a resonant wave period where the reflected wave and incident wave are π radians out of phase, and n = 1, 2, 3, ...

* * * * * * * * * * * * * * * EXAMPLE PROBLEM 4-7 * * * * * * * * * * * * * *

GIVEN: The water depth d_s at the toe of a nearshore slope is 98 feet. The width of the shelf ℓ_s is 98,000 feet (18.6 miles), and the water depth d_2 at the seaward edge of the shelf is 196 feet.

FIND: The resonant wave periods for the shelf.

SOLUTION: The slope of the shelf S_2 for a constant slope is given by

$$S_2 = \frac{d_2 - d_s}{\ell_s} = \frac{196 - 98}{98,000} = 0.001$$

From equation (4-41),

$$T = \frac{8}{n} \frac{d_2^{1/2} - d_s^{1/2}}{S_2 \, g^{1/2}} \, , \; n = 1,2,3,\ldots$$

$$T = \frac{8}{n} \frac{(196^{1/2} - 98^{1/2})}{0.001 \, (32.2)^{1/2}} = \frac{5,800}{n} \, , \; n = 1, 2, 3, \ldots$$

T_1 = 5,800 s (96.7 min), n = 1

T_2 = 2,900 s (48.3) min), n = 2

T_3 = 1,933 s (32.2 min), n = 3

T_4 = 1,450 s (24.2 min), n = 4

etc.

* *

(2) Currents parallel to the coast may act as boundaries which reflect waves. In this case waves generated near a shoreline could be trapped between the shoreline and an offshore current, creating a resonant condition between two boundaries.

d. Mach Stem Formation. Reflected tsunami waves can be refracted so they become trapped and form a mach stem. Graphical solutions for trapped waves for angles $\alpha_1 \leq 45^\circ$ are given in item 11. When $\alpha_1 < 45^\circ$ regular reflection occurs. When $\alpha_1 = 45^\circ$ the end of the wave crest at the shoreline turns perpendicular to the shoreline (see Figure 4-14). Regular reflection no longer occurs when $\alpha_1 > 45^\circ$.

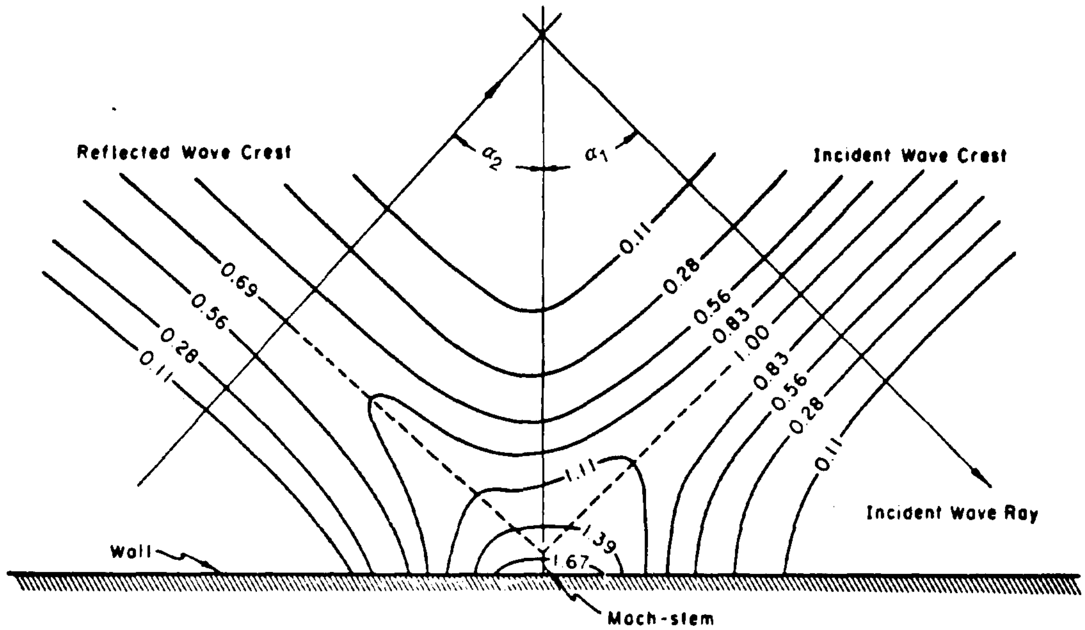

Figure 4-14. Mach stem formation, solitary wave (lines of equal surface elevation above still water normalized to unit incident wave amplitude (item 107))

(1) The incident wave produces two components. The first is a reflected wave, lower than the incident wave, and with the angle, α_2, between the reflected wave ray and the normal to the shoreline defined by $\alpha_2 < \alpha_1$. The second component is a mach stem which moves along the shoreline in the direction of the longshore component of the incident wave, growing in size as it progresses along the shoreline. Figure 4-14 shows the initial growth of a mach stem along a vertical wall for the critical angle $\alpha_1 = 45^\circ$.

(2) The mach stem has a profile at the shoreline similar to the profile of the incident wave, giving the mach stem the appearance of a large wave moving along the shoreline. When the angle of nearshore slope, $\beta < 60^\circ$ and $\alpha_1 > 55^\circ$, the mach stem may form a breaking wave. The mach stem remains attached to the shoreline end of the incident wave crest, so its speed of propagation C_ℓ along the shoreline is given as

$$C_\ell = \frac{C}{\sin \alpha_1} \tag{4-42}$$

where C is the celerity of the incident wave near the shoreline. The development of mach stems during tsunamis is rare, but a mach stem may have developed during the bore-like 1960 tsunami at Hilo, Hawaii.

e. Bay and Harbor Resonance. When a bay or harbor is very long in relation to the tsunami wavelength, the tsunami may cause resonance if a natural mode of oscillation of a bay or harbor corresponds to the period of the tsunami.

(1) Item 96 presents a tabulation of the approximate periods of inlets on the Pacific coast of North and South America based on the formula

$$T_1 = \frac{4L_b}{\sqrt{gd_a}} \qquad (4\text{-}43)$$

where

T_1 = primary period

L_b = length of the inlet

d_a = average depth of the inlet

Values of length, depth, width, period, and relative intensity of secondary oscillations of the water level for inlets on the coast of Alaska and British Columbia, and for Puget Sound, are given in Table 4-2. These values are only approximate because variations in inlet cross section, restricted entrances, and the effects of branched inlets are not considered.

(2) Values of the relative intensity I of secondary undulations are also shown in Table 4-2. I is given by

$$I = \frac{L_b}{Bd_a^{3/2}} \qquad (4\text{-}44)$$

where B is the inlet width. Inlets with higher relative intensities I would be expected to excite larger amplitudes of oscillation. Some bays which have small ratios of L_b/B also have large secondary oscillations. The equations are based on a one-dimensional theory which is not valid for low ratios of L_b/B, and transverse motion can be important in these cases.

(3) Ippen, Raichlen, and Sullivan (item 73) carried out a hydraulic model investigation of an inlet connected to an "infinite ocean." The ocean was simulated in a wave basin using wave absorbers to minimize reflected waves (Figure 4-15). It is assumed in this case that $B_1 \rightarrow \infty$. The experimental results (item 73) are shown in Figure 4-16, where k is the wave number $2\pi/L$. The curves illustrate the dependence of the results on the ratio of wavelength to inlet width, particularly for short, wide inlets.

(4) Each curve in Figure 4-16 was obtained by varying the inlet length for a fixed wavelength. Using equation (4-43) to define T_1, the figure shows that maximum amplification occurs where $T_1/T < 1$. This is equivalent to a resonance condition for a longer inlet. It can be assumed, therefore, that the inlet has an effective length L_e extending into the open sea, and the effective primary period T_{1e}, is

$$T_{1e} = \frac{4L_e}{\sqrt{gd_a}} \qquad (4\text{-}45)$$

Table 4-2

Dimensions, periods of fundamental mode, and intensity of secondary undulations of inlets of Alaska and British Columbia, and of Puget Sound (item 96)

Inlet	L_b, length km	d_a, mean depth km	Period T_1 min	B, mean width km	$\frac{L_b}{B}$	$\frac{L_b/B}{d_a^{3/2}}$
Alaska						
Tarr Inlet-Glacier Bay	111	0.220	159	5.6	19.8	192
Muir Inlet	35	0.215	51	3.5	10.0	100
Lynn Canal	146	0.360	164	6.6	22.1	102
Gastineau Canal	18	0.040	61	1.3	13.8	1,725
Taku Inlet-Stephens Passage	133	0.295	165	13.0	10.2	64
Tracy Arm	43	0.270	56	1.8	23.9	170
Endicott Arm	44	0.260	58	3.3	13.3	100
Frederick Sound	80	0.165	133	22.2	3.6	54
Thomas Bay	20	0.150	35	2.8	7.1	122
Tenakee Inlet	64	0.140	115	3.2	20.0	382
Peril Strait	71	0.210	104	4.0	17.8	185
Bradfield Canal-Ernest Sound	80	0.310	97	5.7	14.0	81
Behm Canal West-Bell Arm	72	0.425	74	5.2	13.8	50
Burroughs Bay-Behm Canal East	113	0.420	174	3.5	32.3	119
Rudyerd Bay	22	0.170	36	0.9	24.4	348
Boca de Quadra	56	0.245	76	1.3	43.1	355
Carroll Inlet	44	0.130	82	1.6	27.5	587
George Inlet	22	0.225	31	1.4	15.7	147
British Columbia						
Portland Canal	115	0.255	153	2.2	52.3	406
Observatory Inlet-Hastings Arm	76	0.385	82	2.2	34.5	144
Alice Arm	19	0.240	26	1.3	14.6	124
Khutzeymateen Inlet	25	0.120	49	1.0	25.0	601
Work Channel	54	0.240	74	2.0	27.0	230
Prince Rupert Inlet	19	0.045	60	1.2	15.6	1,634
Douglas Channel	83	0.330	97	3.5	23.7	125
Kildala Arm	19	0.175	31	1.5	12.7	173
Gardner Canal	91	0.275	117	1.9	47.9	332
Surf Inlet	22	0.220	32	0.9	24.4	236
Laredo Inlet	39	0.295	48	1.5	26.0	162
Sheep Passage-Mussel Inlet	33	0.275	42	1.5	22.0	153
Spiller Channel	46	0.255	61	1.9	24.2	188
Roscoe Inlet	43	0.135	79	1.1	39.1	788

(Continued)

Table 4-2 (Concluded)

Cousins Inlet	12	0.070	31	0.8	15.0	810
Cascade Inlet	26	0.250	35	1.1	23.6	189
Dean Channel	111	0.420	115	2.4	46.3	170
Kwatna Inlet	24	0.345	28	2.0	12.0	59
South Bentinck Arm	37	0.240	51	2.2	16.8	143
Rivers Inlet	46	0.295	57	3.0	15.3	95
Moses Inlet	26	0.200	39	0.9	28.9	323
Smith Inlet	33	0.270	43	1.3	25.4	181
Mereworth Sound	19	0.090	43	0.4	47.5	1,759
Belize Inlet	52	0.255	69	1.1	47.3	367
Nugent Sound	24	0.075	59	0.7	34.3	1,669
Seymour Inlet	67	0.420	70	1.7	39.4	145
Drury Inlet	22	0.040	74	1.3	16.9	2,112
Knight Inlet	130	0.295	161	3.0	43.3	270
Call Inlet	28	0.135	51	1.5	18.7	377
Loughborough Inlet	35	0.190	54	1.7	20.6	249
Bute Inlet	76	0.510	72	3.7	20.5	56
Toba Inlet	37	0.390	40	2.6	14.2	58
Jervis Inlet	89	0.495	85	3.2	27.8	80
Howe Sound	43	0.225	61	7.0	6.1	57
Vancouver Island British Columbia						
Holberg-Rupert Inlet	44	0.165	73	1.4	31.4	469
Quatsino Sound-Neroutsos Inlet	59	0.150	103	2.2	26.8	461
Forward Inlet	11	0.030	43	1.1	10.0	1,925
Klaskino Inlet	11	0.035	40	0.7	15.7	2,398
Ououkinsh Inlet	14	0.085	32	1.2	11.7	472
Port Eliza	11	0.050	33	0.7	15.7	1,404
Espinosa Inlet	14	0.215	20	1.3	10.8	108
Nuchalitz Inlet	15	0.025	64	1.3	11.5	2,909
Tahsis Inlet	29	0.120	56	0.9	32.3	775
Cook Channel-Tlupana Inlet	31	0.150	54	1.9	16.3	281
Zuciarte Channel Mechalat Inlet	48	0.220	69	1.5	32.0	310
Sydney Inlet	20	0.080	48	1.3	15.4	681
Shelter Inlet	19	0.115	38	1.3	14.6	374
Herbert Inlet	23	0.100	49	2.0	11.5	364
Pipestem Inlet	9	0.045	29	0.7	12.9	1,351
Effingham Inlet	17	0.095	37	1.2	14.2	485
Alberni Inlet	69	0.145	122	1.3	53.1	962
Saanich Inlet	23	0.180	37	2.5	9.2	120
Puget Sound						
Puget Sound	111	0.165	184	6.0	18.5	276
Hood Canal	102	0.110	207	2.5	40.8	1,118
Possession Sound-Saratoga Passage	70	0.090	157	3.7	18.9	700

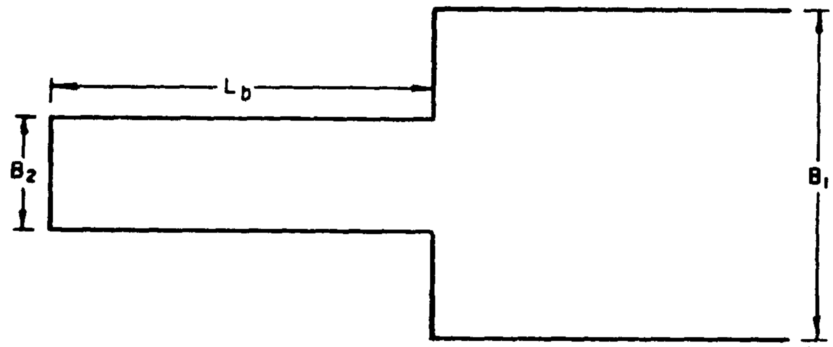

Figure 4-15. Plan view of inlet

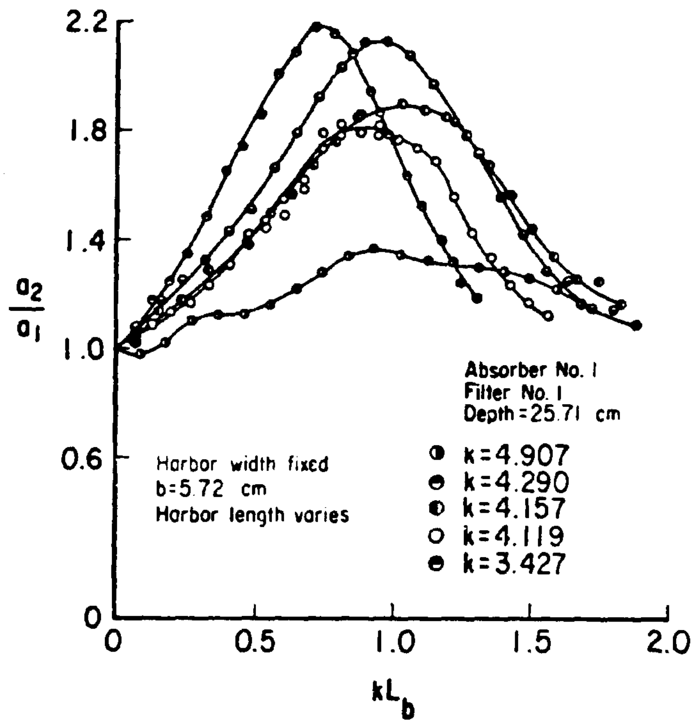

Figure 4-16. Amplification factor versus relative harbor length (from item 73)

The length L_e , is defined by this equation if it is assumed that $T_{1e}/T = 1$ where maximum amplification occurs. The ratio of inlet width to inlet length is also important in determining L_e .

(5) For a fully open inlet or harbor (see Figure 4-15), item 72 defines resonant amplification (the ratio of an amplitude in the harbor to the amplitude at the closed harbor entrance) as

$$\frac{a_2}{a_1} = \frac{1}{\left[(\cos kL_b - \psi_2 \sin kL_b)^2 + \psi_1^2 \sin^2 kL_b\right]^{1/2}} \qquad (4\text{-}46)$$

where ψ_1 and ψ_2 are wave radiation functions given in Figure 4-17. The resonant amplification would occur where $T_{1e}/T = 1$ as before. The functions shown in Figure 4-17 apply to all harbor openings, where b is the width of the opening.

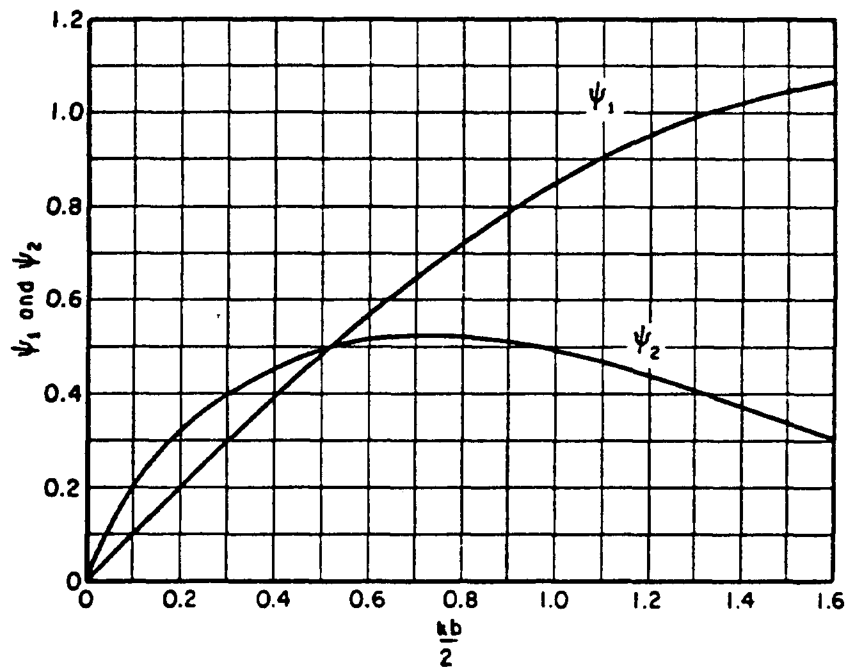

Figure 4-17. Wave radiation functions (from item 72)

* * * * * * * * * * * * * * *EXAMPLE PROBLEM 4-8* * * * * * * * * * * * * * *

GIVEN: A fully open inlet has a width B given by $B = 0.194\ L_b$, where L_b is the length of the inlet. The incident wavelength $L = 25B$.

FIND: The resonant amplification in the inlet.

SOLUTION:

$$\frac{kB}{2} = \frac{2\pi(0.04L)}{2L} = 0.1257$$

From Figure 4-17, where b = B for a fully open inlet

$$\psi_1 = 0.12$$

and

$$\psi_2 = 0.24$$

From equation (4-46),

$$\frac{a_2}{a_1} = \frac{1}{\left[\left(\cos kL_b - \psi_2 \sin kL_b\right)^2 + \psi_1 \sin^2 kL_b\right]^{1/2}}$$

$$\frac{a_2}{a_1} = \frac{1}{\left\{\left[\cos\left(2\pi \frac{0.04}{0.194}\right) - 0.24 \sin\left(2\pi \frac{0.04}{0.194}\right)\right]^2 + (0.12)^2 \sin^2\left(2\pi \frac{0.04}{0.194}\right)\right\}^{1/2}}$$

$$\frac{a_2}{a_1} = 8.16$$

* *

(6) Theoretical results for open and partially closed harbors with both symmetric and asymmetric entrances are given in Figure 4-18. Experimental results generally show that amplification factors are less than those predicted theoretically.

(7) For waves passing from a continental shelf into a harbor, where the dimensions of the harbor and the entry channel are small compared to the local wavelength of the tsunami, the response of the harbor is essentially restricted to the Helmholtz mode, i.e., the lowest mode of resonance. The harbor undergoes a pumping motion where the water level in the harbor is assumed to rise and fall uniformly across the total area of the harbor. The water passing through the entry channel is assumed to have high velocity represented as kinetic energy; on the other hand, the water in the harbor has a much lower velocity, and the rise and fall of the water level in the harbor is represented as potential energy.

(8) An approximate method for determining resonant wavelengths for harbors with entrance channels (Figure 4-19) assumes that the resonant wavelength $L_o(L_c = 0)$ for an equivalent harbor of the same dimensions but having no entrance channel $(L_c = 0)$, can be obtained (item 13). The resonant wavelength for the harbor with an entrance channel is then given by the equation

$$\frac{L_o}{2\pi} = \left[\frac{L_c\ L_b\ B}{b} + \frac{L_o^2\ (L_c = 0)}{(2\pi)^2}\right]^{1/2} \qquad (4\text{-}47)$$

where L_c is the length of the entrance channel. The resonant wavelength where $L_c = 0$ can be obtained using item 92 results discussed in item 92 (see Figure 4-20).

(9) Narrowing the entrance width or increasing the length of the entrance channel will significantly increase the response of the harbor to the Helmholtz mode, which may dominate tsunami response. This narrowing or lengthening also has the effect of decreasing the resonant frequency. Lengthening the entrance channel to a harbor also increases the frictional

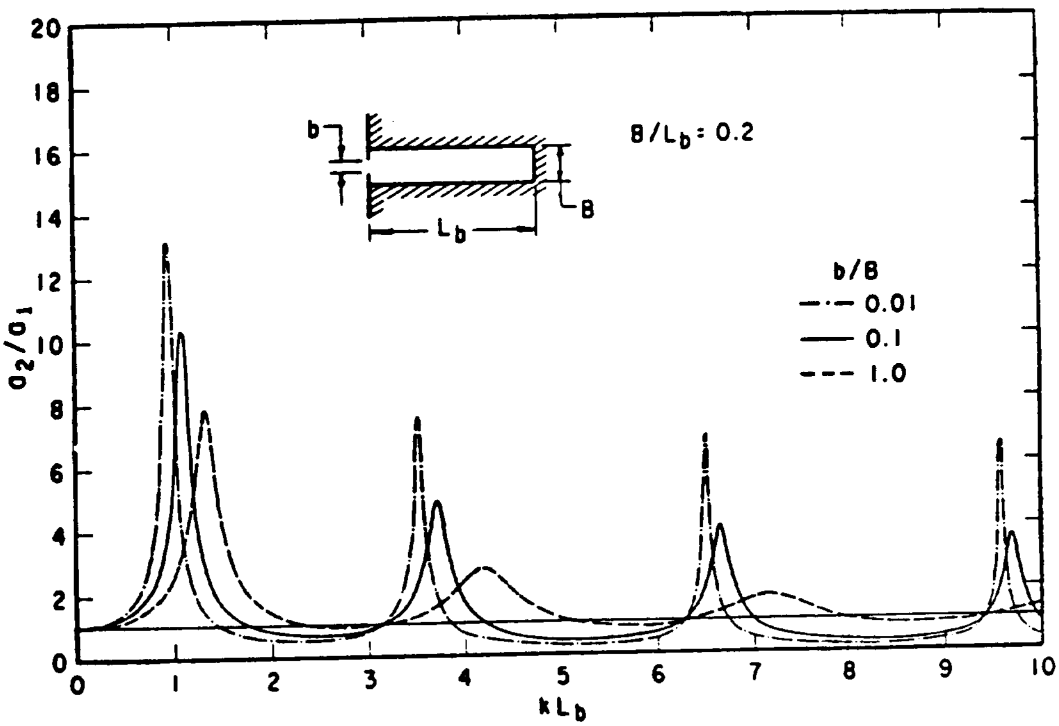

a. Narrow harbor

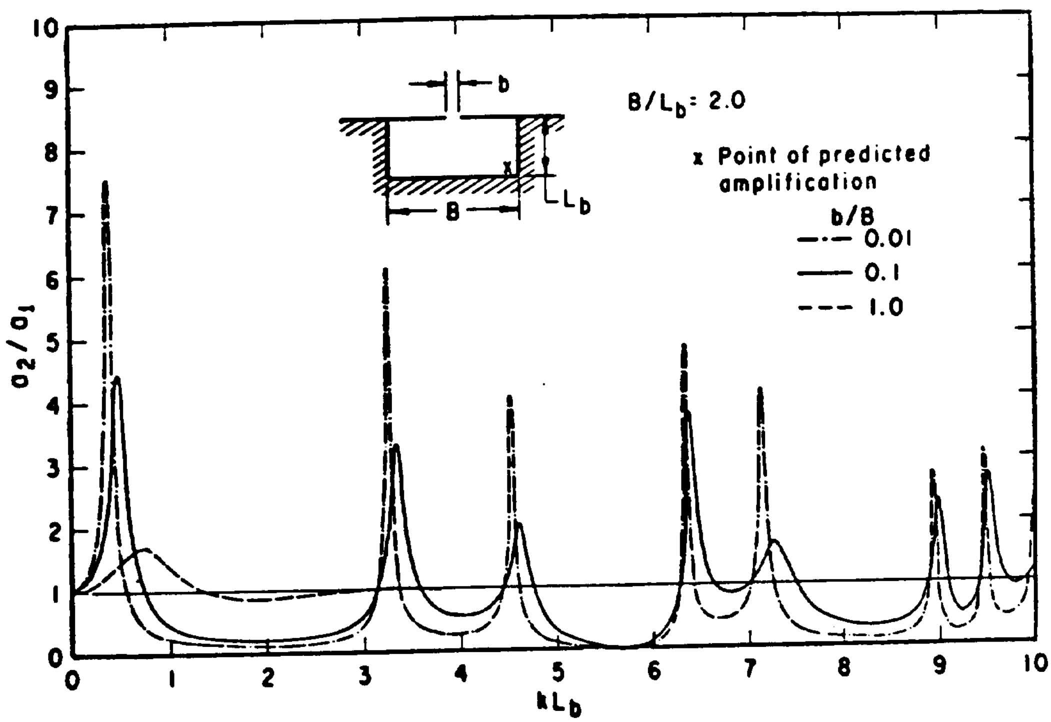

b. Wide harbor

Figure 4-18. Theoretical frequency response curves of harbors (from item 72) (Continued)

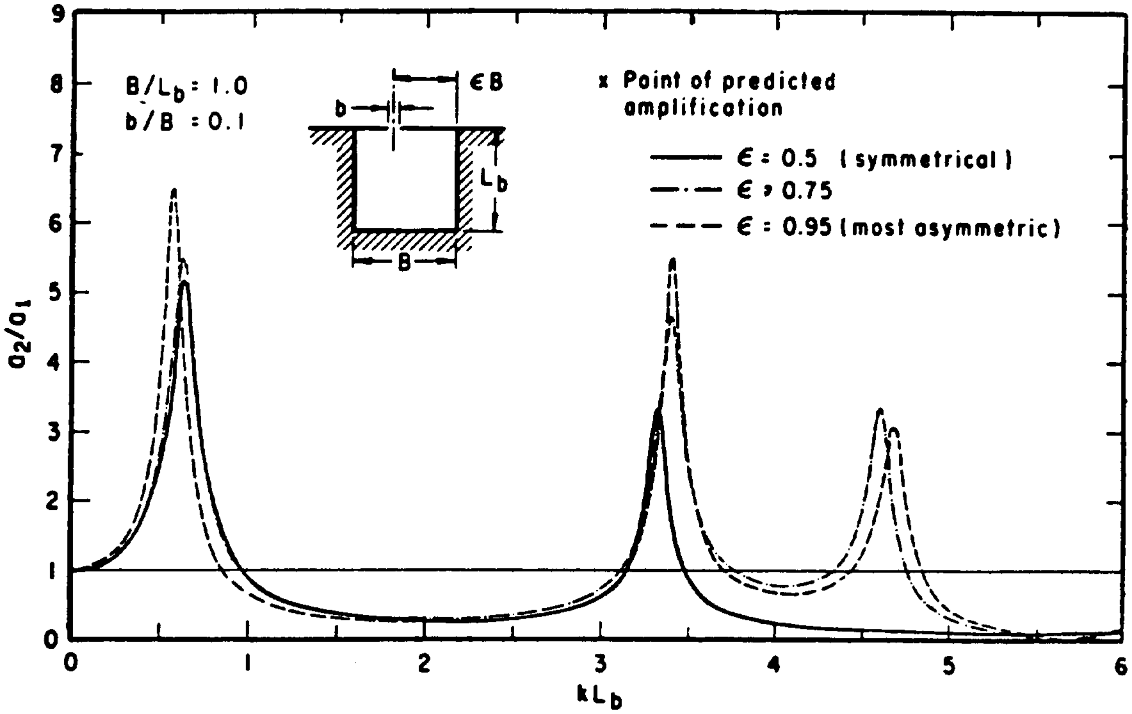

c. Square harbor with asymmetric entrance

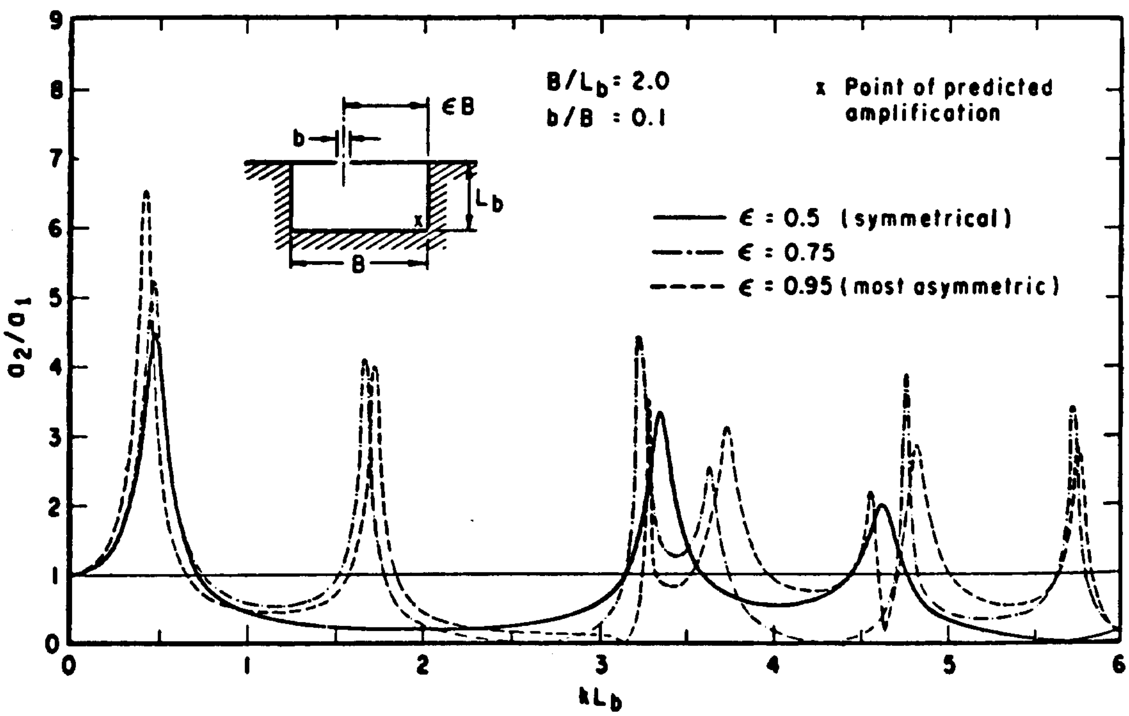

d. Wide harbor with asymmetric entrance

Figure 4-18. (Concluded)

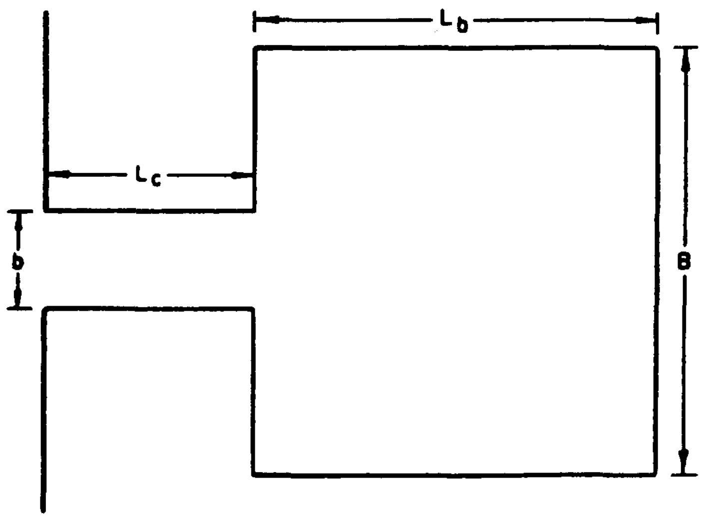

Figure 4-19. Harbor with an entrance channel

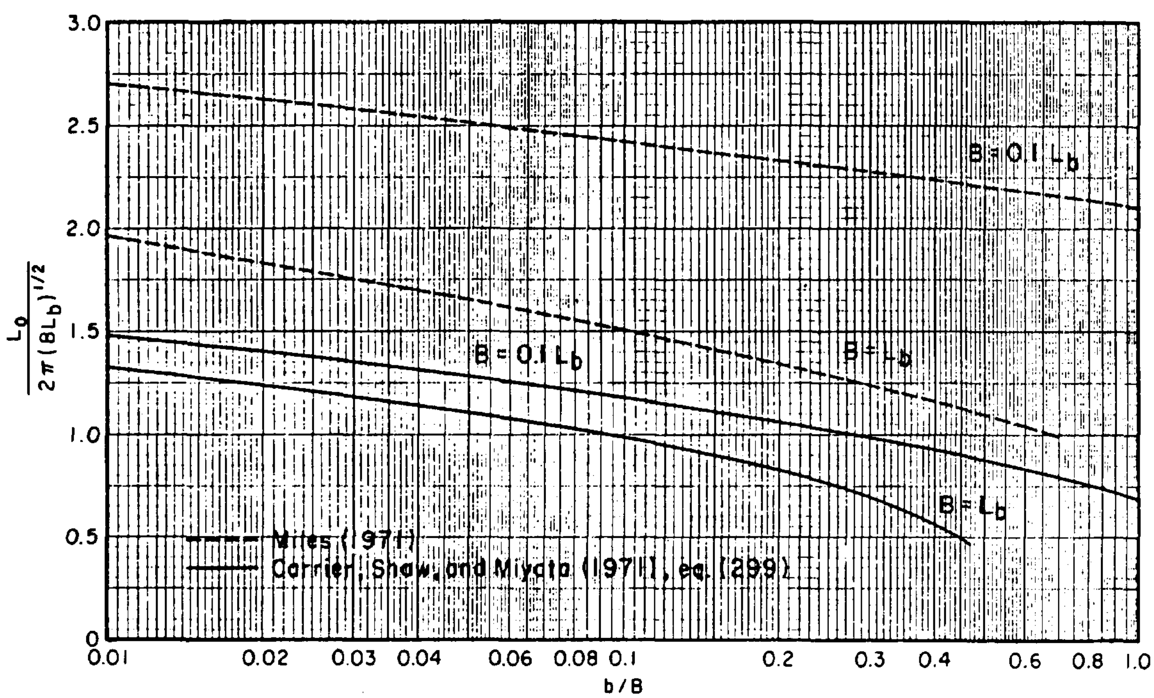

Figure 4-20. Wavelength for Helmholtz resonance (centered harbor entrance, entrance length L_c = 0) (from item 92)

resistance so amplification factors for a very long entrance channel may be significantly reduced (although the resonant frequencies would still be less than for a harbor without an entrance channel; i.e., where $L_c = 0$).

(10) Item 116 presents a numerical means for analyzing harbors responding to the Helmholtz mode of resonance. The method uses

$$\frac{dh_b}{dt} = \frac{Q}{A_b} \tag{4-48}$$

where

h_b = surface elevation of the water in the harbor above some arbitrary fixed datum

Q = flow rate through the entrance channel

A_b = area of the harbor, $A_b = L_b B$

t = time

and d denotes differentiation. The governing differential equation is

$$\frac{dQ}{dt} = \frac{I_g}{2}\left(\frac{1}{A_{bc}^2} - \frac{1}{A_{sc}^2}\right)Q^2 - gI_g(h_b - h_s) - I_g F \tag{4-49}$$

where

$I_g = \left(\int A_c^{-1}\, dx\right)^{-1}$

A_{bc} = cross-sectional area at the bay end

A_{sc} = cross-sectional area at the sea end

h_s = height of the sea level above the arbitrary datum

F = total bottom friction in the entrance channel

A_c = cross-sectional area of flow through the entrance channel at any point x between the seaward end at X_s and the harbor end X_b (A_b is a function of x.)

(11) Several numerical models are available for investigating wave oscillations in an arbitrary-shaped harbor. The hybrid element model developed by item 15 includes the effects of bottom friction and absorption of wave energy at harbor boundaries. Earlier nondissipative models are described in items 18 and 84. Items 54 and 55 discuss application of Chen and Mei's model to studies of Los Angeles and Long Beach harbors. Durham (item 29) applied the model to Barber's Point Harbor, Hawaii, and found the period of the Helmoltz mode of the harbor to be close to that of typical tsunami periods. Farrar and Houston (item 33) investigated the response of this harbor to tsunamis, including dynamic land flooding. It is important to consider the resonant response of harbors during their design in areas where tsunamis are a potential threat.

4-4. Runup and Interaction with Structures. The arrival of a tsunami at a shoreline may cause an increase in water level as much as 20 or 30 feet. Much higher increases are possible in bays and estuaries. The large increase in water level, combined with the surge of the tsunami, can impose powerful forces on shore protection structures and on structures located near the shoreline. Structures may be seriously damaged or destroyed by the tsunami. Damage may be caused by strong currents produced by waves overtopping the structures, the direct force of the surge produced by a wave, the hydrostatic pressure created by flooding behind a structure combined with the loss of equalizing forces at the front of a structure due to extreme drawdown of the water level when the waves recede, and erosion at the base of the structure. Major damage may also be caused by debris carried forward by the tsunami in the nearshore area. To determine the potential damage to structures located along a shoreline, the probable increase in water level caused by the tsunami, i.e., the runup height, must be estimated. Estimates of tsunami runup are also needed for flood zone planning along the shoreline and for operation of the tsunami warning system to evacuate people from endangered areas.

a. Tsunami Runup on a Shoreline. The height of a tsunami will vary from point to point along a coastline. Numerical models for prediction of tsunami height at the shoreline, i.e., the elevation of water at the shoreline due to the tsunami, must be applied to a sufficient number of points along the shoreline to determine this variation. When the variation is large between adjacent points, calculations for tsunami heights should be carried out at additional shoreline points between those points. After the height of the tsunami at a point along the shoreline has been determined, the vertical runup height at that point can be estimated.

(1) When the tsunami height along a section of coastline is relatively constant, and the variations in onshore topography are relatively minor, the runup height may be assumed to be constant along that section of coastline as a first approximation. Variations in tsunami height and shoreline topography will actually cause some variation in runup characteristics along any section of coastline. Because these variations are difficult to predict, the predicted runup heights may contain substantial errors. Where tsunamis of a known height have produced variations in runup at a particular section of coastline, the higher heights should normally be used for conservative design. It should also be noted that the characteristics of the waves may vary from one wave to another at the same coastal point.

(2) An added complication, which is an important consideration in computing runup heights, is the possibility of storm waves occurring simultaneously with the tsunami. The prediction of maximum runup heights would require the consideration of joint probabilities of tsunamis and storm waves as well as the probability of a high tidal stage.

(3) Because a tsunami has a very long period relative to storm waves, it causes an apparent variation in water depth over a long distance. Storm waves riding on top of the tsunami will have a wave celerity corresponding to the depth (including tsunami height) at any particular point. If two storm waves are otherwise equivalent (e.g., the same period and wave height), and one is at the crest of the tsunami while the other is at the leading edge, the storm wave at the tsunami crest will have a higher celerity. Therefore, the tsunami can cause one storm wave to overtake and superimpose itself on another storm wave, producing higher waves at the shoreline.

(4) As a first approximation, the tsunami runup on a shoreline will have a runup height (vertical rise) equal to the wave height at the shoreline. This assumption is based on the idea that a tsunami will act like a rapidly rising tide. This assumption cannot always be used with accuracy. The effects of ground slope, wave period, and the possible convergence or divergence of the runup must be considered.

(5) Tsunamis at a shoreline could be categorized into three types of waves: nonbreaking waves (i.e., a tsunami which acts as a rapidly rising tide); waves which break far from the shoreline and become fully developed bores before reaching the shoreline; and waves which break near the shoreline and act as partially developed bores which are not uniform in height. In addition, there are some cases where reflected waves become bores after reflecting from a shoreline. Except in rare cases, most tsunamis appear as nonbreaking waves.

(6) For the nonbreaking wave, the assumption that the runup height equals the wave height (crest amplitude) at the shoreline is reasonable. Item 59 presents many historical cases where runup was found to correspond to the tsunami height at the shoreline. Unless an area is known historically to be one of the rare locations where tsunamis appear as bores, it should be assumed tsunami runup equals the height at the shoreline. To analyze the runup of breaking waves and fully developed bores, where maximum runup heights have been observed to be much higher than the wave or bore height at the shoreline, it is necessary to consider the actual form of the runup.

(7) Several experimental studies have been performed for flat, uniform slopes with no convergence of the wave crest (item 11). In general, the experiments show that for flatter slopes (less than 8 deg) the runup height appears equal to or less than the wave height at the shoreline. For steeper slopes, the runup height increases as the slope increases, and the ratio of runup height to wave height at the shoreline appears to reach a maximum value for vertical walls. However, the higher runup on the steeper slopes appears to have a relatively shallow depth.

(8) For runup on a shoreline where the slope varies, it is necessary to use a numerical solution to determine the limits of the runup. Freeman and Le Mehaute have carried out numerical calculations for slopes $S \geq 0.1$, but they present no results for very flat slopes. Very little data exist to verify such equations or to determine their full range of application.

(9) Runup is dependent on surface roughness. Only very limited data are presently available for estimating values of surface roughness coefficient. For prototype conditions, the "roughness" may consist of groves of trees or subdivisions of houses. Also, the roughness elements, e.g., trees and houses, may be moved by the waves.

(10) In addition to considering wave runup, it is necessary to consider the drawdown of the water when the wave trough arrives at the shoreline. Not as much attention has been given to wave rundown; however, the drawdown of the water level may result in the seaward collapse of seawalls, damage to ships in a harbor, or exposure of seawater-intake pipelines. It should also be noted that a gradual increase in water level, with very low velocity currents, may

be followed by a sudden withdrawal of water producing very strong currents. No estimates of speed are available for rundown currents. Maximum runup current velocities of up to 3 ft per second have been estimated for actual tsunami events.

(11) Water overflowing a coastal barrier will have a current velocity determined by the difference in height between the top of the barrier and the ground level behind the barrier, as well as the quantity of water overtopping the barrier. The barrier will also limit the height of the runup; however, large drain openings must be provided to prevent water levels from building up behind the barrier if it is overtopped by successive waves.

(12) Surge runup on a dry bed will have a high velocity for a tsunami which acts like a rapidly rising tide. An approximate equation is

$$u = 2(gh)^{1/2} \tag{4-50}$$

where h is the surge height at any point and u the water velocity at the same point.

b. Interaction with Shore Protection Structures. Breakwaters and seawalls may protect coastal areas from tsunamis. When a tsunami occurs, breakwaters may decrease the volume of water flowing into a harbor and onto the coastline. Proper placement of breakwaters may also decrease wave heights by changing the natural period of an inlet discussed in Section 4-3. However, breakwaters may also affect the resonant period of a harbor so that wave heights are increased, and seawalls may reflect waves within a harbor. A high seawall along a coastline may prevent flooding of the backshore areas.

(1) A tsunami may damage shore protection structures; therefore, care must be exercised in the design of the structures. Numerous instances of tsunamis damaging or destroying protective structures have been recorded. The 1946 tsunami in Hawaii overtopped and breached the breakwater at Hilo, removing 8-ton stones to a depth 3 feet below the water surface along nine sections of the breakwater crest with a total length of over 6,000 feet (item 131). Iwasaki and Horikawa (item 75) investigated areas along the northeast coast of Honshu after the 1960 tsunami. They indicated that a sea dike at Kesennuma Bay failed during the 1960 tsunami because the water from the incident waves, which had overtopped the dike, caused extensive erosion receding at a gap in the dike. The receding water gradually widened the gap. They also noted that a quay wall at Ofunato failed because of scouring of the backfilling, and that a quay wall constructed of reinforced concrete sheet piles at Hachinohe collapsed due to a lack of interlocking strength after backfilling was washed away.

(2) Receding water may also seriously scour the seaward base of a revetment or seawall. The combination of this scouring and the increased hydrostatic pressure from initial overtopping may cause failure.

(3) The following empirical equation can be used to estimate the volume of overtopping of a seawall at the shoreline in cubic feet per foot length of wall:

$$V = 3.09 \int_{t_1}^{t_2} \left(\frac{1}{2} h_s \cos \frac{2\pi t}{T} - h_w\right)^{3/2} dt \qquad (4\text{-}51)$$

where

t_2 = time when overtopping ends

t_1 = point in time where overtopping begins

h_s = total wave height in feet (crest-to-trough) of the wave at the shoreline

T = wave period

h_w = wall height

As the wall height h_w is measured in feet from the sea level at the time the tsunami occurs, it varies, but its lowest value (i.e., the greatest overtopping) would occur when the sea level is at the highest tidal stage. Values for overtopping are shown in Figure 4-21.

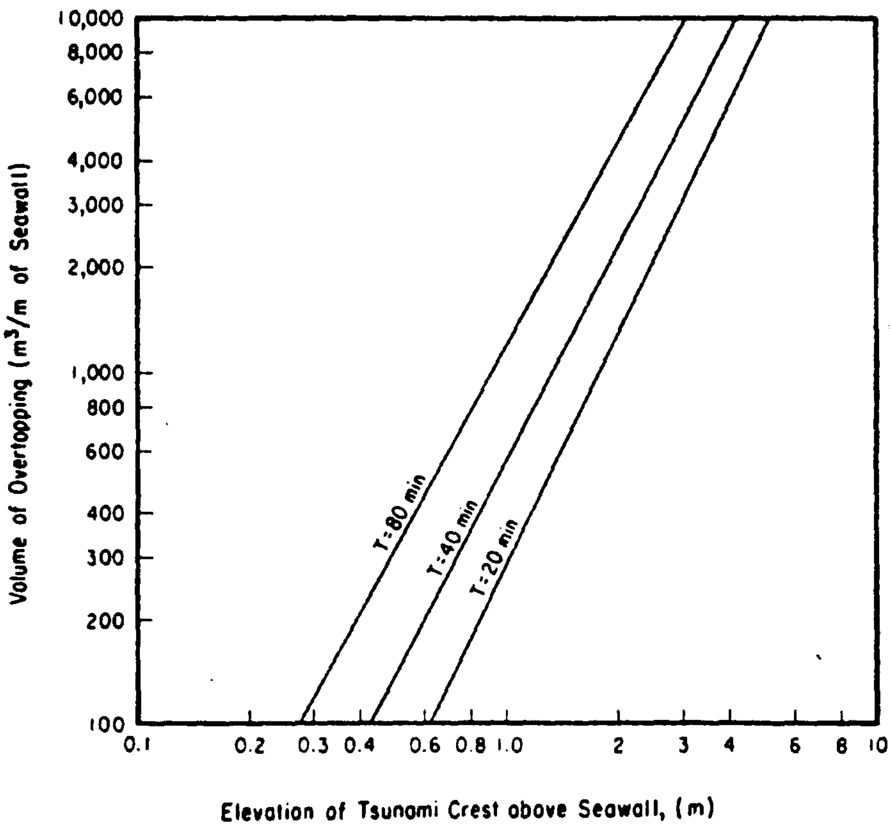

Figure 4-21. Overtopping volumes (after item 140)

(4) The protection provided by a breakwater depends on its location and the width of the navigation channel through the breakwater. Model tests

indicate that a properly placed breakwater can substantially reduce wave heights in a bay or harbor (item 76). The greatest reduction in wave height occurred when the area of the breakwater opening was the least. For tests at one particular site when the ratio of the breakwater opening area to the cross-sectional area of the bay was equal to about 0.1, the wave height was reduced to about 0.25 times the height which would occur without the breakwater. The location of the breakwater would be expected to affect the resonant periods of the bay and the harbor. Therefore, care should be exercised in placing a breakwater in any bay or harbor.

(5) In some instances, trees may offer some protection against a tsunami surge. Groves of trees alone or as supplements to shore protection structures may dissipate tsunami energy and reduce surge heights. Groves of coconut palms may withstand a tsunami surge but may be sheared off by debris carried forward by the tsunami. Other types of trees may be easily uprooted and flattened. Item 118 indicates that dense thickets of hau trees provided effective shields in many places during the 1946 tsunami in Hawaii. Trees which do not survive the tsunami may add debris to the surf and increase the damages resulting from the surge. Also a buildup of debris in front of a structure may result in an increase of its effective area and increased drag force and may cause the entire structure to be swept away by the tsunami (item 88).

c. Other Shoreline Structures. Damage from a tsunami may occur to structures located at the shoreline or along river channels near the shoreline. These include docks and bridges where damage may occur to both the superstructure and supports. Specific examples and photographs are given in item 11.

d. Tsunami Surge on the Shoreline. After the runup height of a tsunami has been established, the effects of this runup on structures and other objects located near the shoreline must be determined. A detailed discussion is given in item 11.

(1) When the tsunami acts as a rapidly rising tide, the resulting incident current velocities are relatively low, and most initial damage will result from buoyant and hydrostatic forces and the effects of flooding. In many instances the withdrawal of the water occurs much more rapidly than the runup and flooding. In some instances, damage may result from the higher current velocities associated with the withdrawal. These velocities would be on the order of those normally associated with an incident surge. More concern is therefore given to a tsunami which approaches the shoreline as a bore (although this is rare).

(2) When the tsunami forms a borelike wave, the runup on the shoreline has the form of a surge on dry ground. This surge should not be confused with the bore approaching the shoreline, as different equations govern the motion and profile of the surge. Laboratory observations (item 93) have noted that a bore approaching a shoreline exhibits a relative steepening of the bore face as the surge moves up on the dry slope. The current velocities associated with the surge are proportional to the square root of the surge height, as discussed in Section 4-4a.

CHAPTER 5

WAVE CLIMATE AND ANALYSIS FOR DESIGN

5-1. Wind Waves. Most coastal projects require an estimate of the characteristics of wind-generated gravity waves at the project site. These waves have periods of between 1 and 25 seconds; hence, they are considerably shorter than the tides, storm surges, and tsunamis discussed in the preceding chapters. Since wind waves occur continuously at exposed project sites, they can be an important concern for operations and maintenance as well as design. Procedures for developing wave characteristics for design are presented in this chapter. The use of wave theory is covered in Section 2. Sections 3, 4, 5, and 6 deal with wave measurement and analysis systems. Sections 7 and 8 deal with numerical and analytical wave models. Section 9 presents alternatives for forming statistical summaries of individual wave estimates to give wave climate information for design.

5-2. Wave Theory. Wave theories can be very useful for estimating certain wave characteristics such as wavelength, wave speed, crest height, wave shape, water particle accelerations, and wave forces. Theories suited for engineering use are commonly based on the following assumptions: presence of a homogeneous, incompressible fluid; lack of surface tension and Coriolis effect; pressure at the surface being uniform and constant; presence of an inviscid fluid; lack of interaction between waves and other water motions; presence of a horizontal fixed impermeable bed; a small wave amplitude and wave shape which does not change with time and space; and presence of long-crested waves (two dimensional). Theories can be applied to areas of gradually varying water depth by assuming the waves are adjusted to the local water depth. The theories should be used only when the bottom slope is flatter than 1 on 10.

a. Small-amplitude Wave Theory.

(1) The most fundamental description of a simple sinusoidal oscillatory wave is by its height H (the vertical distance between crest and trough), length L (the horizontal distance between corresponding points on two successive waves), period T (the time for two successive crests to pass a given point), and depth d (the distance from the bed to the SWL). A graphic definition of terms is given in Figure 5-1.

(2) Small-amplitude wave theory has proven to be a very useful tool for many engineering applications. It is based on the additional assumption that the wave height is small in relation to the water depth and the wavelength. Expressions for various wave characteristics derived from small-amplitude theory are given in Figure 5-2. The approximate limits of validity for the small-amplitude assumption are shown in Figure 5-3.

b. Higher Order Wave Theories. Steep or shallow waves which exceed the range of validity for small-amplitude theory can be estimated with higher order theories. The approximate ranges of validity for higher order theories are shown in Figure 5-3. The higher order theories are more complex and hence more difficult to use. Tabular or graphical presentations of the solutions are generally used. Tabulated solutions from stream function theory are given in item 23. Wave profiles for the 40 cases considered by Dean are shown in Figure 5-4. Many of the profiles differ considerably from the sinusoidal

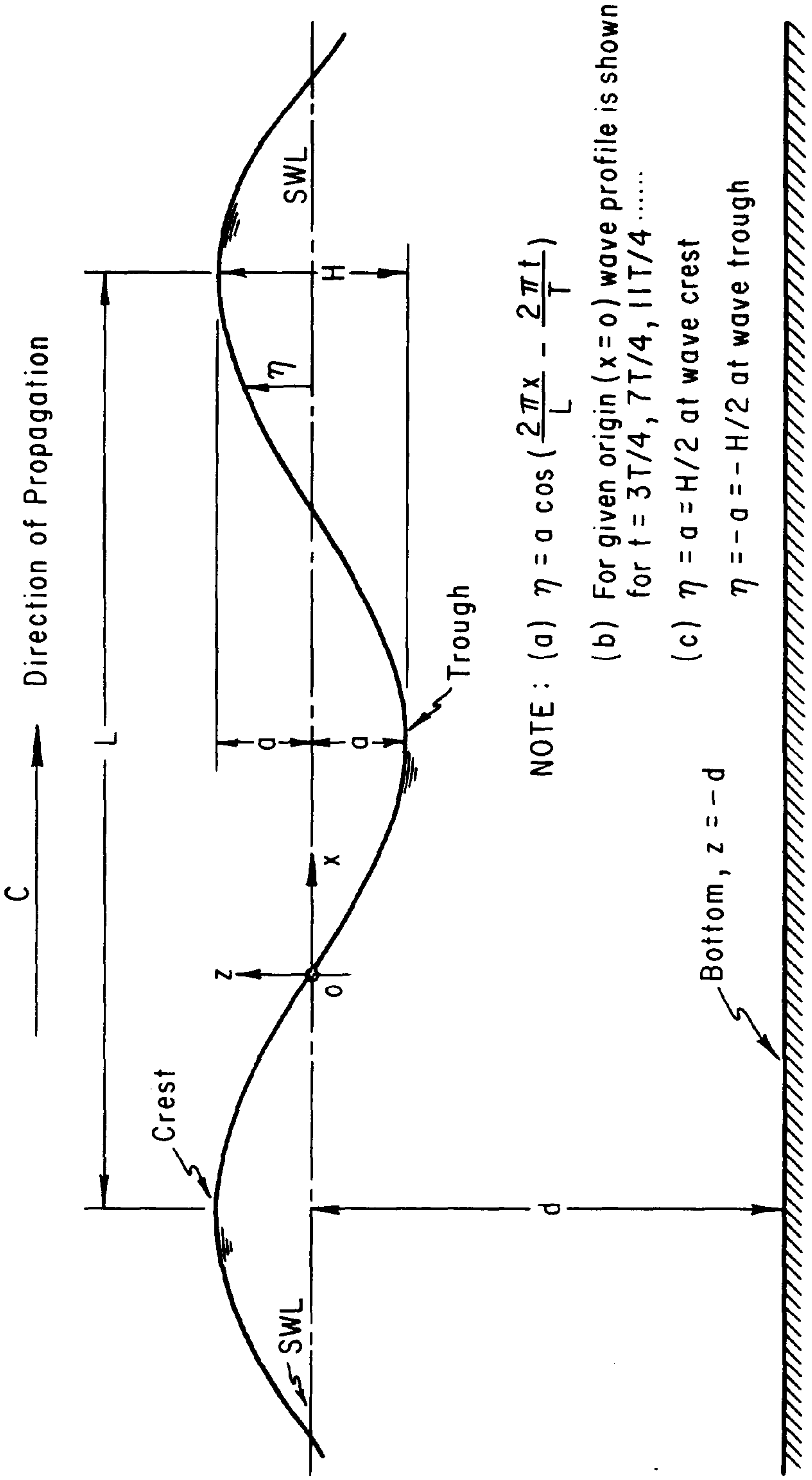

Figure 5-1. Definitions of elementary, sinusoidal, and progressive waves

RELATIVE DEPTH	SHALLOW WATER $\frac{d}{L} < \frac{1}{25}$	TRANSITIONAL WATER $\frac{1}{25} < \frac{d}{L} < \frac{1}{2}$	DEEP WATER $\frac{d}{L} > \frac{1}{2}$
1. Wave profile	Same As $\longrightarrow$	$\eta = \frac{H}{2} \cos \left[\frac{2\pi x}{L} - \frac{2\pi t}{T} \right] = \frac{H}{2} \cos \theta$	Same As $\longleftarrow$
2. Wave celerity	$C = \frac{L}{T} = \sqrt{gd}$	$C = \frac{L}{T} = \frac{gT}{2\pi} \tanh \left(\frac{2\pi d}{L} \right)$	$C = C_0 = \frac{L}{T} = \frac{gT}{2\pi}$
3. Wavelength	$L = T\sqrt{gd} = CT$	$L = \frac{gT^2}{2\pi} \tanh \left(\frac{2\pi d}{L} \right)$	$L = L_0 = \frac{gT^2}{2\pi} = C_0 T$
4. Group velocity	$C_g = C = \sqrt{gd}$	$C_g = nC = \frac{1}{2} \left[1 + \frac{4\pi d/L}{\sinh(4\pi d/L)} \right] \cdot C$	$C_g = \frac{1}{2} C = \frac{gT}{4\pi}$
5. Water Particle Velocity (a) Horizontal	$u = \frac{H}{2} \sqrt{\frac{g}{d}} \cos \theta$	$u = \frac{H}{2} \frac{gT}{L} \frac{\cosh[2\pi(z+d)/L]}{\cosh(2\pi d/L)} \cos \theta$	$u = \frac{\pi H}{T} e^{\frac{2\pi z}{L}} \cos \theta$
(b) Vertical	$w = \frac{H\pi}{T} \left(1 + \frac{z}{d} \right) \sin \theta$	$w = \frac{H}{2} \frac{gT}{L} \frac{\sinh[2\pi(z+d)/L]}{\cosh(2\pi d/L)} \sin \theta$	$w = \frac{\pi H}{T} e^{\frac{2\pi z}{L}} \sin \theta$
6. Water Particle Accelerations (a) Horizontal	$a_x = \frac{H\pi}{T} \sqrt{\frac{g}{d}} \sin \theta$	$a_x = \frac{g\pi H}{L} \frac{\cosh[2\pi(z+d)/L]}{\cosh(2\pi d/L)} \sin \theta$	$a_x = 2H \left(\frac{\pi}{T} \right)^2 e^{\frac{2\pi z}{L}} \sin \theta$
(b) Vertical	$a_z = -2H \left(\frac{\pi}{T} \right)^2 \left(1 + \frac{z}{d} \right) \cos \theta$	$a_z = -\frac{g\pi H}{L} \frac{\sinh[2\pi(z+d)/L]}{\cosh(2\pi d/L)} \cos \theta$	$a_z = -2H \left(\frac{\pi}{T} \right)^2 e^{\frac{2\pi z}{L}} \cos \theta$
7. Water Particle Displacements (a) Horizontal	$\xi = -\frac{HT}{4\pi} \sqrt{\frac{g}{d}} \sin \theta$	$\xi = -\frac{H}{2} \frac{\cosh[2\pi(z+d)/L]}{\sinh(2\pi d/L)} \sin \theta$	$\xi = -\frac{H}{2} e^{\frac{2\pi z}{L}} \sin \theta$
(b) Vertical	$\zeta = \frac{H}{2} \left(1 + \frac{z}{d} \right) \cos \theta$	$\zeta = \frac{H}{2} \frac{\sinh[2\pi(z+d)/L]}{\sinh(2\pi d/L)} \cos \theta$	$\zeta = \frac{H}{2} e^{\frac{2\pi z}{L}} \cos \theta$
8. Subsurface Pressure	$p = \rho g (\eta - z)$	$p = \rho g \eta \frac{\cosh[2\pi(z+d)/L]}{\cosh(2\pi d/L)} - \rho g z$	$p = \rho g \eta e^{\frac{2\pi z}{L}} - \rho g z$

Figure 5-2. Summary of linear (Airy) wave theory wave characteristics

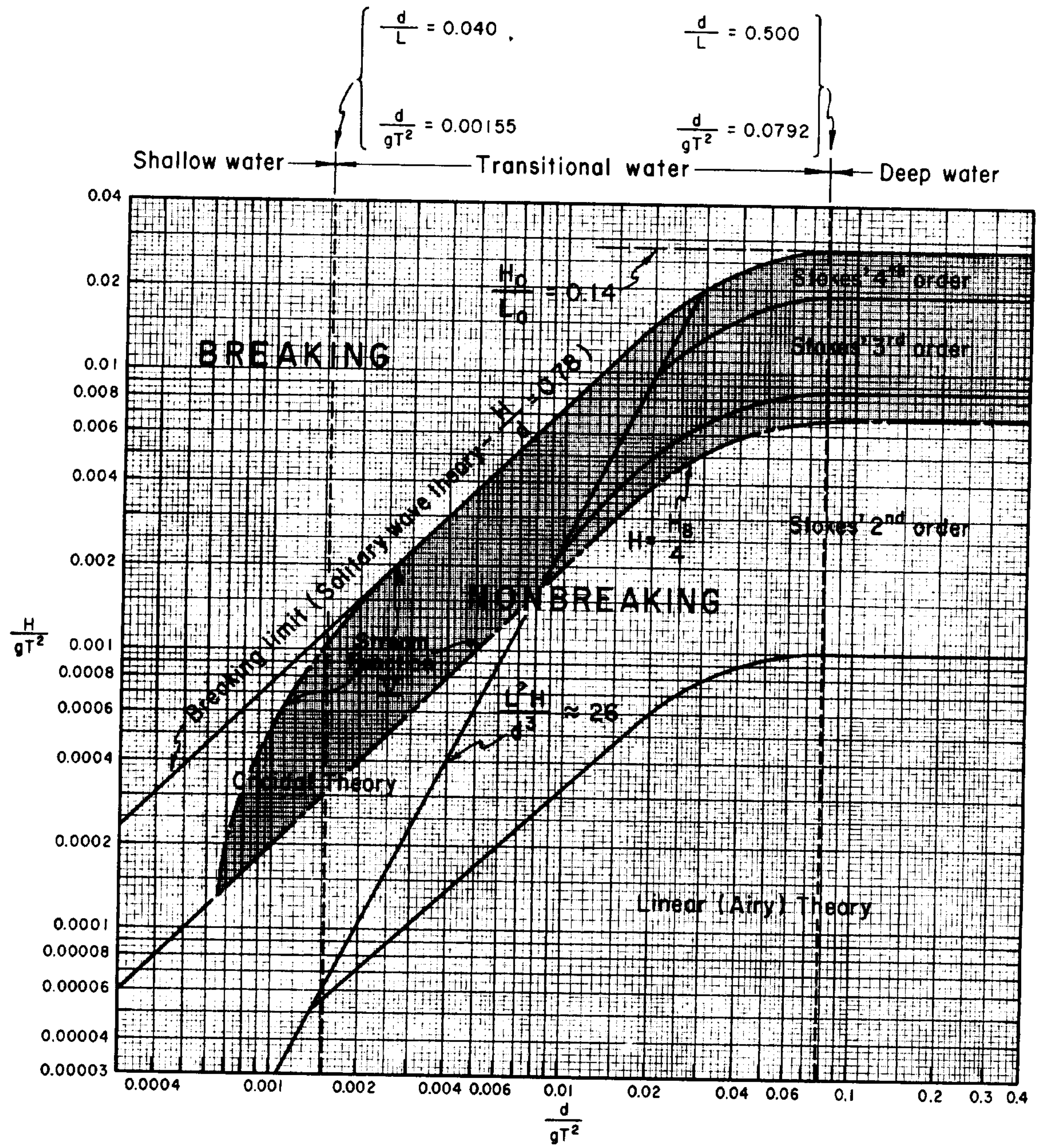

Figure 5-3. Regions of validity for various wave theories (after item 85)

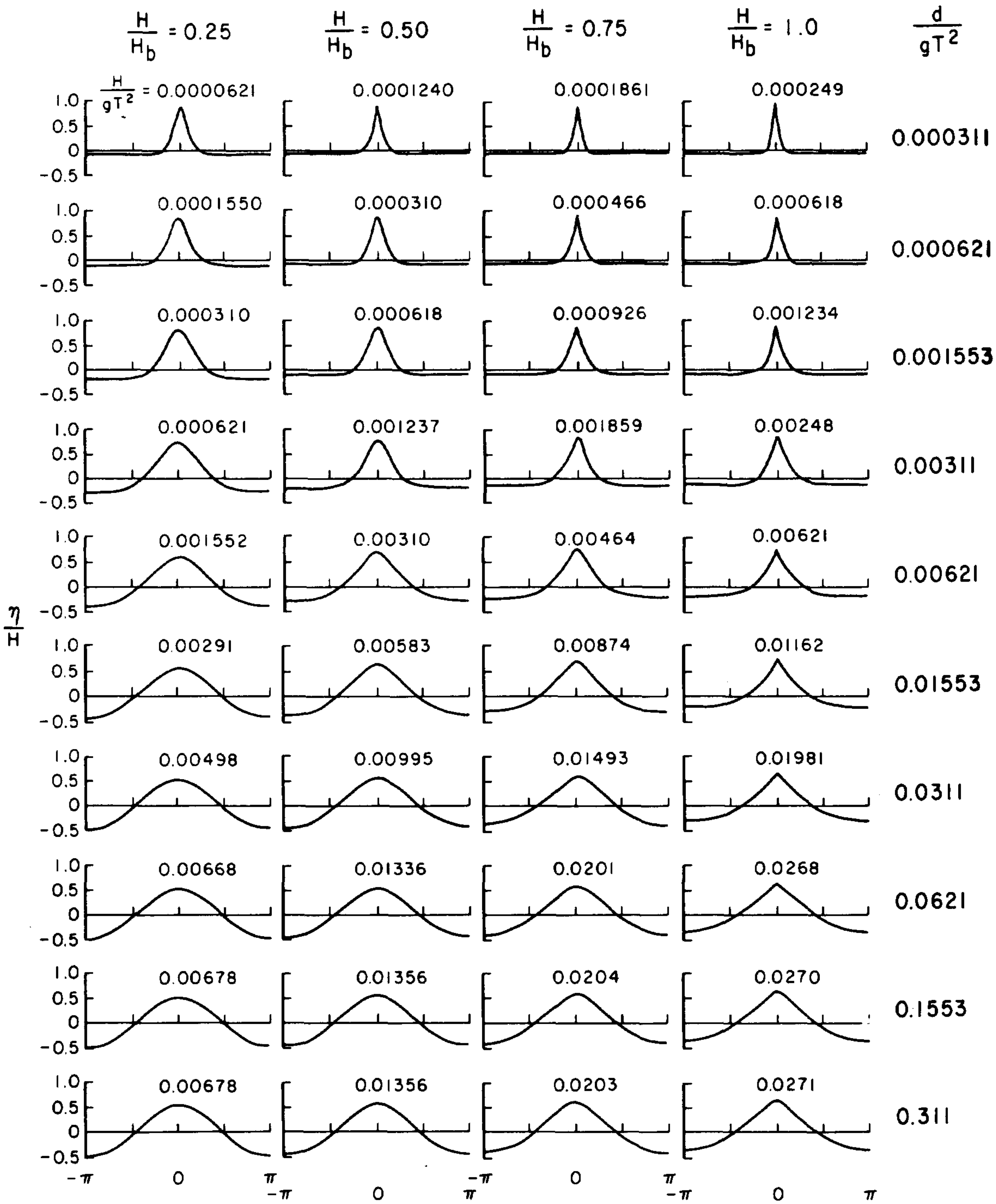

Figure 5-4. Dimensionless wave profiles for 40 cases (numbers on each plot represent the value of H/gT^2 for each case) (after item 23)

profiles assumed by small-amplitude theory. Additional information on higher order wave theories is available in the SPM.

5-3. Wave Observation Techniques. The primary information from any wave observation technique is generally an estimate of significant wave height and period as defined in the following subsection. Many techniques provide additional valuable data. Commonly used techniques are described in the remainder of this section. Their particular advantages and disadvantages are given in Table 5-1.

Table 5-1

Wave Observation Techniques

Technique	Water Depth*	Advantages**	Disadvantages***
Ship board observations	1,2	1,2	1
Shore observations	3	1	1
Staff gage	1,2,3	3,6	2,3
Pressure cell (connected to shore by cable or telemetry)	2,3	4,6	3,4,5
Pressure cell (internally recording)	2,3	4,5	3,4,5,6,7
Accelerometer buoy	1,2	5,6	5,8,9
High frequency radar	1,2	5,6,7	5,9

*Water Depths: 1 = deep, 2 = intermediate, 3 = shallow.

**Advantages: 1 = inexpensive, 2 = large data set already exists, 3 = direct measurement of surface waves, 4 = relatively reliable for unattended use, 5 = relatively simple installation, 6 = adaptable to real-time monitoring, 7 = spatial coverage.

***Disadvantages: 1 = low accuracy; 2 = sturdy support structure required for exposed sites; 3 = subject to fouling by marine growth; 4 = divers needed for installation and maintenance; 5 = indirect measurement of desired surface waves; 6 = prone to loss due to burial, inaccurate positioning, and loss of marker buoys; 7 = frequent maintenance required for power supply and recorder; 8 = prone to loss due to collision or failed mooring; 9 = relatively expensive.

a. Definition of Significant Wave Height and Period. The concept of a "significant wave height" and a "significant wave period" which can be used to characterize a wave field is appealingly simple. It suggests a simple transition from the experimental results in a laboratory wave tank and the theoretical results obtained with theories for uniform waves to the phenomena that occur in the ocean.

(1) The concept of a significant wave height and period was first introduced when sailors were asked to report the height and period of the larger, well-formed waves, and omit entirely the low and poorly formed waves as part of the synoptic weather reports from ships. Comparisons of early wave gage records with observations led to the conclusion that the wave height H_v given by observers was approximately equal to the average height of the one-third highest individual waves $H_{1/3}$. Figure 5-5 provides some perspective on the reliability of this approximation. The figure is based on 905 pairs of visual and instrument observations from a weather ship equipped with a shipboard wave recorder.

(2) The parameter $H_{1/3}$ is referred to as "significant wave height," and the corresponding period is the "significant wave period." Practical techniques for estimating these parameters from wave records are presented in Section 5-4.

b. Observations from Shipboard. Wave observations have been collected by observers aboard ships in passage for many areas of the world over many years. The observations include average height, period, and direction of sea waves (locally generated) and swell waves (generated elsewhere and propagated to the area). In modern observations, the sea direction is assumed to coincide with the wind direction.

(1) The reliability of shipboard observations must be considered. Individual observations are highly variable. However, the observations are generally unbiased so that summaries of many observations can be useful. Height summaries provide useful estimates of the mean and distribution, as illustrated in Figure 5-5. Accuracy is less in the upper end of the distribution because of the small number of observations and the tendency for ships to avoid very high wave conditions. A cumulative distribution of shipboard observed wave heights should be considered reliable up to about the one percent level of occurrence or the point at which 20 observations are represented, whichever criterion is more restrictive.

(2) Wave period is difficult to estimate aboard a moving ship, and only the overall mean period should be used. Wave directions are also somewhat difficult to estimate and should be assumed to have a resolution of 45 degrees or coarser. The availability of shipboard observations is presented in Chapter 6.

c. Observations from Shore.

(1) The major Corps program for collection of wave observations from shore is the Littoral Environment Observation (LEO) program. The LEO program was established to provide data on coastal phenomena at low cost. Volunteer observers obtain daily estimates which include breaker height, wave period,

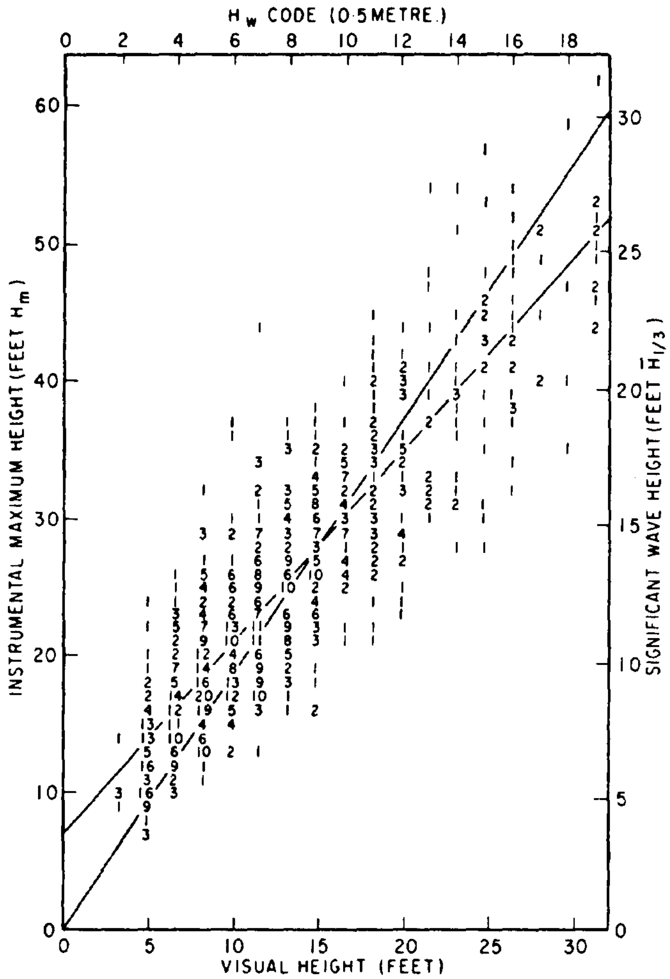

Figure 5-5. Comparison of instrument and observed heights ($H_{1/3} = 1.1\ H_v$) (after item 112)

direction of wave approach, wind speed, and wind direction. Wave height and direction are visual estimates. Other parameters are estimated with simple equipment. The skill and biases of individual observers significantly influence the validity of observations from shore.

(2) Generally, LEO data are summarized annually. To be statistically descriptive of a site, observations must be recorded for at least 20 days of each month for a period of at least 3 years. Additional information on the LEO program is available from item 114. The availability of LEO data summaries is discussed in Chapter 6.

d. Wave Staff Observations. Wave staff observations are obtained with a gage which pierces the water surface. In its simplest form, the wave staff is a vertical rod with visible marks on it at measured intervals. It allows an observer to obtain good quantitative estimates of wave characteristics by watching the undulating water motions at the staff.

(1) Most wave staffs operate as electrical sensors. They detect the instantaneous location of the water surface by using it to change the electrical properties of a circuit. Most electrical wave staffs operate as either resistive, capacitive, or wave guides. Additional information about wave staffs is available from item 106.

(2) In addition to the advantages and disadvantages of the wave staff listed in Table 5-1, the staff is often inexpensive relative to other instrument observation techniques. The observed staff is especially economical, and it can be very useful in low-budget projects. In low-energy environments, the staff gage can be mounted on a spar buoy as an alternative to a rigid mounting structure.

e. Pressure Cell Observations. Pressure cell observations are obtained with a pressure-sensitive gage mounted under the water surface. Pressure cells can be situated anywhere in the water column as long as they are below the elevation of the lowest expected wave trough at the lowest expected tide level. Pressure cells, often placed on a small tripod which rests on the bottom, submerged, sense dynamic pressure fluctuations created by passing surface waves. The magnitude of the fluctuations decreases exponentially with distance below the surface. The pressure fluctuations are converted to an electronic signal which can be recorded at the gage or sent to a shore station by either an armored electrical cable or a surface buoy transmitter. Additional information about pressure cells is available in item 34.

f. Accelerometer Observations. Accelerometer buoy observations are obtained with a surface following buoy which is usually spherical. Buoys, routinely moored in water depths of less than 600 feet, sense vertical acceleration which is usually integrated twice electronically to give a record of surface displacements. Observations may be recorded in the buoy or transmitted to a shore station either directly or via a satellite link.

g. Other Wave Recording Instruments. A variety of other wave recording instruments is available for practical use, although those discussed in the preceding subsections are most widely used. The instruments are categorized as in situ instruments and remote sensing devices.

(1) In situ instruments include acoustic, ultrasonic, optical (laser), and radar instruments, all of which transmit a signal toward the water surface from above or below. The reflected signal is then received and interpreted. Another approach to in situ data recording consists of operating several instruments together at a site and analyzing the records jointly to get additional information, particularly wave direction. Typical combinations are a pressure cell or staff with two orthogonal horizontal current meters, and a spatial array of staffs or pressure cells. More information on these in situ instruments is available from items 106 and 117.

(2) A variety of remote sensing devices is available, as summarized in Figure 5-6. Only a few devices are suitable for routine data collection. The Coastal Imaging Radar System can be used to estimate dominant wave directions (item 91). High-frequency radar, such as the Coastal Ocean Dynamics Applications Radar (CODAR) can be used to estimate coastal wave characteristics, including direction (item 2). Other devices are the Side-Looking Airborne Radar

	Sensor	SLAR	SAR	Coastal Wave Imaging Radar	CODAR	ROWS	Δk	SCR
WAVE PARAMETERS	Status	Operational	Operational	Operational	Operational	Operational	Developmental	Operational
	Height	No	(1)	No	Yes	Yes	Yes	Yes
	Length	Yes	Yes	Yes	Yes	Yes	Yes	Yes
	Direction	Yes	Yes	Yes	Yes	No	Yes	Yes
	Spectrum	Directional Wave number Spectrum	Directional Wave number Spectrum	Directional Wave number Spectrum	Directional Wave height Spectrum	1-D Wave height Spectrum	Directional Wave height Spectrum	Directional Wave height Spectrum
	Spatial Coverage	1-km swath	Aircraft 1-km swath	Up to 5-km radius	40-km radius	Several sq Meters	2-3 km Radius	Swath width = 1/2 aircraft altitude
	Cell Size Resolution	Depends on range	Aircraft 3-m spatial resolution	15-m range resolution	5-km spatial resolution	Several sq Meters	90-m Range Resolution	0.5 -2.0 km^2 cell size
	Platform	Aircraft	Aircraft/ Satellite	Land-based tower	Land-based	Land-based tower	Land-based tower	Aircraft
	System Cost	Expensive	Very Expensive	\$50 K	\$150 K	\$50 K	\$100 K	\$500 K
	Cost/ Typical Data Set	Moderate	\$1000 per 5 km x 5 km patch	\$100	Low	Low	Low	\$2700/hr aircraft flight time
	Comments	Limited spatial resolution.	Increased resolution: more expensive than SLAR.	Inexpensive and reliable for long term operation.	Large spatial coverage. Useful for getting directional spectra offshore.	High spatial resolution.	Provides data at scales between ROWS and CODAR. Uses could include monitoring waves in harbors and entrances.	Aircraft out of Wallops Is., VA. Expensive for remote study sites. Data acquisition quick.

(1) Theoretically possible, but no algorithm developed as yet.

NOTE: 1 km = 0.621 mile, 1m = 3.28 ft,
1 km^2 = 0.386 sq miles, 1 m^2 = 10.75 ft^2

Figure 5-6. Summary of remote sensing systems for measuring ocean waves (after item 24)

(SLAR), Synthetic Aperature Radar (SAR), Remote Orbital Wave Spectrometer (ROWS), dual frequency radar (Δk), and Surface Contouring Radar (SCR).

5-4. Wave Analysis Techniques. Wave records are usually collected as a digital time series of surface elevation or subsurface pressure. Records should be suitably checked and edited before further analysis. Typical steps in analyzing a digital wave record are schematized in Figure 5-7. Appendix D describes parameters that are important in the collection and analysis of digital wave data.

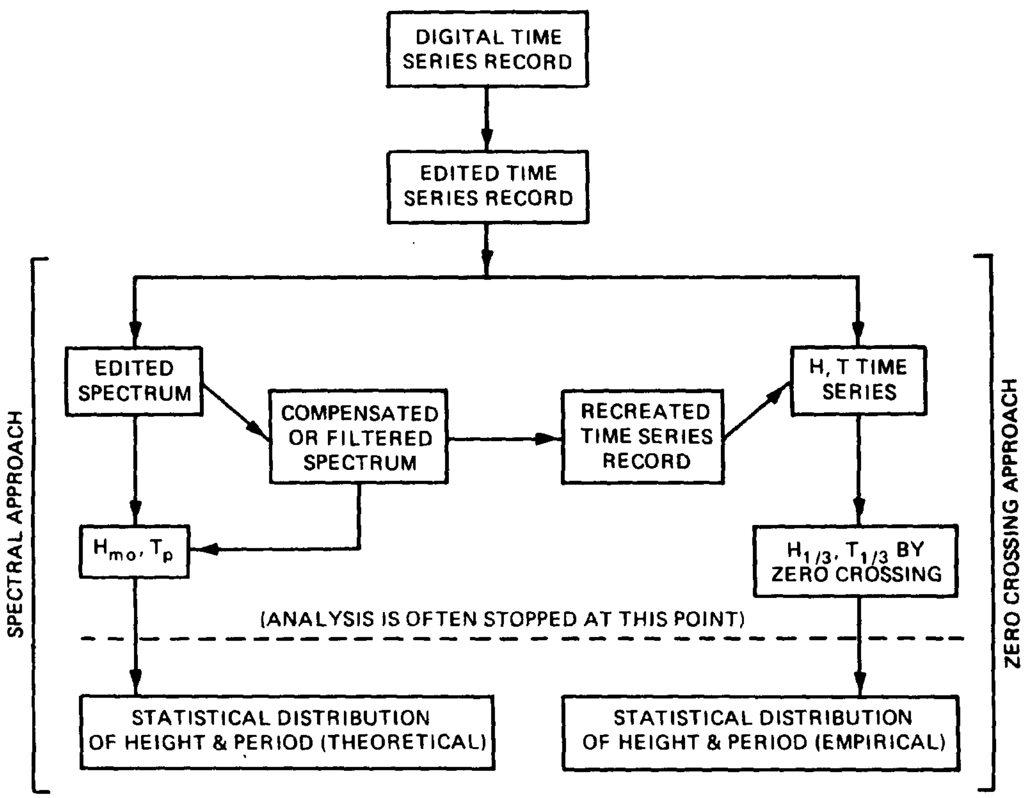

Figure 5-7. Analysis of a digital wave record

a. Wave Record Editing. The editing step should include a check for waves at short and long periods outside the range of wind wave periods, which is 1 to 30 seconds. Potential sources of waves at undesired periods are tides, water level oscillations, surf beats, electronic drift, electronic noise, and transmission interference. If any of these waves are significant in the record, they may distort estimates of wind wave characteristics. Short- and long-period contamination can be identified visually or by numerical tests. It can be removed by filtering or by considering the spectrum discussed in the following subsections.

b. Significant Height and Period. Significant wave height may be estimated from a digital record by direct computation of $H_{1/3}$ from the time series or by first computing a spectrum, as shown in Figure 5-7.

(1) By the spectral approach, significant height is estimated as four times the standard deviation of the record of sea surface elevations. A standardized analysis package for ocean waves should be used when the spectral approach is desired. A comprehensive package has the advantages of automatically removing nonwind wave energy from the results and options for compensating pressure or acceleration signals to give estimates of surface waves. The significant height estimate is referred to as H_{mo} (zero moment wave height) to clearly identify that it was obtained by a spectral approach. Wave period estimated by the spectral approach is the period corresponding to the highest energy density in the spectrum. It is called significant or peak period T_p .

(2) The term H_s is commonly used to designate a generalized significant wave height. When it is used, the method for estimating it and whether it represents $H_{1/3}$ or H_{mo} should be made clear.

(3) Significant height and period may be estimated directly from the time series record by identifying all individual waves in the record. The procedure which is most widely used and most easily applied on a digital computer is the zero-crossing method. The preferred application of this method involves identifying each wave in the record as an event between two successive points at which the wave trace crosses the mean in a downward moving direction (Figure 5-8). Wave height is defined as the elevation difference between the highest point (crest) and lowest point (trough) of each wave. Significant wave height is computed as the average height of the highest one-third zero-crossing waves. Other wave height statistics, such as the root-mean-square wave height, are also easily computed. Significant period is computed as the average period of the one-third highest waves. Significant period may also be estimated as the mean period of all waves, although this estimate may be misleading when two or more prominent wave trains with greatly differing periods occur simultaneously. This procedure is called the zero downcrossing analysis procedure because each wave is defined by two downcrossings of the mean.

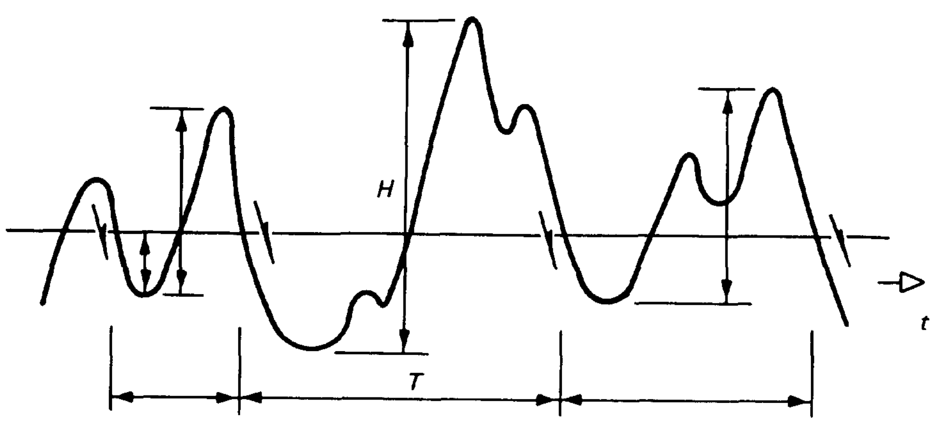

Figure 5-8. Zero downcrossing waves

(4) Both spectral analysis and zero-crossing analysis are useful in practical engineering work. Spectral analysis is more complete; but zero-crossing requires less computer capacity. Zero-crossing analysis also provides unique information when the waves are near breaking and highly nonlinear. Spectral analysis may be necessary prior to zero-crossing analysis if the time series needs to be compensated or filtered (see Figure 5-7).

c. Spectral Analysis. Spectra are becoming widely available through various field wave measurement programs, laboratory tests with programmable wave generators, and numerical wave hindcasting projects. Because of the availability and applications of spectra, practicing coastal engineers need to be familiar with spectra and their interpretation.

(1) Energy Spectrum. A fundamental parameter for characterizing a wave field is some measure of the periodicity of the waves. For many years a significant period, which could be subjectively estimated in various ways, was used. However, the ocean surface often has waves characterized by several distinct periods occurring simultaneously. A record of the variation of sea surface elevation with time, commonly called time series, frequently appears confusing and is difficult to interpret.

(a) Developments in computer technology and in mathematical analysis of time series have provided a practical approach to an objective, more comprehensive analysis of periodicity in wave records. The approach is to express the time series as a sum of sine and cosine functions with different frequency and phase. Thus, the time series of sea-surface deviations from the mean surface $\eta(t)$ is expressed by

$$\eta(t) = \sum_{j=1}^{n} a_j \cos(\omega_j t - \phi_j) \qquad (5\text{-}1)$$

where

a_j = amplitude

ω_j = frequency in radians

t = time

ϕ_j = phase

Frequency is often expressed in terms of hertz units where one hertz is equal to one cycle per second. One hertz is also equivalent to 2π radians per second. If the symbol f_j denotes frequency in hertz, then $2\pi f_j = \omega_j$.

(b) The amplitudes a_j , computed for a time series, give an indication of the importance of each frequency f_j . The sum of the squared amplitudes is related to the variance of sea surface elevations in the original time series and hence to the potential energy contained in the wavy sea surface. Because of this relationship, the distribution of squared amplitudes as a function of frequency can be used to estimate the distribution of wave energy as a function of frequency. This distribution is called the energy spectrum and is often expressed as

$$(E_j)\,(\Delta f)_j = \frac{a_j^2}{2} = S_j \tag{5-2}$$

where

$E_j = E(f_j)$ = energy density in the j^{th} component of the energy spectrum

$(\Delta f)_j$ = frequency bandwidth in hertz (difference between successive f_j)

$S_j = S(f_j)$ = energy in the j^{th} component of the energy spectrum

(c) An energy spectrum computed from an ocean wave record is plotted in Figure 5-9. Frequencies associated with large values of energy density (or large values of $a_j^2/[2(\Delta f)_j]$ (see equation 5-2) represent dominant periodicities in the original time series. Frequencies associated with small values of energy density are usually unimportant. It is common for ocean wave spectra to show two or more dominant periodicities, as in Figure 5-9. When only one frequency is reported from a spectrum, the frequency at which the energy density is highest f_p is usually used. The dominant wave period, or peak period, is given as the reciprocal of f_p.

(d) The appearance of a spectrum can be noticeably influenced by the methods used for calculation and display, neither of which is standardized in coastal engineering activities at present. The most important difference

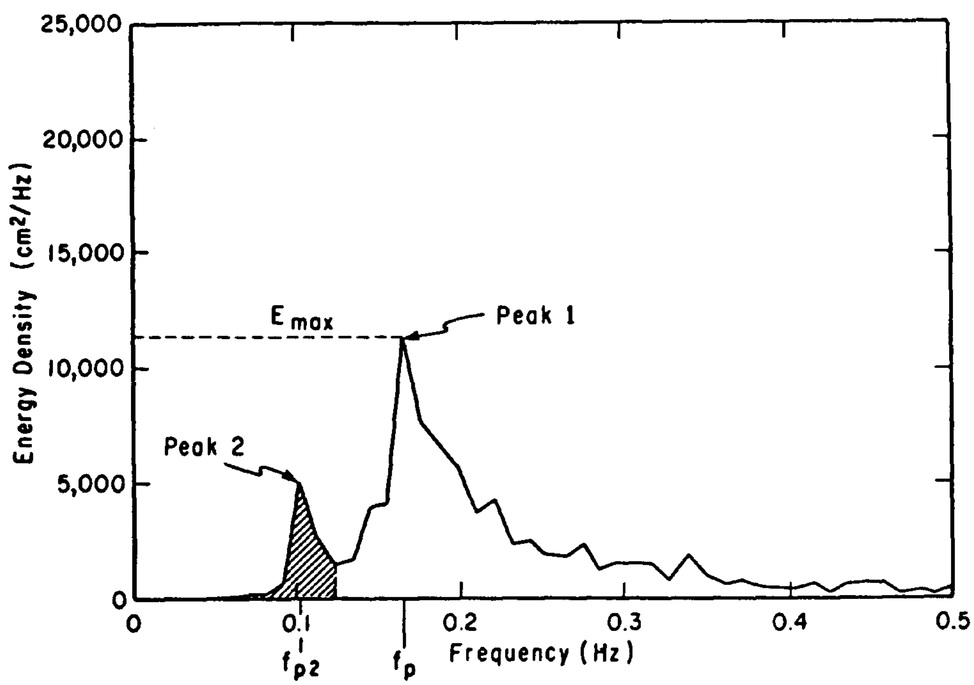

Figure 5-9. Spectrum for Wrightsville Beach, North Carolina, 0700 EST, 12 February 1972 (H_s = 4.2 ft (128 centimeters), Δf = 0.01074 hertz, and depth = 17.7 ft (5.4 meters))

among commonly used methods is whether the spectrum is summarized as energy density at equal frequency intervals or approximately equal period intervals.

(e) Spectral analysis procedures such as cross spectral analysis are available to extract more information when concurrent time series from several gages are obtained. The most important additional information is typically wave direction. Procedures for a triangular array are discussed in item 31 and for an arbitrary gage arrangement in item 4.

(2) Spectral Parameters. The complete energy spectrum is too cumbersome for forming statistical summaries of wave conditions at a site. Thus simple parameters of the spectrum are very useful. The most commonly used spectral parameters are the significant wave height estimate H_{mo} and the peak period T_p.

(a) Several additional parameters are also widely used to better characterize the shape of the spectrum and the importance of nonlinearities in the time series from which the spectrum was computed. One useful parameter is the number of major peaks in the spectrum. This parameter is indicative of the number of independent wave trains present, except when the measurements were taken in or near the surf zone (item 124).

(b) The spectral peakedness parameter proposed by item 36 is indicative of the sharpness of the spectral peak. The spectral peakedness parameter Q_p is computed by

$$Q_p = 2 \sum_{i=1}^{N} f(\Delta f)_i \, S_i^2 \left[\sum_{i=1}^{N} (\Delta f)_i \, S_i \right]^{-2} \tag{5-3}$$

The usefulness of Q_p is illustrated in Figure 5-10 which shows two spectra with nearly the same significant height and peak period but different values of the peakedness parameter.

(3) Parameters of the Distribution of Surface Elevations. Statistical moments of the distribution of sea surface elevations provide additional information. Moments are computed by

$$q_n = \sum_{i=1}^{N} \eta_i^n \, p(\eta_i) \tag{5-4}$$

where

q_n = n^{th} moment of the distribution function of sea surface elevations

N = number of intervals in the distribution function

η_i = sea surface elevation associated with the i^{th} interval in the distribution function

$p(\eta_i)$ = probability associated with η_i

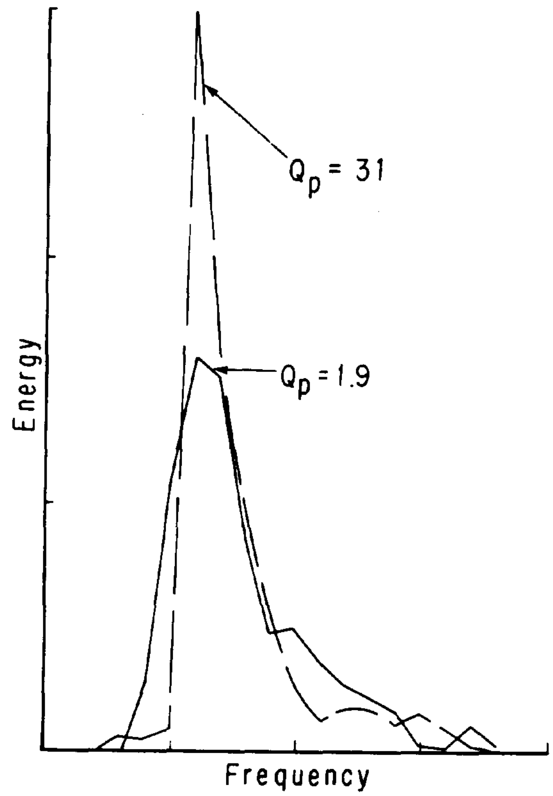

Figure 5-10. Comparison of two measured spectra from the North Atlantic Ocean (H_s = 3.3 m, T_p = 10.5 s)

The zeroth and first moments q_o and q_1 are equivalent to the mean and variance of the distribution function. The third moment, or skewness, of the distribution is a very useful indicator of the extent of nonlinear deformation of wave profiles in the time series. The deformation can be significant for breaking and near breaking waves in shallow water. Since the shape of the spectrum is affected by nonlinear deformation of wave profiles (Figure 5-11), the skewness is helpful in interpreting spectral shape.

d. Coastal Engineering Research Center (CERC) Method for Strip Chart Records. In addition to digital records, pen-and-ink strip chart records are sometimes available. Although strip chart wave records are rarely collected with modern systems, they can be easily analyzed by the method in Appendix E. The method is set up for a 7-minute record length. It can be adapted to other record lengths by using the Rayleigh distribution equation (Section 5-4.e) to compute new entries in the tabulated "number of wave to measure."

e. Distribution of Individual Wave Heights.

(1) The distribution of individual wave heights is well approximated by the Rayleigh distribution function. The probability density function for the Rayleigh distribution is given by

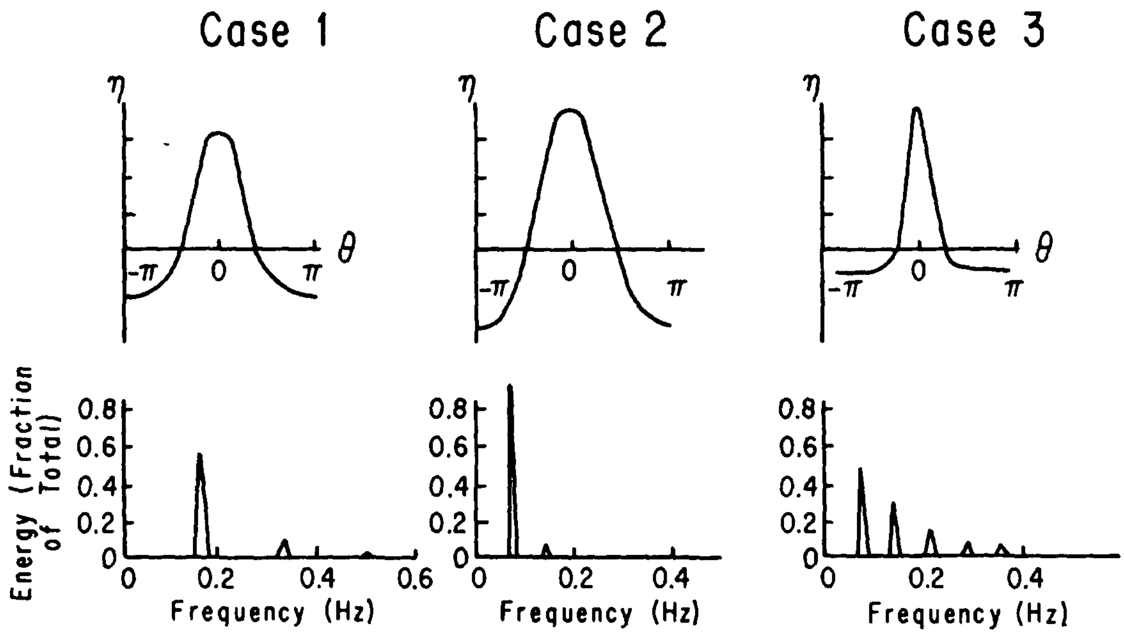

	Case 1	Case 2	Case 3
T	6.0 s	14.0 s	14.0 s
$\frac{H}{d}$ =	0.572	0.076	0.572
d/gT^2 =	0.0142	0.0026	0.0026
d/L =	0.129	0.052	0.046
q_1 =	0	0	0
q_2 =	1.0	1.0	1.0
q_3 =	0.84	0.51	2.02
q_4 =	2.23	1.89	5.82
Q_p =	14.2	13.2	6.8

Figure 5-11. Wave profiles and energy spectra for several cnoidal wave cases (record length = 512 s, spectral bandwidth = 0.00977 hz)

$$p(\hat{H}) = -2 \frac{\hat{H}}{H_{rms}^2} e^{-(\hat{H}/H_{rms})^2} \tag{5-5}$$

where $p(H)$ is the probability of a given wave height H, and H_{rms} is the root-mean-square wave height. The cumulative form of the Rayleigh distribution function is given by

$$P(H>\hat{H}) = e^{-(\hat{H}/H_{rms})^2} \tag{5-6}$$

where $P(H>\hat{H})$ is the number of waves larger than $\hat{H}$ divided by the total number of waves in the record. The cumulative distribution function is plotted in Figure 5-12. The Rayleigh distribution was derived theoretically for the distribution of wave amplitudes in a Gaussian sea state with a narrow spectrum. However it has proved to fit empirical wave height data remarkably well, even in shallow water.

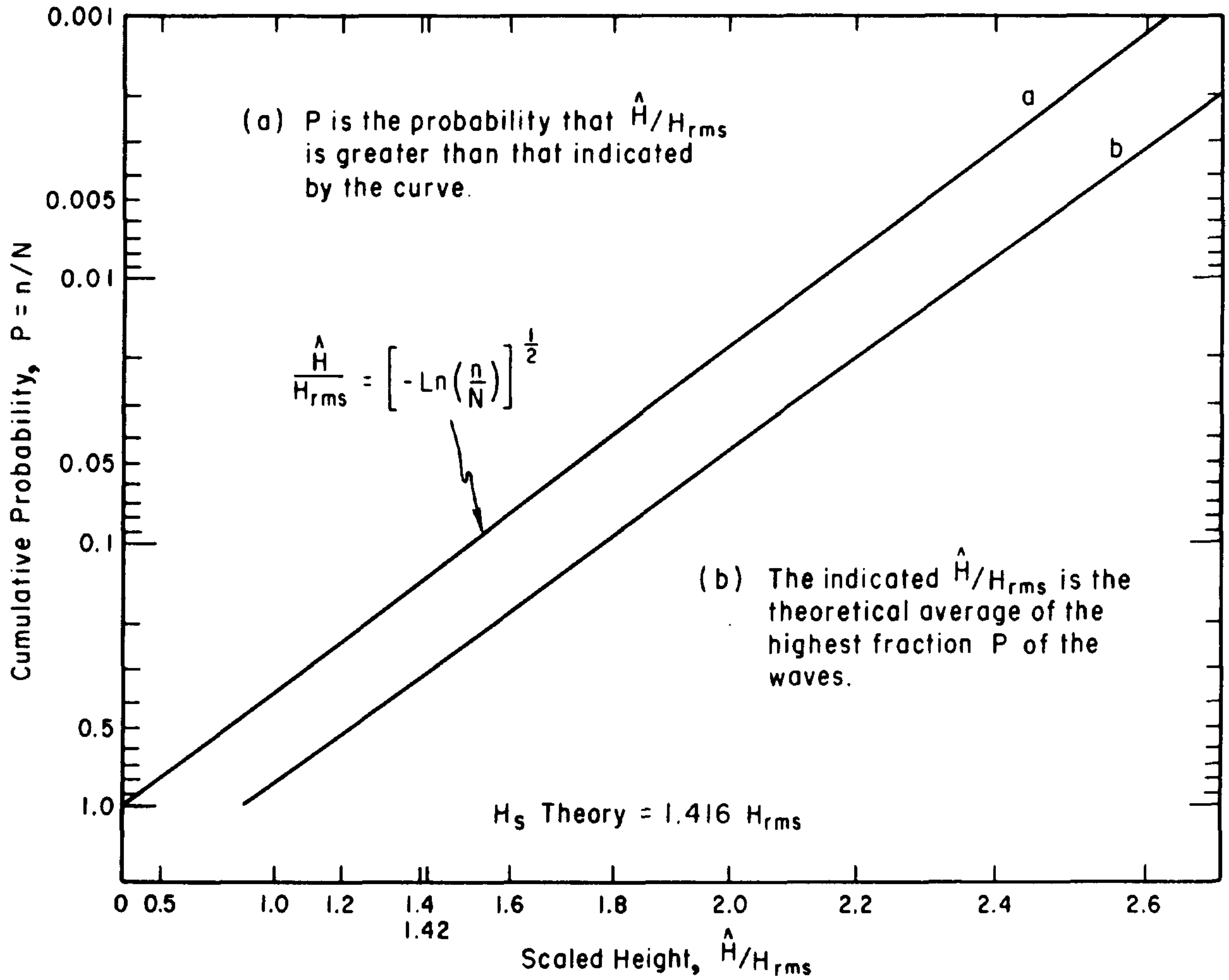

Figure 5-12. Theoretical wave height distributions

(2) The average height for any specified fraction of the higher waves is given by the lower curve in Figure 5-12 in terms of H/H_{rms} . The same information is given in Table 5-2 for commonly used fractions of the higher waves. The table also gives the percentage of heights higher than the average.

f. Distribution of Individual Wave Periods. The distribution of individual wave periods is much more variable than the distribution of individual wave heights. A reasonable approximation for sea waves is given by item 10 as

Table 5-2

Wave Height Relationships Based on the Rayleigh Distribution

Fraction of Higher Waves	Average $\frac{H}{H_{rms}}$	Percentage of Heights Higher than average $\frac{H}{H_{rms}}$
0.001	2.82	0.035
0.01	2.36	0.38
0.10	1.80	3.92
0.33	1.42	13.5
0.50	0.89	20.4

$$p(\hat{T}) = 2.7 \frac{\hat{T}^3}{\bar{T}^4} \exp\left[-0.675\left(\frac{\hat{T}}{\bar{T}}\right)^4\right] \tag{5-7}$$

where $\bar{T}$ is the mean wave period. The relationship between $\bar{T}$ and T_p depends on the particular wave condition. In general, T_p is between 0.95 and 1.5 times $\bar{T}$. This expression should not be used when two or more prominent wave trains with widely differing periods occur simultaneously.

g. Intercomparisons of Analysis Procedures.

(1) The significant wave height obtained by zero-crossing analysis $H_{1/3}$ generally compares well with the estimate from spectral analysis H_{mo}. Empirical evidence indicates $H_{1/3}$ may be 5 percent less than H_{mo} in deep water, but $H_{1/3}$ can significantly exceed H_{mo} in shallow water. Differences are directly related to the change in wave profiles in shallow water such that crests become narrow and high and troughs broad and flat (Figure 5-4). A relationship between $H_{1/3}$ and H_{mo} is plotted in Figure 5-13. Wave steepness ε in the figure is defined as $0.25\ H_{mo}/L_p$, where L_p is the finite depth wavelength of waves at the spectral peak.

(2) Peak spectral period T_p is related to zero-crossing period by

$$T_p = 1.05\ T_{1/3} \tag{5-8}$$

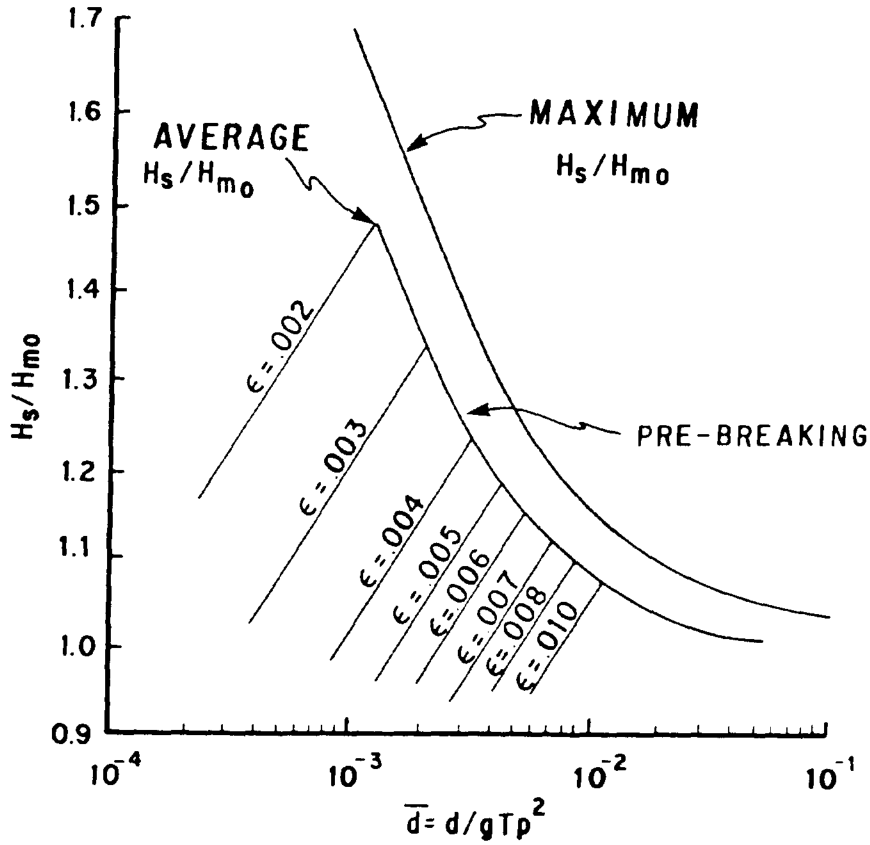

Figure 5-13. Variation of H_s/H_{mo} as a function of relative depth $\bar{d}$ and significant steepness (Both the average and maximum values of the ratio are given. The average value is read from the lower of the prebreaking line or the appropriate steepness line. Values of steepness intermediate to those plotted should be constructed as lines parallel to those plotted and spaced in between by linear interpolation. For values of steepness greater than 0.01, the ratio may be assumed to be 1) (item 125)

In the case of multiple concurrent wave trains, this relationship is unreliable. T_p will represent one of the wave trains, but $T_{1/3}$ will be an average of a variety of wave periods and may not represent any one wave train.

5-5. Comparison of Gage Records.

a. Variability Due to Gage Type. Wave gage types used in coastal waters each have some influence on the data collected. In particular, the pressure sensitive gage provides a record in which high frequency energy is removed or severely attenuated and lower frequency energy is moderately attenuated. A simple procedure for compensating the pressure record to get an estimate of surface wave conditions is to compute significant height and period from the pressure record and to compensate for the effect of gage submersion by a factor based on linear wave theory. The factor is

$$(H_s)_{sfc} = \frac{\cosh \frac{2\pi d}{L}}{\cosh \frac{2\pi(z+d)}{L}} \frac{1}{\rho g} (H_s)_{pres} \qquad (5\text{-}9)$$

where

sfc = surface conditions at the gage

d = water depth

L = local wavelength

z = depth of pressure sensor below the water surface (z is negative)

pres = underwater conditions at the gage

(1) It is generally preferable to apply the compensation equation to frequency components of the energy spectrum rather than significant wave heights. The factor for spectral application is

$$E_{sfc}(f) = \left(\frac{\cosh \frac{2\pi d}{L}}{\cosh \frac{2\pi(z+d)}{L}} \right)^2 \frac{E_{pres}(f)}{(\rho g)^2} \qquad (5\text{-}10)$$

Raw and corrected pressure spectra are illustrated in Figure 5-14. Significant height can be estimated from the compensated spectrum as discussed in Section 5-4. This approach can be expected to give surface wave estimates with errors less than 20 percent when no wavelengths are less than two times the gage depth and waves are not near the point of depth-induced breaking (items 32, 39, and 41).

(2) Another widely used gage type, the accelerometer buoy, tends to produce a spectrum with attenuated energy at the low and high frequency ends of the spectrum. Low frequency attenuation occurs because the buoy experiences very small vertical accelerations due to low frequency waves, and the accelerometer does not respond well. High frequencies are attenuated because the buoy hull does not respond well to wavelengths on the order of the hull dimensions or less. These effects can sometimes be reduced by correcting the spectrum to compensate for buoy response characteristics.

b. Variability of Wave Spectra Due to Gage Location. Wave energy spectra are naturally variable simply because they are based on a finite length record of a wave field which varies in time and space. Spectra computed for successive records of a relatively stationary wave field are

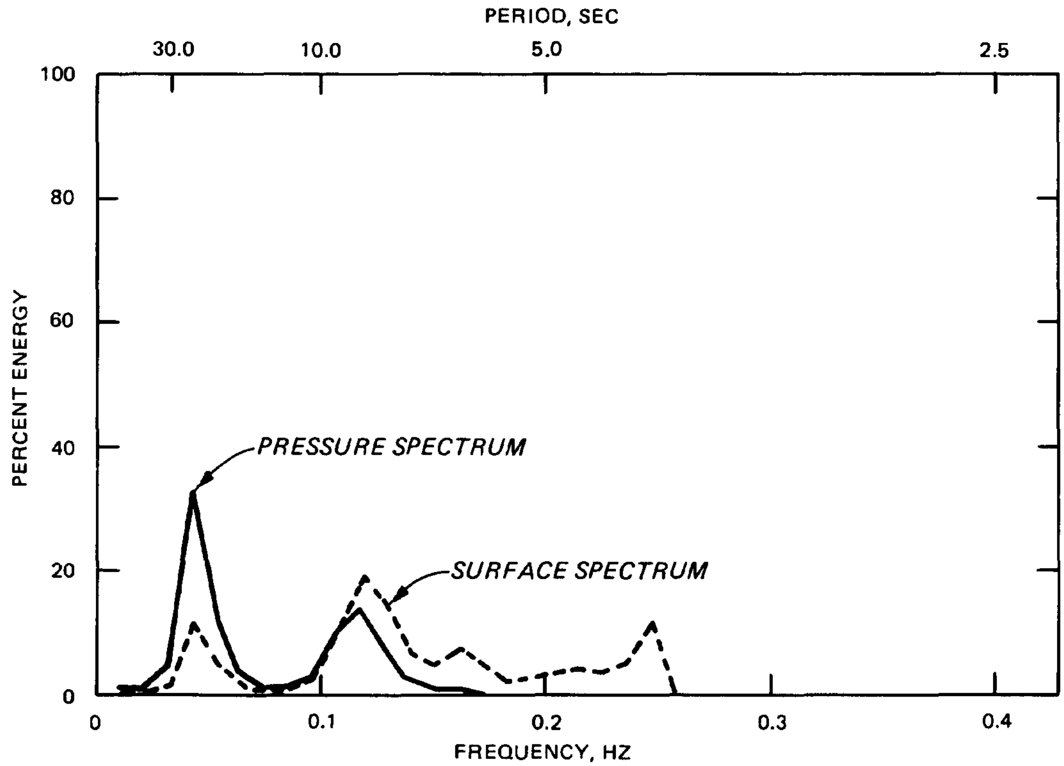

Figure 5-14. Surface spectrum computed from pressure spectrum at Point Mugu, California (gage bottom-mounted in 26-ft water depth)

never identical and often differ noticeably. The magnitude of spectral variation in time is illustrated by spectra derived at 2-hour intervals from two pressure gages along the southern California coast (Figure 5-15). The significant wave height is nearly constant in the figure.

(1) Gages Along Depth Contour.

(a) Spatial variation of the spectrum over short alongshore distances in shallow water is also shown in Figure 5-15. Each spectrum in the top row of the figure can be compared to the spectrum immediately below it to see variations between spectra from two gages 80 feet (24 meters) apart. In this figure, spatial variations are smaller than temporal variations. Spatial variations would be expected to be greater if the gages were farther apart or the water depth varied between measurement points. For gages far apart, processes such as refraction, diffraction, reflection, currents, and winds can induce significant differences in spectra by differentially influencing the wave field.

(b) Variability of spectra induced by finite length data records has been studied by Donelan and Pierson (item 27) who concluded that the theory of stationary Gaussian processes provides accurate estimates of sampling variability. For 17-minute record length, the uncertainties in significant wave

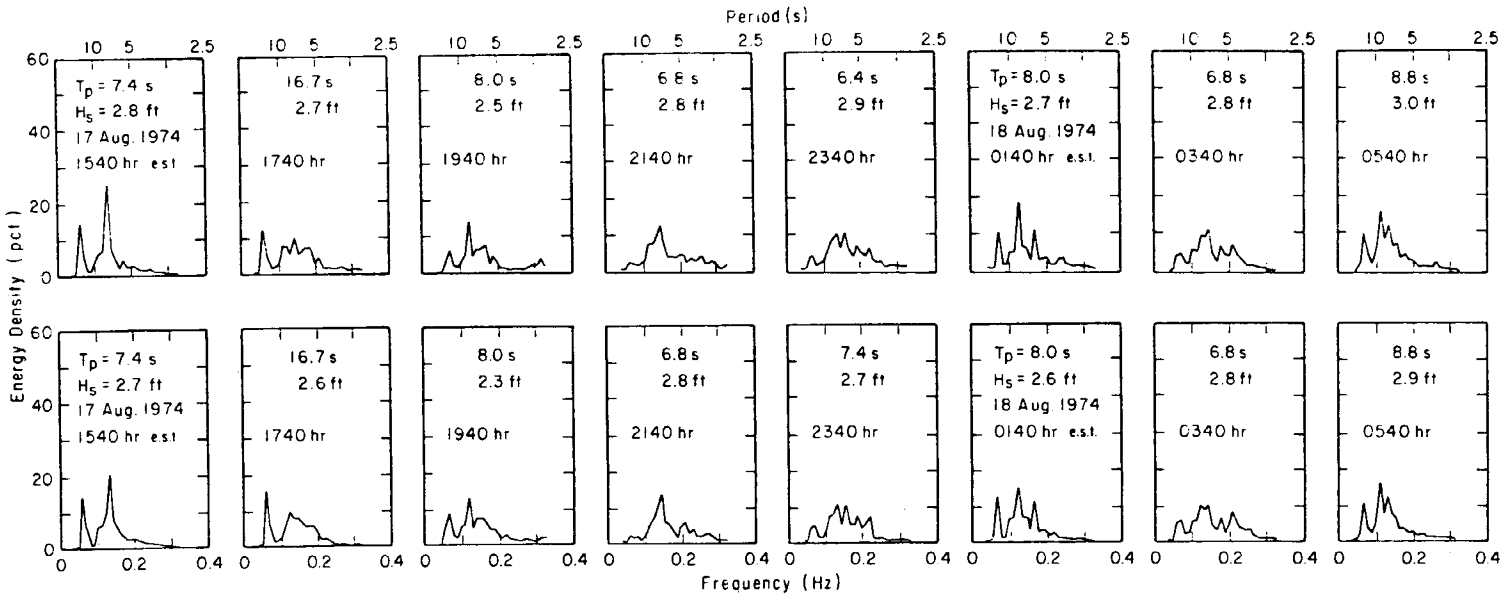

Figure 5-15. Wave energy spectra from bottom-mounted pressure gages at Channel Island Harbor, California (spectra in top row from Gage 1, in bottom row from Gage 2; gages 80 ft (24 m) apart in water depth of 20 ft (6.1 m); spectra compensated for hydrodynamic attenuation due to submergence of the gage)

height and peak frequency estimates are ± 12 percent and ± 5 percent, respectively, at the 90 percent confidence level. Further, the height of the peak of the spectrum is generally overestimated.

(2) Gages Along Line Normal To Shore. Variations between spectra from gages situated along a line perpendicular to shore are shown in Figure 5-16. The spatial variations are more prominent in this figure than in Figure 5-15. Depth-induced variations in spectra and significant heights can be large and systematic. The variations are an important consideration in interpreting data from any shallow-water gage site. The effect of shallow depth on measurements can be estimated by the techniques in Section 5-7.e.(3).

5-6. Evaluation of Common Assumptions About Waves by Comparison with Observations. Many widely used engineering formulas dealing with wind-generated waves have been derived with assumptions about the nature of waves. When real wave conditions are not well described by the assumptions, the propriety of the formulas and designs based upon the formulas is questionable. The validity of some common assumptions is assessed in this section.

a. Gaussian Distribution of Water Surface Elevations.

(1) Relationship Between Surface Elevation Distribution and Wave Profile. The Gaussian distribution is symmetric, indicating that the same probability is associated with elevation x units above the mean and x units below the mean. Such symmetry can be expected for waves which have crest profiles which generally resemble trough profiles in width and excursion from the mean. The distribution of measured sea surface elevations can differ noticeably from the Gaussian distribution when the measurements are taken in shallow water or when the measurements represent steep waves in relatively deep water. Shallow-water waves and steep, deepwater waves tend to have high narrow crests and broad flat troughs (Figure 5-4) that lead to non-Gaussian sea surface elevation distributions. The profiles of high, steep waves tend to become increasingly non-Gaussian between deep water and shallow water, as illustrated by item 77 with hurricane wave data from the Gulf of Mexico. Non-Gaussian waves have some important practical consequences. The crest elevation exceeds the SWL by more than half the wave height, which can accelerate overtopping of coastal dunes and structures and damage to elevated structures such as pier decks. Accelerations and, hence, forces exerted by wave crests are intensified in non-Gaussian waves.

(2) Parameters of Sea Surface Elevation Distribution. Distributions of measured sea surface elevation are often normalized for convenient comparison with the Gaussian distribution. A normalized distribution has mean equal to zero and standard deviation equal to one. The third and fourth moments, λ_3 and λ_4, often called skewness and kurtosis, respectively, of a normalized distribution of sea surface elevation, are defined in Section 5-4. The third and fourth moments thus defined are both equal to zero for a normalized Gaussian distribution. The skewness for shallow-water and for steep, deepwater waves is usually greater than zero. Skewness values up to 0.35 computed from high wave measurements during Hurricane Carla are presented in item 66. Skewness values of up to about 1.5 computed from coastal shallow-water wave measurements are presented in item 124. Positive kurtosis values

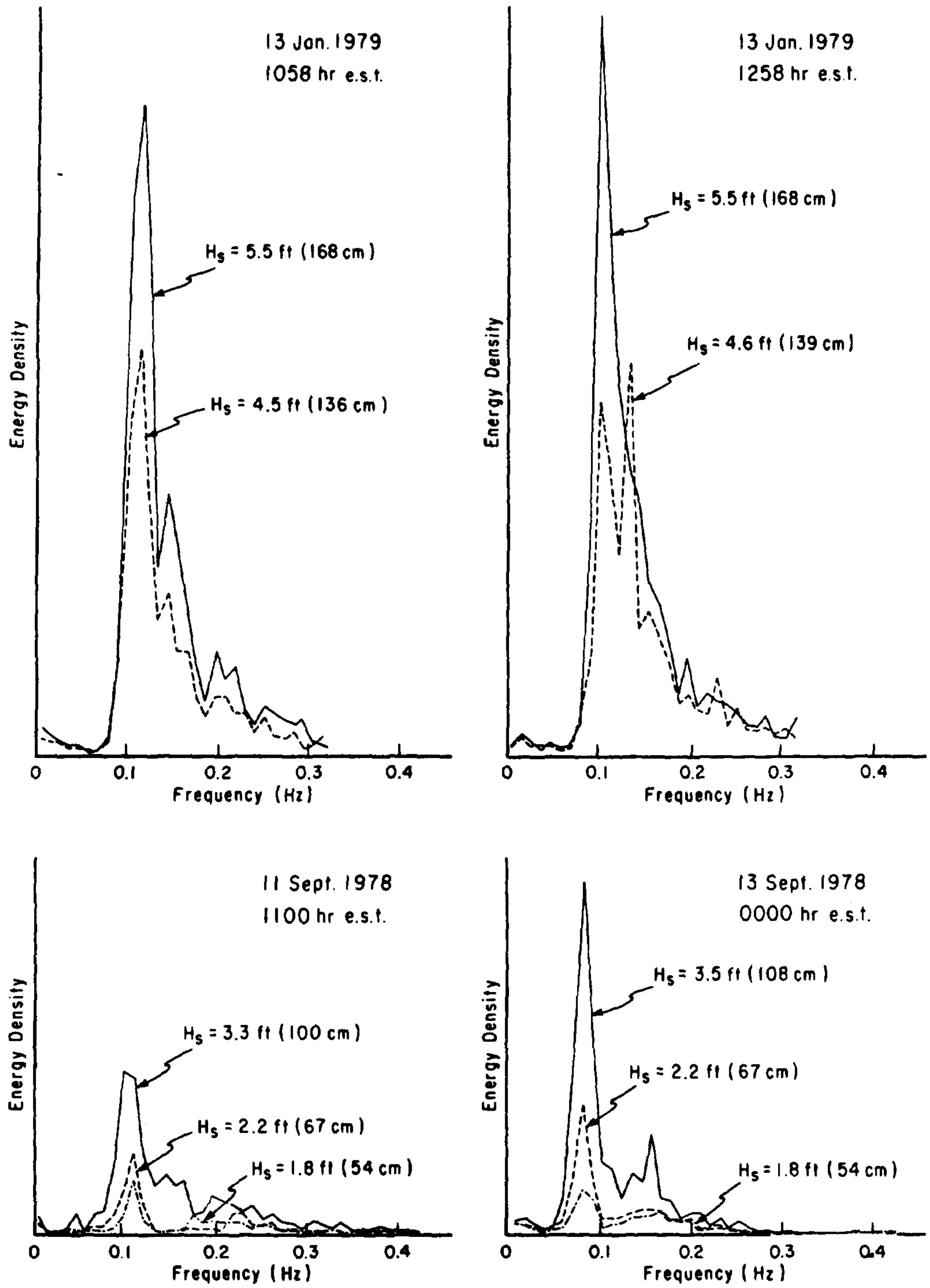

Figure 5-16. Wave energy spectra from pier-mounted continuous wire staff gages at the CERC Field Research Facility (FRF) near Duck, North Carolina, showing variation along a line perpendicular to shore (Solid lines represent a gage at the seaward pier end (depth 29 ft (8.8 m)); dashed lines represent a gage 480 ft (146 m) from the seaward pier end (depth 22 ft (6.6 m)); dot-dashed lines represent a gage 840 ft (256 m) from the pier end (depth 17 ft (5.1 m).)

are also reported. Item 104 also presents extensive documentation of deviations from the Gaussian distribution in storm measurements at the CERC FRF.

b. Rayleigh Distribution of Wave Heights. The use of a Rayleigh distribution for wave heights is a direct consequence of the assumptions of a Gaussian distribution for sea surface elevations and a narrow band spectrum. Since the assumptions are often violated in natural wave conditions, particularly in very shallow coastal waters, the use of the Rayleigh distribution in shallow-water design can only be justified by empirical evidence. Empirical data in the SPM from several shallow-water Atlantic coast gages indicate the Rayleigh distribution is a good approximation (Figure 5-17). As indicated, the Rayleigh distribution is increasingly conservative at cumulative probabilities less than about 0.05. Further evidence in support of the Rayleigh distribution for shallow-water wave heights (including the surf zone) was presented in item 126 and contrary evidence in item 104. The predominant conclusion is that the Rayleigh distribution is quite satisfactory for most engineering applications. The Rayleigh distribution is less satisfactory for describing the extreme wave heights with cumulative probabilities of about 0.01 or less.

c. Continuity of Wave Spectra.

(1) It is often assumed that the sea surface represents a random Gaussian process and that the Fourier transform of a time series of sea-surface elevations represents a continuous spectrum with an infinite number of independent frequency components. An obvious case in which spectral components are not independent is a record of steep waves with peaked crests and flat troughs. Wave profiles may be described as a summation of a wave of the fundamental frequency and waves at frequencies which are integral multiples of the fundamental, often called a Stokes wave. The spectrum has peaks at harmonics of the dominant frequency which are phase-bound to the fundamental and are clearly not independent (Figure 5-11).

(2) The assumption of a continuous spectrum of independent components is adequate for most practical engineering work. However, for very steep waves or waves in very shallow water the assumption is often incorrect. The following steepness and relative depth criteria can be used to indicate cases where the assumption of independent spectral components may be poor:

$$\text{steepness:} \quad \frac{H_s}{gT_p^2} > 0.008$$

or (5-11)

$$\text{relative depth:} \quad \frac{d}{gT_p^2} < 0.01$$

In cases where both steepness and relative depth approach the above guidelines, nonindependence may also be a factor.

d. Wave Grouping. The characteristics of individual waves in a record are highly variable. This observation has led to the assumption that waves

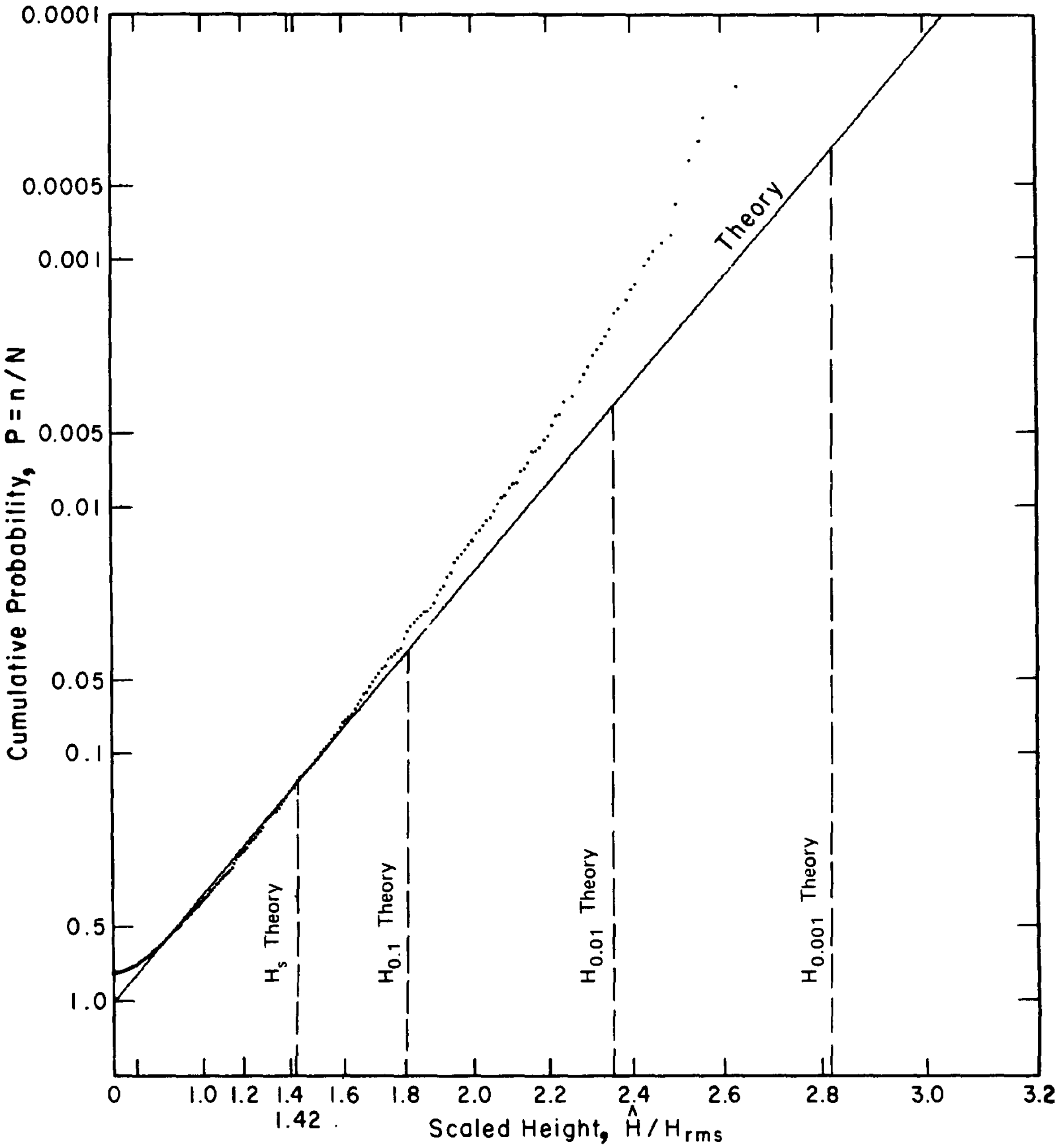

Figure 5-17. Theoretical and observed wave height distributions (Observed shallow-water waves from 72 individual 15-min observations from several Atlantic coast wave gages are superimposed on the Rayleigh distribution curve. A total of 11,678 individual waves is represented.)

occur randomly in the record. However, there is a small but significant correlation between the heights of successive waves in a record. The tendency for high waves to occur in groups is important because it has been demonstrated that high wave groups can be exceptionally destructive to rubble-mound structures (item 80). Also, long period motion induced by quasi-periodic wave groups can generate resonant oscillation of moored, floating structures such as piers, breakwaters, and tethered vessels. It can also lead to oscillation in harbors and bays. Because of the significance of wave grouping, it is often necessary to include consideration of wave groups in laboratory tests of coastal phenomena. Inclusion of wave grouping effects in general criteria for coastal design is beyond the present state of art.

5-7. Simplified Wave Models. The processes of wave growth, propagation, and nearshore transformation can be predicted reasonably well by a variety of methods based on formulas and computer programs of varying complexity. This section presents simple, self-contained methods, and the following section describes more comprehensive methods available. The simplified methods are particularly useful when quick, low-cost estimates are needed. They provide accurate results for areas with simple fetches and bathymetry. For complex areas, comprehensive methods are needed for accurate results; therefore, the simplified methods should be used with great care, if at all.

a. Estimating Wind Conditions. Winds can be estimated for wave growth models by using direct wind measurements, atmospheric pressure measurements, or a combination of both. Use of actual wind records from the site is preferred in protected areas so that local peculiarities of wind intensity such as sheltering from adjacent topography or channelization of winds along valleys is included. If wind records are not available, regional wind records in the United States can be used. Annual extreme fastest mile wind velocity data (with recurrence intervals) can be obtained from Figures 5-18 through 5-20. Figures 5-21 through 5-23 relate specifically to hurricane winds at the coast and 125 miles inland along the Gulf of Mexico and Atlantic states. Figures 5-18 through 5-23 were developed to estimate maximum wind loads for building design. They can be expected to give conservative wave estimates.

(1) Wind Information Adjustments. Wind information must be properly adjusted for use in wave models to avoid introducing bias into the results. The following procedure provides a method for adjusting the wind speed that is reasonably quick and relatively accurate. It must be recognized that the problem of identifying the appropriate wind speed and the resultant wave estimation in irregular water bodies is complex. To achieve a simplified method, the following assumptions are made. First, the wind fields are well organized and can be adequately described by the use of an average wind speed and direction over the entire fetch. Secondly, the wind speed should be corrected to the 33-foot (10-meter) level. Also, the wind speed should be representative of the average wind speed measured over the fetch. When the fetch length is 10 miles (16 kilometers) or less, the wind has not fully adjusted to the frictional characteristics of the waves. In such cases, the overwater wind speed will be estimated to be 120 percent of the overland wind speed U_L. Thermal effects on stability of the air in this case are not applicable. Finally, when the fetch length is greater than 10 miles (16 kilometers), thermal stability effects must be included in the wind speed transformation.

1792

July, 1968

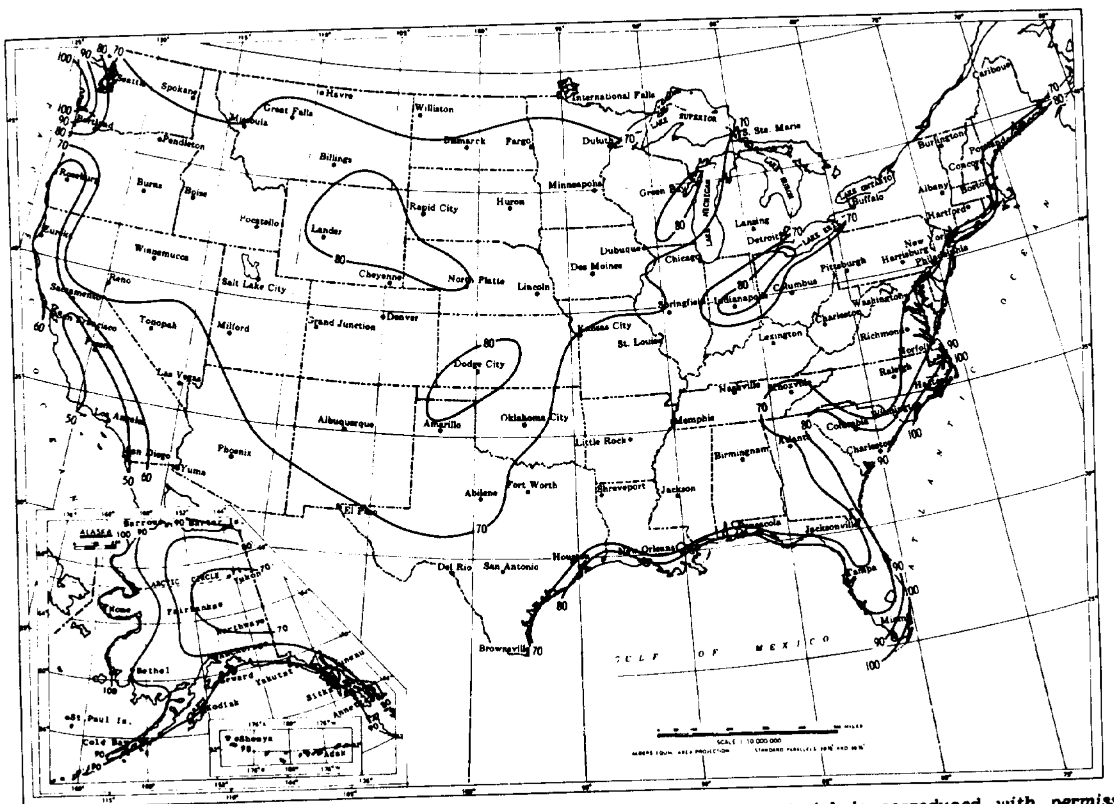

Figure 5-18. Annual extreme fastest-mile wind speed 30 ft above ground, 25-year mean recurrence intervals (wind speed in miles per hour) (item 1)

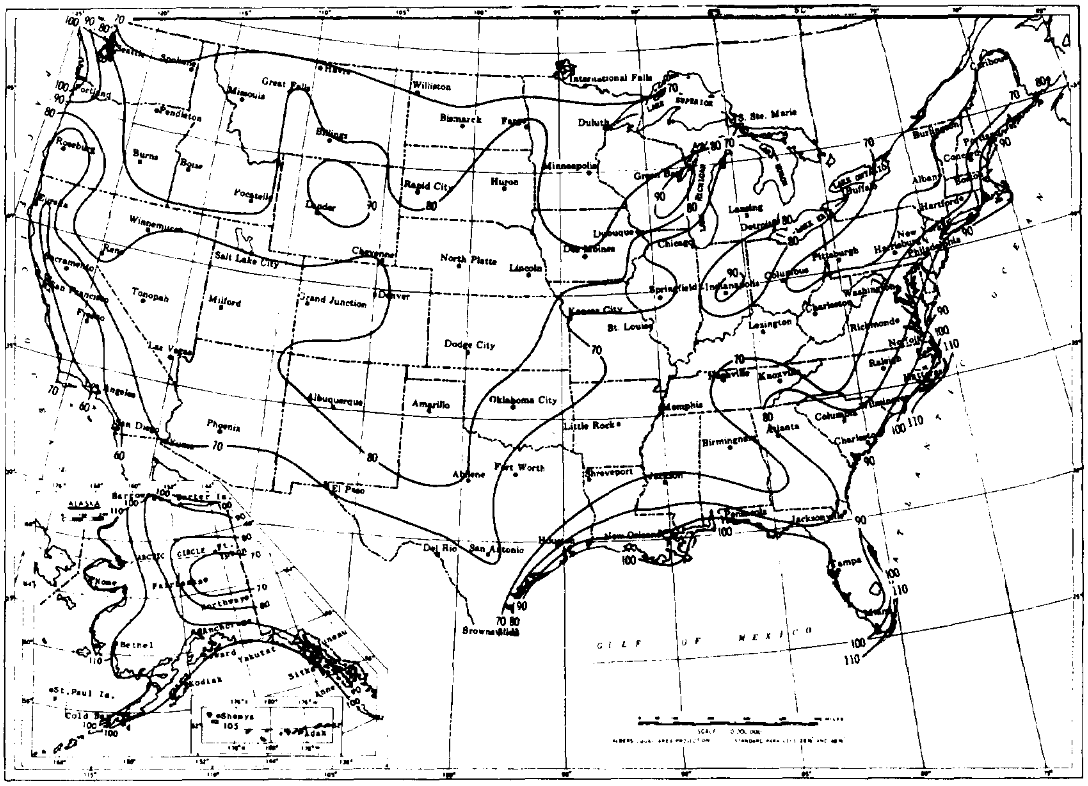

DISTRIBUTIONS OF WINDS 1793

This material is reproduced with permission from American National Standard Building Code Requirements for Minimum Design Loads in Buildings and Other Structures, copyright 1972 by the American National Standards Institute.

Figure 5-19. Annual extreme fastest-mile wind speed 30 ft above ground, 50-year mean recurrence intervals (wind speed in miles per hour) (item 1)

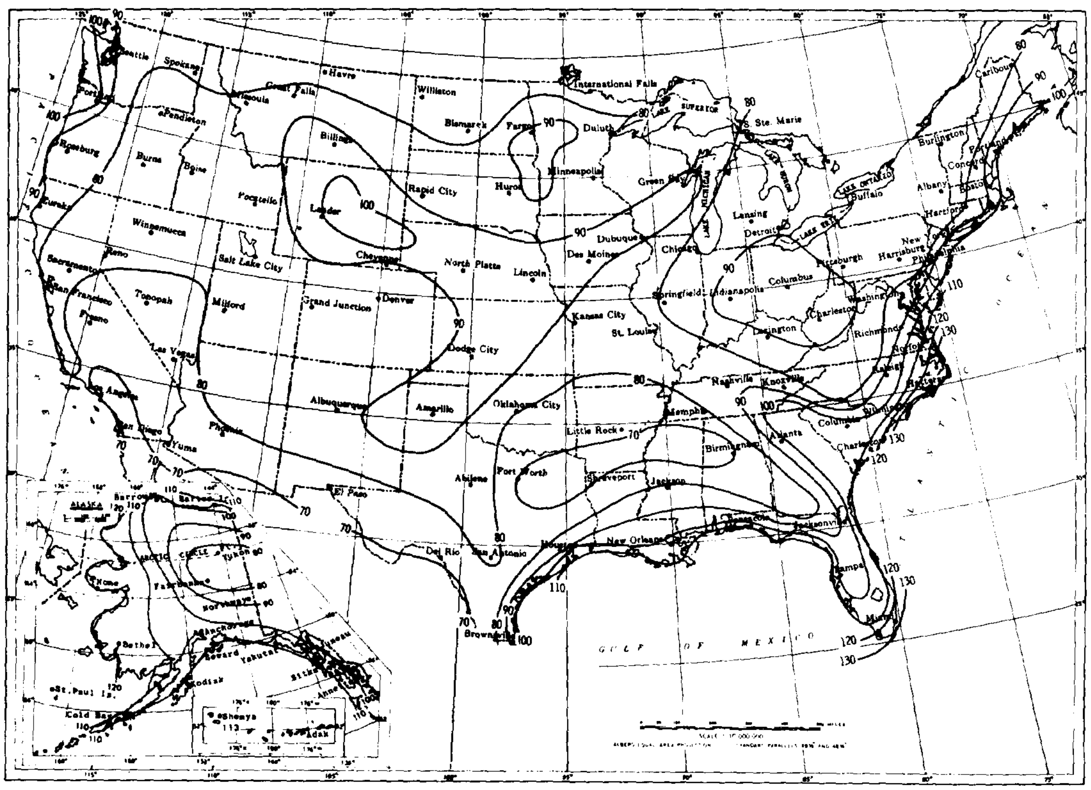

1794

July, 1968

This material is reproduced with permission from American National Standard Building Code Requirements for Minimum Design Loads in Buildings and Other Structures, copyright 1972 by the American National Standards Institute

Figure 5-20. Annual extreme fastest-mile wind speed 30 ft above ground, 100-year mean recurrence intervals (wind speed in miles per hour) (item 1)

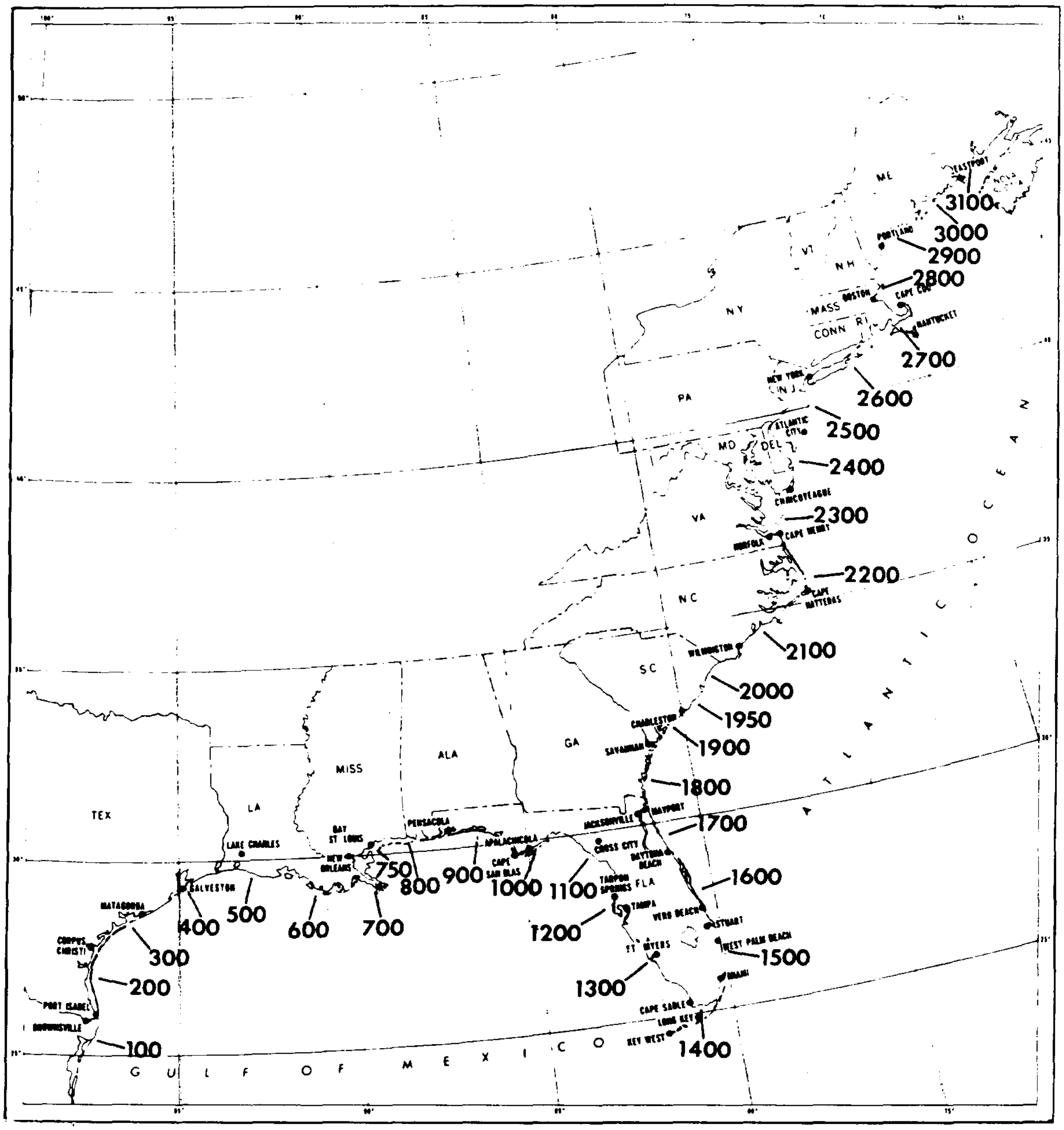

Figure 5-21. Locator map with coastal distance intervals marked in nautical miles (1 n. mi. = 1.9 km)

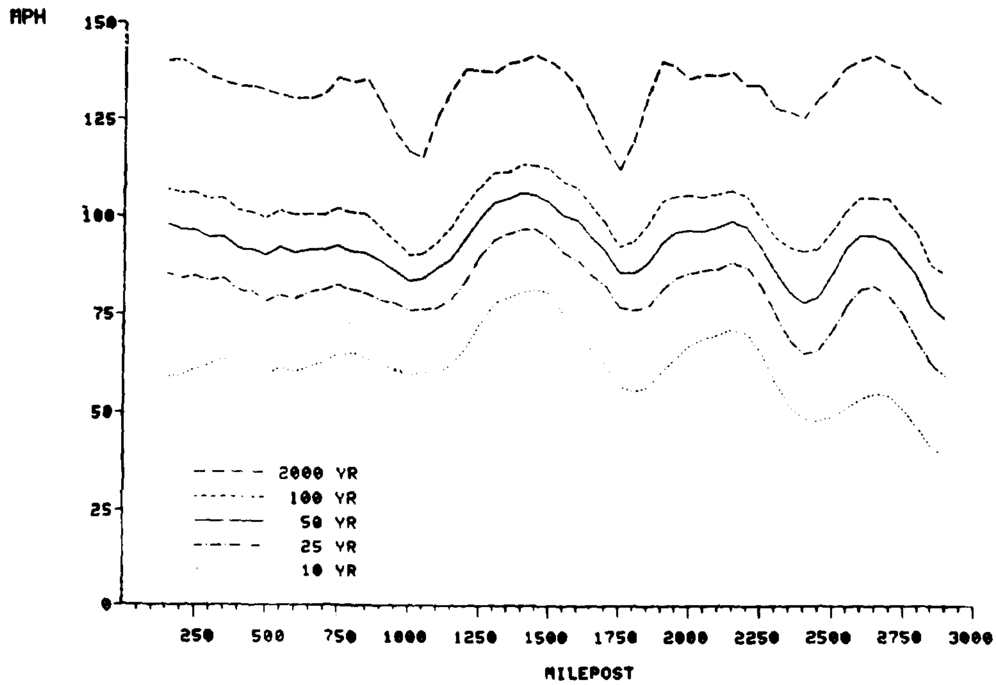

Figure 5-22. Estimated fastest-mile hurricane wind speeds blowing from any direction at 33 ft (10 m) above ground in open terrain near the coastline for various mean recurrence intervals (item 97)

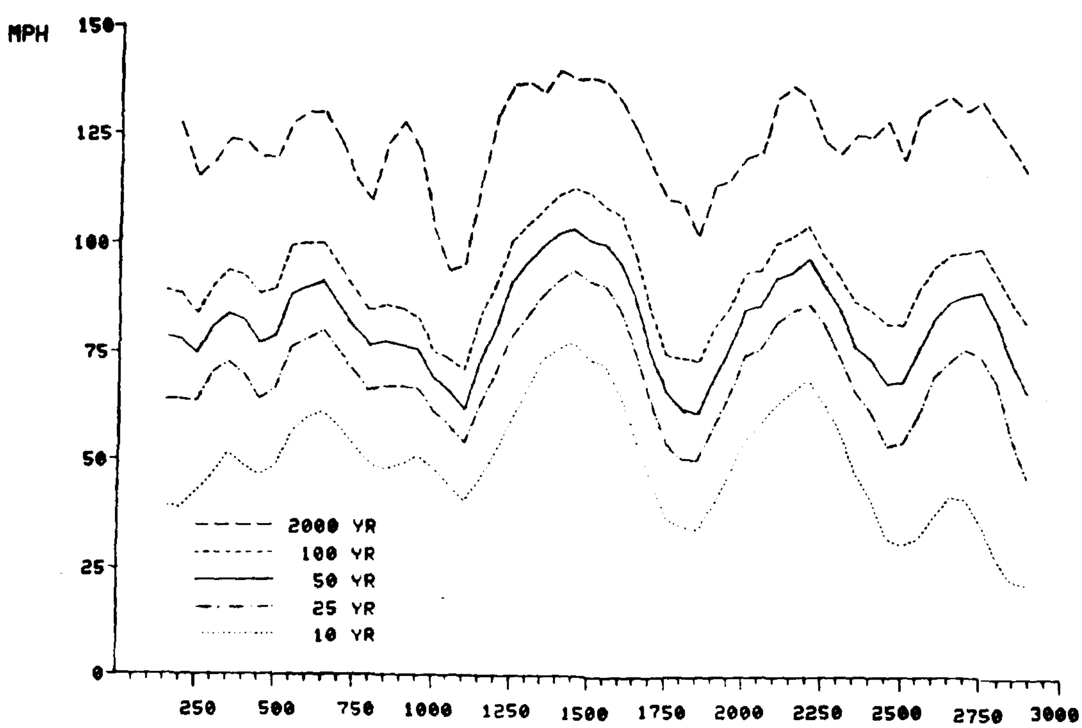

Figure 5-23. Estimated fastest-mile hurricane wind speeds blowing from any direction at 33 ft (10 m) above ground in open terrain at 200 km inland for various mean recurrence intervals (item 97)

(2) The Process of Determining Wind speed Adjustments. After an observed wind speed of known direction, level above the surface, location of observation (i.e., overwater or overland), and method of wind speed description (i.e., fastest mile or a time-averaged speed) have been determined, the following steps should be completed in accordance with Figure 5-24. The figure presents a logic diagram which leads to the adjusted wind speed required to determine the wave height and period in either deep or shallow water. SPM guidance includes an additional step to correct for coefficient of drag. This correction is omitted from the following steps; rather, it has been incorporated into the wave prediction curves to simplify the procedure. An interactive computer program for calculating the adjusted wind speed is available under the Microcomputer Applications for Coastal Engineering (MACE) program (Appendix C).

(a) If the wind speed is observed at any level other than 33 feet, it should be adjusted as follows:

$$U_{33} = \left(\frac{33}{Z}\right)^{1/7} U_Z = R_{33}\, U_Z \tag{5-12}$$

where U_{33} is the wind speed at the 33-foot level, and U_Z is the wind speed at distance Z above the surface. This method is valid where Z is less than 65 feet (20 meters).

(b) Wind speeds are frequently described in a variety of ways such as fastest mile, 5-minute average, 10-minute average, etc. The wind speed must be averaged over the fetch or adjusted so that the average time is equal to or greater than the minimum duration t. Figure 5-25 provides the means to convert the fastest-mile wind speed to an equivalent duration. Figure 5-26 can be used to convert a wind speed of any duration to a 1-hour wind speed.

(c) It should be determined if the overwater fetch distance is less or greater than 10 miles (16 kilometers).

(d) It should be determined if the wind speed were observed overwater or overland. On short fetches it is assumed that the atmospheric boundary layer has not had time to fully adjust to the developing frictional characteristics of the water surface. Wind speeds observed overland U_L must be corrected to overwater wind speeds U_W. For overwater fetches less than 10 miles, $U_W = 1.2\, U_L$. For overwater fetches greater than 10 miles, $U_W = RU_L$, where R is determined from Figure 5-27. The term overland implies a measurement site that is dominantly characterized as inland. If a measurement site is directly adjacent to the water body, it may, for selected wind directions, be equivelent to overwater. Careful analysis of such a site is required.

(e) The air-sea temperature difference should be determined. A wind stability correction is required when the air and water are different temperatures and the fetch is more than 10 miles $U_C = R_T U_W$. If the temperature difference between the air and the sea is known, Figure 5-28 should be used to determine the amplification ratio R_T. When only general knowledge of the condition of the atmospheric boundary layer is available, it should be

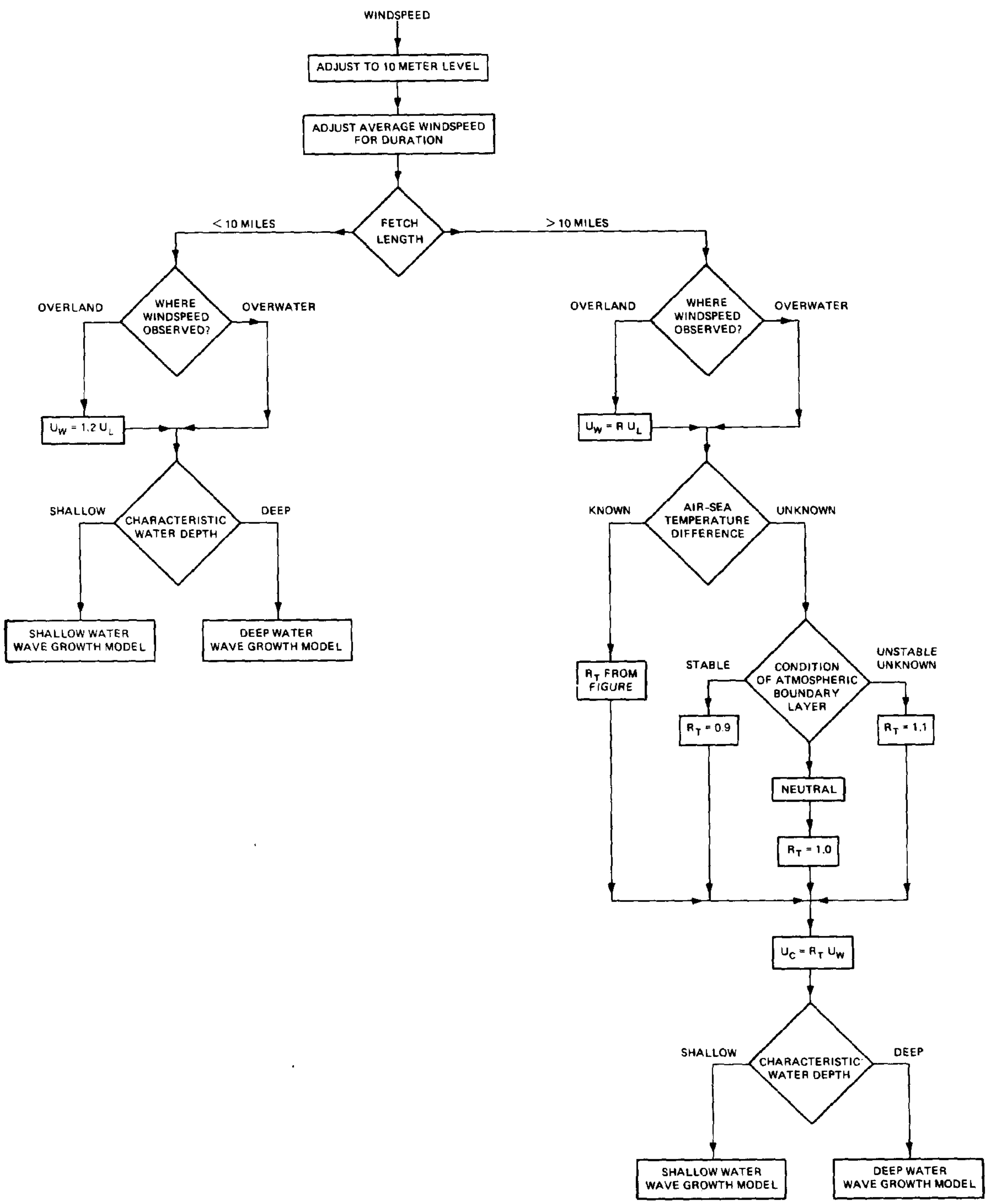

Figure 5-24. Logic diagram for determining wind speed for use in wave forecasting models

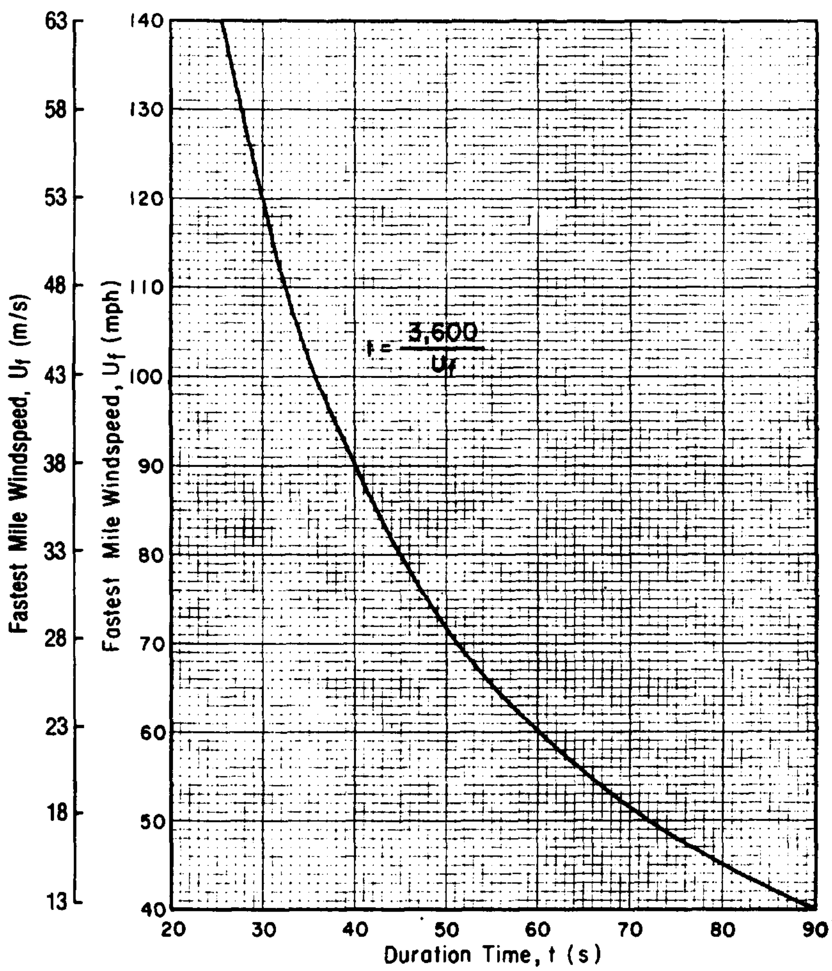

Figure 5-25. Duration of the fastest-mile wind speed as a function of wind speed (for open terrain conditions)

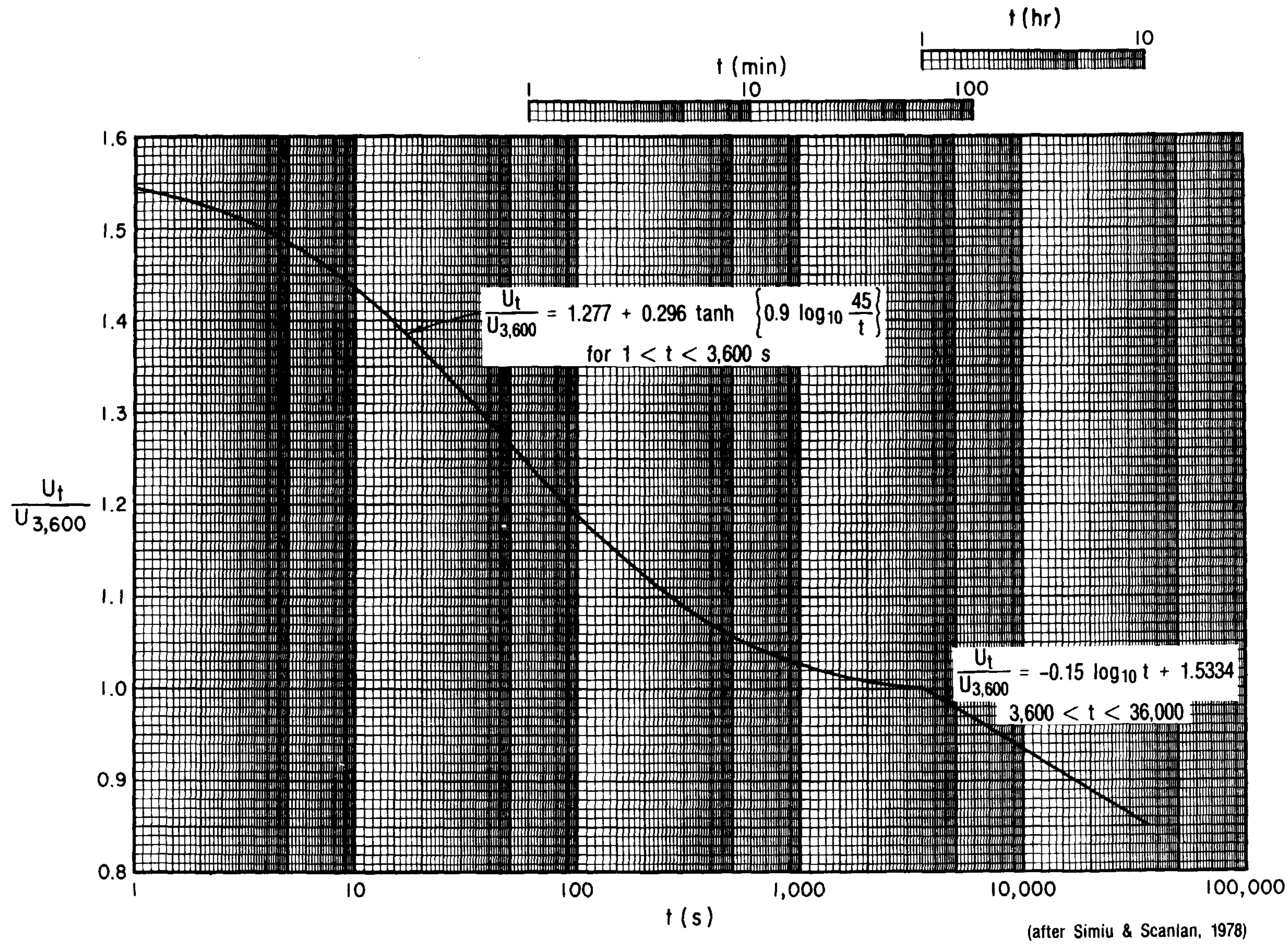

Figure 5-26. Ratio of wind speed of any duration U_t to the 1-hour wind speed U_{3600} (after item 120)

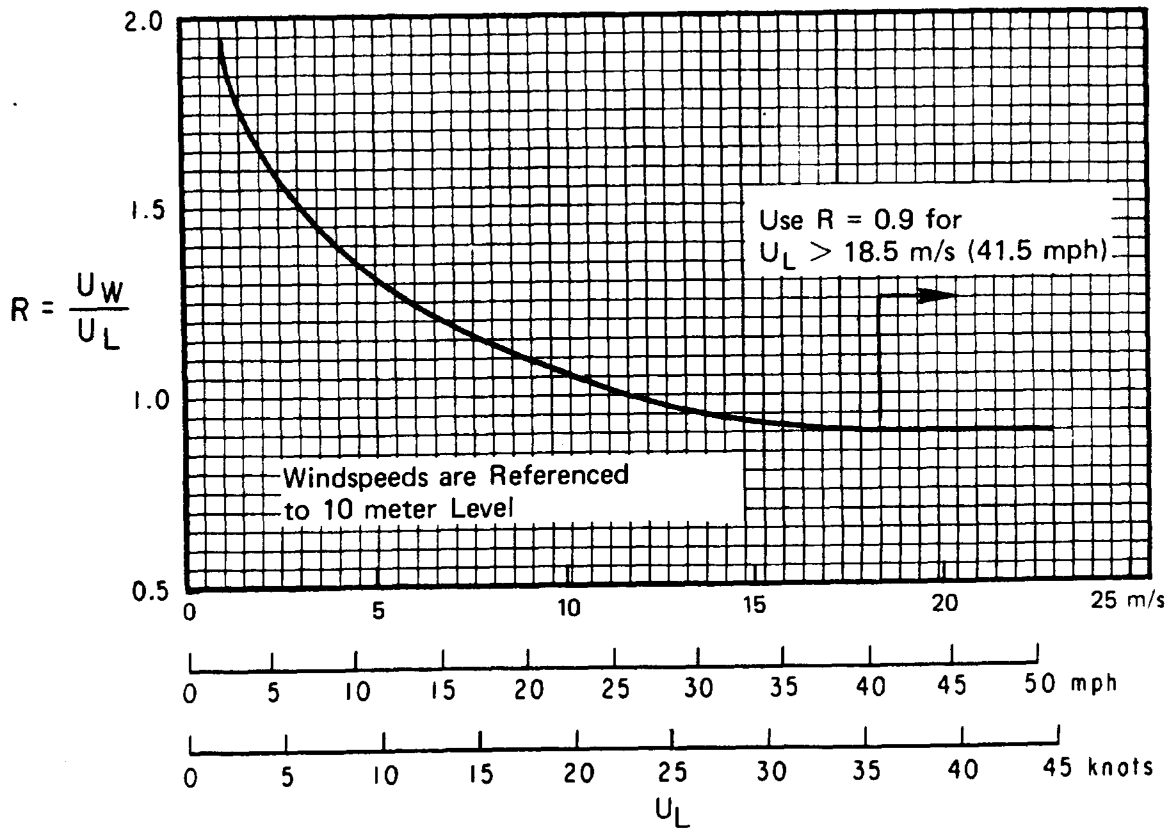

Figure 5-27. Ratio R of wind speed overwater U_W to wind speed overland U_L as a function of wind speed overland U_L (after Item 111)

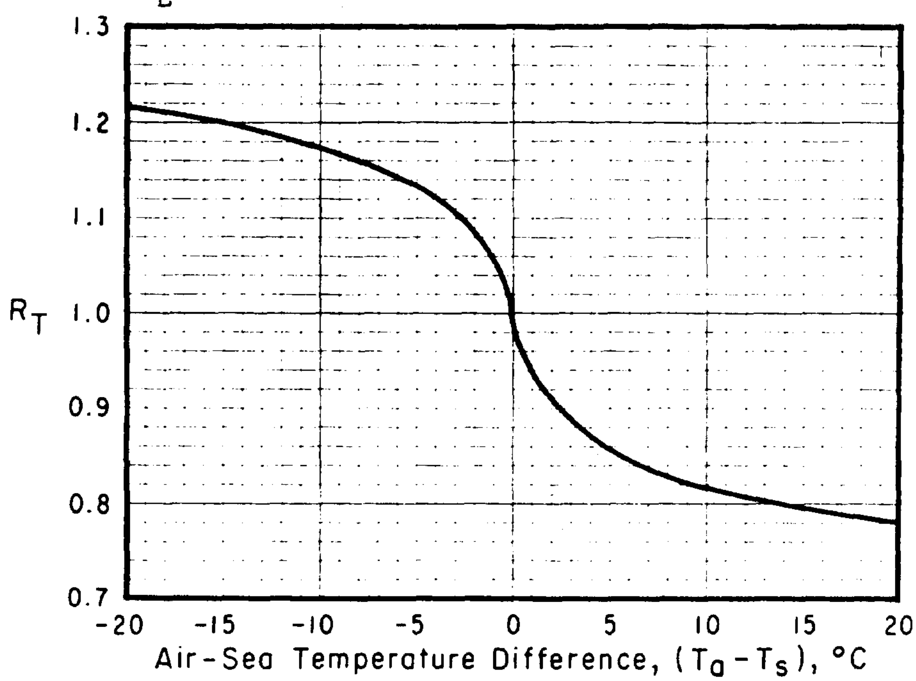

Figure 5-28. Amplification ratio R_T accounting for effects of air-sea temperature difference

categorized as stable, neutral, or unstable according to the following criteria:

Stable - when the air is warmer than the water, the water cools the air just above it and decreases mixing in the air column ($R_T = 0.9$).
Neutral - when the air and water have the same temperature, the water temperature does not affect the mixing in the air column ($R_T = 1.0$).
Unstable - when the air is colder than the water, the water warms the air causing the air near the water surface to rise thus increasing mixing in the air column ($R_T = 1.1$).

An unstable condition, $R_T = 1.1$, should be assumed when the boundary layer condition is unknown. Having a value for R_T , the adjusted wind speed is determined by $U_C = R_T U_W$. Therefore, design wind speed adjustments are:

$$U_C = R_T \; R \; U_L \tag{5-13}$$

(3) Wind Information from Surface Pressure. Wind speed and direction in the open ocean are usually estimated from surface synoptic weather charts. The free air, or geostrophic, wind speed is first estimated from sea level pressure charts. Corrections to the free air wind are then made. Estimation from pressure charts should be used only for large areas, and the estimated values should be compared with observations, if possible, to confirm their validity.

(a) A simplified surface chart for the north Pacific Ocean is shown in Figure 5-29. The area labeled L in the right center of the chart and the area labeled H in the lower left corner of the chart are low- and high-pressure areas. The pressures increase moving outward from L (isobars 972, 975, etc.) and decrease moving outward from H (isobars 1026, 1023, etc.). Scattered about the chart are small arrow shafts with a varying number of feathers. The direction of a shaft shows the direction of the wind; each one-half feather representing a unit of 5 knots (2.5 meters per second) in wind speed.

(b) Figure 5-30 may be used to estimate the free air wind speed. The distance between isobars on a chart is measured in degrees of latitude (an average spacing over a fetch ordinarily used), and the latitude position of the fetch is determined. Using the spacing as ordinate and location as abscissa, the plotted, or interpolated, slant line at the intersection of these two values gives the geostrophic wind speed. For example, in Figure 5-29, a chart with 3-millibar isobar spacing, the average isobar spacing (measured normal to the isobars) over fetch F_2 located at 37 degrees N. latitude, is 0.70 degrees of latitude. The scales on the bottom and left side of Figure 5-30 are used to find a free air wind of 34.5 meters per second (67 knots).

(c) After the free air wind has been estimated, the wind speed at the surface must be estimated. First, the free air wind speed is converted to the 33-foot (10-meter) level speed by multiplying by R_g , as given in

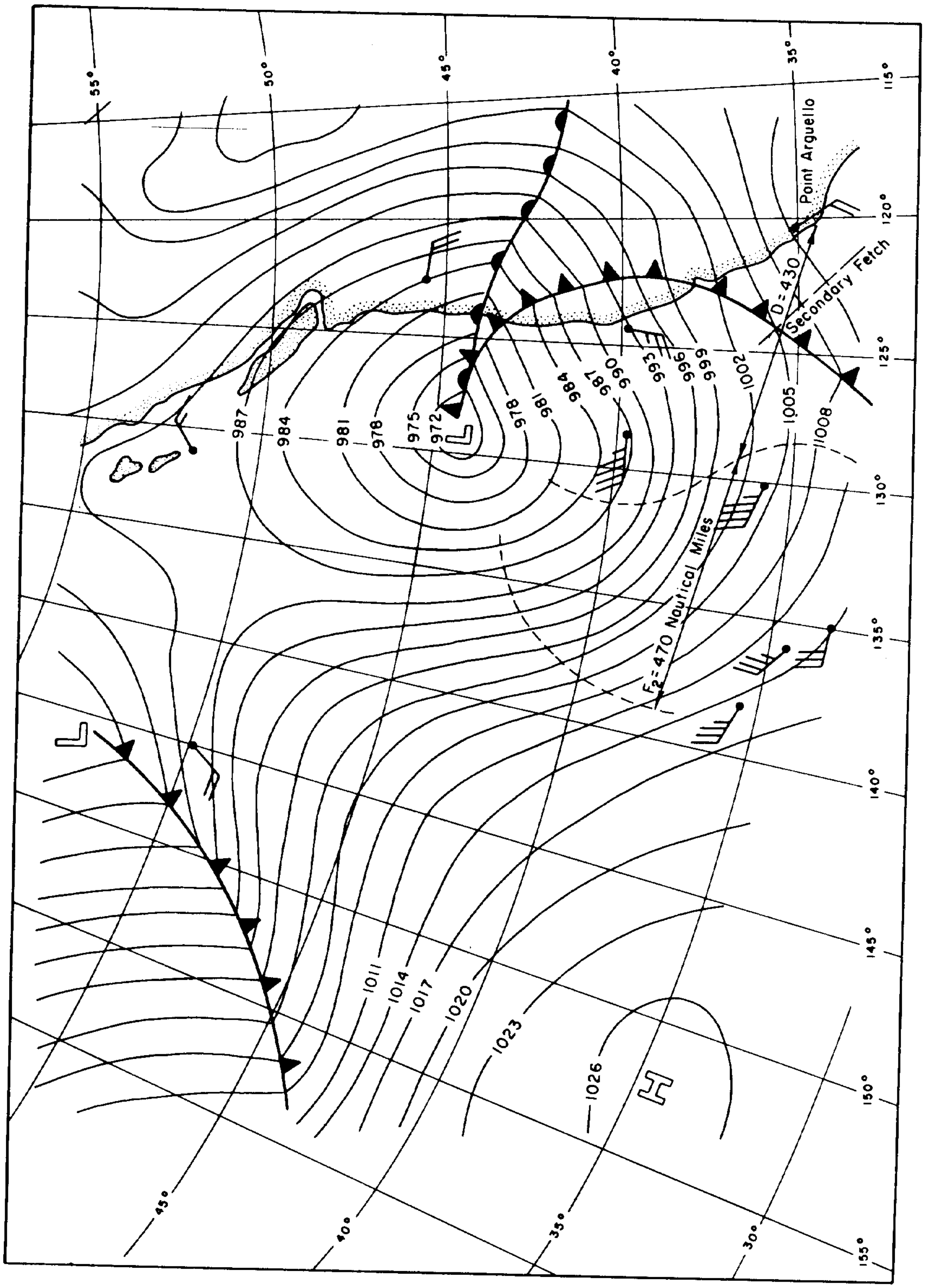

Figure 5-29. Surface synoptic chart for 0030Z, 27 October 1950

$$U_g = \frac{1}{\rho_a f} \frac{\Delta p}{\Delta n}$$

For T = 10° C
Δp = 3 mb and 4 mb
Δn = isobar spacing measured in degrees latitude
p = 1013.3 mb
ρ_a = 1.247×10^{-3} gm/cm^3
f = Coriolis parameter = $2\omega \sin \phi$

where
ω = angular velocity of earth, 0.2625 rad/hr
ϕ = latitude in degrees

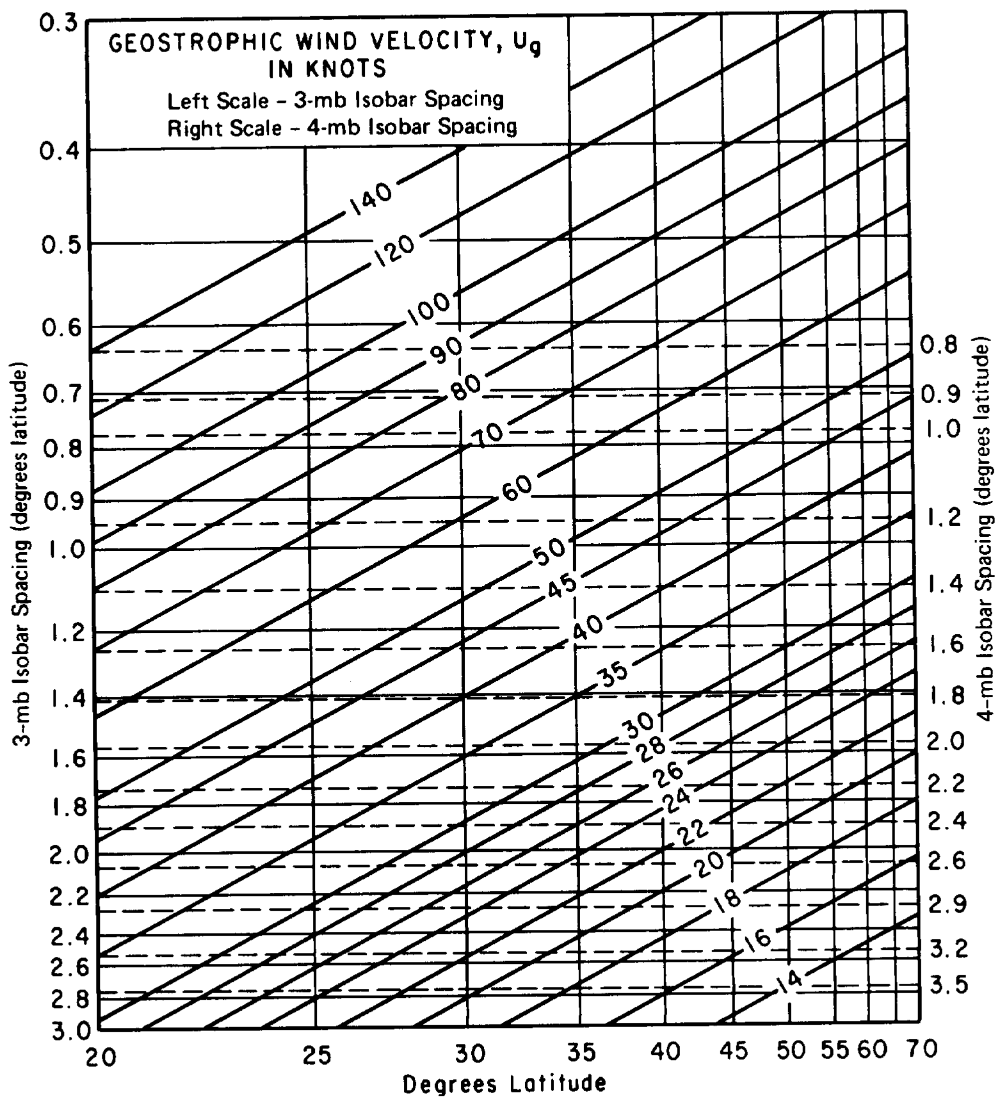

Figure 5-30. Geostrophic (free air) wind scale (after item 9)

Figure 5-31. R_g is a function of the free air wind speed U_g. The resulting velocity is then adjusted for stability effects by the factor R_T given in Figure 5-28.

(4) Wind Duration. Estimates of the duration of the wind are also needed for wave prediction. Synoptic weather charts are prepared only at 6-hour intervals. Thus interpolation to determine the duration may be necessary. Linear interpolation is adequate for most uses. Interpolation should not be used if short-duration phenomena, such as frontal passage or thunderstorms, are present.

(5) Fetch.

(a) A fetch is defined as a region in which the wind speed and direction are reasonably constant. A fetch should be defined such that wind direction variations do not exceed 15 degrees and wind speed variations do not exceed 5 knots (2.5 meters per second) from the mean. A coastline upwind from the point of interest always limits a fetch. An upwind limit to the fetch may also be provided by curvature, or spreading, of the isobars as indicated in Figure 5-32 or by a definite shift in wind direction. Frequently the discontinuity at a weather front will limit a fetch.

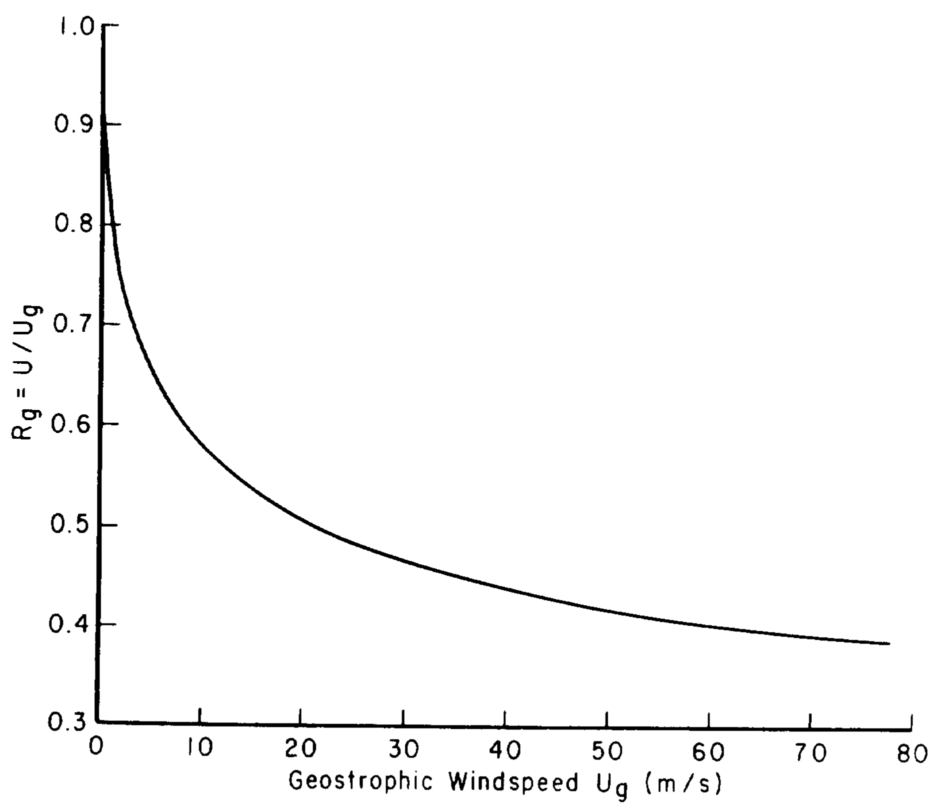

Figure 5-31. Ratio R_g of wind speed U at 10-m elevation to geostrophic (free air) wind speed U_g

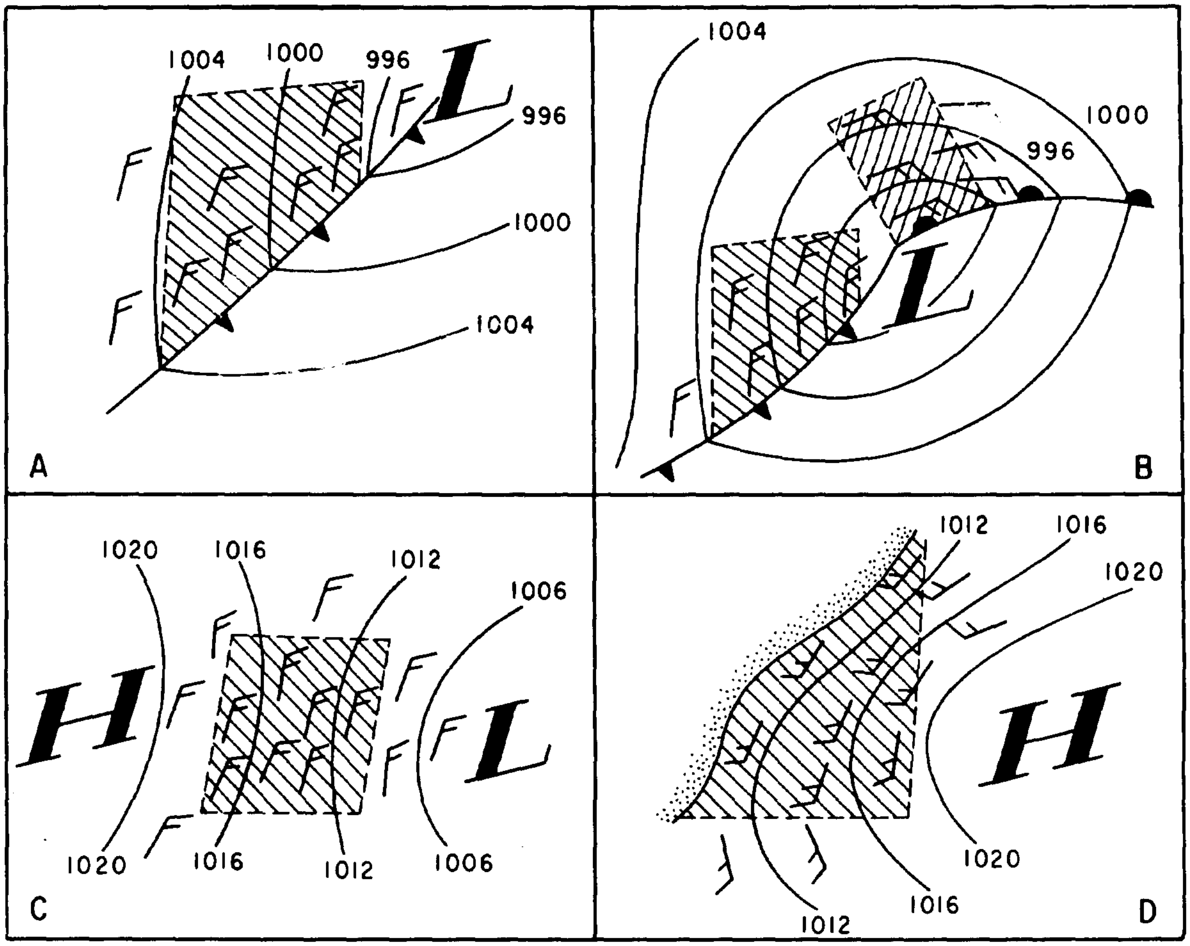

Figure 5-32. Possible fetch limitations

an arc of 24 degrees centered on the wind direction. Radials are placed at 3-degree intervals. Example fetch determinations are provided in Figure 5-33.

b. Wave Prediction in Deep Water. Significant wave height and peak period can be estimated from Figure 5-34 when the wind speed (corrected as discussed previously), duration, and fetch are known. The prediction curve is based on equations developed from the Joint North Sea Wave Project (JONSWAP) experiment (items 47 and 49). The peak period is approximately 5 percent longer than significant period. In most instances they can be assumed equal. The equations in Table 5-3 may be used as an alternative to the figure. The computer program JONSWAP to estimate deepwater significant wave height and peak period is available under the MACE program (C-9, Appendix C). Special procedures for use with hurricanes and other tropical storms are available in the SPM. The computer program HURWAVES to estimate the maximum wind speed, maximum significant wave height, and maximum significant period for slow-moving hurricanes is available under the MACE program (C-5, Appendix C).

c. Wave Prediction in Shallow Water. If the predominant depth of water over the fetch is less than one-half the deepwater wavelength, wave growth is

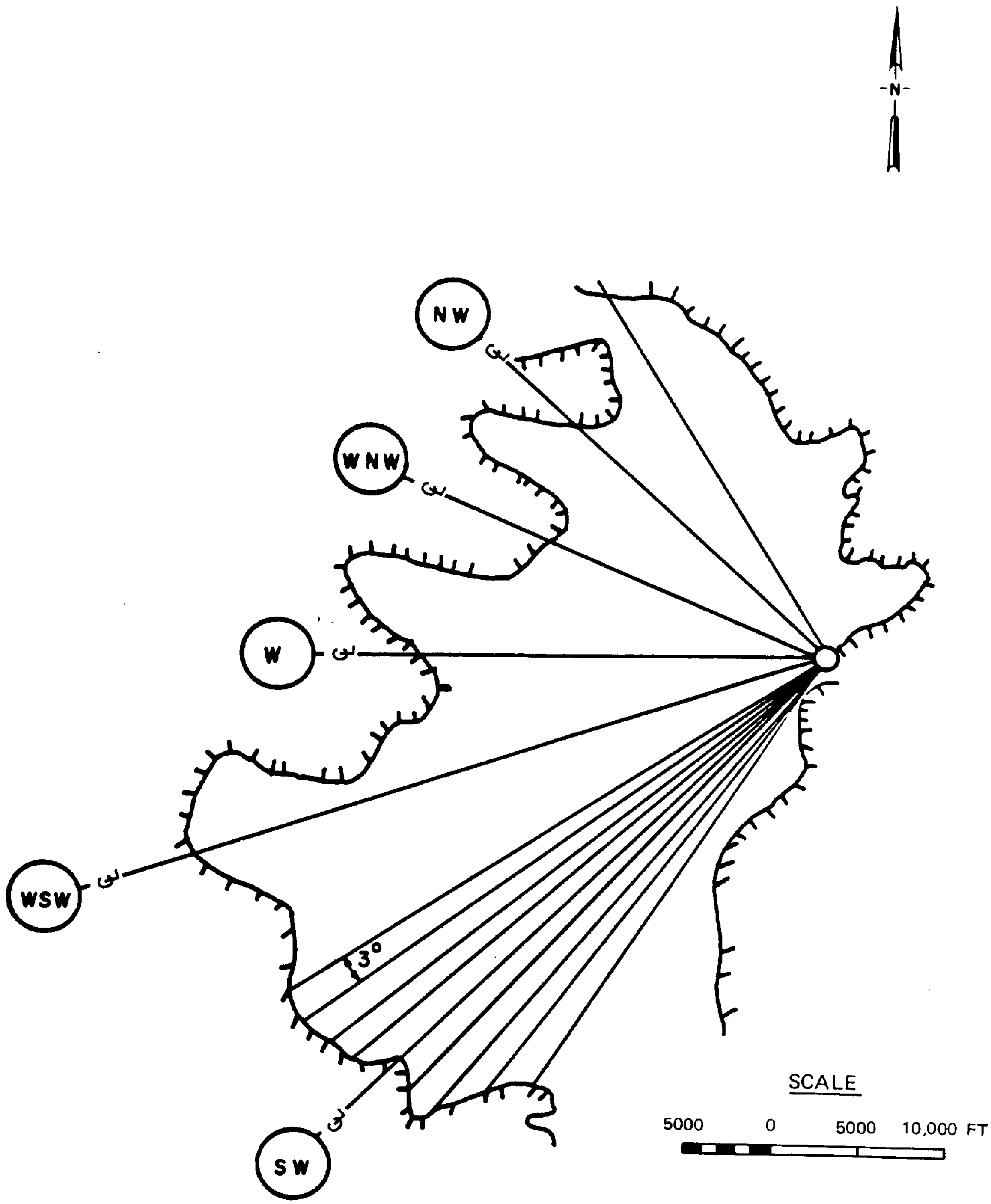

Figure 5-33. Average fetch length for each wind direction

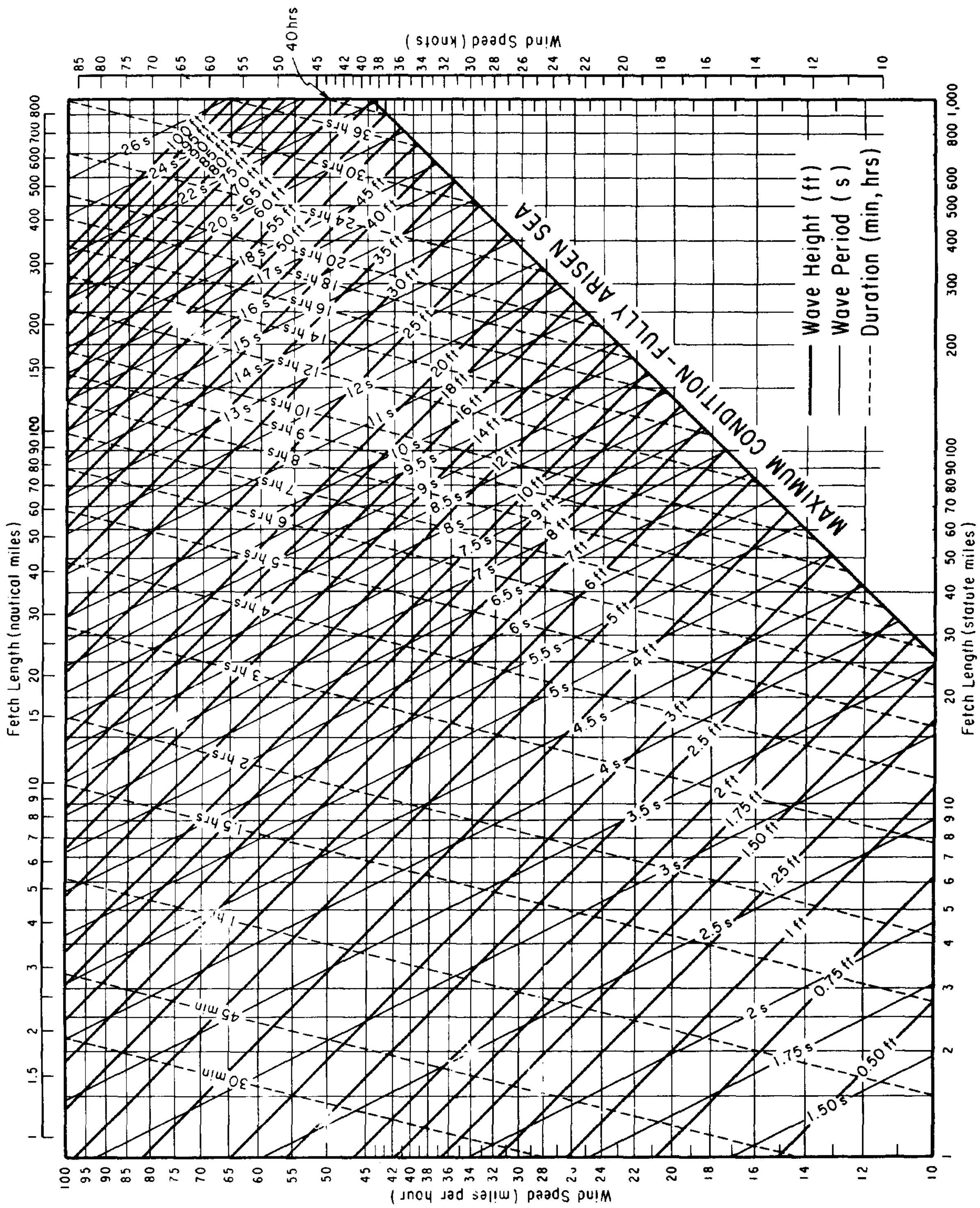

Figure 5-34. Nomograms of deepwater significant wave prediction curves as functions of wind speed, fetch length, and wind duration

Table 5-3

Deepwater Wave Forecasting Equations[a]

Units	
H_s(ft), T_p(s), U_c(miles/hr) F(miles), t(hr)	H_s(ft), T_p(s), U_c(kn) F(nmi), t(hr)
Fetch limited[b] (F, U_c)	
$H_s = 1.77 \times 10^{-2} U_c^{1.23} F^{0.5}$	$H_s = 2.26 \times 10^{-2} U_c^{1.23} F^{0.5}$
$T_p = 46.86 \times 10^{-2} U_c^{0.41} F^{0.33}$	$T_p = 52.0 \times 0^{-2} U_c^{0.41} F^{0.33}$
Duration limited[b] (U_c, t)	
$H_s = 90.79 \times 10^{-4} U_c^{1.58} t^{0.714}$	$H_s = 1.135 \times 10^{-2} U_c^{1.58} t^{0.714}$
$T_p = 24.16 \times 10^{-2} U_c^{0.724} t^{0.411}$	$T_p = 26.76 \times 10^{-2} U_c^{0.724} t^{0.411}$
Fully developed	
$H_s = 0.5634 \times 10^{-2} U_c^{2.46}$	$H_s = 0.7963 \times 10^{-2} U_c^{2.46}$
$T_p = 21.83 \times 10^{-2} U_c^{1.23}$	$T_p = 25.8 \times 10^{-2} U_c^{1.23}$
$t = 53.28 \times 10^{-2} U_c^{1.23}$	$t = 63.2 \times 10^{-2} U_c^{1.23}$

[a]Wind speed U_c in these equations must be corrected as indicated in text.

[b]It has been shown that fetch and duration are not directly interchangeable quantities for wave growth. Consequently, the duration required to reach a given fetch-limited condition cannot be obtained by the interchange of these sets of equations. The wind duration required to reach fetch-limited conditions t_f in hours is estimated by $t_f = 1.91 F^{0.67} U_c^{-0.41}$ with F in miles and U_c in miles per hour.

c. Wave Prediction in Shallow Water. If the predominant depth of water over the fetch is less than one-half the deepwater wavelength, wave growth is affected by the bottom. When shallow-water wave growth occurs, the known wind speed, duration, and fetch should be used to predict significant wave height and period from Figures 5-35 through 5-44. The computer program SHALWAVE to estimate shallow-water significant wave height and peak period is available under the MACE program (C-7, Appendix C). Wave refraction and shoaling are also considerations, as discussed in the following paragraph.

Note: Waves in a water depth of 5 feet with wave periods less than 1.4 secs. are considered to be deepwater waves, i.e. $d/T^2 > 2.56$.

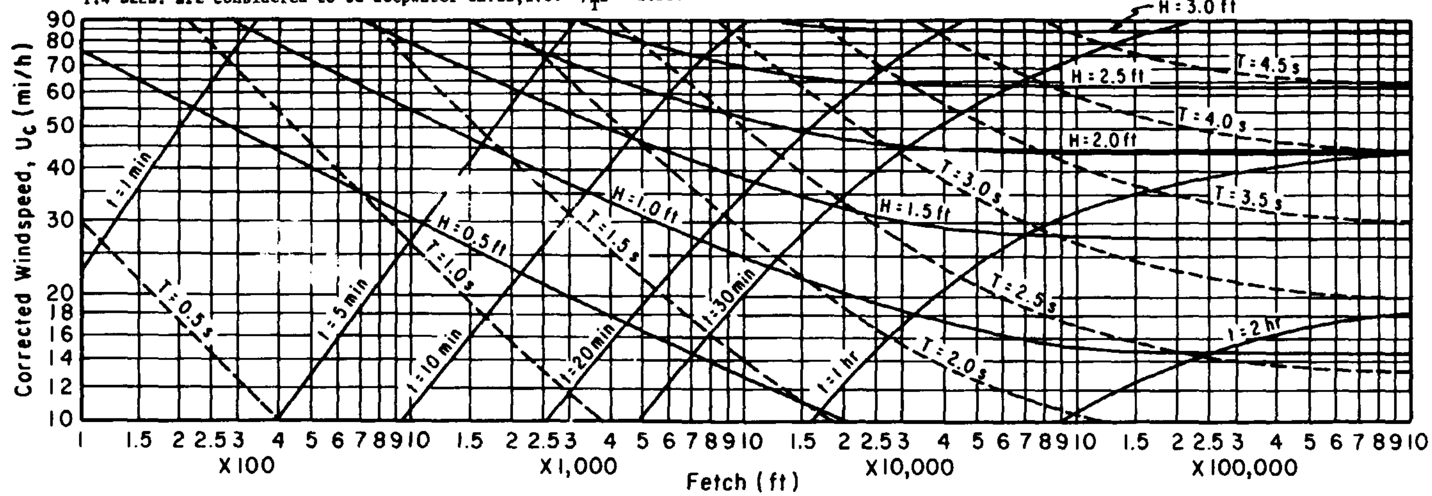

Figure 5-35. Forecasting curves for shallow-water waves (constant depth = 5 ft)

Note: Waves in a water depth of 10 feet with wave periods less than 2.0 secs. are considered to be deepwater waves, i.e. $d/T^2 > 2.56$.

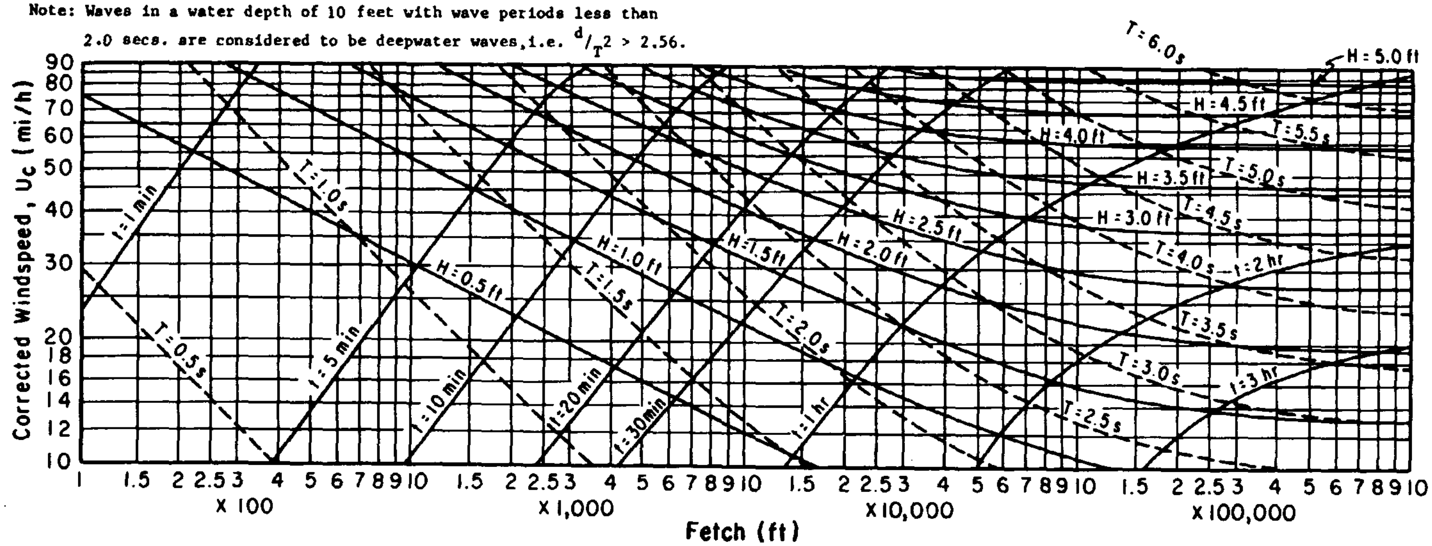

Figure 5-36. Forecasting curves for shallow-water waves (constant depth = 10 ft)

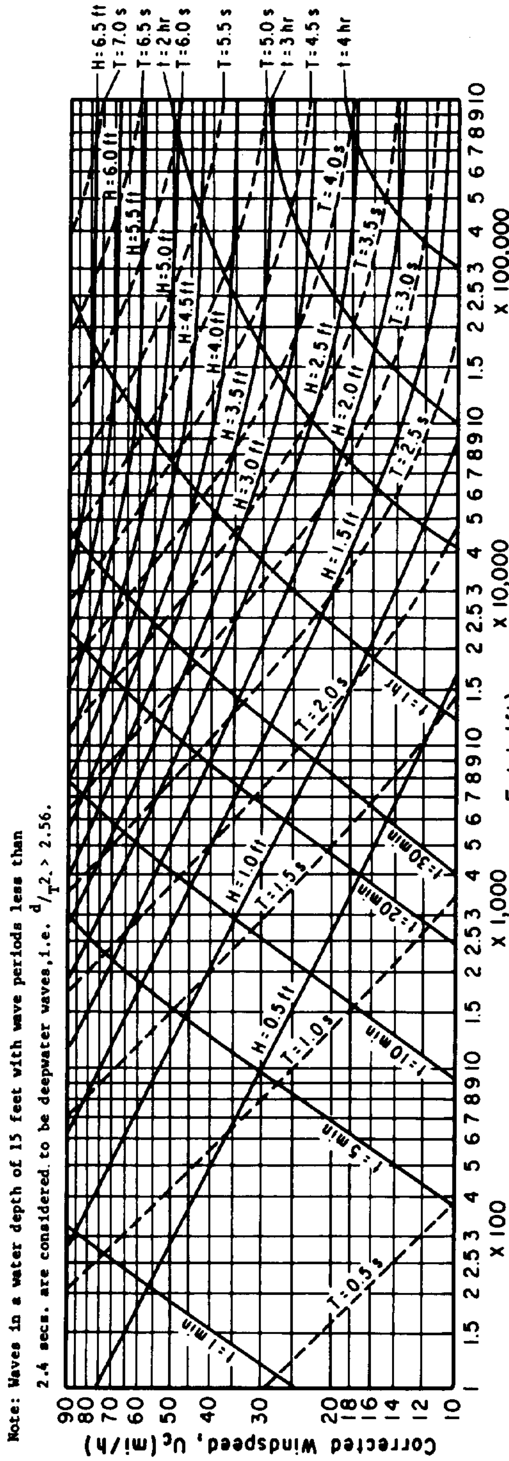

Figure 5-37. Forecasting curves for shallow-water waves (constant depth = 15 ft)

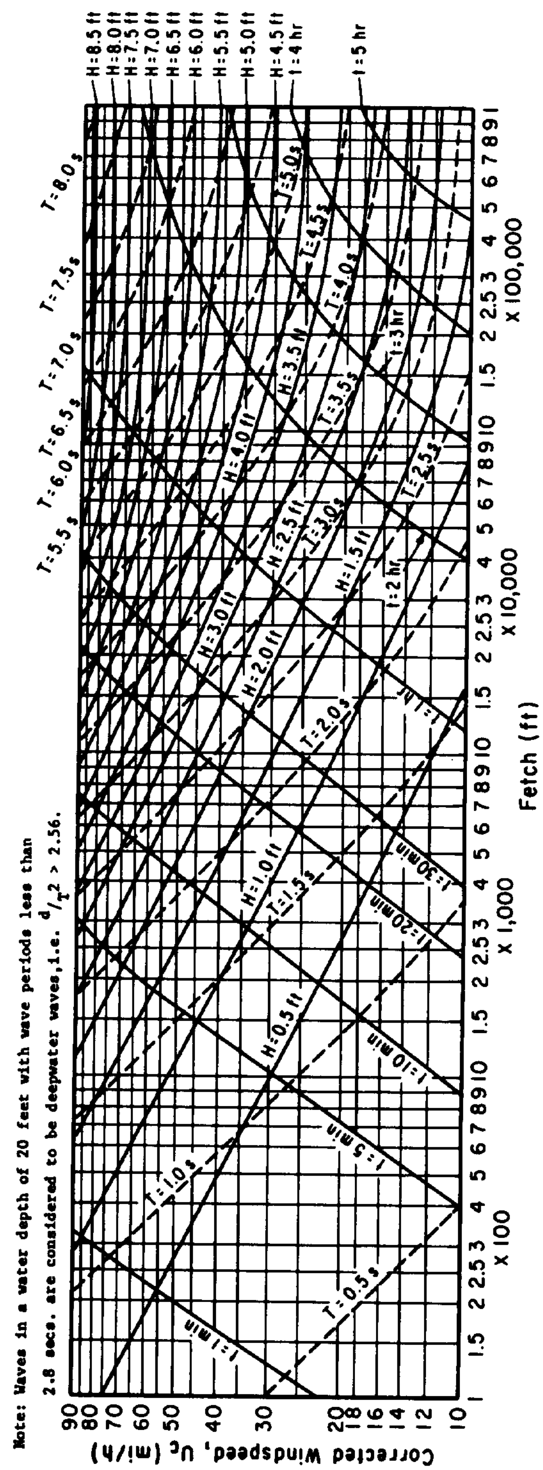

Figure 5-38. Forecasting curves for shallow-water waves (constant depth = 20 ft)

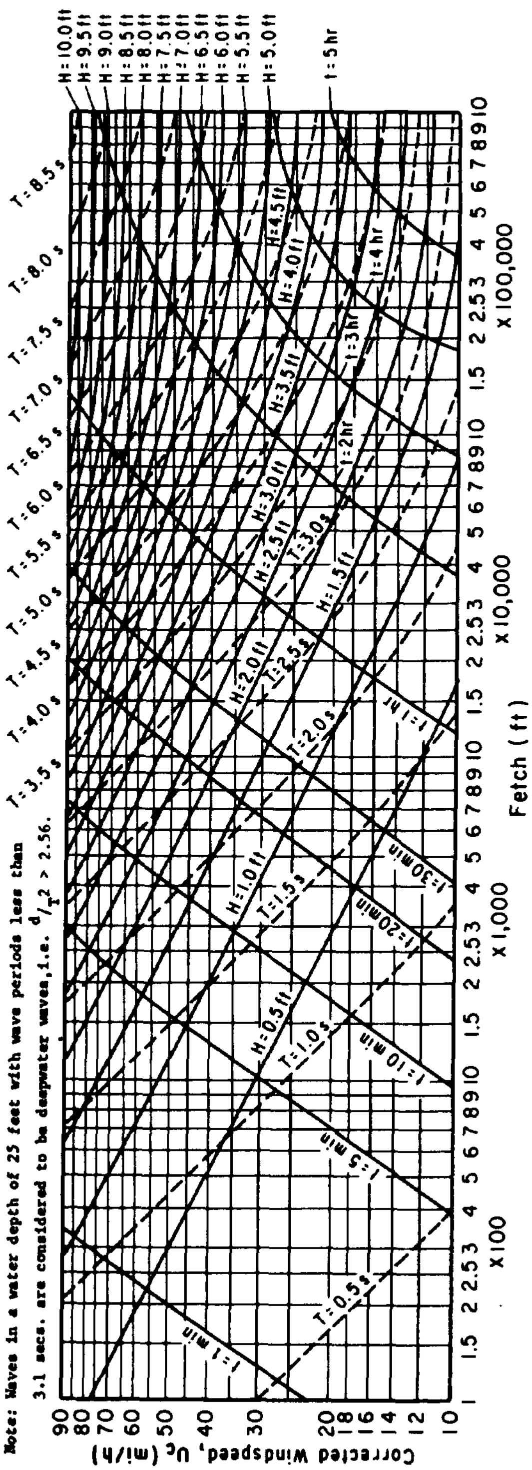

Figure 5-39. Forecasting curves for shallow-water waves (constant depth = 25 ft)

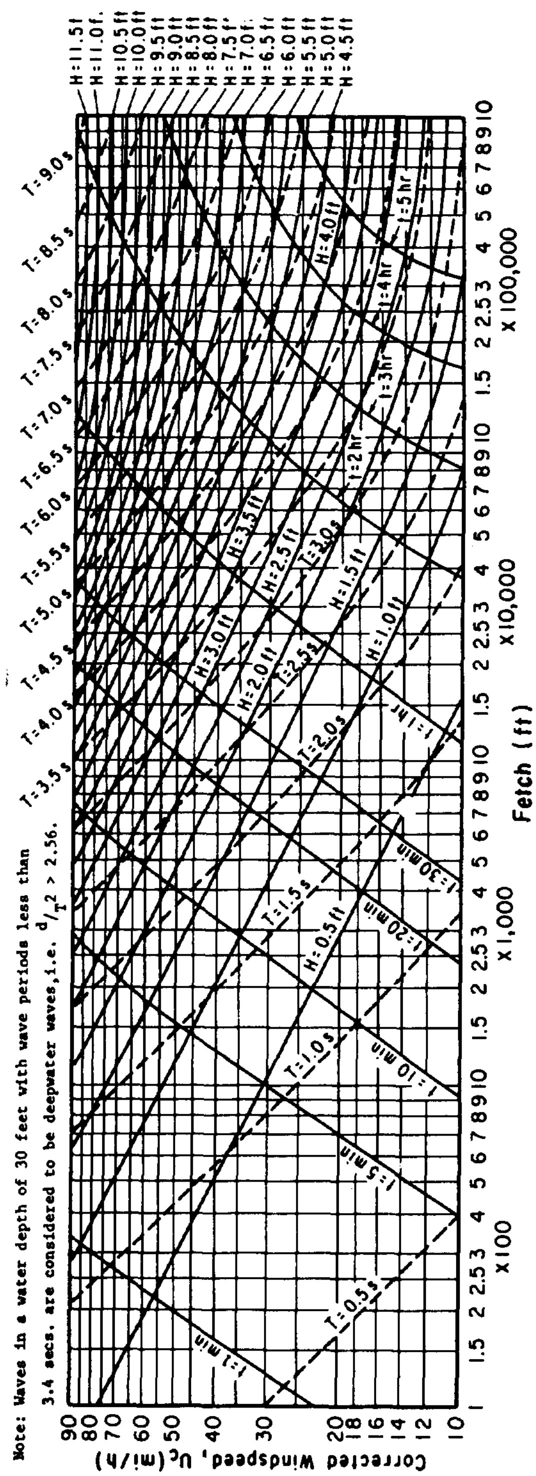

Figure 5-40. Forecasting curves for shallow-water waves (constant depth = 30 ft)

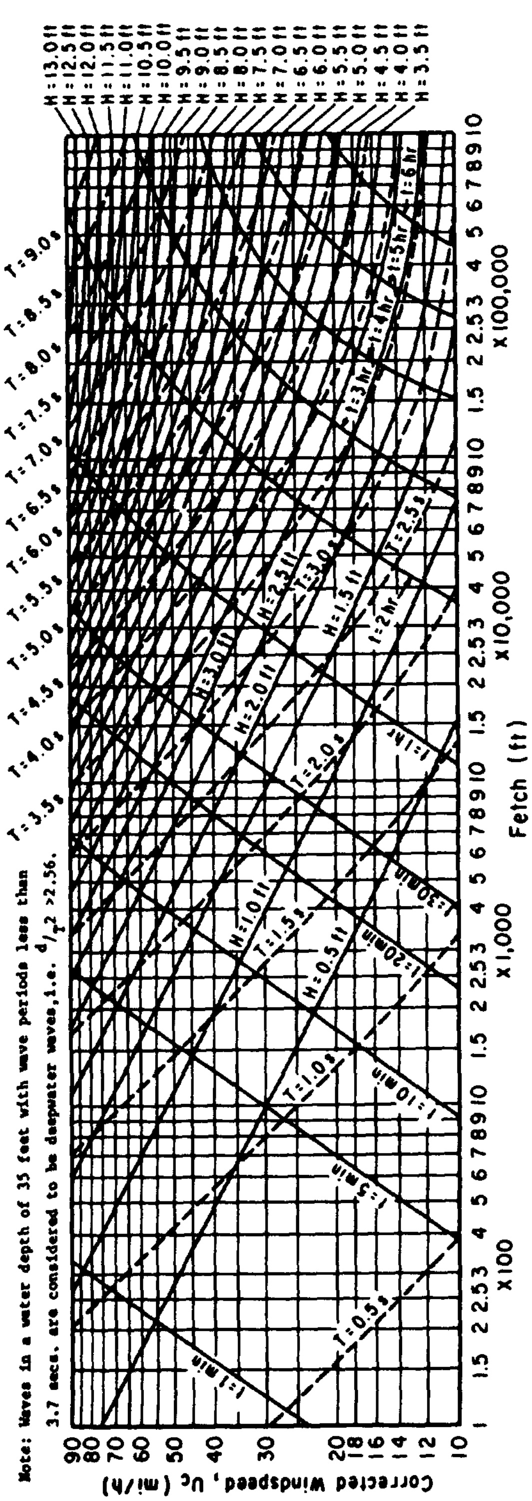

Figure 5-41. Forecasting curves for shallow-water waves (constant depth = 35 ft)

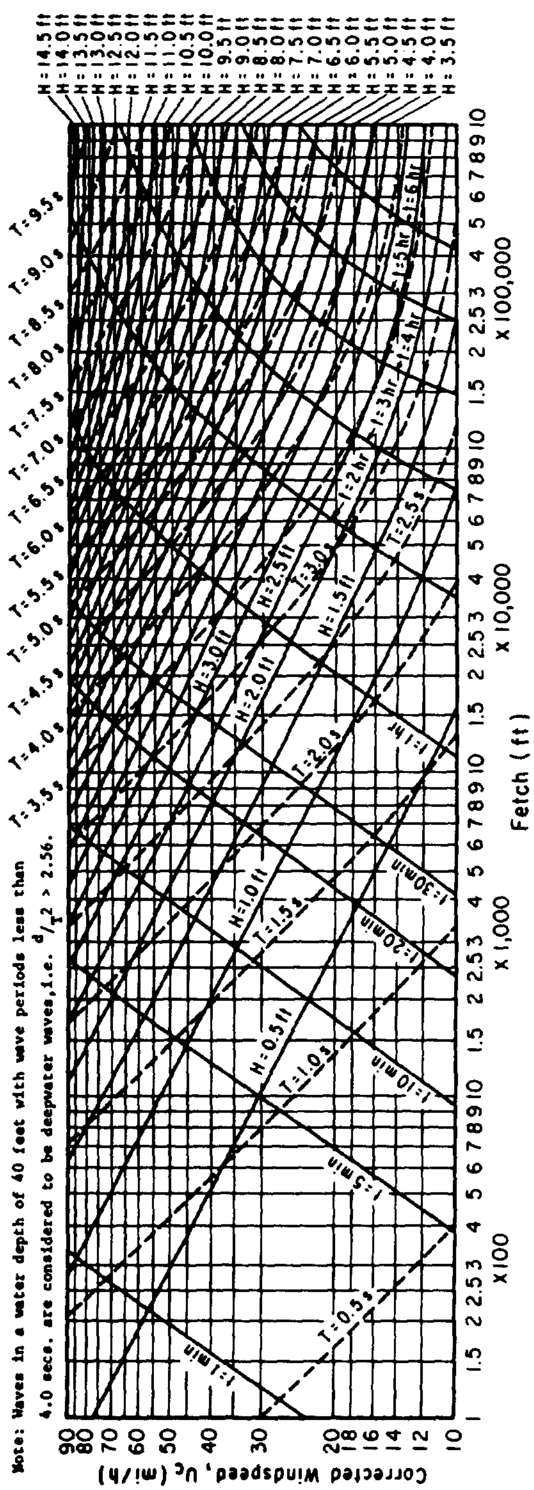

Figure 5-42. Forecasting curves for shallow-water waves (constant depth = 40 ft)

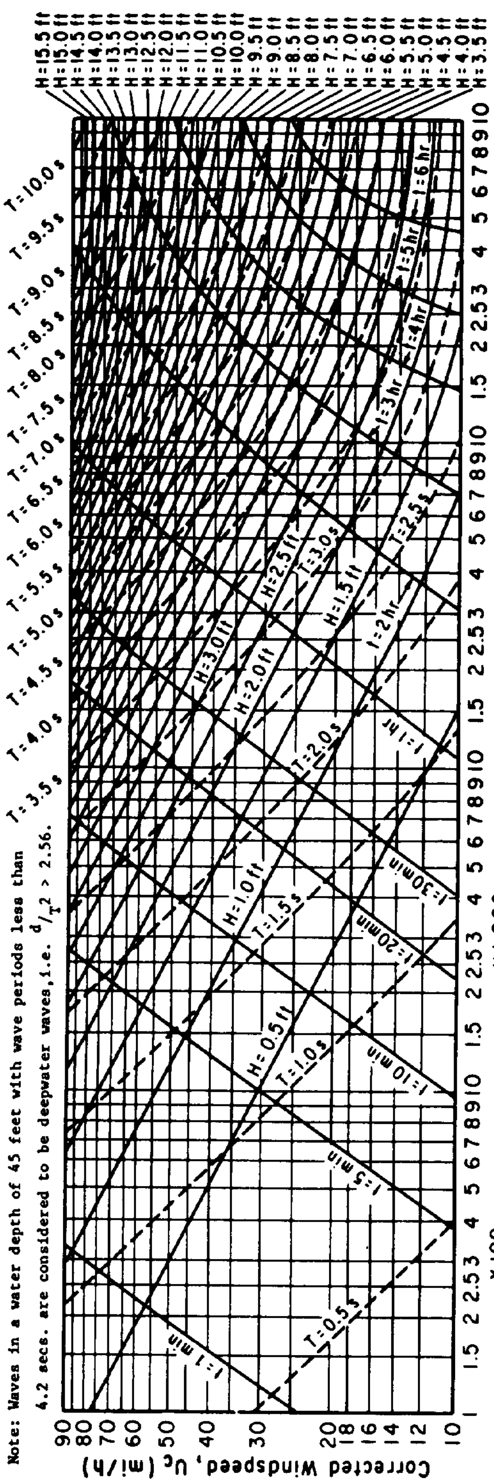

Figure 5-43. Forecasting curves for shallow-water waves (constant depth = 45 ft)

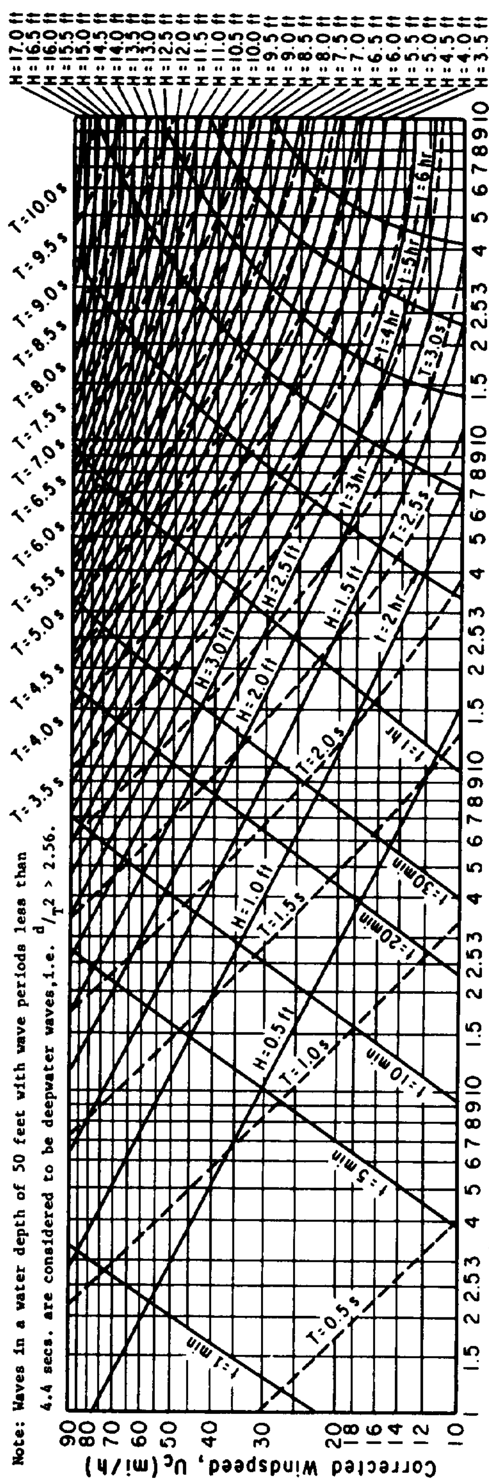

Figure 5-44. Forecasting curves for shallow-water waves (constant depth = 50 ft)

d. Wave Growth and Decay over Flooded, Vegetated Land. Waves grow slower and decay more rapidly over a vegetated bottom because the vegetation increases the frictional resistance. An approximate method to estimate wave growth and decay over a vegetated bottom is presented in the SPM. This method accounts for the high friction by adjusting the fetch length. The computer program WAVFLOOD, available under the MACE program (C-6, Appendix C), uses the same method.

e. Wave Refraction and Shoaling. When waves move into shallow water, their speed decreases. This effect, referred to as shoaling, influences wave height. If the waves are moving at an angle to the bottom contours, they bend so that wave crests are more nearly parallel to the contours. This process, called refraction, also affects wave height. Refraction is generally computed on a site-by-site basis since it depends upon the details of the bottom configuration. Computational methods are described in Section 5-7. Rough estimates of refraction and shoaling effects on wave height and direction can be obtained from Figure 5-45, which is based on the assumption that bottom contours are straight and parallel. The computer program SINWAVES to estimate the effects of refraction and shoaling, assuming linear wave theory and straight, parallel bottom contours, is available under the MACE program (C-8, Appendix C).

f. Spectral Models. Numerous mathematical expressions for the spectral energy density function $E(f)$ have been proposed based on theoretical considerations and analysis of field data. The expressions can be very helpful for characterizing a sea state for modeling of wave growth, structure response to waves, and vessel response to waves. Some accepted spectral models are presented and discussed in the following paragraphs.

(1) Bretschneider Spectrum. The Bretschneider Spectrum applies to deepwater waves which are growing under the influence of a local wind. The spectrum is based on parameters of the wave field. Spectral energy density is given in square foot-seconds by

$$E(f) = 3.36 \, H_s^2 \, T_p \, (fT_p)^5 \left[\exp -1.25(fT_p)^{-4}\right] \tag{5-14}$$

(2) JONSWAP Spectrum. The JONSWAP spectrum also applies to deepwater waves which are generated by a local wind. It is based on extensive wave observations collected in the North Sea as part of the JONSWAP (item 47).

(a) Spectral energy density is given by

$$E(f) = \frac{\alpha \, g^2}{(2\pi)^4 \, f^5} \, e^a \, \gamma^b \tag{5-15}$$

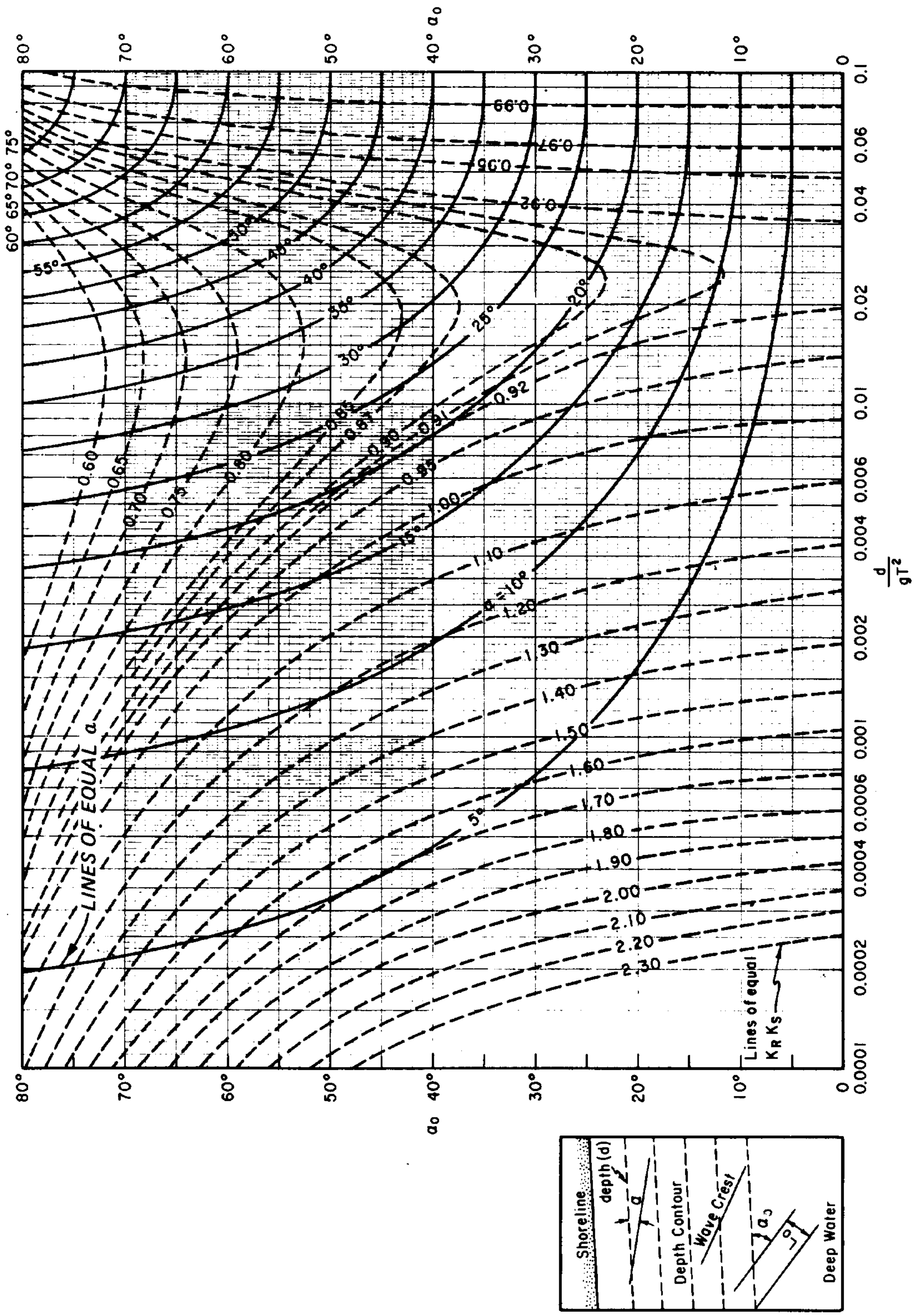

Figure 5-45. Change in wave direction and height due to refraction on slopes with straight, parallel depth contours including shoaling

where

$$a = -1.25\ (f\ T_p)^{-4} \tag{5-16}$$

$$b = \exp\left[\frac{-1}{2\sigma^2}\ (fT_p - 1)^2\right]$$

The parameters α, σ, and γ may be determined either by fitting an observed spectrum or by the following expressions:

$$\begin{aligned} \sigma = 0.07 \quad &\text{for} \quad f \leq f_p \\ 0.09 \quad &\text{for} \quad f \geq f_p \end{aligned} \tag{5-17}$$

$$\alpha = 0.0078\ \kappa^{0.49} \tag{5-18}$$

$$\gamma = 2.47\ \kappa^{0.39} \tag{5-19}$$

$$\kappa = 2\pi\ \frac{U^2}{gL_p} \tag{5-20}$$

where

U = wind speed at 33-ft (10-m) elevation

L_p = wavelength for waves at peak frequency

(b) The above expressions for α and γ differ from the original JONSWAP formulation which was based on fetch and wind speed rather than wavelength and wind speed. The advantage of the above formulation is that it can easily be extended for application in shallow water as discussed in the following paragraphs and by item 67.

(c) The parameters α and γ may also be estimated in terms of parameters of the wave field alone (rather than wind field) by

$$\alpha = 157.9\ \varepsilon^2 \tag{5-21}$$

$$\gamma = 6{,}614\ \varepsilon^{1.59} \tag{5-22}$$

where

$$\varepsilon = \frac{H_s}{4L_p} \tag{5-23}$$

The parameter ε is the significant wave steepness. The parameter γ, called the peak enhancement factor, controls the sharpness of the spectral peak. It typically ranges between 1 and 7 with a mean value of 3.3.

(3) Shallow-Water Spectrum. The Texel, MARSEN, ARSLOE (TMA) spectrum characterizes waves which have been generated primarily in a local deepwater area and then moved into shallow water. MARSEN is an acronym for Marine Remote Sensing Experiment at the North Sea; TMA is an acronym for Atlantic Remote Sensing Land-Ocean Experiment. The spectral form is based on the assumption of complete saturation of energy at frequencies higher than f_p. No refraction effects are included. The spectral form was derived from theoretical work discussed in item 6 and item 83 and extensive field data from the TMA experiments.

(a) The TMA spectrum is given by

$$E_{TMA}\ (f,d) = \frac{\alpha g^2}{(2\pi)^4 f^5}\ \Phi(2\pi f,d)\ e^a\ \gamma^b \tag{5-24}$$

The function $\Phi(2\pi f,d)$ approaches a value of one in deep water and a value of zero as depth decreases (Figure 5-46). It is well approximated by

$$\Phi(2\pi f,d) = \begin{cases} 0.5\ \omega_d^2 & \text{for } \omega_d \leq 1 \\ 1 - 0.5\ (2 - \omega_d)^2 & \text{for } \omega_d > 1 \end{cases} \tag{5-25}$$

where

$$\omega_d = 2\pi f\left(\frac{d}{g}\right)^{1/2}$$

The functions a and b are defined as with the JONSWAP spectrum (equation 5-16). The wavelength L_p in equations (5-20) and (5-23) is based on linear wave theory and an appropriate local water depth. Significant wave height in equation (5-23) is the energy-based parameter H_{mo} (Section 5-4.g). If it can be assumed that the energy-containing frequencies are such that $\omega_d < 1$, H_{mo} is approximated by

$$H_{mo} = 0.350\ (\alpha\ g\ d)^{0.5}\ T_p \tag{5-26}$$

(b) The variation in TMA spectral shape as a function of water depth is illustrated in Figure 5-47. Additional details on the TMA spectrum are given in item 67.

g. Directional Spectral Models. Ocean wave energy can be characterized by a variety of directions as well as by a variety of frequencies. Spectral representations which include both frequency distribution and angular spreading are known as directional spectral models.

(1) Directional spectral models are based on the assumption that the spectrum may be described by the product of two functions:

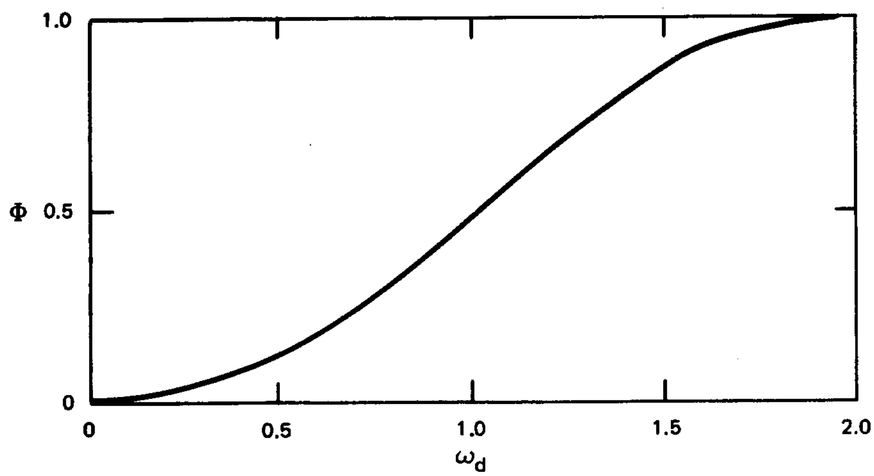

Figure 5-46. Φ as a function of ω_d

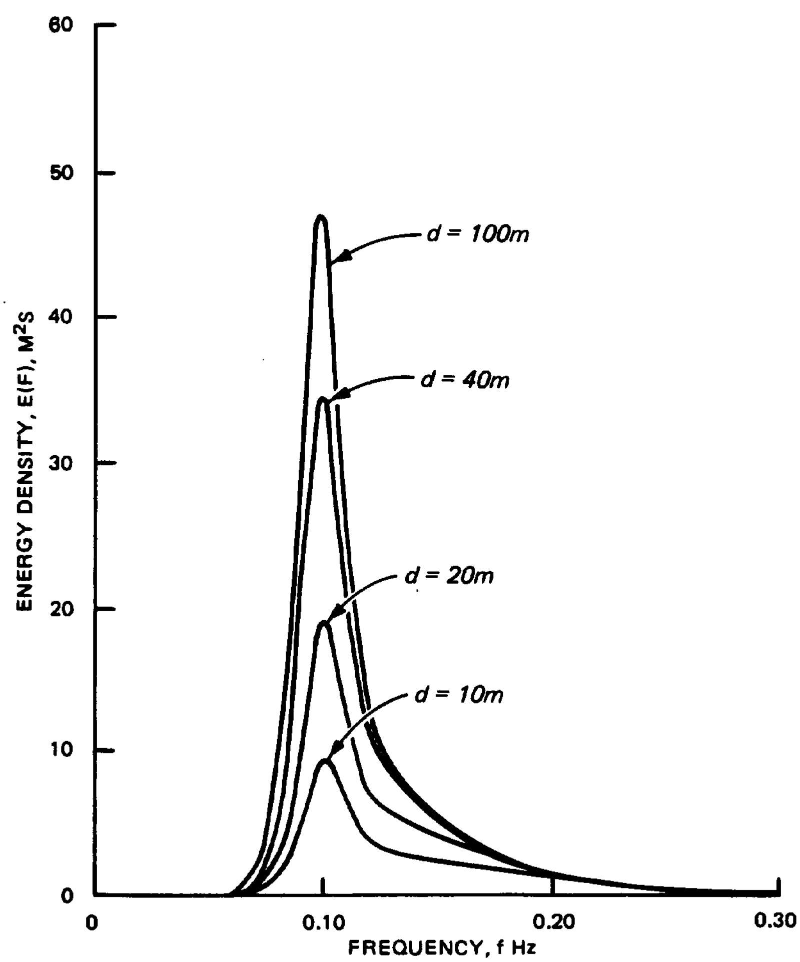

Figure 5-47. A family of TMA wind wave spectra with identical JONSWAP parameters

$$E(f,\theta) = E(f)\ D(f,\theta) \tag{5-27}$$

where

$E(f,\theta)$ = directional spectral density function

$D(f,\theta)$ = angular spreading function

θ = direction in radians

This parameterization can effectively represent the directional nature of a wave field in the absence of complicating influences such as a large change in wind direction or the propagation of swell into a generation area.

(2) A commonly-used form of the spreading function which is independent of frequency (item 87) is

$$D(\theta) = G(s) \cos^{2s}\left(\frac{\theta - \theta_o}{2}\right) \tag{5-28}$$

where

$G(s)$ = function tabulated in Table 5-4

s = constant-valued spreading parameter

θ_o = mean wind direction

The parameter s controls the magnitude of directional spread, as illustrated in Figure 5-48. Increasing the value of s causes a narrowing of the directional spread. Swell is typically represented by narrow spreads and seas by broad spreads.

(3) More complex formulations for the spreading parameter which include a dependence on wind speed and peak spectral frequency have been proposed based on field data in deep water (items 48 and 94).

5-8. Numerical Wave Models. Because of the continually increasing capabilities and availability of digital computers, numerical wave models are becoming essential tools for practical engineering work. Models vary greatly in complexity. The simplest wave growth model is a computer program to solve the equations in Table 5-3. The most complex models are comprehensive spectral models which operate on a grid and simulate natural wave processes including growth, dissipation, propagation, and wave-wave interaction. Numerical modeling definitions and characteristics are presented in the following paragraphs. Examples of how to select an appropriate model for a given engineering project are given. A major wave modeling effort in the Corps, the Wave Information Study (WIS), and the statistics which it has produced are discussed.

a. Numerical Modeling Definitions. Numerical model characteristics are described in the following paragraphs.

Table 5-4

Values of G(s) in the Directional Spreading Function

s	G(s)
1	0.3183
2	0.4244
3	0.5093
4	0.5821
5	0.6467
6	0.7055
7	0.7598
8	0.8104
9	0.8581
10	0.9033
11	0.9463
12	0.9874
13	1.0269
14	1.0650
15	1.1017
16	1.1372

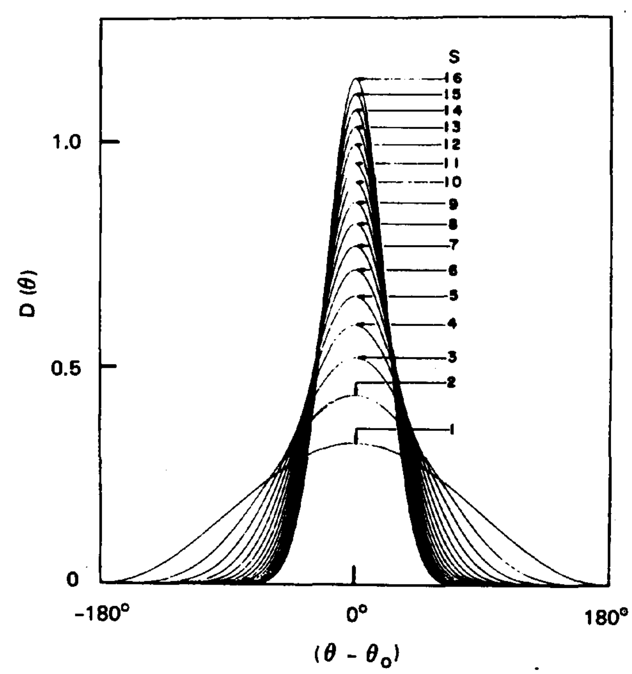

Figure 5-48. Idealized angular distribution

(1) Wave concept. The significant wave model uses monochromatic waves or simple parameters of a spectrum of wave energy (Figure 5-49 a and b). The spectral wave model uses a spectrum of wave energy composed of many different frequency bands (Figure 5-49c).

(2) Time dependence. The steady state model input does not vary with time. However, the time-dependent model input changes with time.

(3) Spatial configuration. The gridded model simulates processes modeled at grid points covering the water body. Finite difference and finite element are alternative approaches for performing numerical calculations. Typically finite difference grid cells are rectangular, and finite element cells are triangular (Figure 5-50a). The nongridded model simulates processes directly over the entire area affecting the point of interest (Figure 5-50b).

(4) Basic formulation. The energy equation model solves energy equations, and the momentum equation model solves momentum equations.

(5) Wave growth. The deepwater model can simulate wave growth in deep water; whereas the shallow-water model can simulate wave growth in shallow water. The hurricane model can simulate wave growth due to hurricanes.

(6) Current models can include the effect of currents.

(7) Propagation models can propagate waves in space (Figure 5-51).

(8) Transformation in shallow water. Refraction and shoaling modeling simulate wave refraction and shoaling. Two approaches are illustrated in Figure 5-52.

(a) Bottom friction model - includes a bottom friction mechanism for energy dissipation.

(b) Percolation model - includes a percolation mechanism for energy dissipation.

(c) Wave breaking model - includes a wave breaking mechanism for energy dissipation.

(d) Nonlinear interaction model - includes a mechanism for nonlinear transfer of energy between frequencies.

(e) Diffraction (bottom-induced) model - includes lateral energy transfer induced by irregular bottom.

(f) Diffraction (structure-induced) model - includes capability for simulating diffraction around surface-piercing structures.

(g) Growth during transformation model - includes capability for simulating additional wave growth by wind during the shallow-water transformation process.

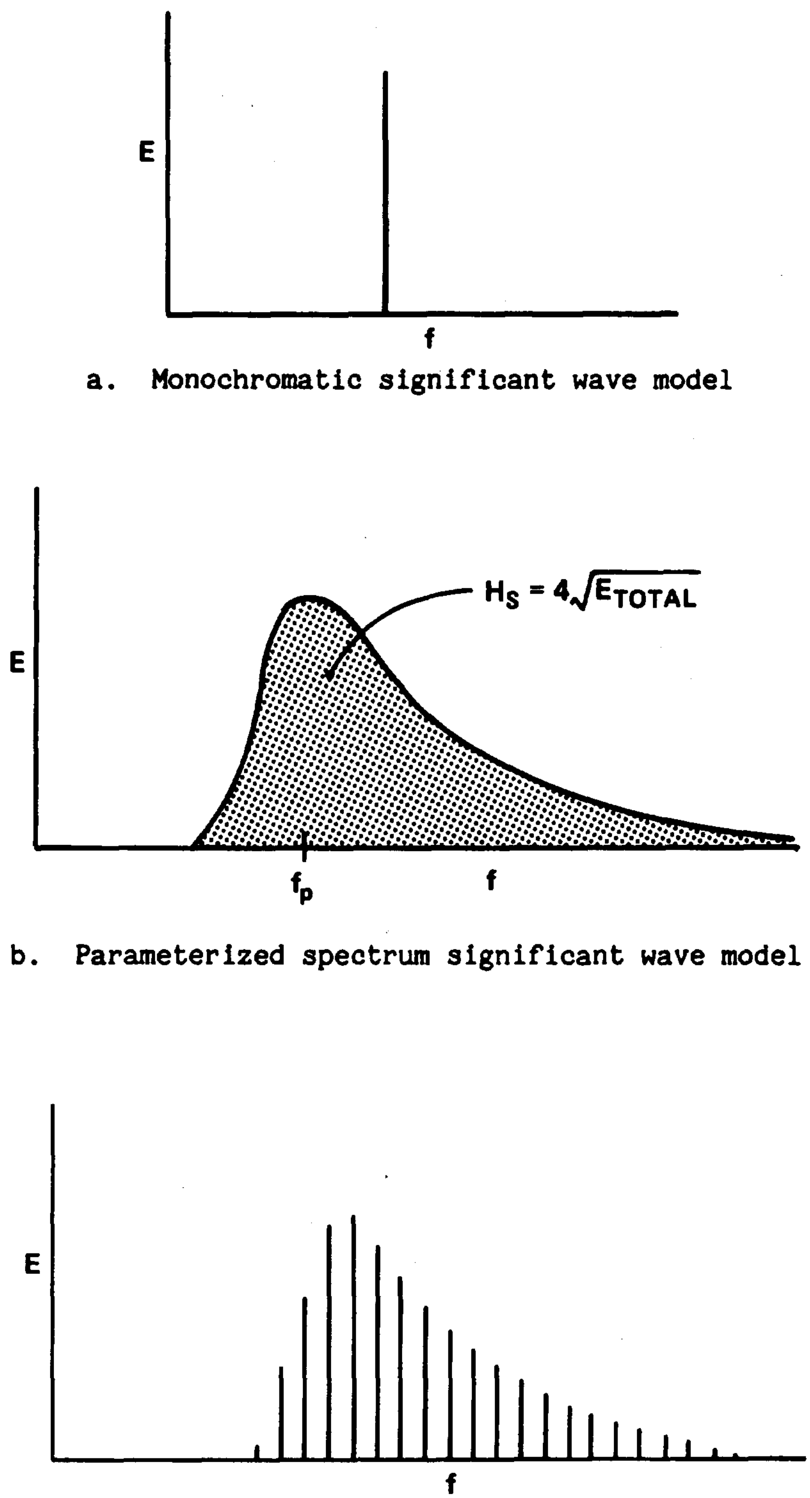

c. Spectral wave model

Figure 5-49. Wave model concepts

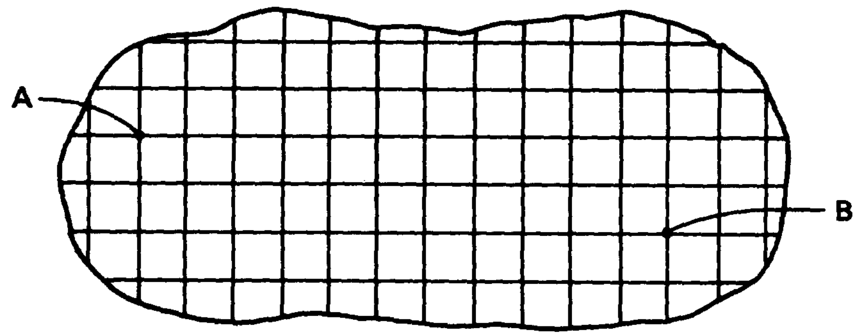

a. Gridded

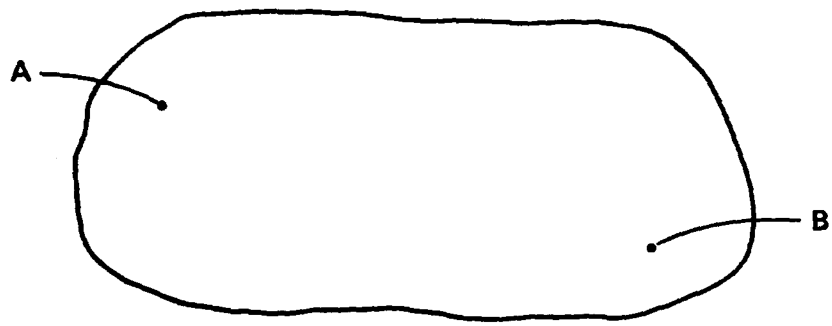

b. Nongridded

Figure 5-50. Spatial configuration of wave models

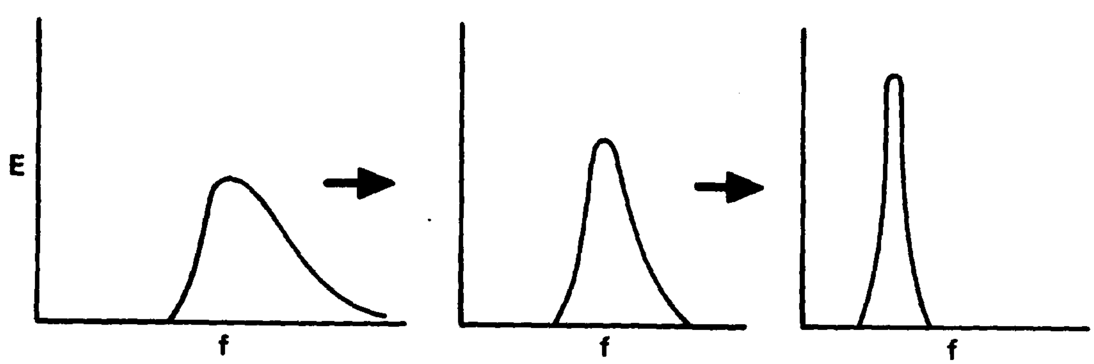

Figure 5-51. Propagation and decay for spectral model

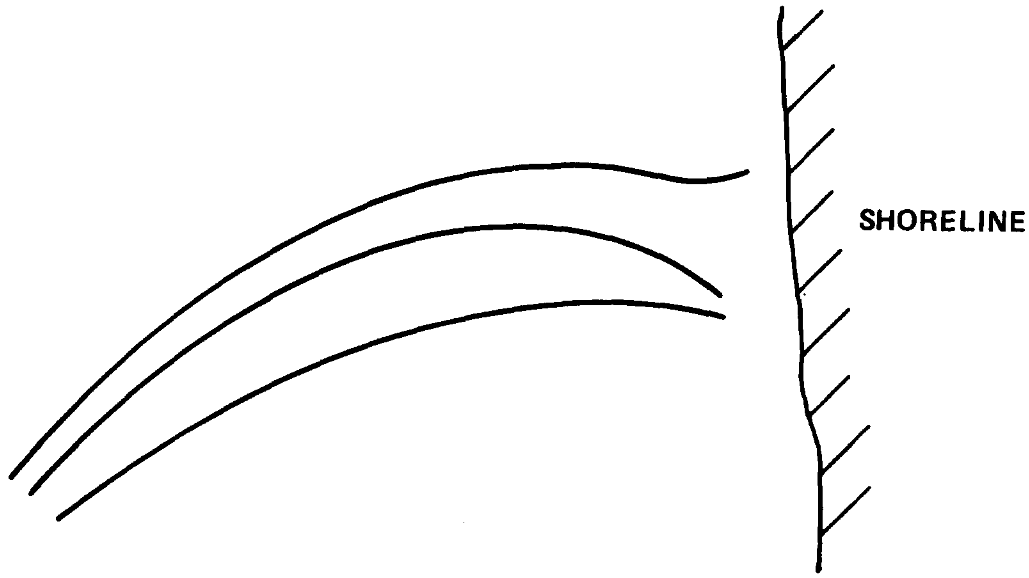

a. Refraction rays

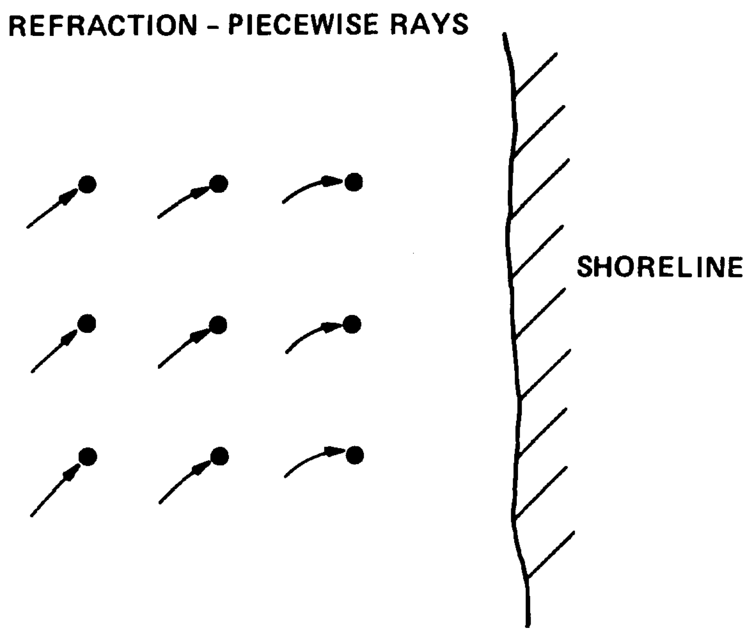

b. Refraction piecewise rays

Figure 5-52. Approaches to modeling wave refraction

(h) Blockage by floating or bottom-resting objects model - can simulate effects of structures or other objects floating on the surface or resting on the bottom.

(9) The model basis is depicted in Figure 5-53. The energy model simulates processes in terms of modifications to wave energy, while the wave height model simulates processes in terms of modifications to wave height.

MODEL BASIS

WAVE ENERGY

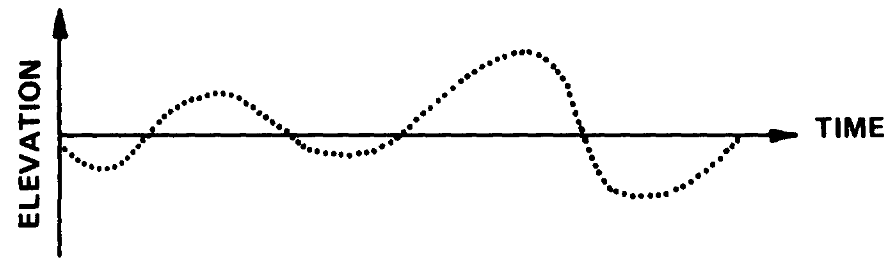

H_S = 4 X (STANDARD DEVIATION)
= 4 X (TOTAL SPECTRAL ENERGY)$^{1/2}$

WAVE HEIGHT

H_S = FUNCTION OF WAVE HEIGHT

Figure 5-53. Model basis

b. Numerical Model Characteristics. To illustrate the range of capabilities of numerical models, a sample of 12 different models available in the Corps is tabulated in terms of the characteristics discussed previously (Figure 5-54). Model 1 in the table represents the manual methods in the SPM. Models 2 through 12 are computerized models which generally increase in complexity with increasing model number. A short description of each model is given in Table 5-5. More detailed descriptions are given in Appendix F.

c. Selection of Numerical models. Considerations in selecting a numerical model are illustrated in the following case studies.

****

Case 1. Application: Wave estimates are needed at Spit A (Figure 5-55) for estimating long-term sediment transport.

Appraisal: The spit is exposed to waves generated in Area B, but it is sheltered from waves generated in Areas C and D. Hence wave generation is considered only in Area B where fetches are up to 80 miles long.

Characteristics	SPM84 1	TMA 2	GODAS 3	TWAVE1 4	SWWM 5	WAVE 6	RCPWAVE 7	WISS 8	WISD 9	ESCUBED 10	SHALWV 11	HARBS 12
Wave concept												
Significant wave												
Monochromatic	x					x	x					x
Parameterized spectrum		x	x		x							
Spectral wave				x				x	x	x	x	
Time dependence												
Steady state	x	x	x	x		x	x			x		x
Time dependent					x			x	x		x	
Spatial configuration												
Ungridded	x	x	x	x	x	x		x				
Gridded												
Finite difference							x		x	x	x	
Finite element												x
Basic formulation												
Energy equation		x		x	x	x	x	x	x	x	x	
Momentum equation												x
Wave growth												
Deep water	x				x				x	x	x	
Shallow water	x				x					x	x	
Hurricanes	x											
Currents										x	x	
Propagation						x	x		x	x	x	x
Transformation in shallow water												
Refraction & shoaling	x			x*		x	x	x		x	x	x
Bottom friction					x					x	x	x
Percolation										x	x	
Wave breaking			x		x		x	x		x		
Nonlinear interaction					x			x		x	x	
Diffraction (bottom-induced)							x					x
Diffraction (structure-induced)	x											x
Growth during transformation					x					x	x	
Blockage by floating or bottom-resting objects												x
Model basis												
Energy		x		x	x			x	x	x	x	
Wave height	x		x			x	x					x

* Assumes straight parallel bottom contours.

Figure 5-54. Overview of numerical wave models

Table 5-5

Model Names

Number	Model Name	Description	Bibliographic Items
1	SPM84	Methods in the Shore Protection Manual	SPM
2	TMA	Parametric model for maximum depth-limited waves; based on TMA shallow-water spectrum	67
3	GODAS	Wave transformation model	37
4	TWAVE2	Simple computer model based on TMA shallow water spectrum	
5	SWWM	Simple shallow-water growth model	78
6	WAVE	Ray refraction model	108
7	RCPWAVE	Refraction and diffraction model	30
8	WISS	Shallow-water model from WIS	79
9	WISD	Deepwater model from WIS	110
10	ESCUBED	Wave growth and transformation model	65
11	SHALWV	Wave growth and transformation model	68
12	HARBS	Harbor model	17

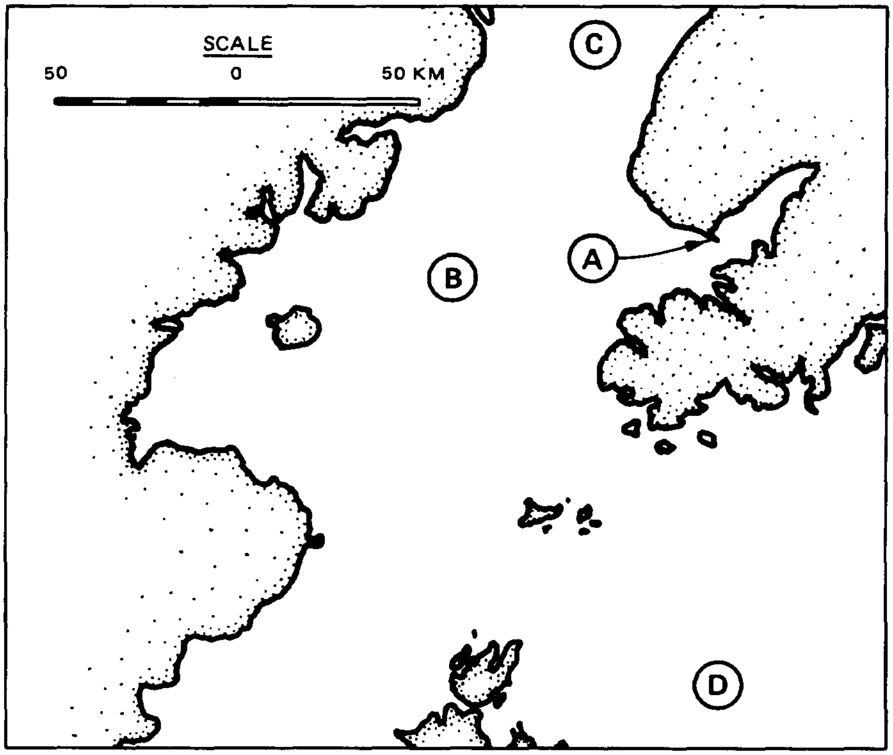

Figure 5-55. Location map for Case Study 1

Climatological wind measurements are available only at the spit. Synoptic weather maps are available. They are of little value in this study because winds are strongly channeled by topographic features (mountain ranges) and bear little relationship to synoptic pressure fields. Also wind fields over Area B are known to often be nonuniform so that the available wind measurements may not be a good representation of winds over the fetch.

The water depth in Area B is relatively great. Waves are in deep water until they approach very near the spit. Bottom contours near the spit are somewhat contorted, including a large shoal offshore from the spit. Currents in the shallow-water area near the spit are believed to be weak, but tidal currents passing the tip of the spit are very strong.

Candidate models: Because the shallow-water area is only a small part of the fetch, the candidate models can be considered in two separate categories as deepwater growth models and shallow, wave transformation models. Candidate deepwater growth models are SPM84, WISD, ESCUBED, and SHALWV. Candidate shallow transformation models include SPM84, TMA, GODAS, TWAVE2, SWWM, WAVE, RCPWAVE, WISS, ESCUBED, SHALWV, and HARBS.

Model selection: Since the wind information for Area B is very sparse in relation to the complexity of the wind fields, it is appropriate to use a simple deepwater wave growth model. Also, the geometry of Area B is relatively simple. Thus the models which operate on a grid appear to be unnecessary for this case. The model SPM84 emerges as the most cost-effective choice for this application.

Since considerations for the deepwater growth model have led to the choice of a simple model, the shallow transformation model should also be relatively simple. It should not depend upon highly accurate input along the seaward boundary. Wave growth in shallow water is negligible. These considerations lead to elimination of the time-dependent models SWWM, WISS, and SHALWV. Since the shallow-water bathymetry is somewhat irregular and good estimates of nearshore wave direction are needed for sediment transport estimates, it is decided that the actual bathymetry must be represented in the model. Thus the nongridded models SPM84, TMA, GODAS, and TWAVE2 are rejected. The model WAVE is an old ray-calculation routine which often leads to crossing rays in complicated nearshore areas. It is not recommended for this application. The remaining models are RCPWAVE, ESCUBED, and HARBS. The limited accuracy of the deepwater input suggests that ESCUBED, a spectral model, is not cost effective in comparison to RCPWAVE and HARBS, which are significant wave models. The nearshore complexity does not appear to be sufficient to warrant the use of HARBS. Therefore, the final selection is RCPWAVE for the shallow-water transformation model.

****

Case 2. Application: Wave estimates are needed at Point A (Figure 5-56) for design of a seawall which will reduce flooding and wave overtopping to acceptable levels.

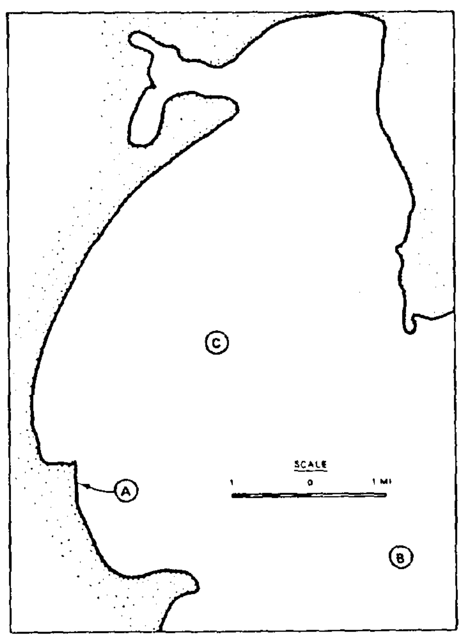

Figure 5-56. Location map for Case Study 2

Appraisal: Point A is exposed to waves generated in the Ocean Area B through the entrance to Bay C. An additional consideration for the north side of Point A is wave energy generated in the northerly reaches of Bay C which propagates toward the project site. Synoptic meteorological data are available for Ocean Area B. Sufficient wind measurements are available in the vicinity of Bay C to establish estimates of the winds over the bay. The entire sound area represents shallow water for all ocean waves of interest in design. Local wave growth in the bay north of the project site may also occur to an appreciable extent in water that is shallow relative to the waves. Bottom contours are irregular. Currents are not expected to be a significant factor in the study. Wave estimates from the WIS are available just seaward of the entrance to Bay C.

Candidate models include WAVE, RCPWAVE, ESCUBED, SHALWV, and HARBS.

Model selection: Accurate overtopping rates are very important in this design project, so a spectral model is favored over a significant wave model. Either ESCUBED or SHALWV would be an acceptable choice. SHALWV is expected to have the advantage of better representing additional wave growth in shallow water but has the disadvantage of higher costs.

****

Case 3. Application: Wave measurements are being collected in deep water along a coast. Just after a major storm it is desired to transfer the deepwater waves to shore for a quick comparison with wave heights reported by coastal residents.

Appraisal. Wave growth between the measurement site and shore is assumed to be inconsequential. It is usually necessary to assume that the bottom contours are straight and parallel to make quick estimates. This assumption is justifiable for this type of application for many US coastal areas.

Candidate models include SPM84, TMA, GODAS, and TWAVE2.

Model selection: The SPM84 model for straight parallel bottom contours is a nomogram derived for monochromatic waves. SPM84 is useful if very quick estimates are needed and access to the computerized candidate models is not available. In most instances TMA, GODAS, or TWAVE2 would be preferable to a monochromatic model.

A wave direction in deep water should be estimated. If significant refraction is expected, TWAVE2 would be a good choice. If refraction appears to be of minor importance, TMA or GODAS would also be suitable. In the case of TMA and TWAVE2, which are energy-based models, it must be remembered that the computed shallow-water wave height will be somewhat lower than the crest-to-trough wave height seen by an observer. Procedures for estimating crest-to-trough height from an energy-based height have been incorporated in TWAVE2. Since the GODAS model is based directly on wave height, it provides a direct estimate of shallow-water height.

****

Case 4. Application: A harbor is being renovated. The harbor is partially protected by a breakwater, which may be rubble mound, sheet pile, floating, etc. A vertical wall along which boats can moor is being designed. Wave forces on the wall must be estimated. Wave forces on moored boats must also be estimated.

Appraisal: It is necessary to estimate wave conditions passing through arbitrary harbor protection works which may have complicated geometry. Wave force estimates on fixed and floating structures must also be provided.

The candidate model is HARBS.

Model Selection: The model HARBS is the reasonable choice for this case involving waves passing complicated structures and estimation of wave forces. When wave forces are needed, the model selected must be formulated in terms of the momentum equation rather than the energy equation.

****

Case 5. Application: A long-term time-history of wave estimates is needed within Area A for design and planning of coastal structures and dredging operations.

Appraisal: Area A is a semi-enclosed body of water sheltered from Area B by barrier islands (Figure 5-57). Area A is approximately 80 nautical miles in length and 10 nautical miles in width. Climatological wind measurements are available at Points C, D, and E. Synoptic weather maps are also available. Comparisons between the three land-based meteorological stations indicate the winds can be considered as uniform over Area A. Therefore, the wind measurements are used in preference to the synoptic maps. The water depth in Area A is relatively shallow, a mean water depth of 10 feet. The bottom contours follow the outline of the land boundaries and are nearly straight and parallel, except for dredged channels. The currents in Area A are believed to be relatively small.

Candidate models: Wave growth in shallow water is the primary consideration in the selection process, eliminating all wave transformation models that require wave input conditions. The following models are considered: SPM84, SWWM, ESCUBED, and SHALWV.

Model selection: The study requires time-histories of wave conditions (storm sequences must be simulated correctly). These considerations lead to the elimination of the steady state wave model ESCUBED. SHALWV is eliminated because of its limitation for modeling poststorm conditions. The study also requires spectral information, eliminating SPM84. Therefore, the final selection is SWWM for the shallow-water wave growth and transformation model.

****

d. Wave Information Study. The WIS is a Corps project to hindcast wave climate over a 20-year period for the Atlantic, Pacific, Gulf of Mexico, and Great Lakes coasts of the US. The hindcast period is from 1956 through 1975.

(1) The WIS project is being executed in three phases (Figure 5-58).

(a) Phase I: Hindcast of deepwater wave data from past meteorological data; model operates on the scale of the ocean basin.

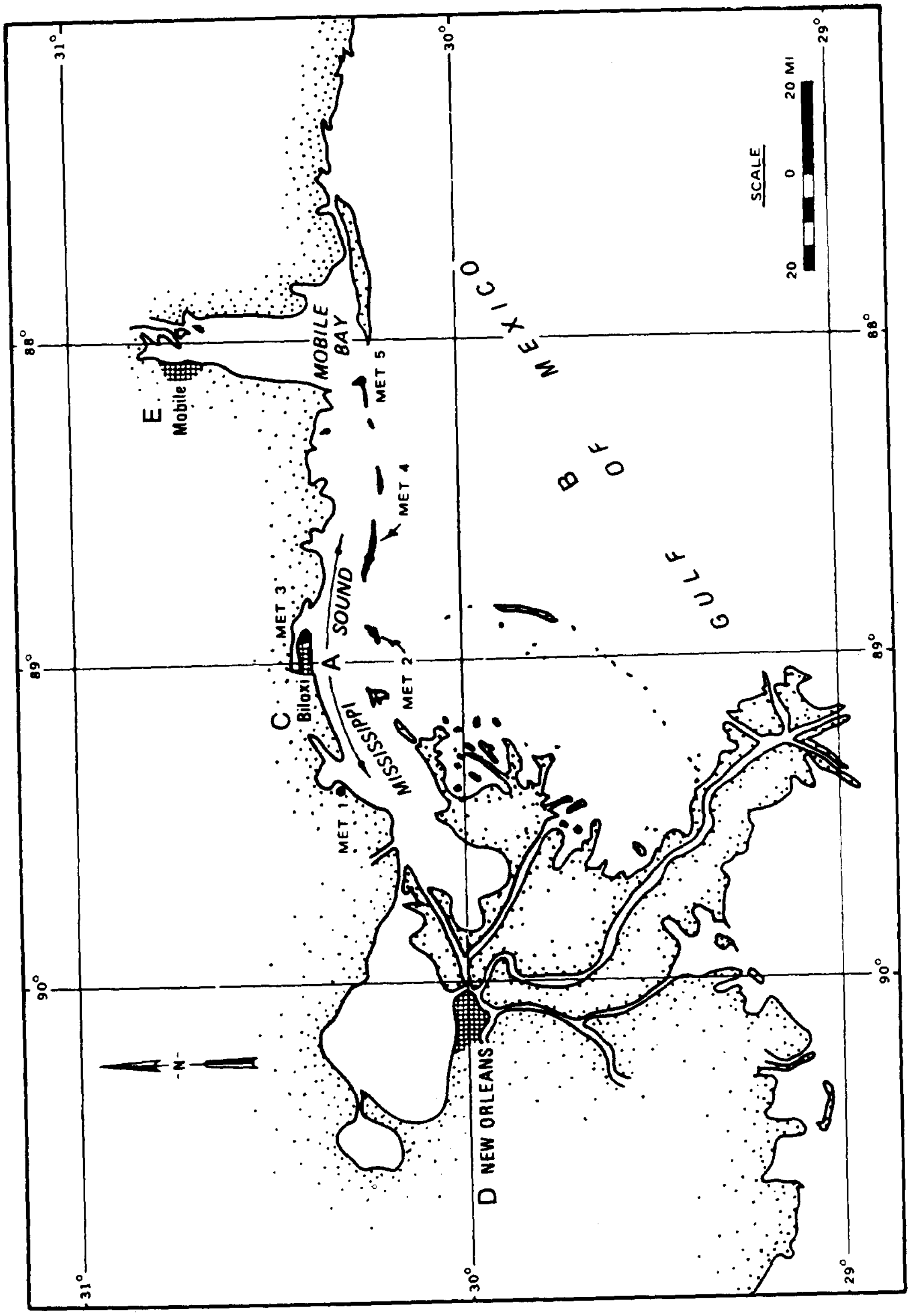

Figure 5-57. Location map for Case Study 5

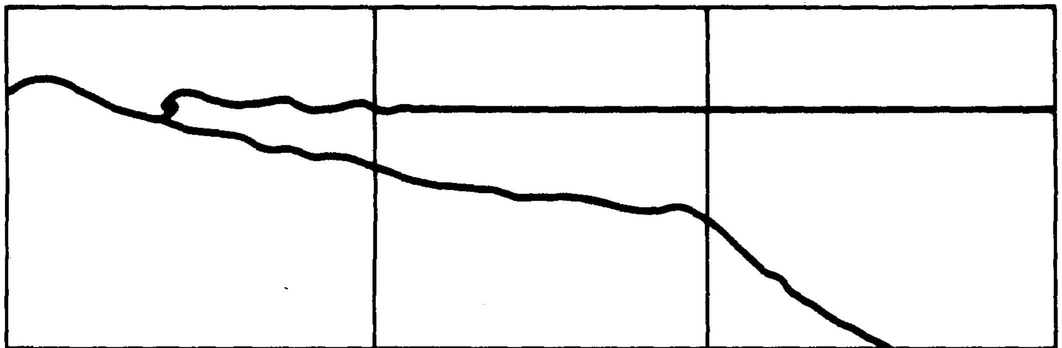

	PHASE III	PHASE II	PHASE I
	NEARSHORE ZONE	SHELF ZONE	DEEP OCEAN
ATMOSPHERIC RESPONSE SCALES	SYNOPTIC, MESOSCALE CONVECTIVE	MESOSCALE AND SYNOPTIC	SYNOPTIC AND LARGE SCALE
ATMOSPHERIC RESPONSE SCALES	Δx LESS THAN 10 MILES Δt LESS THAN 3 HOURS	Δx 10'S OF MILES Δt 3 TO 6 HOURS	Δx 100'S OF MILES Δt GREATER THAN 6 HOURS
WAVE PROCESSES	AIR-SEA INTERACTION REFRACTION DIFFRACTION SHOALING BOTTOM FRICTION LONG WAVES (TIDES AND SURGE)	AIR-SEA INTERACTION	AIR-SEA INTERACTION
	WAVE TRANSFORMATION	SECONDARY ENERGY SOURCE	PRIMARY ENERGY SOURCE

Figure 5-58. Summary of the three phases of WIS hindcasts

(b) Phase II: Hindcast at a finer scale than Phase I to better resolve sheltering effects of continental geometry; model operates on the scale of the continental shelf. Phase I data serve as boundary conditions for the seaward edge of the Phase II area.

(c) Phase III: Transformation of Phase II wave data into nearshore region and inclusion of long waves.

(2) WIS uses a discrete spectral model based on an energy balance equation. The model includes wave growth in deep water and spectral wave propagation. The model is time dependent and, in the case of Phases I and II, operates on a spatial grid. Nearshore effects of sheltering, refraction, shoaling, and nonlinear interaction among various spectral components are included. Refraction in Phase III is based on the assumption of straight parallel bottom contours and uniformity of wave conditions along 10-mile stretches of coast.

(3) The WIS results can be used to get high quality data for project sites typically by using Phase II results as input to a gridded shallow-water transformation model with high quality bathymetric data. Alternatively, the existing WIS data base of shallow-water wave information for simplified bathymetry and coastal configuration can be used for some stages of project planning and execution. More information on the availability and access to WIS data and programs is given in Chapter 6.

5-9. Statistical Summaries of Individual Wave Estimates. Statistical summaries of parameters from individual wave estimates are essential for defining wave climate and for predicting extreme waves at a site. The simplest statistics which are also very useful are the monthly, seasonal, and annual means. Other useful summaries are described in the following sections. The quantity and quality of data available are crucial considerations in all statistical summaries. Less than one year of data can be very misleading due to seasonal variations in wave climate. One complete year can give reliable estimates of routine wave conditions but not of extreme or unusual wave conditions. The possibililty of biases introduced by the data collection and analysis systems must also be considered. One insidious bias on extreme values from observed or measured data is a tendency during very severe storms for missing or unreliable data in an otherwise consistent record. Good overall references on statistical summaries of wave observations are items 38 and 103.

a. Joint Distribution Tables of Wave Height and Period. Significant wave height and period statistics are often summarized as a table giving the number or percentage of occurrence of each significant height/period combination. A typical example is given in Figure 5-59.

b. Sea State Persistence. Sea state persistence is an estimate of how long a particular wave condition will remain. Persistence estimates are useful in planning and operational work. They are usually expressed as tables or plots of the number of consecutive hours or days the significant wave height exceeds various threshold levels. Various distribution functions have been applied to persistence data as discussed in item 38.

c. Long-Term Distributions for Wave Height.

(1) The long-term distribution for wave height is usually represented by the cumulative probability distribution of the data. It is also often fit with a model distribution function. There is no strong theoretical basis for a particular model. Several models are widely used primarily because they often provide good fits to the data.

(a) The probability distribution functions used for long-term distribution of wave heights are given in Figure 5-60. These consist of the lognormal distribution and the Extremal Types I, II, and III distributions. The table includes the cumulative probability $P(\hat{H}) = \mathrm{Prob}(H \le \hat{H})$, that is the probability that the significant wave height $\hat{H}$ is not exceeded by any randomly chosen significant height H. The general expressions for mean and variance are also given for each distribution.

Wave Climatology for Atlantic City, New Jersey[a]

Period sec	Height, ft										
	0-1	1-2	2-3	3-4	4-5	5-6	6-7	7-8	8-9	9-10	Total	Acc total
0.0–1.9	2.2										2.2	2.2
2.0–2.4	–											2.2
2.5–2.9	–											2.2
3.0–3.4	–	1.1									1.1	3.3
3.5–3.9	–	1.1	0.7								1.8	5.1
4.0–4.9	–	1.8	2.9	0.7							5.5	10.6
5.0–5.9	–	1.8	2.6	1.5	0.7	0.4					6.9	17.5
6.0–6.9	0.4	3.3	4.0	1.8	1.5	0.7	0.4	0.4			12.4	29.9
7.0–7.9	0.4	5.5	6.6	2.9	1.5	0.7	0.4	0.4			18.2	48.2
8.0–8.9	0.4	8.0	6.2	2.9	1.1	0.4	0.4	0.4	0.4		20.1	68.2
9.0–9.9	0.4	6.9	4.0	1.5	0.7	0.4	0.7	0.4	0.4	0.4	15.7	83.9
10.0–10.9	0.4	4.4	1.8	0.7	0.4	0.4		0.4	0.4		8.8	92.7
11.0–11.9	0.4	1.8	1.5	0.4	0.4	0.4					4.8	97.4
12.0–12.9		1.1	0.7								1.8	99.3
13.0–13.9		0.7									0.7	100.0
Total	4.4	37.6	31.0	12.4	6.2	3.3	1.8	1.8	1.1	0.4		100.0
Acc. total	4.4	42.0	73.0	85.4	91.6	94.9	96.7	98.5	99.6	100.0	100.0	

[a]Total = 12 months, January 1967 to December 1967. Distribution of height (in percent) as a function of period for 2083 observations. Each entry in the table is rounded individually, therefore, the sum and the accumulated total for each row or column may not agree with the figures as shown in the table.

Figure 5-59. Joint distribution table of significant wave height and period

Distribution (1)	Range (2)	Cumulative probability, $P(H)$ (3)	Mean (4)	Variance (5)
Lognormal	$0 < H < \infty$ $-\infty < \theta < \infty$ $0 < \alpha < \infty$	$(1/\sqrt{2\pi}) \int_0^H \frac{1}{\alpha h} \exp\left[-\frac{1}{2}\left(\frac{\ln(h) - \theta}{\alpha}\right)^2\right] dh$	$\exp\left(\theta + \frac{\alpha^2}{2}\right)$	$\exp(2\theta + \alpha^2)[\exp(\alpha^2) - 1]$
Type I	$-\infty < H < \infty$ $-\infty < \epsilon < \infty$ $0 < \theta < \infty$	$\exp\left\{-\exp\left[-\left(\frac{H - \epsilon}{\theta}\right)\right]\right\}$	$\epsilon + \gamma\theta$ $(\simeq \epsilon + 0.58\theta)$	$\frac{\pi^2}{6}\theta^2$ $(\simeq 1.64\theta^2)$
Type II	$0 < H < \infty$ $0 < \theta < \infty$ $0 < \alpha < \infty$	$\exp\left[-\left(\frac{H}{\theta}\right)^{-\alpha}\right]$	$\theta\Gamma\left(1 - \frac{1}{\alpha}\right)$	$\theta^2\left[\Gamma\left(1 - \frac{2}{\alpha}\right) - \Gamma^2\left(1 - \frac{1}{\alpha}\right)\right]$
Type III_L (Lower Bound)	$\epsilon < H < \infty$ $0 < \theta < \infty$ $0 < \alpha < \infty$	$1 - \exp\left[-\left(\frac{H - \epsilon}{\theta}\right)^{\alpha}\right]$	$\epsilon + \theta\Gamma\left(1 - \frac{1}{\alpha}\right)$	$\theta^2\left[\Gamma\left(1 + \frac{2}{\alpha}\right) - \Gamma^2\left(1 + \frac{1}{\alpha}\right)\right]$
Type III_U (Upper Bound)	$-\infty < H < \epsilon$ $0 < \theta < \infty$ $0 < \alpha < \infty$	$\exp\left[-\left(\frac{\epsilon - H}{\theta}\right)^{\alpha}\right]$	$\epsilon - \theta\Gamma\left(1 + \frac{1}{\alpha}\right)$	$\theta^2\left[\Gamma\left(1 + \frac{2}{\alpha}\right) - \Gamma^2\left(1 + \frac{1}{\alpha}\right)\right]$

Figure 5-60. Probability distributions used to describe long-term wave heights (item 74)

(b) In applying these distributions, data are usually plotted so that, if they follow the selected distribution, they will form a straight line. The linear ordinate scale y in such a plot is related to the cumulative probability, and the linear abscissa scale x is related to $\hat{H}$ according to the relationships given in Figure 5-61. The slope a and the intercept b for the linear relationship $y = ax + b$ are given in the table in terms of the parameters of each distribution.

Distribution (1)	Abscissa scale x (2)	Ordinate scale y (3)	Slope a (4)	Intercept b (5)
Lognormal	$\ln(H)$	$P(H) = \frac{1}{\sqrt{2\pi}} \int_0^y e^{-1/2t^2} dt$	$1/\alpha$	$-\theta/\alpha$
Type I	H	$-\ln\{-\ln[P(H)]\}$	$1/\theta$	$-\epsilon/\theta$
Type II	$\ln(H)$	$-\ln\{-\ln[P(H)]\}$	α	$-\alpha \ln\theta$
Type III_L	$\ln(H - \epsilon)$	$\ln\{-\ln[Q(H)]\}$	α	$-\alpha \ln\theta$
(Lower Bound)	H	$\{-\ln[Q(H)]\}^{1/\alpha}$	$1/\theta$	$-\epsilon/\theta$
Type III_U	$-\ln(\epsilon - H)$	$-\ln\{-\ln[P(H)]\}$	α	$\alpha \ln\theta$
(Upper Bound)	H	$-\{-\ln[P(H)]\}^{1/\alpha}$	$1/\theta$	$-\epsilon/\theta$

Figure 5-61. Scale relationships for probability papers (item 74)

(2) Overall Distribution Functions. The Extremal Type III distribution with lower bound, also called the Weibull distribution, is useful for fitting the cumulative distribution of significant wave heights.

(a) A simplified form of the distribution which can be used for this purpose is given by

$$P(H_s \le \hat{H}_s) = \begin{cases} 1 - \exp\left[-\left(\dfrac{\hat{H}_s - H_{s\,min}}{\sigma_{Hs}}\right)\right] & \hat{H}_s \ge H_{s\,min} \\ 0 & \hat{H}_s < H_{s\,min} \end{cases} \qquad (5\text{-}29)$$

where

$\hat{H}_s$ = a particular value of H_s

$H_{s\,min}$ = minimum (background) significant wave height

σ_{Hs} = standard deviation of significant wave height

In circumstances where only the mean significant wave height $\bar{H}_s$ is known, the distribution function can be approximated by evaluating $H_{s\,min}$ and σ_{Hs} from

$$H_{s\,min} \approx 0.38\,\bar{H}_s$$

and

$$\sigma_{Hs} = \bar{H}_s - H_{s\,min} = 0.62\,\bar{H}_s \qquad (5\text{-}30)$$

(b) The lognormal distribution is also used in this context. Examples of data plotted on Weibull probability paper are given in Figure 5-62 (items 14, 28, and 103). The same data are plotted in Figure 5-63 (items 14, 23, and 103) on lognormal probability paper. The trends illustrated are typical. The Weibull distribution tends to fit the moderate and high wave height ranges, and the lognormal distribution fits the low and moderate wave height ranges.

(3) Extreme Value Distribution Functions. Extreme wave height values are a crucial ingredient in most coastal design. Often the extreme wave heights are limited by the shallow-water depth, as discussed in Section 5-7.e. For deeper water or low energy sites, extreme values are usually described in terms of significant wave height values as a function of return period. Extreme values of other height statistics such as $H_{1/10}$ can be obtained from the significant height data and a model for the distribution of individual wave heights (Section 5-4.e). Consideration of different statistical populations may be required as discussed in item 5.

(a) The basic approaches to predicting extreme wave conditions are extrapolation of long-term distribution of significant wave heights, extreme value analysis with annual maxima, and extreme value analysis with peak significant wave heights of major storms above a certain threshold.

(b) The first approach is relatively easy to apply. However, care must be taken concerning any statistical dependence among successive observations. A method for correcting for statistical dependence is given in item 102.

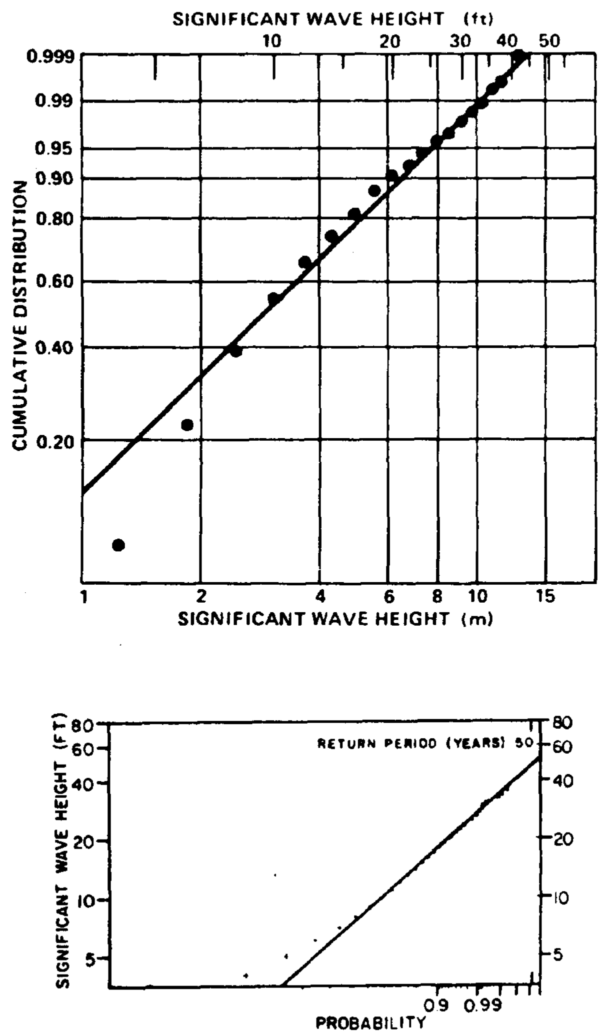

Figure 5-62. Cumulative distribution function of significant wave height plotted on Weibull probability paper

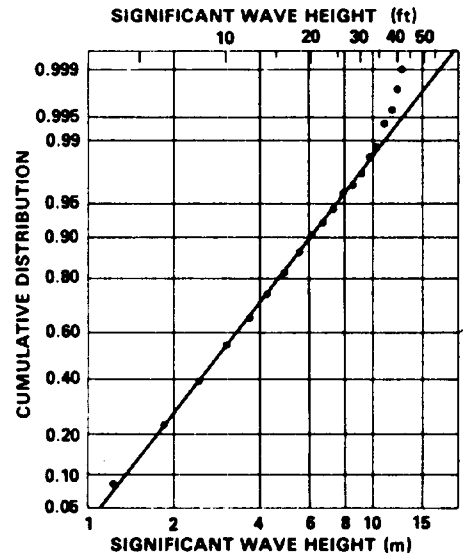

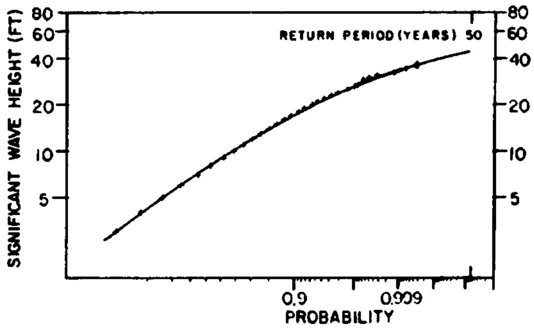

Figure 5-63. Cumulative distribution function of significant wave height plotted on lognormal probability paper

(c) Possible long-term statistical variability must also be considered before observed data can be extrapolated to long return periods. A more sophisticated curve fitting and extrapolation procedure is given in item 103. The reliability of the data base is a primary concern in extreme value analysis, and care should be taken to optimize it.

(4) Extreme Value Analysis. The steps involved in applying extreme value analysis (item 74) are discussed in the following paragraphs.

(a) Assign a probability value to each extreme data point. The data are ordered according to wave height. The subscript m denotes the rank, with m=1 for the largest wave height and m=N for the smallest wave height in a sample of N wave heights. The cumulative probability is given as

$$P(H) = 1 - \frac{m}{N + 1} \tag{5-31}$$

(b) Plot these points on an extreme value probability paper represented in Figure 5-61. Often it is desirable to use more than one probability paper and to select the one which gives the best fit to the data. The lognormal and Type I distributions are most often used.

(c) Fit a straight line through the points to represent a trend. Often the fit is done by eye. Alternatively the best fit line may be derived by matching the mean wave height and the mean squared wave height from the data with those from the model distribution. The model parameters derived by this approach are given in Figure 5-64 in terms of the mean and mean squared wave heights. The Type III distribution is less amenable to this approach because it has three parameters rather than two. It has been omitted from the table.

Distribution (1)	Estimated Parameters $\hat{\alpha}$ (2)	$\hat{\theta}$ (3)	$\hat{\varepsilon}$ (4)
Lognormal	$[\ln(\bar{H^2}) - 2\ln(\bar{H})]^{1/2}$	$2\ln(\bar{H}) - \frac{1}{2}\ln(\bar{H^2})$	—
Type I	—	$\frac{\sqrt{6}}{\pi}[\bar{H^2} - (\bar{H})^2]^{1/2}$	$\bar{H} - \gamma\hat{\theta}$
Type II	$\frac{\bar{H^2}}{(\bar{H})^2} = \frac{\Gamma(1 - 2/\hat{\alpha})}{\Gamma^2(1 - 1/\hat{\alpha})}$	$\frac{\bar{H}}{\Gamma(1 - 1/\hat{\alpha})}$	—

Figure 5-64. Parameters of distributions as estimated by Method of Moments (item 74)

(d) Extrapolate the line to locate a design value corresponding to a chosen return period T_r or a chosen encounter probability P_e . The return period is the average time interval between successive events of the design wave being equalled or exceeded. It is given by

$$T_r = \frac{r}{1 - P(\hat{H})} \tag{5-32}$$

where r is the time interval associated with each data point. The encounter probability P_e is the probability that the design wave is equalled or exceeded during a prescribed time period L . It is given by

$$P_e = 1 - \left(1 - \frac{r}{T_r}\right)^{L/r} \tag{5-33}$$

When return period is determined for a model distribution, encounter probability may be estimated for selected time periods from Figure 5-65. The figure may be used, for example, to determine the percent chance of occurrence of a significant wave height with 100-year return period in time periods of 1, 10, 25, 50, and 100 years. From the figure the percent chances are 1.0, 9.6, 22.2, 39.5, and 63.0.

(e) The computer programs WAVDIST to estimate the parameters of three commonly used extremal probability distributions and FWAVOCUR to determine the expected frequency of extreme wave conditions over a specified time period are available under the MACE program (C-14 and C-15, Appendix C).

GRAPH: Frequency of Wave Occurrence

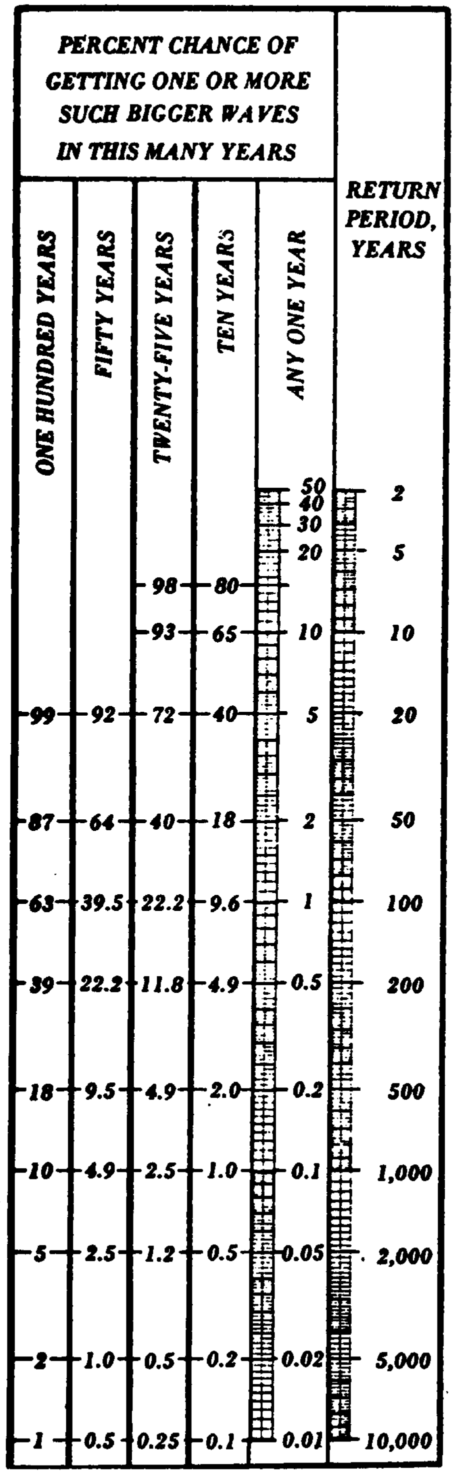

Figure 5-65. Encounter probabilities as a function of return period

CHAPTER 6

AVAILABILITY OF WAVE AND WATER LEVEL DATA

6-1. Available Wave Data. Extensive data sets for climatological use are available as summaries of visual observations from shipboard and as wave hindcasts.

a. Shipboard observations generally represent deepwater wave conditions summarized over areas on the order of 100 miles by 100 miles. Coastal areas of the contiguous US, for which summaries have been published in item 134, are shown in Figure 6-1.

b. Observations from shore have been collected in many US coastal areas under the Corps' LEO program. General areas for which LEO data are available are shown in Figure 6-2. LEO is decribed in item 114.

c. WIS (described in Section 5-8.d), a part of the Coastal Field Data Collection Program, is in the process of hindcasting wave statistics for US coasts including the Great Lakes. Great Lakes data presently available are design wave estimates for 5-, 10-, 20-, 50-, and 100-year return periods. Atlantic and Pacific hindcasts at 3-hour intervals over 20 years are available for the following three WIS phases: deepwater summaries (oceanic scale), intermediate summaries (continental shelf scale), and shallow-water summaries (10-meter water depth). Coastal summary points for WIS hindcasts are illustrated in Figures 6-3 through 6-7. Coastal summary points along the mainland in the southern California Bight are omitted from Figure 6-6 because they are not yet finalized. The extensive data sets generated for the US coast of the Atlantic, Pacific, and Gulf of Mexico are listed in Table 6-1. A list of WIS reports is given in Tables 6-2 and 6-3. Some hindcast data are also available in item 98.

d. Other types of data available include gage measurements discussed in Section 5-3. These types lack the length of record and uniformity of coastal coverage which typify shipboard observations and major hindcasting programs, but they have other obvious advantages for many applications. Item 123 summarizes wave gage data at selected US coastal locations. Since 1972 the National Oceanic and Atmospheric Administration's (NOAA's) National Data Buoy Center (NDBC) has maintained numerous oceanographic buoys throughout the US coastal waters of the Atlantic, Pacific, Gulf of Mexico, and the Great Lakes. A listing of the buoy locations and years of operation is provided in Table 6-4. Table 6-4 is updated to 1984. Further updates or actual buoy data can be obtained from the National Oceanographic Data Center (Table 6-5). More information on available meteorological, water level, and wave data is given in item 19.

6-2. Available Water Level Data. Tides and storm surges are described in Chapters 2 and 3, respectively, of this EM. Chapters 2 and 3 should be reviewed to determine the type of tidal information that is required for the study being performed. Occasionally tide gages are temporarily deployed in coastal areas while work is under way. Although the detail of local gages is desirable, this type of tidal data is usually not well documented and is often difficult to locate. The most comprehensive source of water level data is

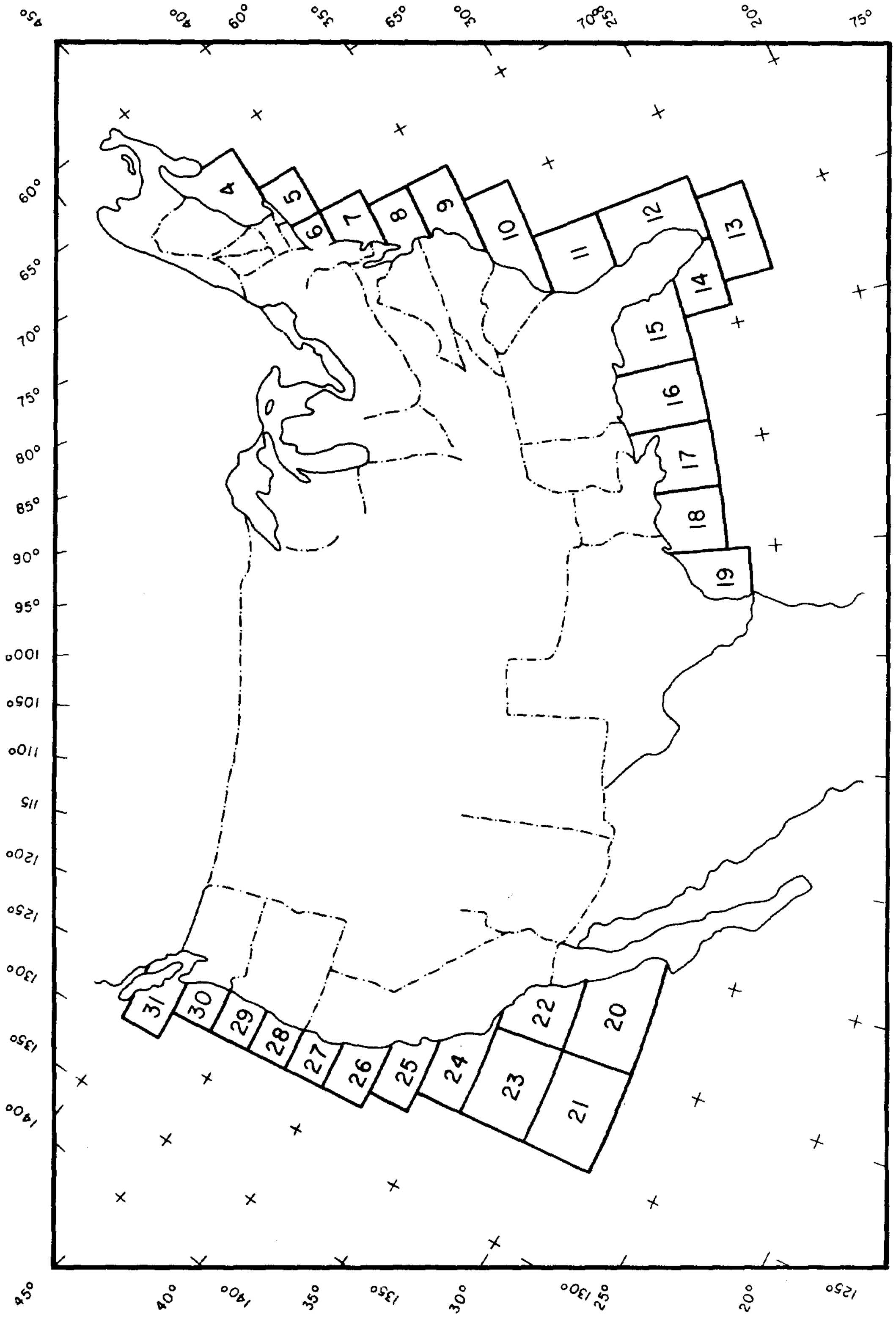

Figure 6-1. North American coastal Summary of Synoptic Meterological Observations (SSMO) Areas

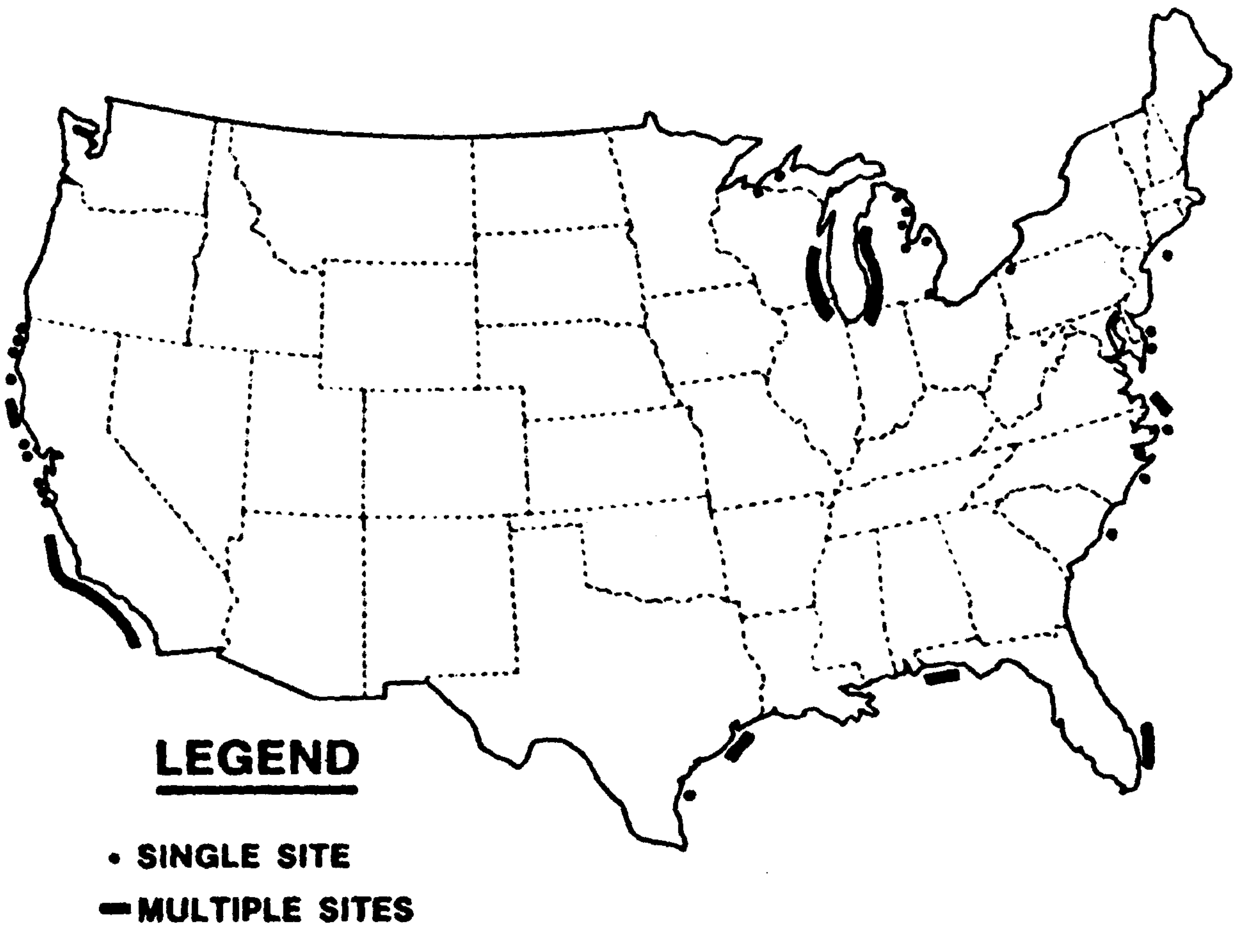

Figure 6-2. LEO sites

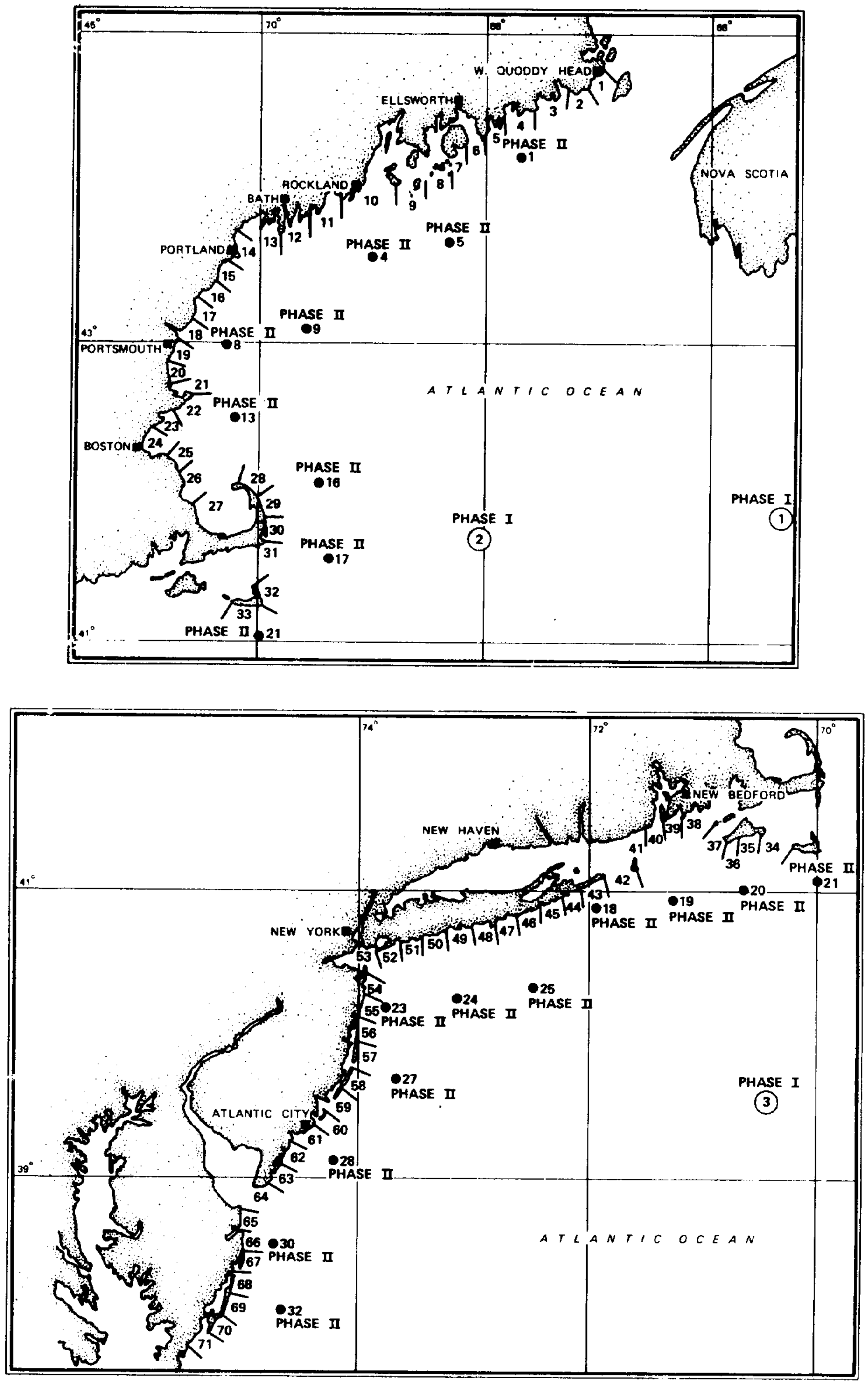

Figure 6-3. WIS locations for US Atlantic coast (Sheet 1 of 3)

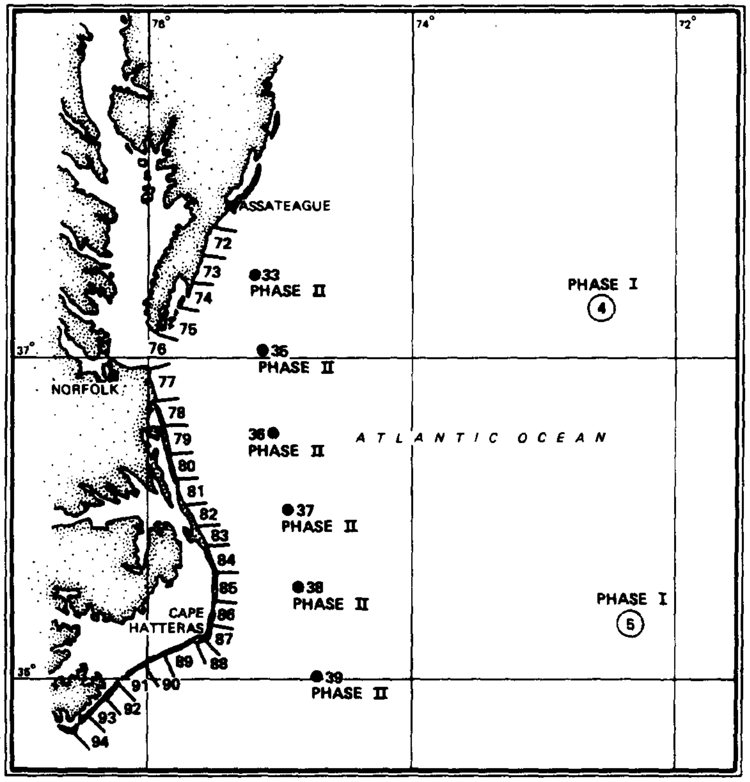

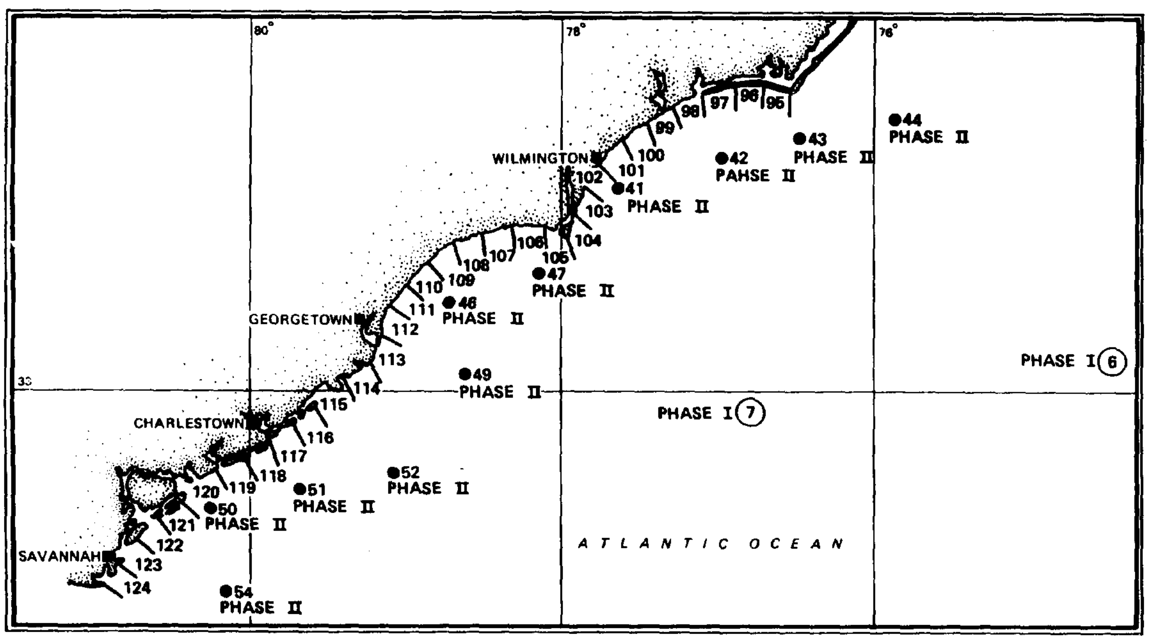

Figure 6-3 (Continued) (Sheet 2 of 3)

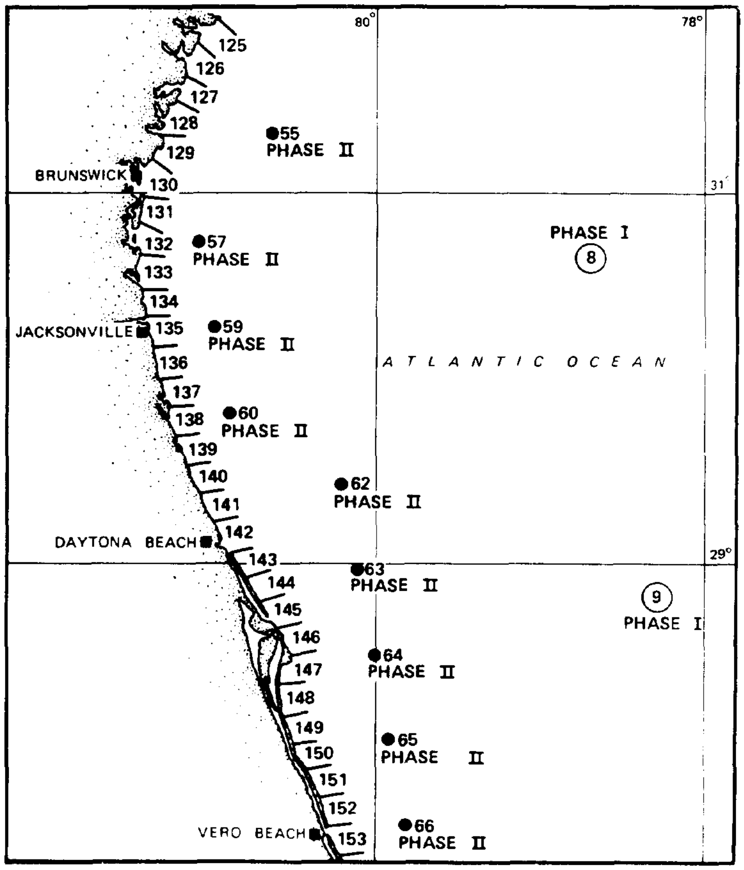

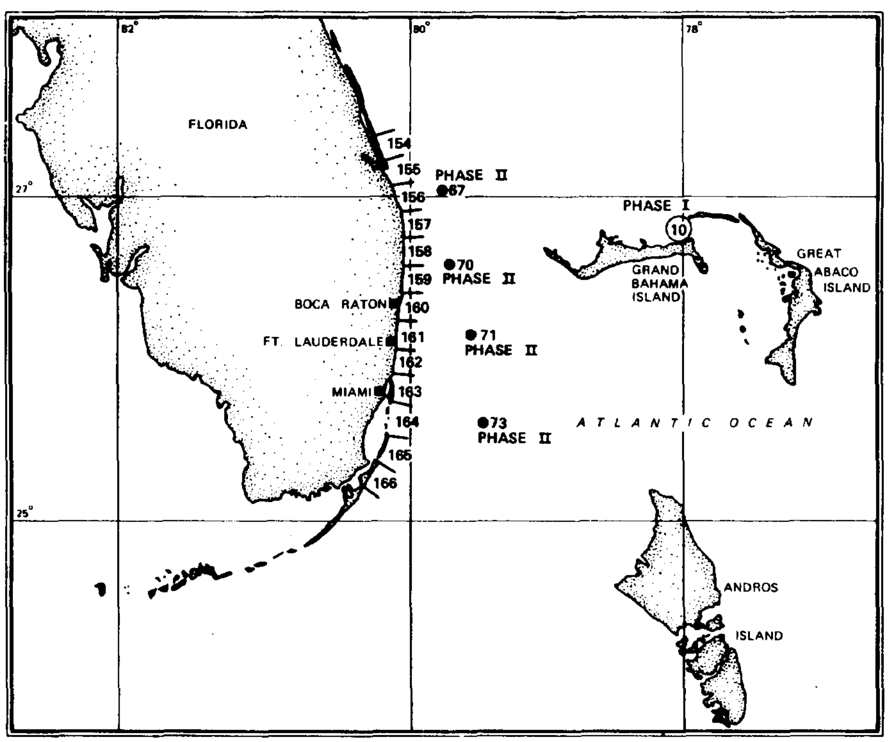

Figure 6-3 (Continued) (Sheet 3 of 3)

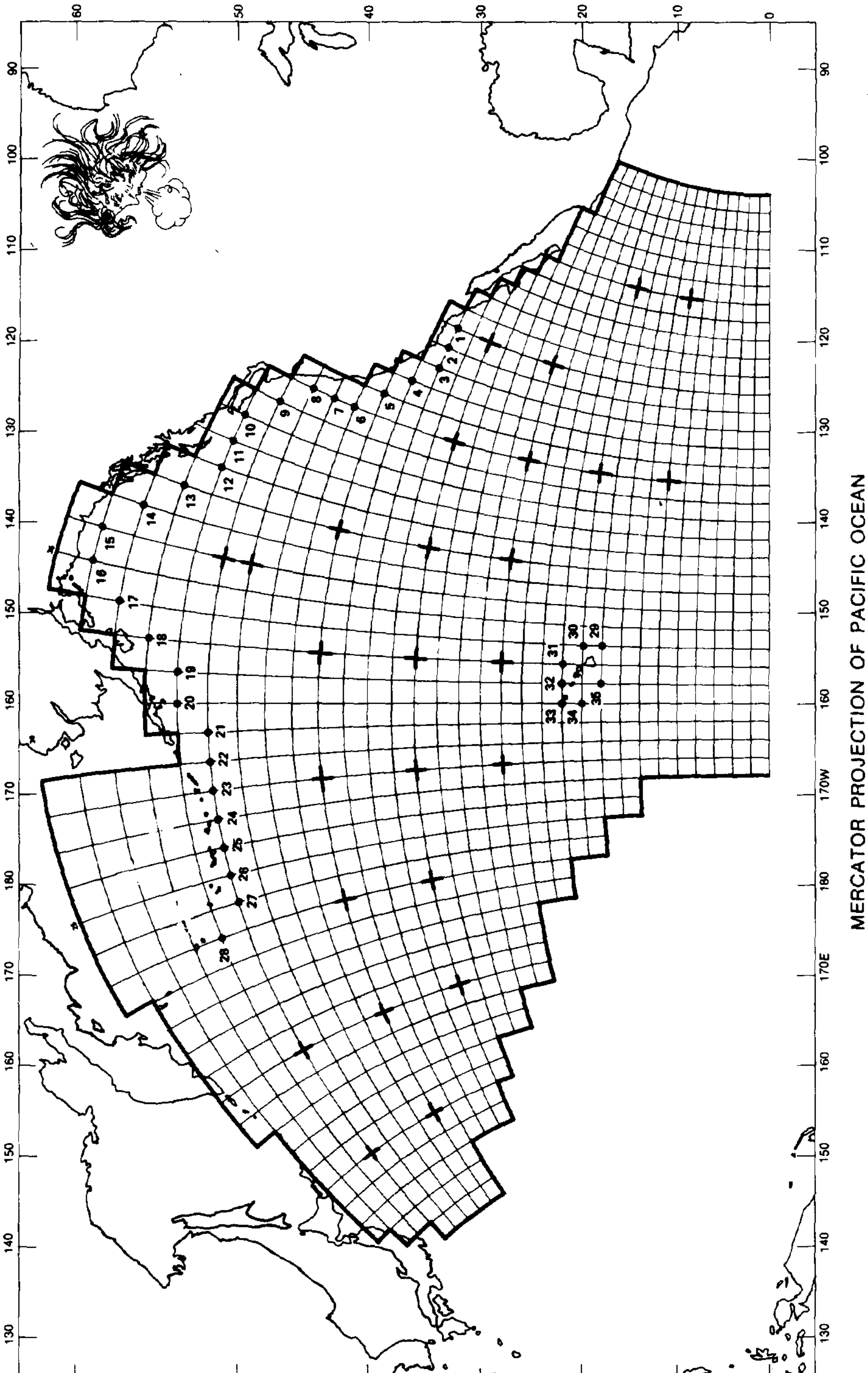

Figure 6-4. WIS Phase I, offshore (+) and coastal (.) locations for Pacific hindcast

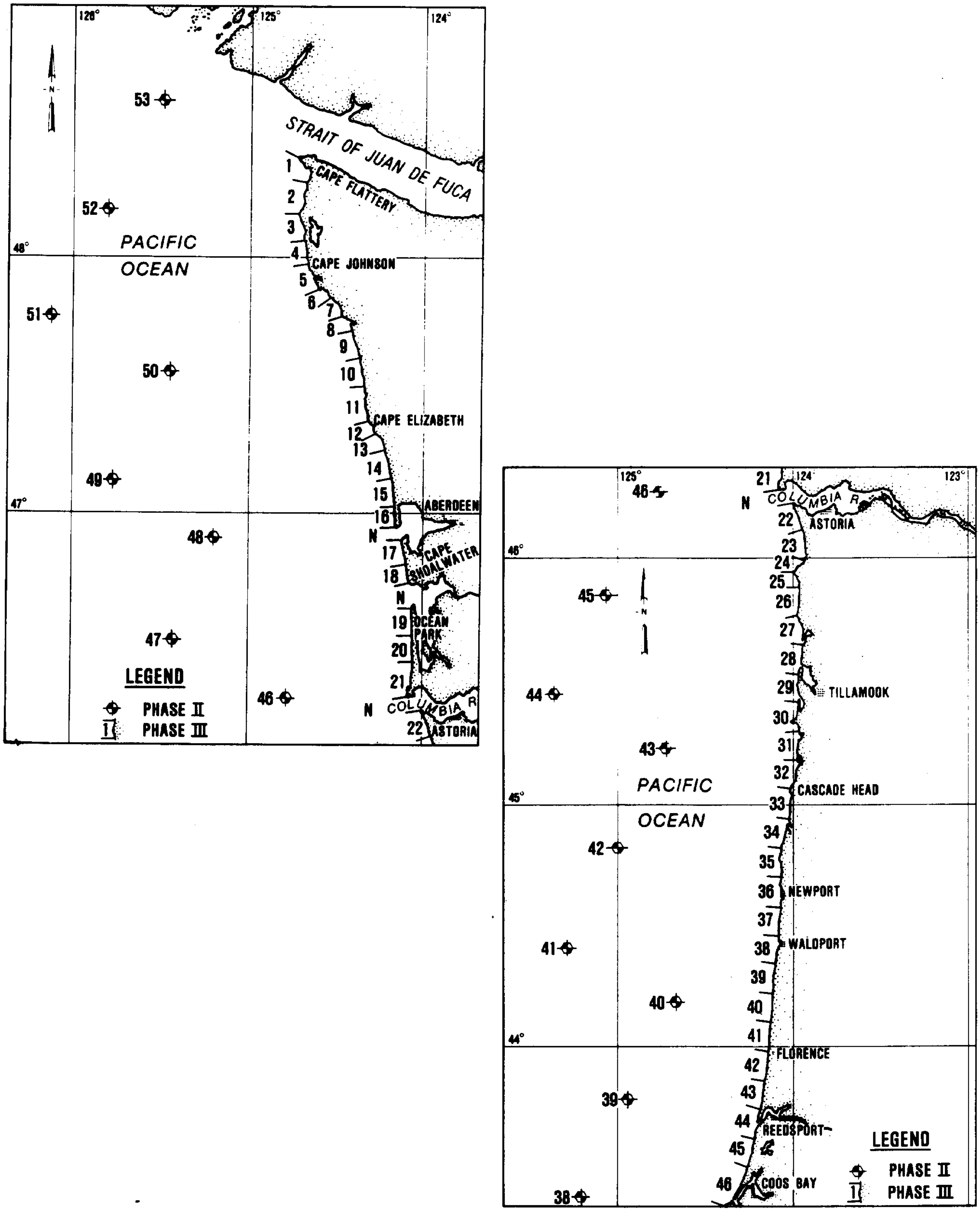

Figure 6-5. WIS Phase II and III locations for US Pacific coast (Sheet 1 of 3)

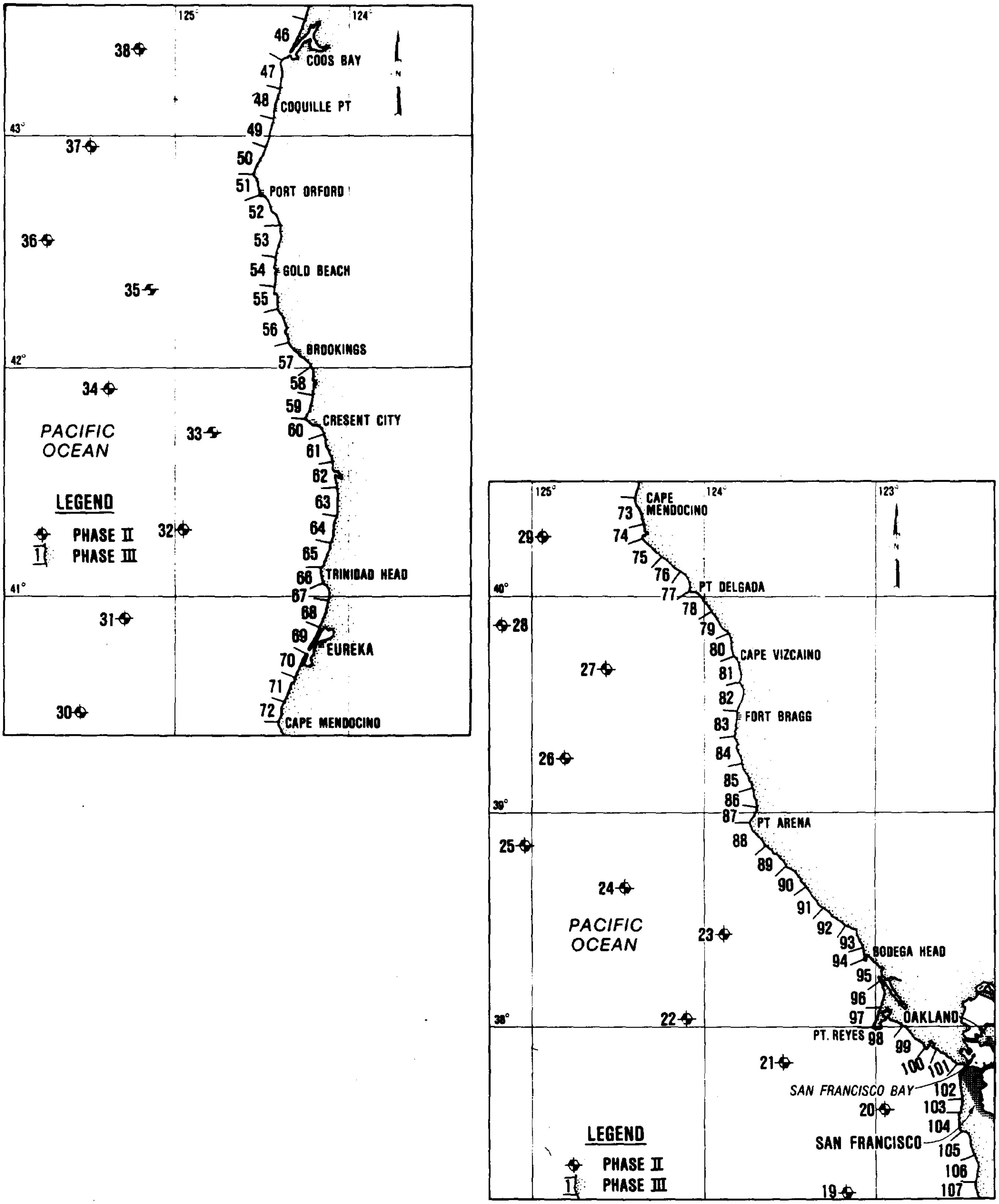

Figure 6-5 (Continued) (Sheet 2 of 3)

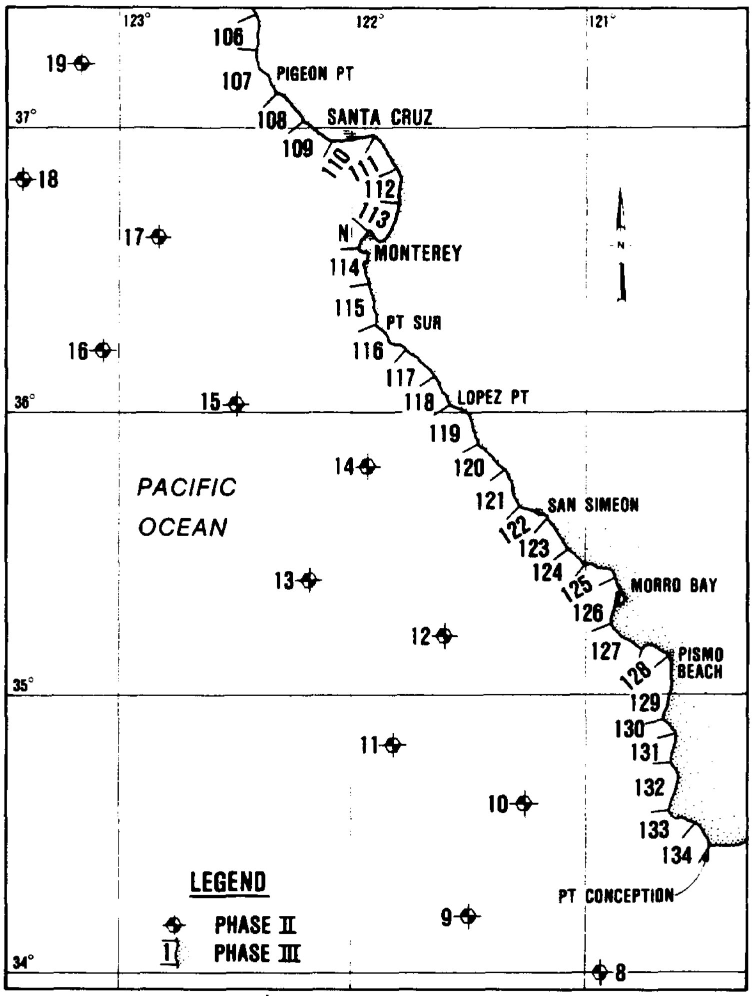

Figure 6-5 (Concluded) (Sheet 3 of 3)

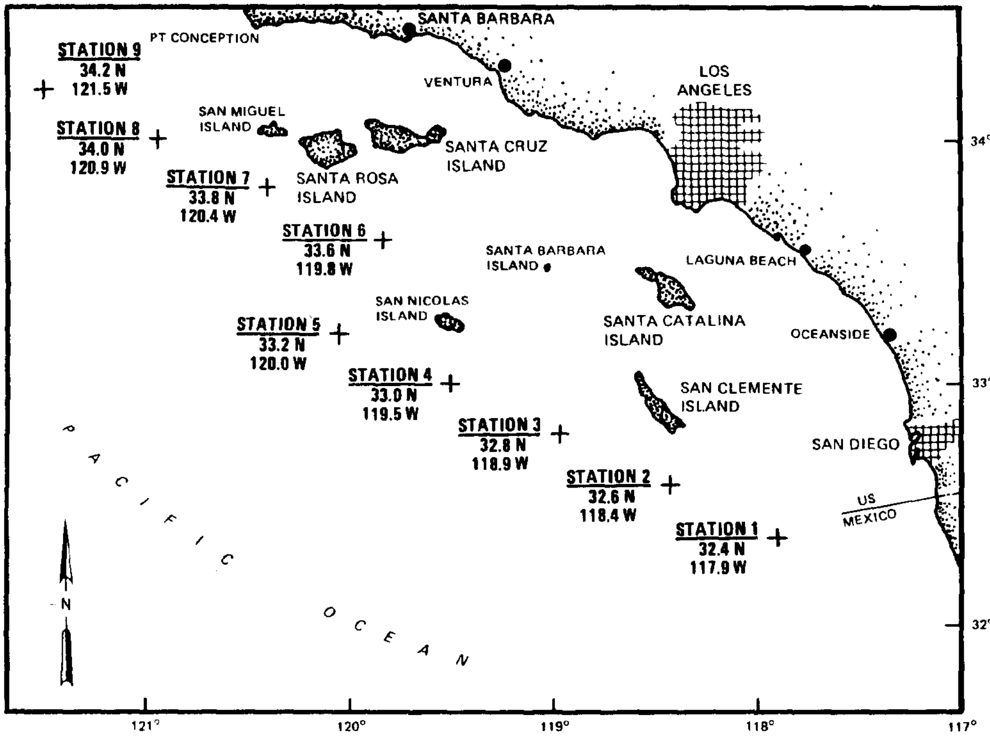

Figure 6-6. WIS, Phase II locations for Southern California Bight

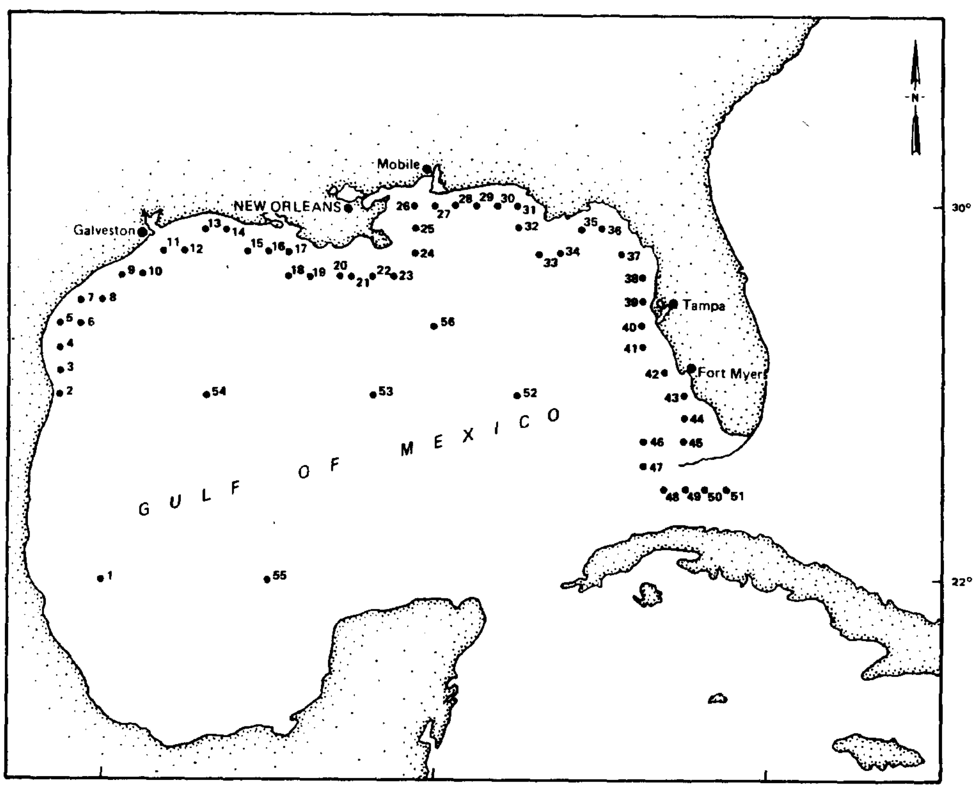

Figure 6-7. WIS locations for Gulf of Mexico

Table 6-1

Summary of WIS Data

Data	Period of Record	Time-Steps GMT	Grid or Stations	Spatial Separation
		Atlantic		
Surface pressure	1956-1975	6-hr	61 x 61	110 km
Phase I wind	1956-1975	3-hr	31 x 31	220 km
Phase II wind	1956-1975	3-hr	41 x 33	55 km
Phase I wave	1956-1975	3-hr	31 x 31	220 km
sea & swell				
parameters	1956-1975	3-hr	13 sites	Variable
2-D spectra	1956-1975	3-hr	96 sites	Variable
Phase II wave	1956-1975	3-hr	41 x 33	55 km
sea & swell				
parameters	1956-1975	3-hr	73 sites	Variable
2-D spectra	1956-1975	3-hr	113 sites	Variable
Phase III wave	1956-1975	3-hr	166 sites	18.5 km
Water level	1927-1981	1-hr	20 sites	Variable
		Pacific		
Surface pressure	1956-1975	6-hr	64 x 123	110 km
Phase I wind	1956-1975	6-hr	32 x 61	220 km
Phase II wind	1956-1975	6-hr	31 x 32	55 km
Phase I wave				
parameters	1956-1975	3-hr	35	Variable
2-D spectra	1956-1975	3-hr	64	Variable
Phase II wave				
parameters	1956-1975	3-hr	53	55 km
2-D spectra	1956-1975	3-hr	53	55 km
Phase III wave				
parameters	1956-1975	3-hr	134	18.5 km
		Gulf of Mexico		
Surface pressure	1956-1975	6-hr	31 x 41	55 km
Wind	1956-1975	6-hr	31 x 41	55 km
Wave				
parameters	1956-1975	3-hr	55	55 km
2-D spectra	1956-1975	6-hr	55	55 km

Table 6-2

Wave Information Studies Reports

Report No.	Bibliographic Information
1.	Corson, W. D., Resio, D. T., and Vincent, C. L. 1980 (July). "Wave Information Study of U. S. Coastlines; Surface Pressure Field Reconstruction for Wave Hindcasting Purposes," TR HL-80-11, Report 1, US Army Engineer, Waterways Experiment Station, Coastal Engineering Research Center, Vicksburg, Mississippi.
2.	Corson, W.D., Resio, D. T., Brooks, R. M., Ebersole, B. A., Jensen, R. E., Ragsdale, D.S., and Tracy, B. A. 1981 (January). "Atlantic Coast Hindcast, Deepwater, Significant Wave Information," WIS Report 2, US Army Engineer, Waterways Experiment Station, Coastal Engineering Research Center, Vicksburg, Mississippi.
3.	Corson, W. D., and Resio, D. T. 1981 (May). "Comparisons of Hindcast and Measured Deepwater, Significant Wave Heights," WIS Report 3, US Army Engineer, Waterways Experiment Station, Coastal Engineering Research Center, Vicksburg, Mississippi.
4.	Resio, D. T., Vincent, C. L., and Corson, W. D. 1982 (May). "Objective Specification of Atlantic Ocean Windfields from Historical Data," WIS Report 4, US Army Engineer, Waterways Experiment Station, Coastal Engineering Research Center, Vicksburg, Mississippi.
5.	Resio, D. T. 1982 (March). "The Estimation of Wind-Wave Generation in a Discrete Spectral Model," WIS Report 5, US Army Engineer, Waterways Experiment Station, Coastal Engineering Research Center, Vicksburg, Mississippi.
6.	Corson, W. D., Resio, D.. T., Brooks, R. M., Ebersole, B. A., Jensen, R. E., Ragsdale, D. S., and Tracy, B. A. 1982 (March). "Atlantic Coast Hindcast Phase II, Significant Wave Information," WIS Report 6, US Army Engineer, Waterways Experiment Station, Coastal Engineering Research Center, Vicksburg, Mississippi.
7.	Ebersole, B. A. 1982 (April). "Atlantic Coast Water-Level Climate," WIS Report 6, US Army Engineer, Waterways Experiment Station, Coastal Engineering Research Center, Vicksburg, Mississippi.
8.	Jensen, R. E. 1983 (September). "Methodology for the Calculation of a Shallow Water Wave Climate," WIS Report 8, US Army Engineer, Waterways Experiment Station, Coastal Engineering Research Center, Vicksburg, Mississippi.

(Continued)

Table 6-2 (Concluded)

9. Jensen, R. E. 1983 (January). "Atlantic Coast Hindcast, Shallow-Water Significant Wave Information," WIS Report 9, US Army Engineer, Waterways Experiment Station, Coastal Engineering Research Center, Vicksburg, Mississippi.

10. Ragsdale, D. S. 1983 (August). "Sea-State Engineering Analysis System: Users Manual," WIS Report 10, US Army Engineer, Waterways Experiment Station, Coastal Engineering Research Center, Vicksburg, Mississippi.

11. Tracy, B. A. 1982 (May). "Theory and Calculation of the Nonlinear Energy Transfer Between Sea Waves in Deep water," WIS Report 11, US Army Engineer, Waterways Experiment Station, Coastal Engineering Research Center, Vicksburg, Mississippi.

12. Resio, D. T., and Tracy, B. A. 1983 (January). "A Numerical Model for Wind-Wave Prediction in Deepwater," WIS Report 12, US Army Engineer, Waterways Experiment Station, Coastal Engineering Research Center, Vicksburg, Mississippi.

13. Brooks, R. M., and Corson, W. D. 1984 (September). "Summary of Archived Atlantic Coast Wave Information Study, Pressure, Wind, Wave, and Water Level Data," WIS Report 13, US Army Engineer, Waterways Experiment Station, Coastal Engineering Research Center, Vicksburg, Mississippi.

14. Corson, W. D., Abel, C. E., Brooks, R. M., Farrar, P. D., Groves, B. J., Jensen, R. E., Payne, J. B., Ragsdale, D. S., Tracy, B. A. 1986 (March). "Pacific Coast Hindcast Deepwater Wave Information," WIS Report 14, US Army Engineer, Waterways Experiment Station, Coastal Engineering Research Center, Vicksburg, Mississippi.

15. Corson, W. D., and Tracy, B. A. 1985 (May). "Atlantic Coast Hindcast, Phase II Wave Information: Additional Extremal Estimates," WIS Report 15, US Army Engineer, Waterways Experiment Station, Vicksburg, Mississippi.

16. Corson, W. D., Abel, C. E., Brooks, R. M., Farrar, P. D., Groves, B. J., Payne, J. B., McAneny, D. S., Tracy, B. A. 1987 (May). "Pacific Coast Hindcast Phase II Wave Information," WIS Report 16, US Army Engineer, Waterways Experiment Station, Vicksburg, Mississippi.

Table 6-3

Wave Information Studies, Design Wave Information for the Great Lakes Reports

Report No.	Bibliographic Information
1.	Resio, D. T., and Vincent, C. L. 1976 (January). "Design Wave Information for the Great Lakes; Report 1: Lake Erie," TR H-76-1, US Army Engineer, Waterways Experiment Station, Coastal Engineering Research Center, Vicksburg, Mississippi.
2.	Resio, D. T., and Vincent, C. L. 1976 (March). "Design Wave Information for the Great Lakes; Report 2: Lake Ontario," TR H-76-1, US Army Engineer, Waterways Experiment Station, Coastal Engineering Research Center, Vicksburg, Mississippi.
3.	Resio, D. T., and Vincent, C. L. 1976 (June). "Estimation of Winds Over Great Lakes," MP H-76-12, US Army Engineer, Waterways Experiment Station, Coastal Engineering Research Center, Vicksburg, Mississippi.
4.	Resio, D. T., and Vincent, C. L. 1976 (November). "Design Wave Information for the Great Lakes; Report 3: Lake Michigan," TR H-76-1, US Army Engineer, Waterways Experiment Station, Coastal Engineering Research Center, Vicksburg, Mississippi.
5.	Resio, D. T., and Vincent, C. L. 1977 (March). "Seasonal Variations in Great Lakes Design Wave Heights: Lake Erie," MP H-76-21, US Army Engineer, Waterways Experiment Station, Coastal Engineering Research Center, Vicksburg, Mississippi.
6.	Resio, D. T., and Vincent, C. L. 1977 (August). "A Numerical Hindcast Model for Wave Spectra on Water Bodies with Irregular Shoreline Geometry," Report 1, MP H-77-9, US Army Engineer, Waterways Experiment Station, Coastal Engineering Research Center, Vicksburg, Mississippi.
7.	Resio, D. T., and Vincent, C. L. 1977 (September). "Design Wave Information for the Great Lakes; Report 4: Lake Huron," TR H-76-1, US Army Engineer, Waterways Experiment Station, Coastal Engineering Research Center, Vicksburg, Mississippi.
8.	Resio, D. T., and Vincent, C. L. 1978 (June). "Design Wave Information for the Great Lakes; Report 5: Lake Superior," TR H-76-1, US Army Engineer, Waterways Experiment Station, Coastal Engineering Research Center, Vicksburg, Mississippi.
9.	Resio, D. T., and Vincent, C. L. 1978 (December). "A Numerical Hindcast Model for Wave Spectra on Water Bodies with Irregular Shoreline Geometry," Report 2, MP H-77-9, US Army Engineer, Waterways Experiment Station, Coastal Engineering Research Center, Vicksburg, Mississippi.

Table 6-4

Listing of NOAA Buoy Locations and Years

Buoy No.	Latitude, °N	Longitude, °W	Years
	Great Lakes		
45001	48.0	87.6	79-84
45002	45.3	86.3	79-84
45003	45.3	82.8	80-84
45004	47.2	86.5	80-84
45005	41.7	82.5	80-84
45006	47.3	90.0	81-84
45007	42.7	87.1	81-84
45008	44.3	82.4	81-84
	Atlantic		
41001	34.9	72.9	72-84
41002	32.3	75.3	74-84
41004	32.6	78.7	78-82
41005	31.7	79.7	79-82
41006	29.3	77.3	82-84
44001	38.7	73.6	75-79
44002	40.1	73.0	75-80
44004	38.5	70.7	77-84
44005	42.7	68.3	78-84
41003	30.3	80.4	NA
	Gulf of Mexico		
42001	25.9	89.7	75-84
42002	26.0	93.5	76-84
42003	26.0	85.9	76-84
42007	30.1	88.9	81-84
42008	28.7	85.3	80-84
42009	29.3	87.5	80-84
42011	29.6	93.5	81-84
	Pacific		
46001	56.3	148.3	72-84
46002	42.5	130.3	75=84
46003	51.9	155.7	76-84
46004	51.0	136.0	76-84
46005	46.1	131.0	76-84
46006	40.7	137.7	77-84
46010	46.2	124.2	79-84
46011	34.9	120.9	80-84
46012	37.4	122.7	80-84
46013	38.2	123.3	81-84
46014	39.2	124.0	81-84
46016	63.3	170.3	81-84
46017	60.3	172.3	81-84
46022	40.8	124.5	82-84
46023	34.3	120.7	82-84
46024	33.8	119.5	82-84
46025	33.6	119.0	82-84
46026	37.8	122.7	82-84
51001	23.4	162.3	81-84

Table 6-5

Access to Coastal Wave and Water Level Data and Programs

Source	Type of Information
OL-A USAF Environmental Technical Applications Center (MAC) Federal Building Asheville, NC 28801 (704) 259-0218 (Non-Department of Defense users should contact the National Climatic Data Center at the above address.) (704) 259-0682	Global, meteorological, and oceanographic data and data products.
National Oceanographic Data Center User Service (Code OC21) 1825 Connecticut Ave., NW Washington, DC 20235 (202) 673-5549	Variety of oceanographic data.
Coastal Engineering Information and Analysis Center USAEWES PO Box 631 Vicksburg, MS 39180 (601) 634-2012	Coastal Engineering Information Management (CEIMS) LEO Retrieval System, gage data from the Corps Coastal Field Data Collection Program and other sources.
Coastal Oceanography Branch USAEWES PO Box 631 Vicksburg, MS 39180 (601) 634-2027	State-of-the-art computer programs for wave growth and transformation, WIS hindcast wave parameters, and two-dimensional spectra.
Corps Computer Program Library USAEWES IM-RS PO Box 631 Vicksburg, MS 39180 (601) 634-2300	Documented computer programs for wave measurement analysis and wave growth and transformation.
Automated Coastal Engineering Group USAEWES PO Box 631 Vicksburg, MS 39180 (601) 634-2017	Wave and tide analysis programs.

(Continued)

Table 6-5 (Concluded)

National Geophysical Data Center NOAA E/GC 3 325 Broadway Boulder, CO 80303 (303) 497-6338	Digital bathymetric data for US coasts, including Alaska, Hawaii, and Puerto Rico.
California Coastal Data Information Program Scripps Institute of Oceanography Mail Code A022 University of California, San Diego LaJolla, CA 92093 (619) 534-3033	US West Coast gage network and gage at CERC's FRF in North Carolina.
Field Coastal Data Network Coastal & Oceanographic Engineering Department 336 Weil Hall University of Florida Gainesville, FL 32611 (904) 392-1051	Coastal Florida wave gage network.
Navy/NOAA Oceanographic Data Distribution system operated by: Science Applications International Corporation 205 Montecito Avenue Monterey, CA 93940 (408) 375-3063	Global forecast wave and weather data.
NOAA National Ocean Service Tidal Datums and Information Section 6001 Executive Blvd. Rockville, MD 20852 (301) 443-8467	Tidal Tables, Tidal Current Tables, and digital data for selected locations.
Alaska Coastal Data Collection Program Plan Formulation Section US Army Engineer District, Alaska Pouch 898 Anchorage, Alaska 99506-0898 (907) 753-2620	Wind and wave data for coastal Alaska.

NOAA's NOS which provides global tide predictions in tables of times and heights of high and low tides (Figure 6-8), tidal current tables for US coasts, tidal current charts for selected harbors, and other summaries of tidal predictions for selected areas. Measured water level data are also available for selected locations from NOS. For details concerning NOS water level products and services, the NOS Tidal Datums and Information Section should be contacted (Table 6-5). NOS water level data were used in WIS Report 7 to develop statistical summaries and extremal estimates of tides, storm surges, and total water level for selected locations along the US Atlantic coast. Harris (SR-7) used results from tide prediction equations to develop extremal estimates of astromical tides for US coasts. Open coast flood levels in the Great Lakes are available from item 128.

6-3. Access to Data and Programs. A listing of publications which contains extensive summaries of meteorological and oceanographic data and related computer programs is provided below. In addition to wave and water level data, the sources listed can include wind speed and direction, air and sea temperature and other information required for wave and water-level studies. Access to coastal wave and water level data and programs is described in Table 6-5. The telephone numbers provided in Table 6-5 are for the points-of-contact for the programs and systems. The points-of-contact for each system will instruct potential users on how to access the programs or systems.

a. Listed below are data products and program summary publications.

(1) Changery, M. J., 1978 (December). "National Wind Data Index: Final Report," National Climatic Data Center, Asheville, NC 28801.

(2) Hatch, W. L. 1983 (July). "Selective Guide to Climatic Data Sources," Key to Meteorological Records Documentation NO. 4.11, National Climatic Data Center, Asheville, NC 28801.

(3) National Oceanic and Atmospheric Administration, 1985 (May). "Index of Tide Stations: United States of America and Miscellaneous Other Stations," National Ocean Service, Tidal Datum Section, Rockville, MD 20852.

(4) National Oceanic and Atmospheric Administration, 1985 (November). "National Ocean Service Products and Services Handbook," NOS, Sea and Lake Levels Branch, Rockville, MD 20852.

(5) US Army Engineer Waterways Experiment Station, 1985 (October). "WES Engineering Computer Programs Library Catalog," Vicksburg, MS 39180.

(6) US Department of Commerce, 1977. "Climatic Atlas of the Outer Continental Shelf Waters and Coastal Regions of Alaska," Research Unit No. 347, National Climatic Data Center, Asheville, NC 28801.

(7) US Department of Commerce, National Climatic Data Center, 1986 (April). "Climatic Summaries for NDBC Data Buoys," National Data Buoy Center, NSTL Station, MS 39529.

(8) US Navy, Naval Oceanography Command, 1983 (October). "US Navy Hindcast, Spectral, Ocean Wave Model Climatic Atlas: North Atlantic Ocean," NAVAIR 50-1C-538, Naval Oceanography Command, NSTL Station, MS 39529.

b. Data collected under the Corps' LEO program can be accessed and manipulated through a database system developed at CERC (Figure 6-9). The LEO Retrieval System is described in item 119.

c. The Sea State Engineering Analysis System (SEAS) enables Corps users to access WIS data and form a variety of summaries (Figure 6-10). SEAS is a user-friendly system which consists of a database of hindcast wave parameters, a retrieval system, and a library of statistical routines to produce desired summaries.

d. An interactive system developed at Scripps Institute of Oceanography (SIO) is available for accessing parameters from the SIO-based network of wave gages. The network includes primarily West Coast gages, many of which are supported by the Corps' Coastal Field Data Collection Program.

e. A system similar to SIO's interactive system is operated by the University of Florida for wave gages along the Florida Coast.

f. Global forecast wave and weather information is available through the Navy/NOAA Oceanographic Data Distribution System (NODDS). The forecast wave data are calculated using the Navy's Global Spectral Ocean Wave Model. NODDS is operated by Science Applications International Corporation under contract to the Jet Propulsion Laboratory (Figure 6-11).

g. CEIMS is a computerized system being developed by CERC. It will provide indexes to a wide variety of coastal data. It will also provide direct access to selected data sets and processing programs.

h. Besides the comprehensive LEO, SEAS, SIO, and CEIMS systems, there is a variety of computer programs for analyzing wave measurements and modeling wave growth, propagation, and transformation in currents and/or shallow water. Documented Corps programs are available through the Corps Computer Program Library. MACE programs related to waves and coastal flooding are listed in Appendix C.

i. An interactive environmental data reference service is described in item 3.

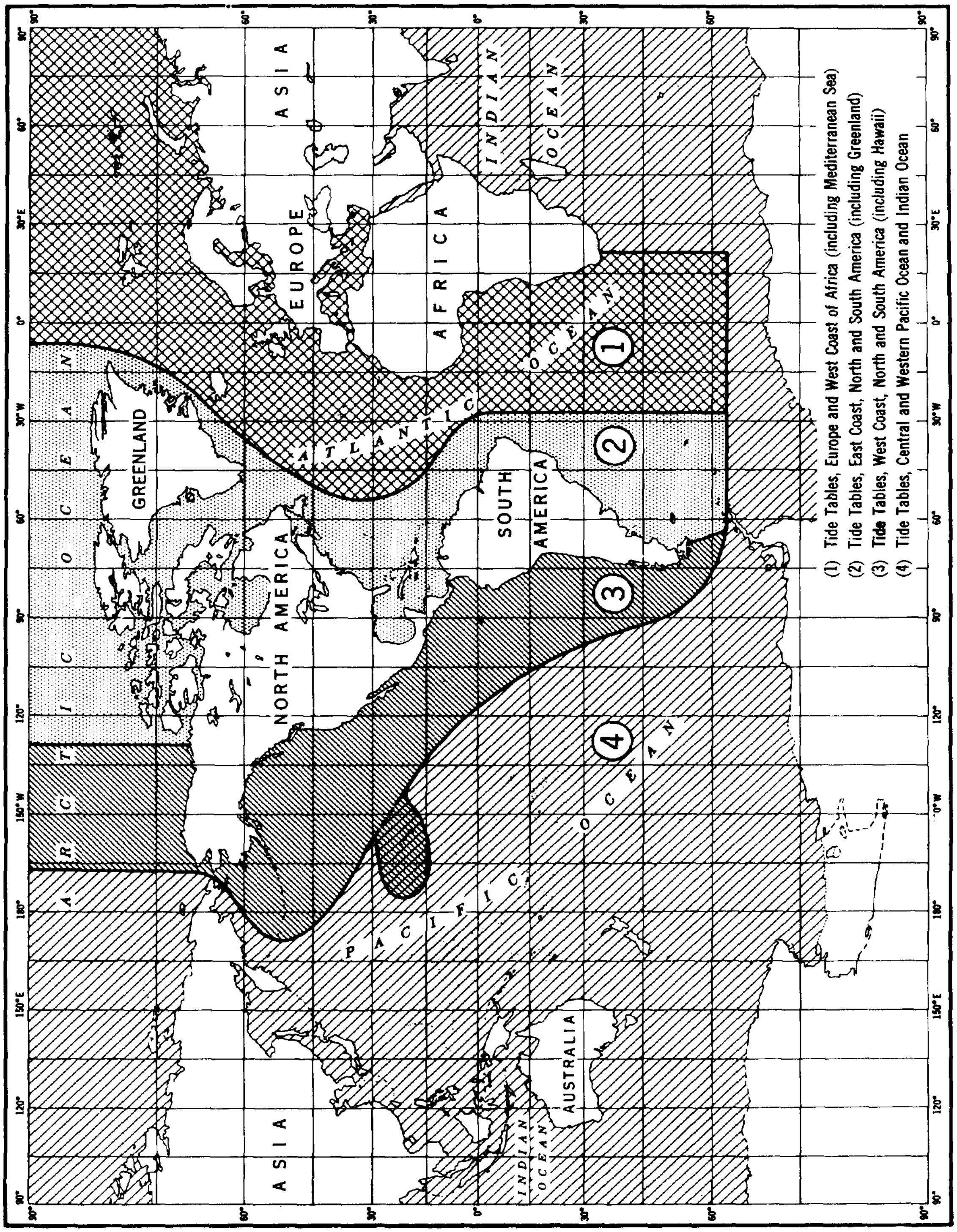

Figure 6-8. NOS index to tide table coverage

LEO PERCENT OCCURRENCE OF WAVE PERIOD VS WAVE HEIGHT

13113-KING AND PRINCE BEACH, GEORGIA DATA COLLECTED 11JAN79 TO 28AUG81

HGT (FT)	0	1	2	3	4	5	6	7	8	9	10	11	12	13	PERCENT
---------	0.9	1.9	2.9	3.9	4.9	5.9	6.9	7.9	8.9	9.9	10.9	11.9	12.9	+	
PER (SEC)															
0-> 1.9	1.	0.	0.	0.	0.	0.	0.	0.	0.	0.	0.	0.	0.	0.	2.
2-> 3.9	5.	6.	2.	1.	0.	1.	0.	0.	0.	0.	0.	0.	0.	0.	15.
4-> 5.9	9.	13.	9.	4.	2.	1.	0.	0.	0.	0.	0.	0.	0.	0.	38.
6-> 7.9	5.	6.	8.	4.	2.	1.	0.	0.	0.	0.	0.	0.	0.	0.	26.
8-> 9.9	1.	2.	3.	3.	1.	0.	0.	0.	0.	0.	0.	0.	0.	0.	10.
10->11.9	0.	1.	2.	1.	0.	0.	0.	0.	0.	0.	0.	0.	0.	0.	6.
12->13.9	0.	0.	1.	0.	0.	0.	0.	0.	0.	0.	0.	0.	0.	0.	2.
14->15.9	0.	0.	0.	0.	0.	0.	0.	0.	0.	0.	0.	0.	0.	0.	0.
16->17.9	0.	0.	0.	0.	0.	0.	0.	0.	0.	0.	0.	0.	0.	0.	0.
18->19.9	0.	0.	0.	0.	0.	0.	0.	0.	0.	0.	0.	0.	0.	0.	0.
20->21.9	0.	0.	0.	0.	0.	0.	0.	0.	0.	0.	0.	0.	0.	0.	0.
22 +	0.	0.	0.	0.	0.	0.	0.	0.	0.	0.	0.	0.	0.	0.	0.
PERCENT	22.	29.	25.	14.	6.	4.	0.	0.	0.	0.	0.	0.	0.	0.	

CALM = 17. PERCENT (95 OBSERVATIONS) TOTAL OBSERVATIONS = 573

Figure 6-9. Example of output from LEO Retrieval System

DATE: 09/26/86 PAGE: 1

SEAS SYSTEM REPORT NO. 101
STATION HINDCAST DATA

STATION: P2010		--- SEA READINGS ---			-- SWELL READINGS --			----- COMBINED -----		
DATE		HEIGHT	PERIOD	DIRECT	HEIGHT	PERIOD	DIRECT	HEIGHT	PERIOD	DIRECT
YY/MM/DD	HOUR	(CM)	(SECS)	(DEG)	(CM)	(SECS)	(DEG)	(CM)	(SECS)	(DEG)
75/10/10	00:00	150.	8.	290.	126.	11.	306.	196.	8.	290.
75/10/10	03:00	147.	8.	287.	129.	11.	304.	196.	8.	287.
75/10/10	06:00	147.	8.	284.	135.	11.	302.	200.	8.	284.
75/10/10	09:00	145.	8.	280.	143.	11.	301.	204.	8.	280.
75/10/10	12:00	146.	8.	278.	153.	11.	299.	211.	11.	299.
75/10/10	15:00	208.	11.	288.	76.	13.	297.	221.	11.	288.
75/10/10	18:00	228.	13.	289.	40.	14.	298.	231.	13.	289.
75/10/10	21:00	224.	11.	288.	88.	13.	296.	241.	11.	288.
75/10/11	00:00	246.	13.	289.	43.	14.	297.	250.	13.	289.
75/10/11	03:00	255.	13.	290.	44.	14.	297.	259.	13.	290.
75/10/11	06:00	263.	13.	290.	44.	14.	297.	267.	13.	290.
75/10/11	09:00	267.	13.	290.	46.	14.	296.	271.	13.	290.
75/10/11	12:00	269.	13.	291.	45.	14.	296.	273.	13.	291.
75/10/11	15:00	272.	13.	291.	45.	14.	296.	276.	13.	291.
75/10/11	18:00	273.	13.	291.	44.	14.	295.	277.	13.	291.
75/10/11	21:00	258.	11.	292.	106.	13.	295.	279.	11.	292.
75/10/12	00:00	262.	11.	292.	104.	13.	295.	282.	11.	292.
75/10/12	03:00	261.	11.	292.	101.	13.	295.	280.	11.	292.
75/10/12	06:00	261.	11.	293.	100.	13.	295.	280.	11.	293.
75/10/12	09:00	260.	11.	293.	99.	13.	295.	278.	11.	293.
75/10/12	12:00	259.	11.	293.	100.	13.	295.	278.	11.	293.
75/10/12	15:00	260.	11.	293.	100.	13.	295.	279.	11.	293.
75/10/12	18:00	261.	11.	293.	102.	13.	295.	280.	11.	293.
75/10/12	21:00	263.	11.	293.	103.	14.	295.	282.	11.	293.
75/10/13	00:00	268.	11.	294.	105.	14.	295.	288.	11.	294.
75/10/13	03:00	262.	11.	294.	107.	14.	295.	283.	11.	294.
75/10/13	06:00	253.	11.	294.	110.	14.	295.	276.	11.	294.
75/10/13	09:00	248.	11.	294.	112.	14.	295.	272.	11.	294.
75/10/13	12:00	200.	9.	295.	182.	13.	295.	270.	9.	295.
75/10/13	15:00	180.	8.	295.	198.	13.	295.	268.	13.	295.
75/10/13	18:00	180.	8.	295.	197.	13.	295.	267.	13.	295.
75/10/13	21:00	182.	8.	295.	196.	13.	295.	267.	13.	295.
75/10/14	00:00	166.	8.	296.	206.	13.	295.	265.	13.	295.
75/10/14	03:00	160.	8.	296.	204.	13.	295.	259.	13.	295.
75/10/14	06:00	158.	8.	295.	202.	13.	295.	256.	13.	295.
75/10/14	09:00	65.	5.	306.	246.	13.	295.	254.	13.	295.
75/10/14	12:00	65.	5.	306.	243.	13.	295.	252.	13.	295.
75/10/14	15:00	65.	5.	306.	241.	13.	295.	250.	13.	295.
75/10/14	18:00	65.	5.	306.	240.	13.	295.	249.	13.	295.
75/10/14	21:00	65.	5.	306.	238.	13.	295.	247.	13.	295.
75/10/15	00:00	65.	5.	305.	237.	13.	295.	246.	13.	295.
75/10/15	03:00	57.	5.	305.	236.	13.	295.	243.	13.	295.
75/10/15	06:00	41.	5.	319.	237.	13.	295.	241.	13.	295.
75/10/15	09:00	41.	5.	318.	235.	13.	295.	239.	13.	295.
75/10/15	12:00	41.	5.	318.	234.	11.	295.	238.	11.	295.
75/10/15	15:00	41.	5.	318.	233.	11.	295.	237.	11.	295.
75/10/15	18:00	41.	5.	318.	231.	11.	295.	235.	11.	295.
75/10/15	21:00	41.	5.	318.	229.	11.	295.	233.	11.	295.

Figure 6-10. Example of listing from WIS SEAS for a portion of the 20-year hindcast

```
87060300   LAT  35.0N LON    72.5W  00Z  3 JUN 87 TAU  0
GSOWM          DIR(FROM),    -LOCAL WIND 250.0DEG 11.0KTS  WHITE CAP  0
PERIOD(TOTAL)     45  135  165  195  225  255  285  315
 12.4      1       1    0    0    0    0    0    0    0
  9.7      3       0    2    1    0    0    0    0    0
  8.6      3       0    2    1    0    0    0    0    0
  7.5      1       0    0    1    0    0    0    0    0
  6.3     10       0    0    0    0    3    5    3    0
  4.8     48       0    0    0    3   14   19   12    1
  3.2     22       0    0    1    2    5    8    5    2
 DIR(TOTAL)        1    4    4    5   22   32   20    3
     SIG HT   3.8FT   AVG HT   2.70FT      THRESHOLD=    .01
```

Figure 6-11. Example of NODDS forecast, including directional wave energy spectrum

CHAPTER 7

SELECTION OF DESIGN WATER LEVELS AND DESIGN WAVES

7-1. Selection of Design Criteria. The selection of design water levels and design waves requires consideration of the critical conditions as discussed in 1-6.a. Probabilities of exceedance for the critical conditions are estimated by applying the information in this manual, as illustrated in Figure 1-1.

a. Exceedance probabilities can be formulated in several different ways. For functional design criteria they are generally formulated in terms of either the probability of exceeding the critical threshold in any given year or the number of days (or hours) per year the threshold will be exceeded. Probabilities for structural design criteria are generally formulated in the same terms. Another useful formulation is in terms of probability of exceeding the critical threshold in an n-year period, where n is an integer value.

b. The basic steps for analyzing and, if desired, fitting of extreme value wave data to a distribution function are described in Chapter 5. The usual procedure is to estimate a distribution function for extreme values and use it to extrapolate to return periods longer than the original record length. This procedure should be done with care. Measured data sets that include wave conditions from 1 to 5 years usually do not include enough storm events to perform a reliable prediction of long-term wave conditions. The general rule-of-thumb is that it is not good to extrapolate to more than three times the extent of the data set. Thus, for a 5-year data set, the longest return period condition that could be reliably predicted would be the 15-year condition. It is evident that reliable prediction of the 50-year wave condition often used for structural design purposes would require at least 17 years of data. Wave data records covering 17 or more years are usually only available as hindcast data derived from synoptic weather records. For this reason, hindcast data are most widely used for making long-term predictions. In particular, the WIS hindcast results which presently cover a 20-year period should be used for Corps projects where applicable (Chapters 5 and 6).

c. A more careful estimate of the required length of data record in order to reliably estimate extreme wave statistics is provided in item 138. The analysis includes only the effect of sample variability due to small sample size and assumes a Weibull distribution for significant wave heights. No consideration is given to gaps in the data, shallow depth-induced limitations on wave energy, measurement inaccuracies, etc. The Weibull distribution is expressed as

$$P\left(H_s < H\right) = - \exp\left[-\left(\frac{H-H_o}{\bar{H}}\right)^{\gamma}\right] \qquad (7\text{-}1)$$

where $\bar{H}$ and γ are scale and shape parameters, and H_o is a background wave height level. The average percentage deviation from the predicted extreme value is shown as a function of record length and desired return period in Figure 7-1 for a value of γ equal to 1.00. For higher values of γ, shorter records are required. Similar information is provided in Table 7-1, which also indicates the influence of the time interval between observations and the value of γ.

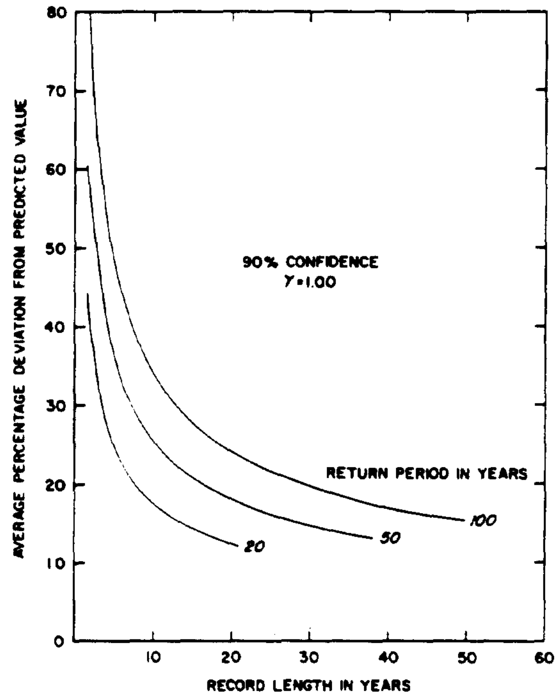

Figure 7-1. Accuracy of prediction of record length (Δt = 6 hr), γ = 1.00

d. Another good source of information on procedures for fitting data to extreme value distribution functions and estimating confidence intervals is given in item 135.

Table 7-1

Data Duration Required as Function of Return Period*

Return period, in years (1)	Δt, in hours (2)	Required Record Length, in Years γ = 1.0 (3)	γ = 1.2 (4)	γ = 1.4 (5)
20	3	7	5	3
20	6	8	6	4
20	12	9	6	5
20	24	10	7	5
50	3	14	10	8
50	6	16	11	8
50	12	18	13	9
50	24	21	15	11
100	3	25	18	13
100	6	28	20	15
100	12	33	23	17
100	24	37	26	19

*Confidence level = 90%; uncertainty = 20%.

7-2. Example Problems. Five example problems to illustrate procedures for estimating design waves and water levels are presented.

******************************EXAMPLE PROBLEM 7-1******************************

GIVEN: An offshore entrance channel is to be surveyed. Water level measurements are available at a gage in an estuary landward of the open coast.

FIND: Water level on the open coast during surveys for calculation of dredged material quantities.

SOLUTION: This problem requires more information for solution. It is presented here to emphasize an important practical concern of which engineers should be aware and to suggest some solutions. In general, the magnitude of the tide on the open coast is not well represented by gages located in an estuary. The water levels in the estuary and several miles offshore may differ by several feet, which would cause serious errors in calculated dredged material quantities. Figure 7-2 illustrates the tide offshore and in the estuary at Beaufort Inlet, North Carolina. The maximum difference in water level between the gages is greater than 2.5 feet in this example. Overdredging will occur when the estuary water level is higher, and under-dredging will occur when the offshore water level is higher.

The best solution to this problem is to install a permanent tide gage offshore to use as a reference for offshore surveys. Alternatively a temporary offshore gage could provide valuable information. A temporary gage would indicate the magnitude of the differences in water level between the estuary and the offshore channel. It could be used to establish a datum. Also, a temporary gage would show when in the tidal cycle the difference in water level is the least. Figure 7-2 shows that the difference in water level is a minimum during the falling tide for Beaufort Inlet. This information is site specific and cannot be transferred directly to other locations. NOS has operated short-term gages at many sites. NOS records should be reviewed before installing a temporary gage.

******************************EXAMPLE PROBLEM 7-2******************************

GIVEN: The reservoir shown in Figure 7-3. A rubble-mound seawall is to be built at Station A. No local wind or wave records are available. Average water depth along the fetch is 65 feet. Water depth at the structure is 75 feet.

FIND: The wind setup and design wave associated with a 25-year recurrence interval.

SOLUTION: This problem can be solved with several alternative tools. Manual methods presented in this EM are used for the following solutions. MACE programs (Appendix C) could be used for microcomputer solution of the problem. A program for use on mainframe computers is available through the Corps Computer Program Library (see Table 6-5) as "Wave Runup and Wind Setup-Computational Model-H7780," Program No. 723-F3-M007A.

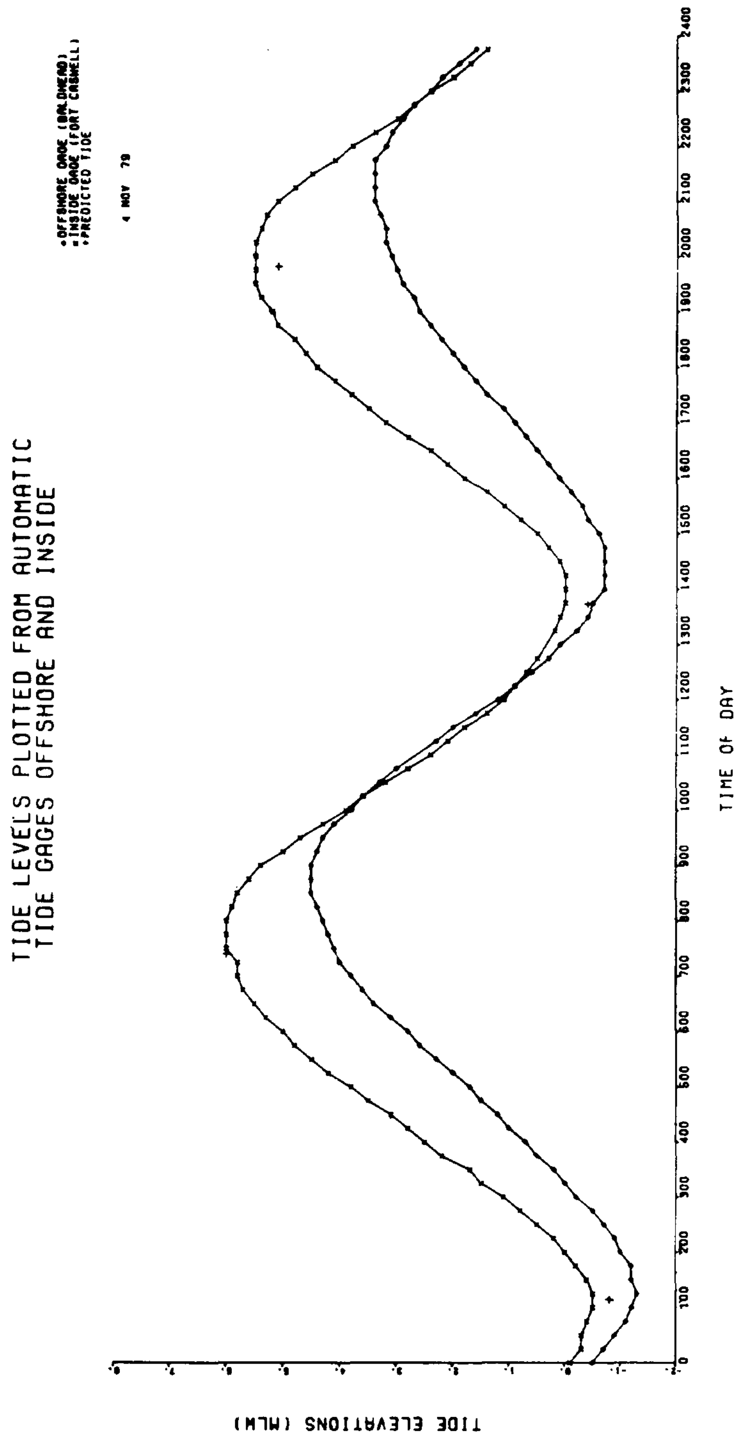

Figure 7-2. Tide levels offshore and in the estuary at Beaufort Inlet, NC

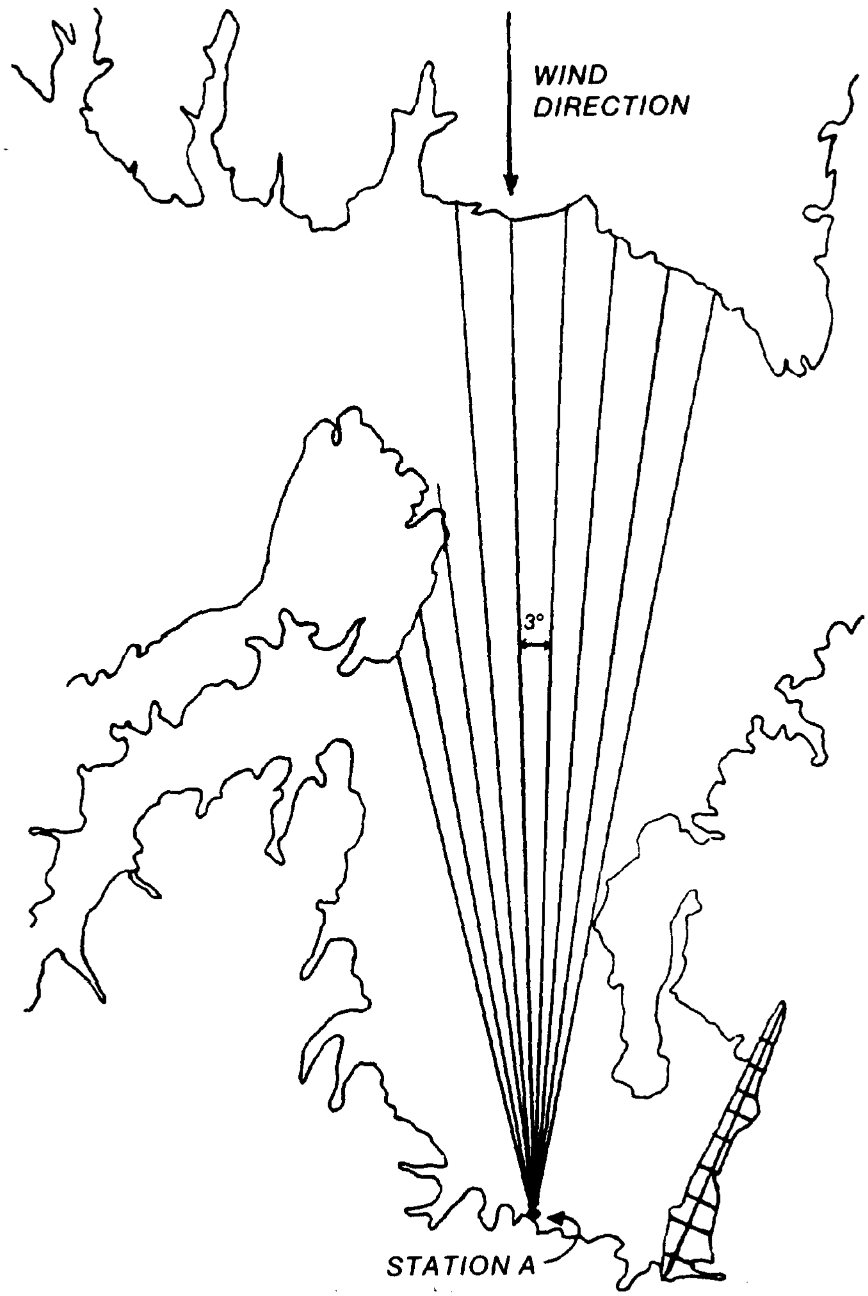

Figure 7-3. Reservoir for example problem 7-2
(scale, 1 inch = 7,500 feet)

FETCH: The fetch is defined as the radial average over an arc of 24 degrees centered on the wind direction. In Figure 7-3, the 24-degree arc is divided into 3-degree intervals with lengths 3.00, 3.30, 3.55, 5.40, 5.30, 5.35, 5.20, 5.05, and 4.95 inches. This gives an average fetch length of

$$\frac{41.10 \text{ in.}}{9} \; \frac{7{,}500 \text{ ft}}{1 \text{ in.}} \; \frac{1 \text{ mi}}{5{,}280 \text{ ft}} = 6.5 \text{ mi}$$

WIND SPEED: Wind speed at reservoir sites is best estimated from local measurements, although even these usually need to be carefully interpreted because of localized influences of surrounding topography. In this example, there are no local data or data from the surrounding area which might be suitable. Therefore, a very approximate and generally conservative procedure is used. The fastest-mile wind speed 30 feet above the ground for the 25-year recurrence interval is determined from Figure 5-18. For this example, 70 miles per hour is used.

WIND SPEED ADJUSTMENTS: The adjustment to the 33-foot level, from equation (5-12), is

$$R_{33} = \left(\frac{33}{30}\right)^{1/7} = 1.01$$

From Figure 5-25, the duration of the fastest-mile wind speed U_f is 51 seconds. The factor to convert the 51-second duration wind speed to the 1-hour duration is 1.0/1.26 = 0.8 from Figure 5-26. Therefore, the 1-hour duration wind speed is 56 miles per hour (70 miles per hour × 0.8). The factors to convert the 1-hour duration to 1.5 and 2 hours are 0.98 and 0.96, also from Figure 5-26. The 1.5- and 2-hour duration wind speeds are 55 and 54 miles per hour, respectively.

The adjustment of the wind speed from overland to overwater R is 1.2 because the fetch is less than 10 miles.

The air-sea temperature difference is not known, so an unstable condition, $R_T = 1.1$, is assumed.

CORRECTED WIND SPEEDS:

$$\begin{aligned} U_{fc} &= R_{33} \times R \times R_T \times U_f \\ &= 1.01\ (1.2)(1.1)(70) \\ &= (1.33)(70\ \text{mph}) \\ &= 93\ \text{mph} \end{aligned}$$

$$\begin{aligned} U_{1\ hr} &= (1.33)(56\ \text{mph}) \\ &= 74\ \text{mph} \end{aligned}$$

$$\begin{aligned} U_{1.5\ hr} &= (1.33)(55\ \text{mph}) \\ &= 73\ \text{mph} \end{aligned}$$

$$\begin{aligned} U_{2\ hr} &= (1.33)(54\ \text{mph}) \\ &= 72\ \text{mph} \end{aligned}$$

DESIGN WAVE: The wave heights and periods associated with the fetch, wind duration, and adjusted wind speed are determined from Figure 5-34 for deepwater wave growth.

Adjusted Wind Speed mph	Wind Duration hr	Wave Height ft	Wave Period s	Remarks
74	1	8.0	4.7	Duration limited
73	1.5	8.9	5.1	Fetch limited
72	2	8.7	5.0	Fetch limited

The design wave is taken as the maximum condition from the above calculations. The deepwater design wave height is 8.9 feet, and the period is 5.1 seconds. The wave length is calculated to verify the assumption of deepwater wave growth.

$$
\begin{aligned}
L_o &= 5.12(T)^2 \\
&= 5.12\,(5.1)^2 \\
&= 133 \text{ feet}
\end{aligned}
$$

The water depth d of 65 feet is only slightly less than half the wave length, 133/2 = 66 feet. Therefore, the assumption of deepwater wave growth is reasonable.

The design wave characteristics are

$$
\begin{aligned}
H_s &= 8.9 \text{ feet} \\
T &= 5.1 \text{ seconds} \\
L_o &= 133 \text{ feet}
\end{aligned}
$$

WIND SETUP. The wind setup S for the design wave is calculated from equation (3-1) as follows:

$$S = \frac{U^2F}{1400\ d}$$

$$S = \frac{(73)^2(6.5)}{1400(65)}$$

$$S = 0.4$$

The wind setup at Station A for the design wave is 0.4 feet.

Since the water depth at Station A is relatively great (75 feet), bottom-induced wave breaking will not occur; and the effect of wave setup can be ignored.

****

******************************EXAMPLE PROBLEM 7-3******************************

GIVEN: A coastal breakwater is to be rehabilitated. Deepwater percent occurrence wave statistics for the station nearest the breakwater are available from WIS Phase II in the SEAS data base. Charts of local bathymetry are available. The water depth is -26 feet MLLW at the toe of the breakwater, and the nearshore bottom slope is 1:35. The extreme range of water levels expected at the breakwater during its design life is -1 foot to +9 feet MLLW.

FIND: Design wave height.

SOLUTION: DEEPWATER WAVES. The deepwater wave climate offshore of the breakwater is defined by the SEAS deepwater percent occurrence wave statistics. Table 7-2 is an example of the statistics for deepwater waves approaching from a direction band of 22.5 degrees centered on 225 degrees azimuth.

REFRACTION AND SHOALING: The wave climate at the toe of the breakwater is determined by applying a numerical wave transformation model. Table 7-2 indicates the higher wave conditions are a mix of sea and swell. Therefore, a spectral wave transformation model would appear to be most accurate. However, overriding requirements for speed and simplicity in designing the breakwater rehabilitation lead to the choice of the monochromatic wave model RCPWAVE in this case.

A bathymetric grid is created as an input to RCPWAVE (Figure 7-4). The grid extends from the breakwater to a water depth sufficient to allow deepwater input at the seaward boundary. The grid cell in the immediate vicinity of the breakwater section to be repaired is identified, and the wave model output at this cell is used to describe the wave climate at the toe of the structure.

RCPWAVE, a linear model, is run with a unity (1 foot) input wave height to give the combined refraction/diffraction/shoaling coefficients for various input wave periods and directions. All mid-band wave periods (from the 8-period bands in Table 7-2) for all deepwater directions which are physically able to propagate toward the breakwater are evaluated. The two extreme SWL's, -1 foot and +9 feet MLLW, are used to assess the role of water level. Thus RCPWAVE is run a total of 112 times, calculated as follows:

$$(8 \text{ wave periods}) \times (7 \text{ wave directions}) \times (2 \text{ water levels}) = 112 \text{ runs}$$

The nearshore transformation coefficients from RCPWAVE, which include the effects of refraction, diffraction by submerged bottom features, and shoaling, are then applied to the deepwater wave heights. For example, the coefficient for a wave period of 8.8 seconds and direction of 225 degrees is multiplied by deepwater wave heights of 8.2, 11.5, 14.8, 18.0, 21.3, and 24.6 feet to give corresponding shallow-water wave heights at the rehabilitation site. Notably, the mid point of each wave height range is used and height/period combinations with zero percent occurrence are omitted. Nearshore wave transformation typically changes the wave height and direction.

The final step in estimating nearshore wave transformation is to transfer the percent occurrence values from deep to shallow water. In this process, it is assumed that the percent occurrence of waves in each wave height band is

Table 7-2

SEAS Percent Frequency-of-Occurrence (x 1000)*

Height m	Height ft	Peak Period, sec							
		4.4-6.0	6.1-8.0	8.1-9.5	9.6-10.5	10.6-11.7	11.8-13.3	13.4-15.3	15.4-18.1
0.0-1.0	0.0- 3.3								
1.0-2.0	3.3- 6.6	1	1						
2.0-3.0	6.6- 9.8	23	75	42	6	13	8		
3.0-4.0	9.8-13.1		193	107	107	54	107	5	
4.0-5.0	13.1-16.4		94	287	78	142	121	30	
5.0-6.0	16.4-19.7		3	237	203	80	128	37	
6.0-7.0	19.7-23.0			54	242	219	94	66	1
7.0-8.0	23.0-26.2			1	65	229	106	53	5
8.0-9.0	26.2-29.5				5	78	85	30	5
9.0-10.0	29.5-32.8					5	46	10	
10.0 +	32.8 +						22	10	
Total		24	366	728	706	820	717	241	11

*Azimuth degrees = 225.0.

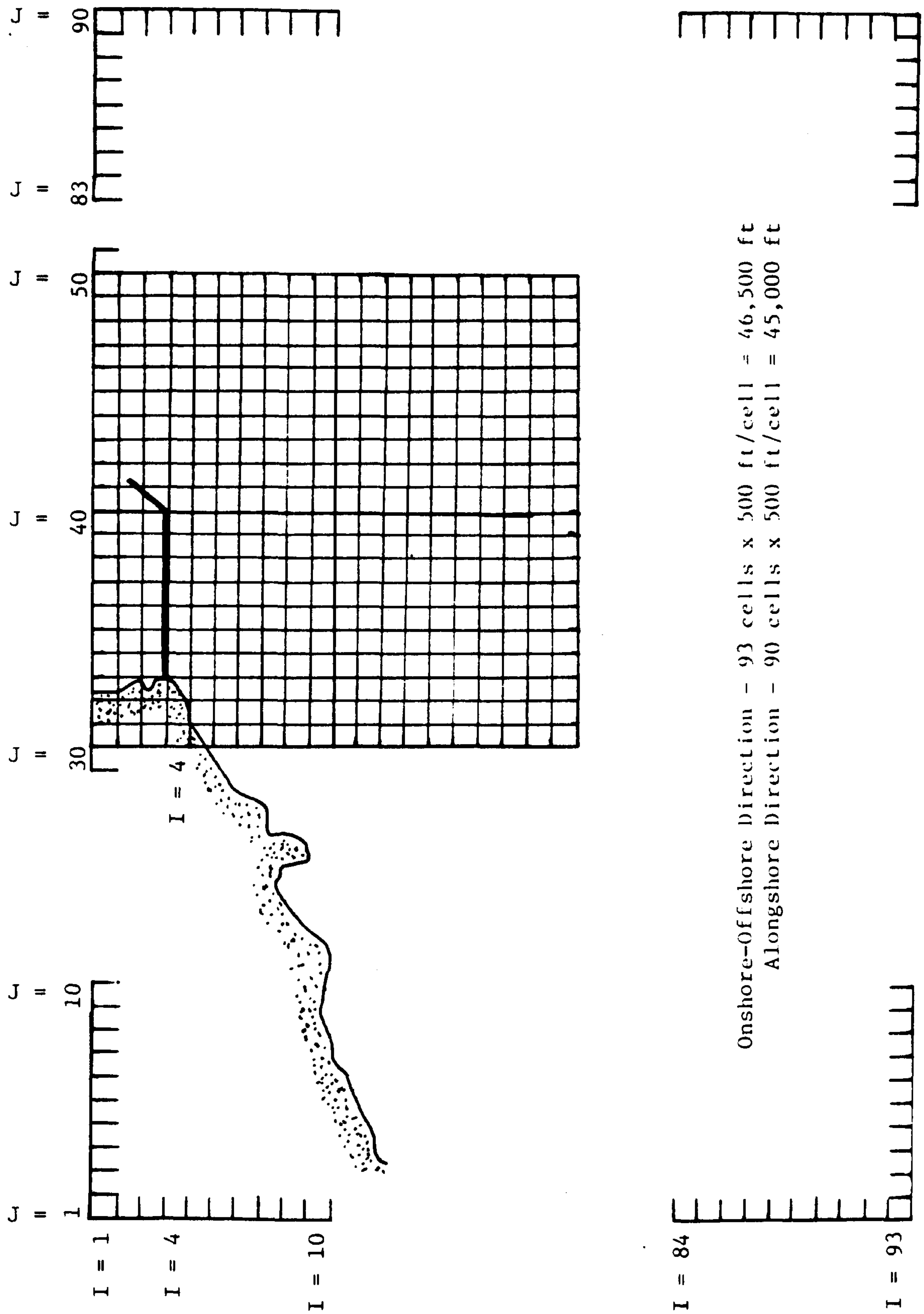

Figure 7-4. Computational grid layout for RCPWAVE application

uniformly distributed over the band. A proportional amount of the percent occurrence in each deepwater wave height band is transferred to the appropriate shallow-water wave height bands. Similar treatment is given to direction bands. Table 7-3 is one of the shallow-water tables derived by this procedure.

WAVE BREAKING: It is important to investigate the possibility of depth-limited wave breaking at the structure. The maximum wave height that can occur at the toe of the breakwater is estimated by Figure 7-4 (SPM) for the range of wave periods. Figure 7-5 shows the depth-limited wave height at the toe of the breakwater for the two extreme water levels and the range of wave periods. These maximum wave heights are incorporated into Table 7-3.

The SPM approach used here is based on monochromatic, or swell, wave conditions. The depth-limited breaking wave height for locally generated sea waves can be expected to be lower. Field data from a number of exposed ocean sites indicate the depth-limited wave height for seas is between 0.5 and 0.6 times the depth.

DESIGN WAVE HEIGHT: Based on Table 7-3 and Figure 7-5, the most severe wave height at the site during the 20-year WIS interval was a breaking wave condition with 34.9-foot height, 14.4-second period, and 225-degree direction. It is assumed that this event coincided with a time of maximum water level. This assumption is usually conservative and in some areas highly conservative. It should be reevaluated in every investigation.

The 14.4-second period represents the midpoint of a band. A more definitive wave period value can be obtained by examining wave periods from the individual high wave events. Another alternative is to assume the worst case (i.e. the longest wave period in the interval). This approach was used for the example. A wave period of 15.3 seconds leads to a breaking wave height of 35.3 feet. Therefore, the design wave height is 35.3 feet with 15.3-second period, 225-degree direction, and +9 foot MLLW water level.

Table 7-3 gives percent occurrence from the 20-year WIS data base. There is a small probability that events more severe than any during the 20 years can occur. The information in tables such as Table 7-3 could be used along with extremal methods discussed in Chapter 5 to estimate more rare events if required by a project.

*****************************EXAMPLE PROBLEM 7-4*****************************

<u>GIVEN</u>: A beach fill is to be designed for a site along the mid-Atlantic coast. A storm water level frequency curve is available from a previous study. Deepwater wave information is available from WIS.

<u>FIND</u>: Design water level.

<u>APPROACH</u>:

a. Problem overview.
b. Determine 100-year tide and storm surge.
c. Determine wave height at breaking and wave runup.

Table 7-3

Wave Percent Occurrence (x 1,000) at Breakwater Repair Section*

Height m	Height ft	Period Band, sec 4.4-6.0	6.1-8.0	8.1-9.5	9.6-10.5	10.6-11.7	11.8-13.3	13.4-15.3	15.4-18.1
0.0-1.0	0.0-3.3								
1.0-2.0	3.3-6.6	5	22	13	1				
2.0-3.0	6.6-9.8	19	134	90	13	20	5	4	
3.0-4.0	9.8-13.1		165	261	121	69	61	7	
4.0-5.0	13.1-16.4		44	465	128	169	115	15	
5.0-6.0	16.4-19.7		1	254	317	184	148	34	1
6.0-7.0	19.7-23.0			34	317	264	160	46	3
7.0-8.0	23.0-26.2				85	348	97	59	4
8.0-9.0	26.2-29.5				11	202	107	56	3
9.0-10.0	29.5-32.8					43	130	31	
10.0 +	32.8 +				32.9 ft	3**	33	8	
		Breaking Wave Height =			33.9 ft		110**		
					34.9 ft			46**	
Total		24	366	1117	993	1302	966	306	11

*Tide elevation = +9 feet MLLW; direction-of-approach at the breakwater = 225.0 degrees.
**Percent frequency-of-occurrence of depth-limited breaking waves (x 1,000)

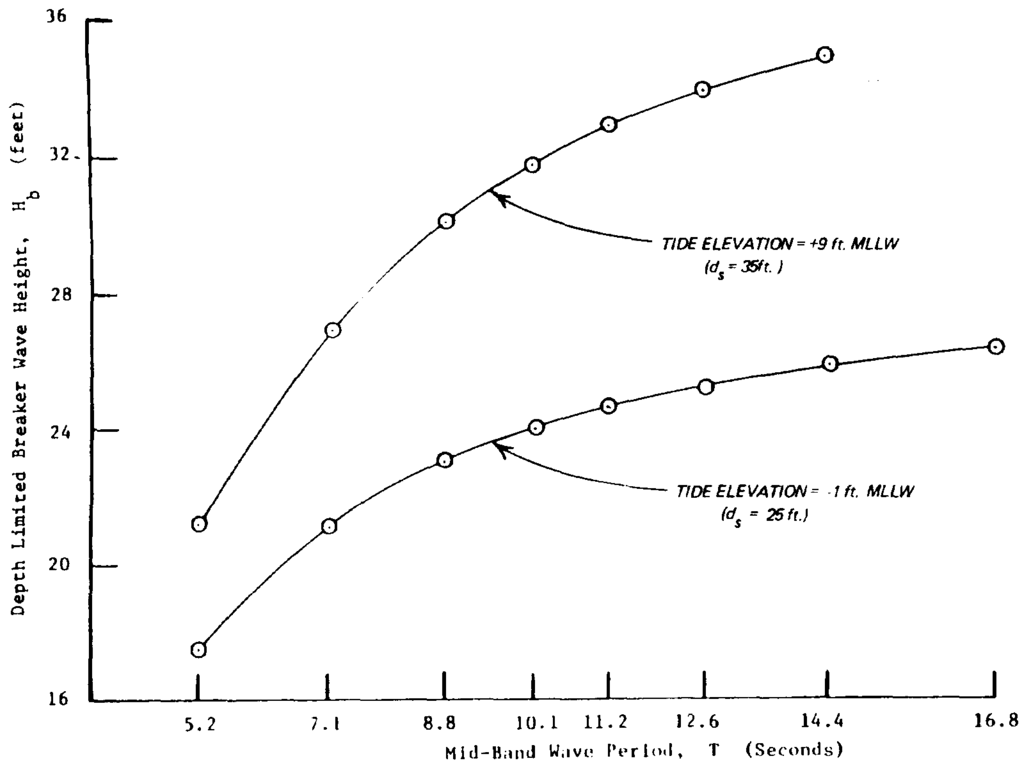

Figure 7-5. Maximum wave breaker height H_b which can be attained at the breakwater repair section

d. Consider wave setup.
e. Design water level summary.

SOLUTION: PROBLEM OVERVIEW. A beach fill project is frequently designed to provide beach erosion control and storm protection. The berm and sand dune (or berm) profile are an integral part of the design. Incorporating a dune section on the profile helps to prevent storm waters from flooding the lower back beach areas and provides a stockpile of sand to buffer the erosional effects of storm attack. As the storm surge rises and wave action reaches the dune, sand erodes and nourishes the eroded beach berm and foreshore. In addition, eroded dune sand contributes to offshore storm bar formation which helps protect the beach by limiting the onshore wave height.

A range of design water levels and waves coupled with different durations is recommended for evaluation of the beach berm width and foreshore profile design. The site location and proposed use benefits of the project must be considered in selecting these ranges. The ranges of water levels and wave conditions should be representative of the overall design water level explained in Section 1-6 for the selected return period. Ranges should include both the maximum and minimum conditions and several intermediate conditions. Consideration should also be given to wave approach angle and potential for a strong longshore transport regime.

Only one design water level will be illustrated in this example, the 100-year event for dune design. Other water levels and wave conditions for the beach design can be found following the same procedure.

TIDE AND STORM SURGE FOR THE 100-YEAR EVENT: Figure 7-6 shows the water level frequency curve for the project site. For this curve hurricanes and extratropical events (i.e. northeasters) were studied separately, and annual frequencies of each were summed to obtain the overall annual frequency. From Figure 7-6, the 100-year event tidal elevation including storm surge is +8.7 feet NGVD.

BREAKING WAVE HEIGHT AND RUNUP: Figure 7-7 from WIS Report 2 represents the return period in years for various significant wave heights at the deepwater WIS station nearest the study area. The published data do not include tropical storms at present. The 100-year and 50-year significant wave heights (53.8 and 48.2 feet, respectively) would break at considerable distance offshore and thus would not be pertinent to project design. Maximum breaker heights to which the berm and dune might reasonably be subjected were found by superimposing the 100-year storm tide and surge level of +8.7 feet (NGVD) onto the existing bathymetry in the area. This superimposition determines the design water level on which the waves are transmitted.

With an average 1:50 bottom slope and a wave period of 10 seconds (see Table 6-2 (WIS Report 2)), the maximum breaker height at several water depths was computed from Figure 7-4 in the SPM. This approach differs from the methodology of Equation 3-5 (also Figure 2-73, SPM) because it includes the initiation of wave breaking seaward of a structure where water depths are somewhat greater than at the structure. Since Figure 7-4 (SPM) gives more conservative results than Figure 2-73 (SPM), Figure 7-4 (SPM) was used. Results are given in Table 7-4.

The SPM approach used here is based on monochromatic, or swell, wave conditions. The depth-limited breaking wave height for locally generated sea waves, which is more appropriate in this example, can be expected to be lower. However, procedures for including the initiation of wave breaking seaward of a structure are not yet available for sea waves.

Maximum runup must be considered for design of a dune or berm elevation. Maximum runup heights above design SWL were computed using the composite slope method (SPM) and maximum breaker heights estimated from Figure 7-4 (SPM), with a placed beach profile of 1V:5H slope for the dune, berm height of +8.75 (NGVD), and a foreshore of 1V:15H. Wave setup is included within this method.

The results of this analysis indicate maximum runup on the design beach fill occurs with $H_{bmax} = 16.7$ feet and $T = 10$ sec. Wave heights greater or less than 16.7 feet will result in lower runup. In practice this runup may be limited if the beach erodes and a scarp develops.

WAVE SETUP: Wave setup S_w can be calculated separately using H and d_b if necessary. Various erosion models are available to design dune widths and beach fills. Depending upon project location and the model used, it may be necessary to calculate setup.

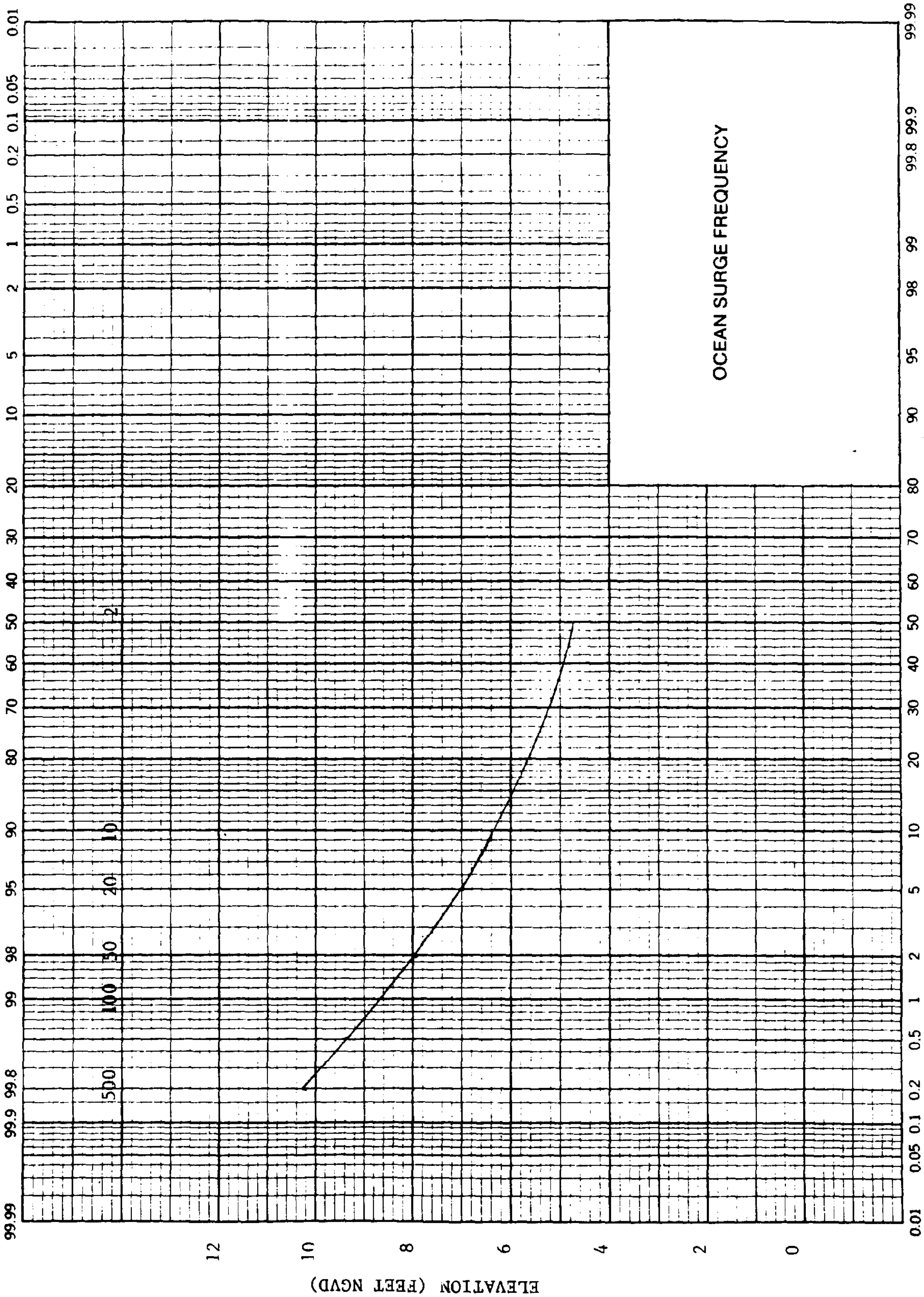

Figure 7-6. Storm water level frequency

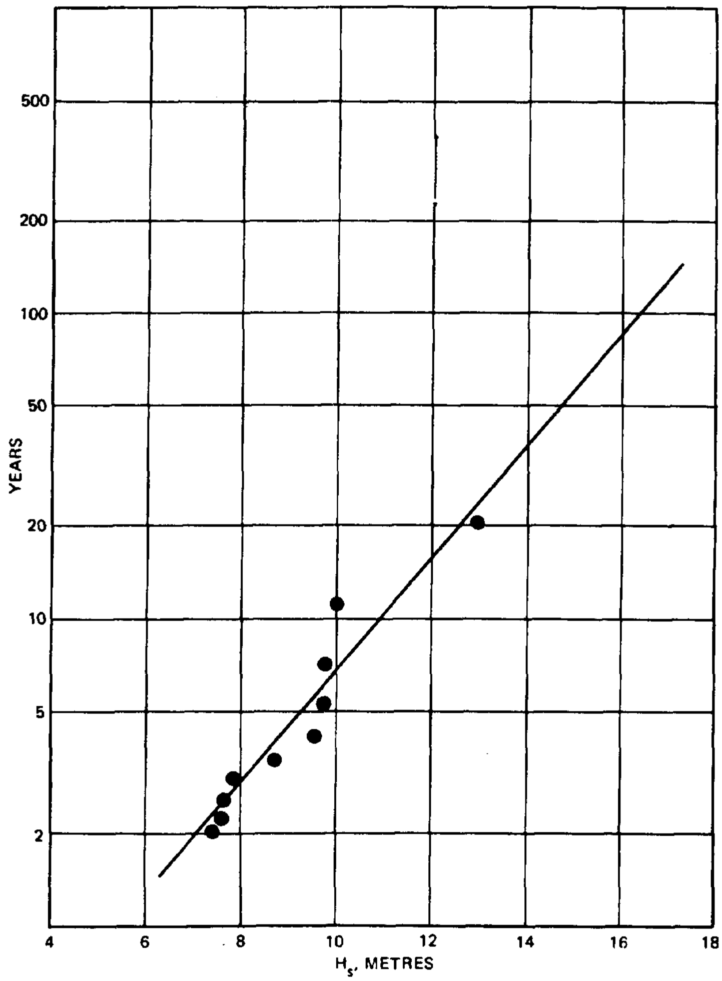

Figure 7-7. Return period of deepwater significant wave heights

Table 7-4

Maximum Wave Height Versus Maximum Runup

d_s ft	H_{bmax} ft	T_{max} s	R_{max} ft
8.7	13.5	10.0	13.2
12.0	11.4	10.0	11.3
18.0	16.7	10.0	13.7
24.0	21.4	10.0	13.2

Setup can be computed by Equation (3-4) or equivalently from Figure 3-50 (SPM). To use Figure 3-50 compute

$$\frac{H_b}{gT^2} = \frac{16.7}{(32.2)(10.0)^2} = 0.0052$$

For a slope of 1:50, the figure gives

$$\frac{S_w}{H_b} = 0.131$$

$$S_w = (0.131)(16.7)$$

$$S_w = 2.2 \text{ ft}$$

DESIGN WATER LEVEL SUMMARY: In summary, the water elevation for flood control and dune elevation design is +8.75 feet (NGVD) without wave setup, and +10.95 feet (NGVD) with wave setup. The deepwater breaking wave height is 16.7 feet.

*****************************EXAMPLE PROBLEM 7-5*****************************

GIVEN: A harbor breakwater is to be designed in one of the Great Lakes. Great Lakes open-coast flood levels, standardized frequency curves for design water level, and design wave information for the Great Lakes are available. A return period of 200 years is to be used for design.

FIND: Design water level and associated deepwater wave height.

APPROACH: Because the design water level and the deepwater wave height are related, they must be determined interactively as discussed in Section 1-6. The approach is as follows:

a. Determine lake levels and associated return periods.

b. Determine peak rise or storm setup and associated return periods.

c. Consider joint return periods of a. and b. and sum a. and b.

d. Determine wave heights and associated return periods.

e. Consider joint return periods of c. and d. and combine c. and d. to select the worst condition.

The 200-year return period is used as a convention for projects involving flood control. It represents a rare event, but it has not been established by any economic optimization procedure.

SOLUTION: LAKE LEVEL. Design water level is the joint occurrence of the long-term average lake level with a short-period fluctuation due to storm setup. Insignificant tidal fluctuations occur in the Great Lakes, and they are not considered in the design water level. Two ways to estimate the design water level are presented. The IGLD is used as the reference datum for computing long-term average lake level.

In the first method, combined average annual lake levels and instantaneous peak rise are extracted from Table 7-5 (item 128). This table shows lake levels referenced to both IGLD and MSL for 10-, 50-, and 100-year return periods. The breakwater site is located in Reach G.

In the second method, long-term average lake levels and peak rise are found separately. Annual mean lake levels are obtained from Figure 7-8 which shows the frequency curve of annual mean levels (item 129).

STORM SETUP: The maximum short-period fluctuation due to storm setup was obtained from Figure 7-9 which shows the frequency curve of peak rise at the breakwater site (item 130). Extraction of peak rise data from measurements is sometimes difficult, and this information is less reliable than that in Table 7-5. An alternative procedure is to estimate peak rise with a numerical model for wind-driven surge.

TOTAL WATER LEVEL: The joint return period is estimated by multiplying the individual event return periods (see Equation (2-4)), as follows:

$$p(a + b) = \left[p(a)\right] \left[p(b)\right]$$

where p is the combined probability of two events occurring in any year, and $p(a)$ and $p(b)$ are the probabilities of the individual events, as discussed in paragraph 2.5.d. This methodology is based on the assumption that events a and b are independent, which is not entirely correct for extreme water levels and wave heights. The probability of occurrence in any year is equal to the reciprocal of the return period, which is equal to 0.005 for a 200-year return period event. Water level and storm setup are summed. See Table 7-6 for joint returns and sum of water level and peak rise. This information is already included in the Method 1 approach using Table 7-5.

DESIGN WAVE: Deepwater design waves are obtained from the reports listed in Table 6-3. Table 7-7 shows the significant wave heights in feet for harbor site 21.

JOINT RETURN PERIOD OF WAVE HEIGHT AND WATER LEVEL: Various combinations of wave height and water level are calculated, as shown in Table 7-8. The extreme value is selected, and the design water level and deepwater significant wave height can be determined. Although wave height plus design water elevation is not a real value, it can be used to indicate the most critical design condition.

From Table 7-8, the extreme value for combined events having 200-year return period from Method 1 is 590.5 feet, yielding a design water elevation of 575.4 feet and a deepwater wave height of 15.1 feet. Low Water Datum (LWD) for this lake is 568.6 feet. Therefore, from Method 1 the design water level is +6.8 feet above LWD. From Method 2 the extreme value for combined events having a 200-year return period is 589.3 feet, yielding a design water

Table 7-5

Open Coast Flood Levels

Reach	Elevations* of Open-Coast Flood Levels at Various Return Periods							
	10-yr		50-yr		100-yr		500-yr	
	IGLD	MSL	IGLD	MSL	IGLD	MSL	IGLD	MSL
A	578.0	579.3	579.1	580.4	579.5	580.8	580.3	581.6
B	577.6	578.9	578.6	579.9	579.0	580.3	579.8	581.1
C	577.1	578.4	578.1	579.4	578.5	579.8	579.2	580.5
D	576.7	578.0	577.7	579.0	578.0	579.3	578.7	580.0
E	576.2	577.5	577.2	578.5	577.5	578.8	578.2	579.5
F	575.8	577.2	576.7	578.1	577.0	578.4	577.6	579.0
G	575.4	576.8	576.2	577.6	576.5	577.9	577.1	578.5
H	574.9	576.4	575.7	577.2	576.0	577.5	576.6	578.1
J	574.8	576.3	575.6	577.1	575.8	577.3	576.4	577.9
K	574.6	576.1	575.4	576.9	575.6	577.1	576.2	577.7
L	574.4	575.9	575.2	576.7	575.4	576.9	575.9	577.4
M	574.2	575.7	575.0	576.5	575.2	576.7	575.7	577.2
N	574.1	575.6	574.8	576.3	575.0	575.5	575.5	577.0
P	573.9	575.4	574.6	576.1	574.8	576.3	575.3	576.8
Q	573.7	575.3	574.4	576.0	574.6	576.2	575.1	576.7
R	573.9	575.5	574.6	576.2	574.8	576.4	575.3	576.9
S	574.0	575.6	574.8	576.4	575.0	576.6	575.5	577.1
T	574.2	575.8	575.0	576.6	575.2	576.8	575.8	577.4
U	574.3	575.9	575.2	576.8	575.4	577.0	576.0	577.6
V	574.5	576.1	575.3	576.9	575.6	577.2	576.2	577.8
W	574.6	576.1	575.5	577.0	575.8	577.3	576.4	577.9
X	574.8	576.3	575.7	577.2	576.0	577.5	576.7	578.2
Y	574.9	576.4	575.9	577.4	576.2	577.7	576.9	578.4
Z	575.1	576.6	576.1	577.6	576.4	577.9	577.1	578.6
AA	575.9	577.3	576.8	578.2	577.1	578.5	577.7	579.1

* Elevations are in feet IGLD (1955) and mean sea level of 1929.

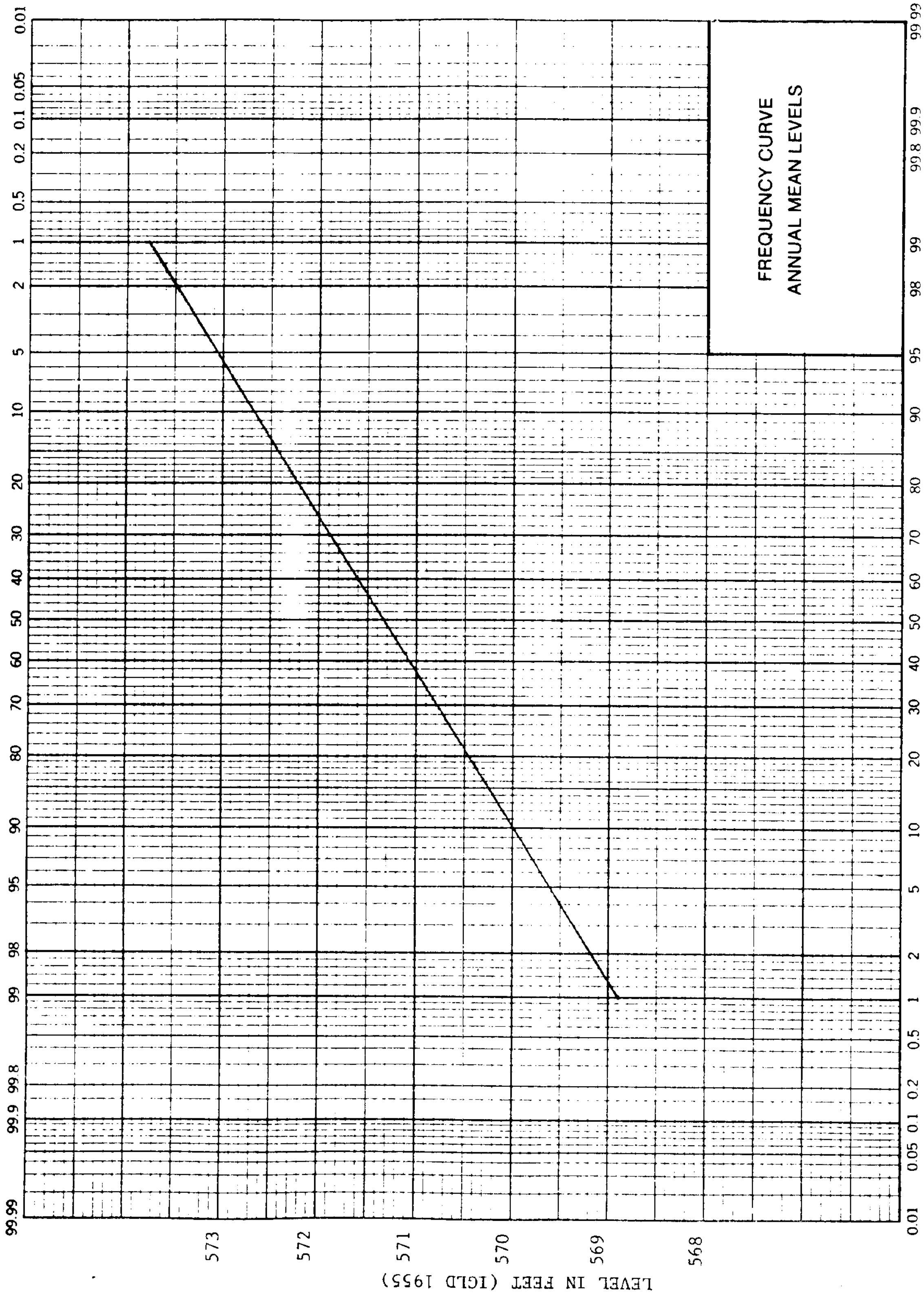

Figure 7-8. Annual mean lake level frequency curve

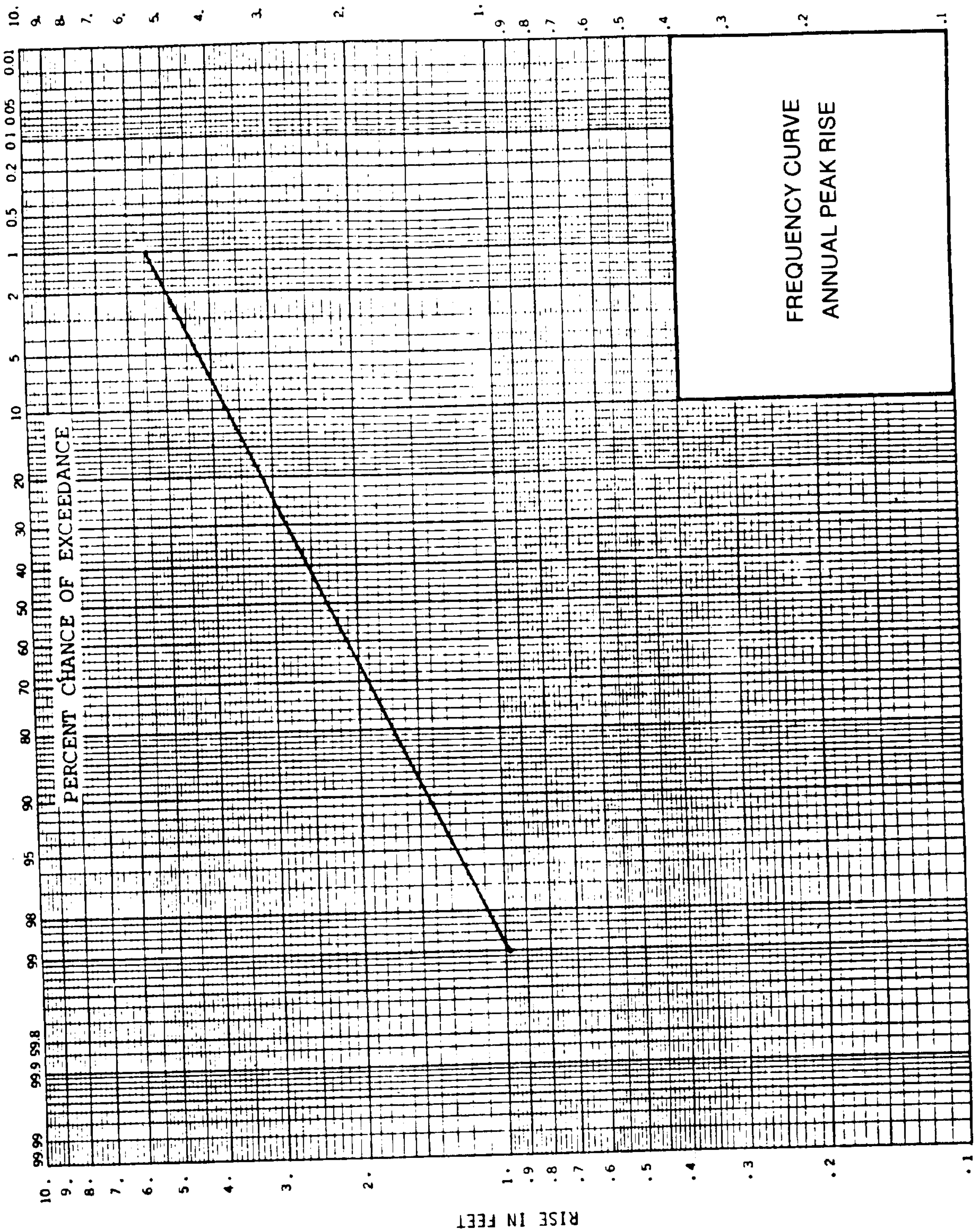

Figure 7-9. Annual peak rise frequency curve

Table 7-6

Estimation of Total Water Level

Lake Level			Peak Rise			Still-Water Elevation		
Return Period yr	Probability	Referenced to IGLD ft	Return Period yr	Probability	ft	Referenced to IGLD ft	Return Period yr	Probability
Method 1								
						575.4	10	0.1
Method 2								
10	0.1	572.7	1	1.0	1.0	573.7	10	0.1
10	0.1	572.7	2	0.5	2.3	575.0	20	0.05
10	0.1	572.7	4	0.25	3.0	575.7	40	0.025
20	0.05	573.0	1	1.0	1.0	574.0	20	0.05
20	0.05	573.0	2	0.5	2.3	575.3	40	0.025

Table 7-7

Wave Heights H_s for Approach Directions and Seasons Combined*

Site	Return Periods, yr 5	10	20	50	100
1	10.6	12.2	13.7	15.7	17.3
2	10.3	12.0	13.8	16.2	18.0
3	9.6	11.0	12.5	14.5	16.0
4	10.0	11.4	12.9	14.9	16.4
5	9.5	10.7	12.0	14.1	15.8
6	11.6	12.7	13.9	15.5	16.9
7	11.0	12.2	13.5	15.3	16.8
8	10.6	11.6	12.6	14.0	15.0
9	11.1	12.7	14.4	16.7	18.5
10	12.8	13.9	14.9	16.3	17.4
11	12.2	13.4	14.7	16.4	17.7
12	12.1	13.2	14.4	16.1	17.3
13	12.9	14.1	15.2	16.7	17.9
14	13.1	14.2	15.4	17.0	18.2
15	13.0	14.4	15.7	17.5	18.8
16	13.5	14.7	15.9	17.6	18.9
17	13.6	14.8	16.1	17.8	19.2
18	12.8	13.7	14.6	15.9	16.9
19	13.2	14.0	14.8	16.0	16.9
20	13.1	13.9	14.7	15.9	16.8
21**	13.4	14.3	15.1	16.3	17.2
22	11.1	12.0	12.9	14.2	15.2
23	12.0	12.8	13.7	14.9	15.9
24	15.9	17.3	18.8	20.8	22.3

*In feet.
**Breakwater site.

Table 7-8

Joint Return Period of Wave Height and Water Level

Still-Water Elevation (SWE)			Significant Deepwater Wave Height (Hs)			Still-Water Elevation + Hs		
Referenced to IGLD ft	Return Period yr	Probability	ft	Return Period yr	Probability	Referenced to IGLD ft	Return Period yr	Probability
				Method 1				
575.4	10	0.1	15.1	20	0.05	590.5	200	0.005
				Method 2				
573.7	10	0.1	15.1	20	0.05	588.8	200	0.005
575.0	20	0.05	14.3	10	0.10	589.3	200	0.005
575.7	40	0.025	13.4	5	0.20	589.1	200	0.005
574.0	20	0.05	14.3	10	0.10	588.3	200	0.005
575.3	40	0.025	13.4	5	0.20	588.7	200	0.005

elevation of 575.0 feet and a deepwater wave height of 14.3 feet. From Method 2 the design water level is +6.4 feet above LWD. The results from Method 1 are slightly more conservative in this case and should be used for design.

Although a single elevation estimate is often used for design, it is important to note that some uncertainty is associated with the estimate. The various estimates in Table 7-8 give an indication of the range of uncertainty. Confidence bands may also be estimated by statistical methods. A conservative approach is used in this example. Engineering judgment may dictate a less conservative approach for some applications.

****

APPENDIX A

BIBLIOGRAPHY

1. American National Standards Institute. 1972. American National Standard Building Code Requirements for Minimum Design Loads in Buildings and Other Structures, ANSI A58.1, 1430 Broadway, New York, NY.

2. Barrick, D. E. 1982. "Status of HF Radars for Wave-Height Directional Spectral Measurements," Measuring Ocean Waves: Proceedings of a Symposium and Workshop on Wave-Measurement Technology, Marine Board, US National Research Council, Washington, DC, pp 112-118.

3. Blumenthal, R. B., and O'Quinn, B. 1981 (Oct). "The Coastal Environmental Reference Service," Reference Publication 35, Naval Oceanographic Office, NSTL Station, Bay St. Louis, MS.

4. Borgman, L. E. 1979. "Directional Wave Spectra from Wave Sensors," Ocean Wave Climate, Earle, M. D., and Malahoff, A. eds., Plenum Press, New York, NY.

5. Borgman, L. E., and Resio, D. T. 1977. "External Prediction in Wave Climatology," Ports 77, 4th Annual Symposium of the Waterway, Port, Coastal and Ocean Division, American Society of Civil Engineers, Vol 1, pp 394-412.

6. Bouws, E., Gunther, H., Rosenthal, W., and Vincent, C. L. 1985 (Jan). "Similarity of the Wind Wave Spectrum in Finite Depth Water, Part I - Spectral Form," Journal of Geophysical Research, Vol 90, No. C1, pp 975-986.

7. Braaten, N. F., and McCombs, C. E. 1963. "Mean Sea Level Variations as Indicated by a 1963 Adjustment of First-Order Leveling in United Stations," (preprint), US Coast and Geodetic Survey, Washington, DC.

8. Brandsma, M., Divoky, D., and Hwang, L-S. 1975 (Apr). "Seawave- A Revised Model for Tsunami Applications," Final Report, National Science Foundation, Washington, DC.

9. Bretschneider, C. L. 1953. "Revised Wave Forecasting Relationships," Proceedings of the 2nd Coastal Engineering Conference, American Society of Civil Engineers, pp 1-5.

10. Bretschneider, C. L. 1959 (Aug). "Wave Variability and Wave Spectra for Wind-Generated Gravity Waves," CERC Technical Memorandum 118, US Army Engineer Waterways Experiment Station, Vicksburg, MS.

11. Camfield, F. E. 1980 (Feb). "Tsunami Engineering,"CERC Special Report 6, US Army Engineer Waterways Experiment Station, Vicksburg, MS.

12. Carrier, G. F. 1970. "The Dynamics of Tsunamis," Mathematical Problems in Geophysical Sciences, Geophysical Fluid Dynamics, American Mathematical Society, Vol 1, pp 157-187.

13. Carrier, G. F., Shaw, R. P., and Miyata, M. 1971 (Dec). "Channel Effects in Harbor Resonance," Journal of the Engineering Mechanics Division, Vol 97, No. EM6.

14. Carter, D. J. T., and Draper, L. 1979. "Waves at Ocean Weather Station ALPHA," Report 69, Institute of Oceanographic Sciences, Wormley, Godalming, England.

15. Chen, H. S. 1984 (Dec). "Hybrid Element Modeling of Harbor Resonance," Proceedings of the 4th International Conference on Applied Numerical Modeling, National Cheng Kung University, Tainan, Taiwan, pp 312-316.

16. Chen, H. S., Divoky, D., and Hwang, L-S. 1975 (Apr). "Nearfied Tsunami Behavior," Final Report, National Science Foundation, Washington, DC.

17. Chen, H. S., and Houston, J. R. 1986 (Aug). "Calculation of Water Oscillation in Coastal Harbors HARBS and HARBD User's Manual," Instruction Report, US Army Engineer Waterways Experiment Station, Vicksburg, MS.

18. Chen, H. S., and Mei, C. C. 1974. "Oscillation and Wave Forces in an Offshore Harbor (Applications of the Hybrid Finite Element Method to Water-Wave Scattering)," Report No. 190, Massachusetts Institute of Technology, Cambridge, MA.

19. Chu, Y.-H., Lund, R. B., and Camfield, F. E. 1986 (Dec). "Sources of Coastal Engineering Information," Technical Report CERC-87-1, US Army Engineer Waterways Experiment Station, Vicksburg, MS.

20. Cochrane, J. D., and Arthur, R. S. 1948. "Reflection of Tsunami," Journal of Marine Research, Vol 7, No. 3, pp 239-251.

21. Crawford, P. L. 1987 (Apr). "Tsunami Predictions for the Coast of Alaska: Kodiak Island to Ketchikan," Technical Report CERC-87-7, US Army Engineer Waterways Experiment Station, Vicksburg, MS.

22. Dean, R. G. 1964 (Feb). "Long Wave Modification by Linear Transitions," Journal of the Waterways and Harbors Division, American Society of Civil Engineers, Vol 90, No. WW1, pp 1-29.

23. Dean, R. G. 1974 (Nov). "Evaluation and Development of Water Wave Theories for Engineering Applications," Special Report 1, 2 Vols, US Army Engineer Waterways Experiment Station, Vicksburg, MS.

24. Dean, R. G. 1982. "Summary of Symposium," Measuring Ocean Waves: Proceedings of a Symposium and Workshop on Wave-Measurement Technology, Marine Board, US National Research Council, Washington, DC., pp 1-13.

25. Dean, R. G., and Dalrymple, R. A. 1984. Water Wave Mechanics for Engineers and Scientists, Prentice-Hall, Englewood Cliffs, NJ.

26. Doodson, A. T., and Warburg, H. D. 1941. Admiralty Manual of Tides, Her Majesty's Stationery Office, London, England.

27. Donelan, M., and Pierson, W. J. 1983 (May). "The Sampling Variability of Estimates of Spectra of Wind-Generated Gravity Waves," Journal of Geophysical Research, Vol 88, No. C7, pp 4381-4392.

28. Draper, L., and Squire, E. M. 1967. "Waves at Ocean Weather Ship Station India (59 N, 19 W)," Transactions of the Royal Institute of Naval Architecture, London.

29. Durham, D. L. 1978. "Numerical Analysis of Harbor Oscillations for Barbers Point Deep-Draft Harbor," Technical Report H-78-20, US Army Engineer Waterways Experiment Station, Vicksburg, MS.

30. Ebersole, B. A., Cialone, M. A., and Prater, M. D. 1986 (Mar). "Regional Coastal Processes Numerical Modeling System Report 1: RCPWAVE--A Linear Wave Propagation Model for Engineering Use," Technical Report CERC-86-4, US Army Engineer Waterways Experiment Station, Vicksburg, MS.

31. Esteva, D. C. 1977 (Jul). "Evaluation of the Computation of Wave Direction with Three-Gage Arrays," Technical Paper 77-7, US Army Engineer Waterways Experiment Station, Vicksburg, MS.

32. Esteva, D. C., and Harris, D. L. 1971. "Comparison of Pressure and Staff Wave Gage Records," Proceedings of the 12th Coastal Engineering Conference, American Society of Civil Engineers.

33. Farrar, P. D., and Houston, J. R. 1982 (Oct). "Tsunami Response of Barbers Point Harbor, Hawaii," Miscellaneous Paper HL-82-1, US Army Engineer Waterways Experiment Station, Vicksburg, MS.

34. Forristall, G. Z. 1982. "Subsurface Wave-Measuring Systems," Measuring Ocean Waves: Proceedings of a Symposium and Workshop on Wave-Measurement Technology, Marine Board, US National Research Council, Washington, DC.

35. Garcia, A. W., and Houston, J. R. 1975 (Nov). "Type 16 Flood Insurance Study: Tsunami Predictions for Monterey and San Francisco Bays and Puget Sound," Technical Report H-75-17, US Army Engineer Waterways Experiment Station, Vicksburg, MS.

36. Goda, Y. 1970 (Sep). "Numerical Experiments on Wave Statistics with Spectral Simulation," Report of the Port and Harbour Research Institute, Japan, Vol 9, No. 3, pp 3-57.

37. Goda, Y. 1975. "Irregular Wave Deformation in the Surf Zone," Coastal Engineering in Japan, Vol 18, pp 13-26.

38. Goda, Y. 1979 (Mar). "A Review on Statistical Interpretation of Wave Data," Report of the Port and Harbour Research Institute, Vol 18, No. 1, pp 5-32.

39. Grace, R. A. 1978. "Surface Wave Heights from Pressure Records," Coastal Engineering, Vol 2, No. 1, pp 55-67.

40. Goring, D. G. 1978 (Nov). "Tsunamis - The Propagation of Long Waves onto a Shelf," W.M. Keck Laboratory Report, No. KH-R-38, California Institute of Technology, Pasadena, CA.

41. Guza, R. T., and Thornton, E. B. 1980 (Mar). "Local and Shoaled Comparisons of Sea Surface Elevations, Pressures and Velocities," Journal of Geophysical Research, Vol 85, No. C3, pp 1524-1530.

42. Hammack, J. L. 1972 (Jun). "Tsunamis - A Model of Their Generation and Propagation," Report No. KH-R-28, W.M. Keck Laboratory of Hydraulics and Water Resources, California Institute of Technology, Pasadena, CA.

43. Hammack, J. L., and Segur H. 1978. "Modeling Criteria for Long Water Waves," Journal of Fluid Mechanics, Vol 84, pp 359-373.

44. Harris, D. L. 1959. "An Interim Hurricane Storm Surge Forecasting Guide," National Hurricane Research Project, Report No. 32, US Weather Bureau, Washington, DC.

45. Harris, D. L. 1963. "Characteristics of the Hurricane Storm Surge," Technical Paper No. 48, US Department of Commerce, Washington DC.

46. Harris, D. L., and Lindsay, C. V. 1957 (May). "An Index of Tide Gages and Tide Gage Records for the Atlantic and Gulf Coasts of the United States," Report No. 7, National Hurricane Research Project, US Weather Bureau, Washington, DC.

47. Hasselmann, K., Barnett, T. P., Bouws, E., Carlson, H., Cartwright, D. E., Enke, K., Ewing, J. A., Gienapp, H., Hasselmann, D. E., Kruseman, D., Meerburg, A., Muller, D., Olberg, D. J., Richter, K., Sell, W., and Walden, H. 1973. "Measurements of Wind Wave Growth and Swell Decay During the Joint North Sea Wave Project (JONSWAP)," Deutsches Hydrographisches Institut, Hamburg, Germany.

48. Hasselmann, D. E., Dunckel, M., and Ewing, J. A. 1980 (Aug). "Directional Wave Spectra Observed during JONSWAP 1973," Journal of Physical Oceanography, Vol 10, No. 8, pp 1264-1280.

49. Hasselmann, K., Ross, D. B., Muller, P., and Sell, W. 1976 (Mar). "A Parametric Wave Prediction Model," Journal of Physical Oceanography, Vol 6, No. 2, pp 200-228.

50. Hicks, S. D. 1984. "Tide and Current Glossary," National Oceanic and Atmospheric Administration, National Ocean Service, US Department of Commerce, Washington, DC.

51. Hicks, S. D., et al. 1983 (Jan). "Sea Level Variations for the United States, 1855-1980," US Department of Commerce, Washington, DC.

52. Hidaka, K. 1935a (Dec). "A Theory of Shelf Seiches, and Seiches in a Channel," Memoirs of the Imperial Marine Observatory, Kobe, Japan, Vol 6, No. 1, pp 9-11.

53. Hidaka, K. 1935b (Dec). "Seiches Due to Submarine Bank," Memoirs of the Imperial Marine Observatory, Kobe, Japan, Vol 6, No. 1, pp 1-7.

54. Houston, J. R. 1976 (Sep). "Long Beach Harbor Numerical Analysis of Harbor Oscillations, Report 1, Existing Conditions and Proposed Improvements," Miscellaneous Paper H-76-20, US Army Engineer Waterways Experiment Station, Vicksburg, MS.

55. Houston, J. R. 1977 (Feb). "Los Angeles Harbor Numerical Analysis of Harbor Oscillations," Miscellaneous Paper H-77-2, US Army Engineer Waterways Experiment Station, Vicksburg, MS.

56. Houston, J. R. 1979 (Nov). "State-of-the-art for Assessing Earthquake Hazards in the United States; Report 15. Tsunamis, Seiches, and Landslide-Induced Water Waves," Miscellaneous Paper S-73-1, US Army Engineer Waterways Experiment Station, Vicksburg, MS.

57. Houston, J. R. 1980a (Sep). "Type 19 Flood Insurance Study: Southern California," Technical Report HL-80-18, US Army Engineer Waterways Experiment Station, Vicksburg, MS.

58. Houston, J. R. 1980b (Sep). "Tsunami Elevation Prediction for American Samoa," Technical Report HL-80-16, US Army Engineer Waterways Experiment Station, Vicksburg, MS.

59. Houston, J. R., and Butler, H. L. 1979 (Feb). "A Numerical Model for Tsunami; Final Report," Technical Report HL-79-2, US Army Engineer Waterways Experiment Station, Vicksburg, MS.

60. Houston, J. R., Carver, R. D., and Markle, D. G. 1977 (Aug). "Tsunami-Wave Elevation Frequency of Occurence for the Hawaiian Islands," Technical Report H-77-16, US Army Engineer Waterways Experiment Station, Vicksburg, MS.

61. Houston, J. R., and Chou, L. W. 1983. "Numerical Modeling of Explosion Waves," Technical Report HL-83-1, US Army Engineer Waterways Experiment Station, Vicksburg, MS.

62. Houston, J. R., and Garcia, A. W. 1974 (May). "Type 16 Flood Insurance Study: Tsunami Predictions for Pacific Coastal Communities," Technical Report H-74-3, US Army Engineer Waterways Experiment Station, Vicksburg, MS.

63. Houston, J. R., and Garcia, A. W. 1978 (Dec). "Type 16 Flood Insurance Study: Tsunami Predictions for the West Coast of the Continental United States," Technical Report H-78-26, US Army Engineer Waterways Experiment Station, Vicksburg, MS.

64. Houston, J. R., et al. 1975 (Jul). "Effect of Souce Orientation and Location in the Aleutian Trench on Tsunami Amplitude Along the Pacific Coast of the Continental United States," Research Report H-75-4, US Army Engineer Waterways Experiment Station, Vicksburg, MS.

65. Hubertz, J. M. 1986. "A User's Guide to a Steady-State Shallow-Water Directional Spectral Wave Model," Instructional Report CERC-86-1, US Army Waterways Experiment Station, Vicksburg, MS.

66. Hudspeth, R. T., and Chen, M. C. 1979 (Feb). "Digital Simulation of Nonlinear Random Waves," Journal of the Waterway, Port, Coastal and Ocean Division, American Society of Civil Engineers, Vol 105, No. WW1, pp 67-85.

67. Hughes, S. A. 1984 (Dec). "Summary and Applications of the TMA Shallow-Water Spectrum," Technical Report 84-7, US Army Engineer Waterways Experiment Station, Vicksburg, MS.

68. Hughes, S. A. and Jensen, R. E. 1986 (Jun). "A User's Guide to SHALWV: Numerical Model for simulation of Shallow-Water Wave Growth, Propagation, and Decay," Instruction Report CERC-86-2, US Army Engineer Waterways Experiment Station, Vicksburg, MS.

69. Hwang, L-S., Butler, H. L., and Divoky, D. 1972. "Tsunami Model: Generation and Open-Sea Characteristics," Bulletin of the Seismological Society of America, Vol 62, No. 6, pp 1579-1596.

70. Hwang, L-S., and Divoky, D. 1975 (Mar). "Numerical Investigations of Tsunami Behavior," Final Report, National Science Foundation, Washington, DC.

71. Iida, K. 1970. "The Generation of Tsunamis and the Focal Mechanism of Earthquakes," Tsumamis in the Pacific Ocean, East-West Center Press, Honolulu, Hawaii.

72. Ippen, A. T., and Goda, Y. 1963 (Jul). "Wave Induced Oscillation in Harbors: The Solution for a Rectangular Harbor Connected to the Open Seas," Report No. 59, Hydodynamics Laboratory, Massachusettes Institute of Technology, Cambridge, MA.

73. Ippen, A. T., Raichlen, F., and Sullivan, R. K. 1962 (Jul). "Wave Induced Oscillations in Harbors: Effect of Energy Dissipators in Coupled Basis Systems," Report No. 52, Hydrodynamics Laboratory, Massachusetts Institute of Technology, Cambridge, MA.

74. Isaacson, M. S., and MacKenzie, N. G. 1981 (May). "Long-Term Distributions of Ocean Waves: a Review," Journal of the Waterway, Port, Coastal and Ocean Division, American Society of Civil Engineers, Vol 107, No. WW2, pp 93-109.

75. Iwasaki, T., and Horikawa, K. 1960. "Tsunami Caused by Chile Earthquake in May, 1960 and Outline of Disasters in North-eastern Coasts of Japan," Coastal Engineering in Japan, Vol III, p 33.

76. Iwasaki, T., Miura, A., and Terada, S. 1961. "On the Effect of the Breakwater in Case of Tsunami, Part 1 (The Model Experiment of Tsunami in Kesennuma Bay)," The Technology Reports of the Tohoku University, Sendai, Japan, Vol 25, No. 2.

77. Jahns, H., and Wheeler, J. 1973 (Apr). "Long-Term Wave Probabilities Based on Hindcasting of Severe Storms," Journal of Petroleum Technology, Vol 25, pp 473-486.

78. Jensen, R. E. 1983a (Apr). "Mississippi Sound Wave-Hindcast Study," Technical Report HL-83-8, US Army Engineer Waterways Experiment Station, Vicksburg, MS.

79. Jensen, R. E. 1983b (Sep). "Methodology for the Calculation of a Shallow-Water Wave Climate," WIS Report 8, US Army Engineer Waterways Experiment Station, Vicksburg, MS.

80. Johnson, R. R., Mansard, E. P. D., and Ploeg, J. 1979. "Effects of Grouping on Breakwater Stability," Proceedings of the 16th Coastal Engineering Conference, American Society of Civil Engineers.

81. Kajiura, K. 1963. "On the Partial Reflection of Water Waves Passing Over a Bottom of Variable Depth," Proceedings of the 10th Pacific Science Congress on Tsunami Hydrodynamics, International Union of Geodesy and Geophysics, Monograph No. 24, pp 206-230.

82. Kajiura, K. 1979. "Tsunami Propagation," Proceedings of the National Science Foundation Tsunami Workshop, Coto De Caza, CA, pp 43-104.

83. Kitaigorodskii, S. A., Drasitskii, V. O., and Zaslavskii, M. M. 1975. "On Phillip's Theory of Equilibrium Range in the Spectra of Wind-Generated Gravity Waves," Journal of Physical Oceanography, Vol 5, pp 410-420.

84. Lee, J. J. 1969 (Dec). "Wave Induced Oscillation in Harbors of Arbitrary Shape," Report No. KH-20, W.M. Keck Laboratory of Hydraulics and Water Resources, California Institute of Technology, Pasadena, CA.

85. Le Méhauté, B. 1969. "An Introduction to Hydrodynamics and Water Waves," Water Wave Theories, Vol II, TR ERL 118-POL-3-2, US Department of Commerce, Environmental Science Services Administration, Washington, DC.

86. Levy, D. M., and Keller, J. B. 1961. "Water Wave Production by Point Sources and Extended Sources," Proceedings of the 10th Pacific Science Congress on Tsunami Hydrodynamics, International Union of Geodesy and Geophysics, Monograph No. 24, pp 162-166.

87. Longuet-Higgins, M. S., et al. 1963. "Observations of Sea Waves Using the Motions of a Floating Buoy," Ocean Wave Spectra, Prentice-Hall, Englewood Cliffs, NJ.

88. Magoon, O. T. 1965. "Structural Damage By Tsunamis," Proceedings of the Coastal Engineering Specialty Conference, American Society of Civil Engineers, pp 35-68.

89. Malloy, R. J. 1964. "Crustal Uplift Southwest of Montague Island, Alaska," Science, Vol 146, pp 1048-1049.

90. Marmer, H. A. 1951. "Tidal Datum Planes," Special Publication No. 135, revised ed., US Coast and Geodetic Survey, US Government Printing Office, Washington, DC.

91. Mattie, M. G., and Harris, D. L. 1979. "A System for Using Radar to Record Wave Direction," Technical Report 79-1, US Army Engineer Waterways Experiment Station, Vicksburg, MS.

92. Miles, J. W. 1971. "Resonant Response of Harbors: An Equivalent-Circuit Analysis," Journal of Fluid Mechanics, Vol 46, Part 2, pp 241-265.

93. Miller, R. L. 1968 (Jun). "Experimental Determination of Runup of Undular and Fully Developed Bores and an Examination of Transition Modes and Internal Structure," Technical Report No. 8, Department of Geophysical Sciences, University of Chicago, Chicago, IL.

94. Mitsuyasu, H., et al. 1975 (Oct). "Observations of the Directional Spectrum of Ocean Waves Using a Cloverleaf Buoy," Journal of Physical Oceanography, Vol 5, No. 4, pp 750-760.

95. Murty, T. S. 1977. "Seismic Sea Waves - Tsunamis," Bulletin 198, Department of Fisheries and the Environment, Fisheries and Marine Service, Ottawa, Canada.

96. Murty, T. S., Wigen, S. O., and Chawla, R. 1975. "Some Features of Tsunamis on the Pacific Coast of South and North America," Series No. 36, Marine Sciences Directorate, Department of the Environment, Ottawa, Canada.

97. National Bureau of Standards. 1980. "Hurricane Wind Speeds in the United States," Building Science Series 124, Gaithersburg, MD.

98. National Marine Consultants. 1960. "Wave Statistics for 7 Deep Water Stations along the California Coast, Santa Barbara," USAE Districts Los Angeles and San Francisco, CA.

99. National Oceanic and Atmospheric Administration. 1977a (Feb). "Classification, Standard of Accuracy, and General Specifications of Geodetic Control Surveys," Federal Geodetic Control Committee, National Ocean Survey, Rockville, MD.

100. National Oceanic and Atmospheric Administration. 1977b (Sep). "Establishment of Gulf Coast Water Datum," Federal Register, Vol 42, No. 179.

101. National Research Council. 1987. "Responding to Changes in Sea Level, Engineering Implications," Report by the Committee on Engineering Implications of Changes in Relative Mean Sea Level, Marine Board, Washington, DC.

102. Nolte, K. G. 1973. "Statistical Methods of Determining Extreme Sea States," Proceedings of the 2nd International Conference on Port and Ocean Engineering Under Artic Conditions, pp 705-742.

103. Ochi, M. K. 1982. "Stochastic Analysis and Probabilistic Prediction of Random Seas," Advances in Hydroscience, Chow, V. T., Ed., Vol 13, Academic Press, New York, NY.

104. Ochi, M. K., Malakar, S. B., and Wang, W-C. 1982 (Oct). "Statistical Analysis of Coastal Waves Observed During the ARSLOE Project," Report UFL/COEL/TR-045, Coastal and Oceanographic Engineering Department, University of Florida, Gainesville, FL.

105. Outlaw, D. G. 1982 (Jan). "Lake Pontchartrain and Vicinity Hurricane Protection Plan," Technical Report HL-82-8, US Army Engineer Waterways Experiment Station, Vicksburg, MS.

106. Parker, A. G. 1982. "Wave Measurements Using Surface-Mounted Instruments," Proceedings of a Symposium and Workshop on Wave Measurement Technology, Marine Board, US National Research Council, Washington, DC.

107. Perroud, P. H. 1957 (Sep). "The Solitary Wave Reflection Along a Straight Vertical Wall at Oblique Incidence," University of California, Institute of Engineering Research, Berkeley, CA, Series 99, Issue 3.

108. Poole, et al. 1977 (Dec). "Minimal Resource Computer Program for Automatic Generation of Ocean Wave Ray or Crest Diagrams in Shoaling Waters," NASA Technical Memo 74076, National Aeronautics and Space Administration Langley Research Center, Hampton, VA.

109. Rappleye, H. S. 1932 (Nov). "The 1929 Adjustment of the Level Net," The Military Engineer, Vol 24, No. 138, pp 576-578.

110. Resio, D. T., and Tracy, B. A. 1983 (Jan). "A Numerical Model for Wind-Wave Predictions in Deep Water," WIS Report 12, US Army Engineer Waterways Experiment Station, Vicksburg, MS.

111. Resio, D. T., and Vincent, C. L. 1976. "Estimation of Winds Over the Great Lakes," Miscellaneous Paper H-76-12, US Army Engineer Waterways Experiment Station, Vicksburg, MS.

112. Ross, D. B. 1967. "Recent Developments in Remote Sensing of Deep Ocean Wave, The New Thrust Seaward," Transactions of the 3rd Annual MTS Conference, Marine Technological Society, Washington, DC., pp 371-393.

113. Saville, T., McClendon, E. W., and Cochran, A. L. 1962 (May). "Freeboard Allowances for Waves in Inland Reservoirs," Journal of the Waterways and Harbors Division, American Society of Civil Engineers, pp 93-124.

114. Schneider, C. 1981 (Mar). "The Littoral Environment Observation (LEO) Data Collection Program," Coastal Engineering Technical Aid 81-5, US Army Engineer Waterways Experiment Station, Vicksburg, MS.

115. Schureman, P. 1941. "Manual of Harmonic Analysis and Prediction of Tides," Special Publication No. 98, US Department of Commerce, National Oceanic and Atmospheric Administration, National Ocean Service, Washington, DC.

116. Seelig, W. N., Harris, D. L., and Herchenroder, B. E. 1977 (Nov). "A Spatially Integrated Numerical Model of Inlet Hydraulics," GITI Report 14, Coastal Engineering Research Center, US Army Engineer Waterways Experiment Station, Vicksburg, MS.

117. Seymour, R. J. 1982. "Review of Wave Measurement Using the Situ Systems," Measuring Ocean Waves: Proceedings of a Symposium and Workshop on Wave-Measurement Technology, Marine Board, US National Research Council, Washington, DC.

118. Shepard, F. P., MacDonald, G. A., and Cox, D. C. 1950. "The Tsunami of April 1, 1946," Bulletin of Scripps Institute of Oceanography, Vol 5, No. 6, pp 391-528.

119. Sherlock, A. R., and Szuwalski, A. 1987. "A User's Guide to the Littoral Environment Observation Retrieval System," Instruction Report CERC-87-3, US Army Engineer Waterways Experiment Station, Coastal Engineering Research Center, Vicksburg, MS.

120. Simiu, E., and Scanlan, R. N. 1978. Wind Effect on Structures: An Introduction to Wind Engineering, John Wiley & Sons, New York.

121. Smith, R. A. 1967 (Apr). "Annotated Bibliography on Water Waves Caused by Explosion--1946 to 1966," DASIAC Special Report 58, DASA Information and Analysis Center, Pasadena, CA.

122. Swanson, R. L. 1974 (Oct). "Variability of Tidal Datums and Accuracy in Determining Datums from Short Series of Observation," Technical Report NOS 64, National Oceanic and Atmoshperic Administration, National Ocean Survey, Rockville, MD.

123. Thompson, E. F. 1977 (Jan). "Wave Climate at Selected Locations Along U.S. Coasts," Technical Report 77-1, US Army Engineer Waterways Experiment Station, Vicksburg, MS.

124. Thompson, E. F. 1980. "Interpretation of Wave Energy Spectra," Coastal Engineering Technical Aid 80-5, US Army Engineer Waterways Experiment Station, Vicksburg, MS.

125. Thompson, E. F., and Vincent, C. L. 1985 (Sep). "Significant Wave Height for Shallow Water Design," Journal of the Waterway, Port, Coastal and Ocean Division, Vol 111, No. 5, pp 828-842.

126. Thornton, E. B., and Guza, R. T. 1983 (Jul). "Transformation of Wave Height Distribution," Journal of Geophysical Research, Vol 88, No. C10, pp 5925-5938.

127. Tuck, E. O. 1979. "Models for Predicting Tsunami Propagation," Proceedings of the National Science Foundation Tsunami Workshop, Coto de Caza, CA, pp 43-104.

128. US Army Engineer District, Detroit. 1977. "Great Lakes Open-Coast Flood Levels," Detroit, MI.

129. US Army Engineer District, Detroit. 1979. "Standardized Frequency Curves for Design Water Level Determination on the Great Lakes," Detroit, MI.

130. US Army Engineer District, Detroit. 1979. "Standard Frequency Curves, Annual and Quarterly Water Level Rise by Station, 24 Great Lakes Recording Stations,' Detroit, MI.

131. US Army Engineer District, Honolulu. 1960. "Hilo Harbor, Hawaii: Report on Survey for Tidal Wave Protection and Navigation," Hawaii Region, Honolulu, HI.

132. US Army Engineer Waterways Experiment Station, Coastal Engineering Research Center. In preparation. "Data Collection Sampling and Analysis Parameters and Their Interrelationships," Coastal Engineering Technical Note, Vicksburg, MS.

133. US Coast and Geodetic Survey. 1965. "Manual of Tide Observation," Publication 30-1, US Department of Commerce, Washington, DC.

134. US Naval Weather Service Command. 1976. Summary of Synoptic Meteorological Observations, prepared by the National Climatic Data Center, Asheville, NC.

135. US Water Resources Council. 1976. "A Unified National Program for Flood Plain Management," Washington, DC.

136. Van Dorn, W. G. 1965. "Source Mechanism of the Tsunami of March 28, 1964 in Alaska," Proceedings of the 9th Coastal Engineering Conference, American Society of Civil Engineers, pp 166-190.

137. Van Dorn, W. G., Le Méhauté, B., and Hwang, L-S. 1968 (Oct). "Handbook of Explosion-Generated Water Waves, Volume I - State-of-the-Art," Report No. TC-130, Tetra Tech, Inc., Pasadena, CA.

138. Wang, S., and LeMéhauté, B. 1983 (May). "Duration of Measurements and Long-Term Wave Statistics," Journal of Waterway, Port, Coastal and Ocean Engineering, Vol 109, No. 2, pp 236-249.

139. Wiegel, R. L. 1964. Oceanographical Engineering, Prentice-Hall, Englewood Cliffs, NJ.

140. Wiegel, R. L. 1970. "Tsunamis," Earthquake Engineering, R. L. Weigel, ed., Prentice-Hall, Englewood Cliffs, NJ.

141. Wilson, B. W. 1963 (Apr). "Long Waves Generated by Nuclear Explosions," Appendix I, Investigation of Long Waves and Their Effects on the Coastal and Harbor Environment of the Lower Chesapeake Bay, Vol. II, Report No. DASA-1355, National Engineering Science Co., Pasadena, CA.

142. Wilson, B. W. 1969 (Feb). "Earthquake Occurrence and Effects in Ocean Areas," Technical Report CR. 69.027, US Naval Civil Engineering Laboratory, Port Hueneme, CA.

143. Wilson, B. W. 1972 (Dec). "Estimate of Tsunami Effect at San Onofre Nuclear Generating Station Units 2 and 3, California," Southern California Edison Co., Los Angeles, CA.

144. Wilson, B. W., and Torum, A. 1968 (May). "The Tsunami of the Alaskan Earthquake, 1964; Engineering Evaluation," CERC Technical Memorandum 25, US Army Engineer Waterways Experiment Station, Vicksburg, MS.

145. Wilson, B. W., Webb, L. M., and Hendrickson, J. A. 1962 (Aug). "The Nature of Tsunamis; Their Generation and Dispersion in Water of Finite Depth," Technical Report No. SN 57-2, National Engineering Science Co., Washington, DC.

146. Zetler, B. D. and Cummings, R. A. 1967 (Jan). "A Harmonic Method for Predicting Shallow-Water Tides," Journal of Marine Research, Vol 25, No. 1, pp 103-114.

APPENDIX B

NOTATION

Symbol	Unit	Definition
a	ft	wave amplitude
	ft	length of semimajor axis of elliptical-shaped tsunami generating area, equation (4-8)
	ft	horizontal distance from a vertical wall at the shoreline to a depth equal to twice the depth at the wall, equation (4-32)
	--	parameter in the JONSWAP spectrum, equations (5-15,16)
A	--	dimensionless amplitude of a resonant wave, equations (4-37,38)
	ft^2	total area of earthquake uplifting, equation (4-4)
A_b	ft^2	area of the harbor, equation (4-48)
A_{bc}	ft^2	cross-sectional area at the bay end of the harbor, equation (4-49)
A_c	ft^2	cross-sectional area of flow through the harbor entrance channel, equation (4-49)
A_i	ft^2	incremental area of earthquake uplifting, equation (4-3)
a_j	ft	amplitude of the j^{th} component of the energy spectrum, equation (5-1)
$A(K_1)$	ft	amplitude of tidal constituent K_1, equation (2-2)
$A(M_2)$	ft	amplitude of tidal constituent M_2, equation (2-2)
A_{ns}	ft	site-specific amplitude of tidal constituent n, equation (2-1)
A_o	--	dimensionless amplitude of resonant wave at the shoreline, equation (4-38)
$A(O_1)$	ft	amplitude of tidal constituent O_1, equation (2-2)
A_{sc}	ft^2	cross-sectional area at the sea end of the harbor, equation (4-49)
$A(S_2)$	ft	amplitude of tidal constituent S_2, equation (2-2)

a_x	ft/sec^2	horizontal water particle acceleration
a_z	ft/sec^2	vertical water particle acceleration
a_1	ft	amplitude of oscillation in the harbor
a_2	ft	amplitude of oscillation at the closed harbor entrance
b	--	parameter in the JONSWAP spectrum, equations (5-15,16)
	ft	length of semiminor axis of elliptical-shaped tsunami generating area, equation (4-8)
	ft	width of inlet entrance channel, equation (4-47)
B	Hz	resolution bandwidth parameter
	ft, km	mean inlet width, equation (4-44), Table 4-2
b_j	ft	distance between refracted wave rays at station j, equation (4-38)
B_j	1/ft^2	parameter, equation (4-38)
c	ft	maximum uplifted elevation of elliptical-shaped tsunami generating area at coordinates (x=0,y=0,z=0), equation (4-8)
C	ft/sec	wave celerity
	--	parameter, equation (4-38)
C_g	ft/sec	group wave celerity
C_1	ft/sec	Mach stem propagation speed, equation (4-42)
CPI	in Hg	central pressure index
c_R	--	coefficient of roughness and permeability
d	ft	still-water depth
	ft	average water depth over a fetch, equation (3-1)
	--	derivative, equations (4-37,48)
d_a	ft, km	mean depth of inlet, equation (4-43), Table 4-2
d_b	ft	water depth at wave breaking
D_f	km	earthquake focal depth, equation (4-1)
$D(f,\theta)$	--	angular spreading function, equation (5-27)

D_j	ft^2	parameter, equation (4-38)
d_s	ft	water depth at the toe of a nearshore slope, equation (4-41)
	ft	water depth at a vertical wall at the shoreline, equation (4-32)
d_1	ft	initial water depth
	ft	water depth at the seaward limit of a steep transition
d_2	ft	water depth under the transmitted wave
	ft	water depth at the seaward limit of the slope, equation (4-41)
e	--	constant = 2.71828..., natural logarithm base
E	ergs	earthquake energy, equation (4-2)
	ft-lbs	energy, equations (4-3,4)
E(f)	ft^2-sec	spectral energy density as a function of frequency, equation (5-15)
$E(f,\theta)$	ft^2-sec	spectral energy density as a function of frequency and direction, equation (5-27)
E_j	ft^2-sec	energy density in the j^{th} component of the energy spectrum, equation (5-2)
E_{pres}	ft^2-sec	energy at an underwater gage
e_s	--	standard error
E_{sfc}	ft^2-sec	energy at the surface
$E_{TMA}(f,d)$	ft^2-sec	energy density of TMA spectrum as a function of frequency and direction, equation (5-24)
exp(x)	--	e^x
f	Hz	wave frequency
F	miles	fetch length, equation (3-1)
	ft^2/sec^2	total bottom friction in a harbor entrance channel, equation (4-49)
f_{ny}	--	node factor of tidal constituent n for a specific year, equation (2-1)

	Hz	Nyquist frequency
f_p	Hz	frequency of the energy spectrum at which the energy density is highest
f_s	Hz	sampling frequency
g	ft/sec^2	gravitational acceleration
GCLWD	ft	Gulf Coast Low Water Datum
G(s)	--	function contained in the directional spreading function, equation (5-28)
h	--	nondimensional tide level, equation (2-8)
	ft	tsunami surge height, equation (4-50)
H	ft	wave height
	m	tsunami wave height, equation (4-5)
$\bar{H}$	--	scale parameter for Weibull distribution, equation (7-1)
$\hat{H}$	ft	particular value of H, equations (5-5,6)
$(h^2)_{avg}$	ft^2	average value of the square of the earthquake unlifted heights, equation (4-4)
h_b	ft	surface elevation of the water in a harbor above some arbitrary fixed datum, equations (4-48,49)
H_b	ft	wave height at wave breaking
h_c	--	specified normalized tide level, equation (2-8)
h_i	ft	height of earthquake uplifting over the incremental area A_i, equation (4-3)
H_i	ft	incident wave height
H/L	--	wave steepness
$(H/L)_c$	--	critical wave steepness for wave reflection, equations (4-28,29)
H_{mo}	ft	zero moment wave height
h_o	ft	height of the local MSL datum above the datum of reference, equation (2-1)
H_o'	ft	equivalent unrefracted deepwater significant wave height, equation (3-2)

H_r	ft	reflected wave height
H_{rms}	ft	root-mean-square wave height
h_s	ft	total wave height at shoreline, equation (4-51)
	ft	height of the sea level above an arbitrary datum, equation (4-49)
H_s	ft	significant wave height
$\bar{H}_s$	ft	mean significant wave height, equation (5-30)
$\hat{H}_s$	ft	particular value of H_s, equation (5-29)
$H_{s_{min}}$	ft	minimum (background) significant wave height, equations (5-29,30)
$(H_s)_{pres}$	ft	significant wave height at an underwater gage
$(H_s)_{sfc}$	ft	significant wave height at the surface
H_t	ft	transmitted wave height
H_v	ft	wave height given by visual observer
h_w	ft	seawall height, equation (4-51)
$h_{ys}(t)$	ft	tide at station s during year y at time t equation (2-1)
$H_{1/3}$	ft	average height of the one-third highest individual waves
$H_{1/10}$	ft	average height of the one-tenth highest individual waves
h_+,	--	tabulated tide limit immediately above h_c equation (2-8)
h_-,	--	tabulated tide limit immediately below h_c equation (2-8)
I	--	relative intensity of secondary harbor undulations, equation (4-44)
I_g	ft	geometry integral, equation 4-49
IGLD	--	International Great Lakes Datum
k	1/ft	wave number
K_r	--	reflection coefficient, equation (4-24)
K_t	--	transmission coefficient, equation (4-23)

l	--	effective slope length, equations (4-26,27)
L	ft	wave length
	yr	prescribed time period in which a design wave is equalled or exceeded, equation (5-33)
L_b	ft, km	length of inlet, equation (4-43), Table 4-2
L_c	ft	length of inlet entrance channel, equation (4-47)
L_e	ft	effective inlet length, equation (4-45)
L_f	km	earthquake fault length, equation (4-6)
L_o	ft	resonant wavelength, equation (4-47)
L_p	ft	wavelength at peak frequency
l_s	ft	shelf width
m	--	beach slope, equation (3-5)
M	--	earthquake magnitude on Richter scale
MHHW	ft	mean higher high water
MHW	ft	mean high water
MLLW	ft	mean lower low water
MLW	ft	mean low water
MSL	ft	mean sea level
MTL	ft	mean tide level
N	--	number of intervals in the distribution function, equation (5-4)
	--	number of tidal constituents used in tide prediction equation, equation (2-1)
	--	dimensionless horizontal displacement of a water particle, equation (4-38)
	yr	average return interval of a storm event
NAVD	--	North American Vertical Datum
NGVD	--	National Geodetic Vertical Datum
nu	--	chi-square degrees of freedom

p	--	probability distribution function
P	--	cumulative distribution function
	--	probability of occurrence
P_e	--	encounter probability for a particular wave height, equation (5-33)
PMH	--	Probable Maximum Hurricane
P_n	in Hg	hurricane peripheral pressure
P_o	in Hg	hurricane central pressure
P_+	--	tabulated cummulative probability of the tide immediately above h_c , equation (2-8)
P_-	--	tabulated cummulative probability of the tide immediately below h_c , equation (2-8)
Q	ft^3/sec	flow rate through an entrance channel, equation (4-48)
q_n	ft^n	n^{th} moment of the distribution function of sea surface elevations, equation (5-4)
Q_p	--	spectral peakedness parameter, equation (5-3)
r	yr	time interval associated with each data point for calculated return period, equation (5-32)
R	--	type of tide (diurnal, semidurnal, or mixed)
	mi, nm	radius of maximum winds for a hurricane
	--	ratio of wind speed over water to wind speed over land
R_g	--	ratio of wind speed at 10-m level to geostrophic or free air wind speed
R_T	--	amplification ratio accounting for the effects of air-sea temperature difference on the wind speed
R_{33}	--	adjustment to correct wind speed to 33-ft level, equation (5-12)
s	--	constant-valued spreading parameter in the directional spreading function, equation (5-28)
S	--	beach slope, equation (4-22)
	ft	setup relative to the still-water level, equation (3-1)

S_b	ft	setup at the breaker line relative to the still-water level, equation (3-2)
S_j	ft^2	energy in the j^{th} component of the energy spectrum, equation (5-2)
SPH	--	Standard Project Hurricane
S_w	ft	wave setup at the mean shoreline, equation (3-4)
S_1	--	slope of the steep transition
S_2	--	slope of the shelf, equation (4-41)
S_3	--	nearshore slope
t	sec	time
	hr	time of predicted tide reckoned from some initial epoch, equation (2-1)
	hr	wind speed duration
T	sec	wave period
	min	tsunami period, equation (4-7)
	sec	resonant wave period, equations (4-40,41)
$\bar{T}$	sec	mean wave period, equation (4-45)
$\hat{T}$	sec	particular value of wave period
T_a	°C	air temperature
T_f	hr	fetch-limited duration
T_{1e}	sec	effective primary period, equation (4-45)
T_p	sec	significant or peak period
T_r	yr	return period of a particular wave height
	sec	record length
t_s	sec	time for a wave to travel the distance l_s
T_s	°C	sea temperature
t_1	sec	the point in time when overtopping begins, equation (4-51)

T_1	sec, min	period of the first mode of wave oscillation, equation (4-35)
t_2	sec	the time when overtopping ends, equation (4-51)
T_2	sec	period of the second mode of wave oscillation, equation (4-36)
$T_{1/3}$	sec	average period of the highest one-third waves
u	ft/sec	horizontal velocity of a water particle in the direction of wave motion
U	mph	wind speed
U_C	mph	adjusted wind speed
U_f	mph	fastest-mile wind speed
U_g	m/sec	geostrophic wind speed
u_{max}	ft/sec	maximum horizontal velocity of a water particle in the direction of wave motion
U_L	mph	overland wind speed
U_w	mph	overwater wind speed
U_z	mph	wind speed at elevation z
U_{33}	mph	wind speed at 33-ft elevation
V	ft^3/ft	Volume of overtopping per ft of seawall at the shoreline
V_f	mph	speed of forward motion of a hurricane
w	ft/sec	vertical water particle velocity
x	--	horizontal Cartesian coordinate
	--	major axis of elliptical-shaped tsunami generating area, equation (4-8)
	--	independent variable, equation (G-1)
X_b	--	coordinate of the harbor end of the harbor entrance channel, equation (4-49)
X_s	--	coordinate of the seaward end of the harbor entrance channel, equation (4-49)
y	--	minor axis of elliptical-shaped tsunami generating area, equation (4-8)

·	--	dependent variable, equation (G-1)
z	--	vertical Cartesian coordinate
Z	ft	distance above the water surface, equation (5-12)
Z_1	--	parameter defined in equation (4-22)
α	deg	angle between wave ray and a line normal to a tangent to the shoreline
	deg	hurricane inflow angle
	--	parameter in JONSWAP spectrum
β	rad, deg	angle of beach slope
γ	--	peak enhancement parameter in JONSWAP spectrum, equations (5-15,19,22)
	--	shape parameter in Wiebull distribution, equation (7-1)
Δ	ft	horizontal distance between stations j and j+1 for calculating resonant wave amplitude, equation (4-38)
Δf	Hz	frequency increment
$(\Delta f)_j$	Hz	frequency bandwidth of the j^{th} component of the energy spectrum, equation (5-2)
Δs	ft	total difference in water surface elevation between the breaker line and the mean shoreline, equation (3-3)
Δt	sec	sampling interval
	hr	time-step in numerical model, Figure 5-58
Δx	mi	grid spacing in numerical model, Figure 5-58
ζ	ft	vertical water particle displacement
ε	--	significant wave steepness, equation (5-23)
η	ft	water surface elevation above the undisturbed surface
θ	rad	direction in directional spectral model, equation (5-27)
	deg	hurricane track angle
θ_o	deg	mean wind direction, equation (5-28)
θ_1	deg	incident wave angle, equations (4-18,19,20)

θ_2	deg	transmitted wave angle, equations (4-18,19,21)
κ	--	parameter in JONSWAP spectrum, equations (5-18,19,20)
κ_{ns}	deg	phase lag or epoch of tidal constituent n for specific site, equation (2-1)
λ_3	ft^3	skewness, third moment of the sea surface elevation
λ_4	ft^4	kurtosis, fourth moment of the sea surface elevation
ν_{ny}	--	equilibrium argument for tide prediction equation, equation (2-1)
ξ	ft	horizontal displacement of the water particle from its undisturbed position, equation (4-12)
ξ_{max}	ft	maximum value of ξ , equations (4-14,17)
π	--	constant = 3.14159...
ρ	$slugs/ft^3$	water density
	--	distance offshore divided by the distance from a vertical wall to a depth equal to twice the depth at the wall, equation (4-37)
σ	--	parameter in JONSWAP specturm
σ_{H_s}	ft	standard deviation of significant wave heights, equation (5-29)
σ_n	deg/hr	frequency or angular speed of tidal constituent n , equation (2-1)
$\phi(2\pi f,d)$	--	function in TMA spectrum to account for water depth, equations (5-24,25)
ϕ_j	rad	phase of the j^{th} component of the energy spectrum, equation (5-1)
ψ_1,ψ_2	--	wave radiation frequencies, equation (4-46)
ω	rad/sec	angular frequency, equation (4-38)
ω_d	--	parameter to approximate $\phi(2\pi f,d)$, equation (5-25)
ω_j	rad/sec	angular frequency of the j^{th} component of the energy spectrum, equation (5-1)
∂	--	partial derivative, equation (4-33)
∞	--	infinity

APPENDIX C

MICROCOMPUTER APPLICATIONS FOR COASTAL ENGINEERING (MACE) PROGRAM RELATED TO WAVES AND COASTAL FLOODING

C-1. Availability. MACE programs in Microsoft BASIC may be obtained from the Engineering Computer Programs Library Section, Technical Information Center, US Army Engineer Waterways Experiment Station, PO Box 631, Vicksburg, MS 39180-0631.

C-2. Program TIDEHT (MACE-2). Purpose: The program TIDEHT estimates the elevation of the water surface at any time or the time at increments of elevation based on the predictions of National Oceanic and Atmospheric (NOAA) tide tables

C-3. Program TIDEC (MACE-3). Purpose: The program TIDEC estimates the tidal current speed at any time based on the predictions of the NOAA tidal current tables.

C-4. Program WIND (MACE-5). Purpose: The program WIND takes observed wind speeds, the observation elevation, the location of the observation (overwater or overland), the method of wind speed description (fastest-mile or time-averaged speed), the fetch distance, and general knowledge of the condition of the atmospheric boundary layer and calculates the adjusted wind speed or wind stress factor suitable for wave forecasting.

C-5. Program HURWAVES (MACE-8). Purpose: The program HURWAVES estimates the maximum gradient wind speed, the maximum sustained wind speed, the maximum significant wave height, and the maximum significant wave period for slow-moving hurricanes.

C-6. Program WAVFLOOD (MACE-9). Purpose: The program WAVFLOOD applies Camfield's method as presented in the SPM to approximate wave growth or decay over flooded, vegetated land.

C-7. Program SHALWAVE (MACE-10). Purpose: The program SHALWAVE takes water depth, fetch length, and wind stress factor (an option is offered to adjust the measured wind speed if wind stress factor is not available) and estimates the spectrally based significant wave height, the peak spectral wave period, and the minimum wind duration to reach this condition for waves generated in shallow water.

C-8. Program SINWAVES (MACE-11). Purpose: The program SINWAVES applies linear wave theory to calculate wave conditions at varying depths, estimate breaking conditions, and provide functions similar to that of Tables C-1 and C-2 in the SPM.

C-9. Program JONSWAP (MACE-12). Purpose: The program JONSWAP takes a fetch length, wind stress factor (an option is offered to adjust the measured wind speed if wind stress factor is not available), and duration as input and calculates the corresponding JONSWAP deepwater spectrally based significant wave height and the peak spectral period for fetch-limited, duration-limited, or fully developed seas in deep water.

C-10. Program WAVTRANS (MACE-13). Purpose: The program WAVTRANS estimates wave transmission by overtopping given a breakwater cross-section geometry and information on the incident wave conditions.

C-11. Program WAVRUNUP (MACE-14). Purpose: The program WAVRUNUP estimates irregular wave runup heights on rough slopes given incident wave conditions and the structure's slope and slope material.

C-12. Program BWLOSS1 (MACE-15). Purpose: The program BWLOSS1 estimates economic losses due to wave attack as a function of wave height. The program optionally provides an estimate of expected annual economic losses due to wave attack, given the parameters of the long-term (extremal) cumulative probability distribution of significant wave heights.

C-13. Program BWLOSS2 (MACE-16). Purpose: The program BWLOSS2 fits a long-term cumulative probability distribution to transmitted wave height data and estimates expected annual economic losses due to wave attack after a protective breakwater has been built.

C-14. Program WAVDIST (MACE-17). Purpose: The program WAVDIST estimates the parameters of the three commonly used extremal probability distributions for prediction of extreme wave conditions.

C-15. Program FWAVOCUR (MACE-20). Purpose: The program FWAVOCUR determines how frequently extreme wave conditions are expected over a specified time period.

APPENDIX D

DIGITAL WAVE DATA COLLECTION AND ANALYSIS PARAMETERS

D-1. Purpose. This appendix describes the parameters used in the collection and analysis of digital wave data. The selection of appropriate sampling and analysis parameters is essential for a successful data collection program. Detailed information is given in item 132.

D-2. Duration. Duration is the total time data is collected. Duration is typically measured in days, months, or years. Several years of data are necessary to discern annual trends or to make extremal predictions.

D-3. Burst Interval. Burst interval is the time between sample records. Sample records may be recorded continuously or every few hours (typically every 1, 2, 3, 4, or 6 hours). Also, a threshold may be defined so that data are collected continuously during storm conditions but only intermittently during calm conditions.

D-4. Sampling Frequency, Sampling Interval, and Nyquist Frequency. These three sampling parameters are interrelated, so choosing one of the three determines the other two.

a. The sampling frequency f_s (in Hertz) is related to the sampling interval Δt (in seconds) by

$$f_s = \frac{1}{\Delta t}$$

One Hertz is one sample per second. Typical values of the sampling frequency are 1, 2, or 4 Hz. The Nyquist frequency is the highest frequency that can be detected when sampling at the selected sampling frequency. The Nyquist frequency f_{ny} is defined

$$f_{ny} = \frac{1}{2\Delta t} = \frac{f_s}{2}$$

b. Two undesirable phenomena, aliasing and hidden oscillations, can occur when sampling at a constant rate. Aliasing is the folding back of energy from frequencies higher than the Nyquist frequency into frequencies related to harmonics of the Nyquist frequency, i.e.,

$$(2\ f_{ny} + f),\ (4\ f_{ny} + f),\ \ldots\ (2n\ f_{ny} + f) \quad n = 1, 2, 3 \ldots$$

where f is any frequency between zero and the Nyquist frequency. Hidden oscillations are the loss of kinetic energy at a particular frequency because the same point in the cycle of the process is always sampled; therefore, the information about the cyclic nature of the process is lost.

c. Three methods to prevent these undesirable phenomena are:

(1) Reduce the higher frequencies present to less than the Nyquist frequency by low-pass filtering the signal prior to digitization with an analog, anti-aliasing filter.

(2) Randomly vary the sampling interval such that the sampling interval approaches a uniform distribution.

(3) Select a constant sampling interval at least twice the highest frequency component present.

The third method is used most often because it does not require special equipment. Generally, high frequencies contain relatively little energy, so they are of little interest. Typically the upper frequency limits of interest are 0.35 Hz for ocean waves, 0.50 Hz for waves in bays and lakes, and 0.25 Hz for low-frequency harbor oscillations.

D-5. Total Number of Points, Record Length, and Frequency Increment.

a. The total number of data points N and the record length T_r (in seconds) are related by

$$T_r = N\Delta t$$

Traditionally, the total number of data points has been a power of 2 (typical values are 1,024, 2,048, and 4,096) because fast fourier transform (FFT) routines to transfer the data from the time domain time series to the frequency domain wave spectra required it. Now FFT's are available in multiples of powers of 2, 3, and 5. Typical values of the record length are 17 to 68 minutes. Longer record lengths give higher resolution and greater confidence in the spectral estimates, but the environment conditions must not change significantly during the sample.

b. The frequency increment Δf (in Hertz) in the frequency domain is analogous to the time domain sampling interval Δt

$$\Delta f = \frac{1}{T_r}$$

Wave energy density spectra are calculated from the measured time series at discrete values which are integer multiples of the frequency increment. There will be N/2 wave energy density values ranging from Δf to the Nyquist frequency, where N is the total number of data points in the time domain.

D-6. Number of Averages, Resolution Bandwidth, and Degrees of Freedom. These last three parameters are concerned with analysis of the data after it is collected.

a. Energy density values are estimates of the true wave spectrum. An infinite number of data points and an infinite number of samples would be required to calculate the true energy density. Since this is impossible, the spectral estimates are usually averaged in the time domain (ensemble averaging) or the frequency domain (band averaging) to increase the confidence in the estimate; but as confidence is increased by averaging, resolution is lost. If the raw spectral estimates are band averaged in the frequency domain, the number of average numbands is related to the resolution bandwidth B (in Hertz) by

$$B = \frac{\text{numbands}}{T_r}$$

Typical values of the number of averages are 8 and 16. The corresponding resolution bandwidth is 0.00781 Hz and 0.01563 Hz for a 1,024-second record length.

b. If spectral estimates are assumed constant within the bandwidth, they are considered chi-square variables with degrees of freedom nu given by

$$\text{nu} = 2 \text{ numbands}$$

The number of degrees of freedom is used to calculate the confidence intervals on the autospectral energy density estimates. The larger the nu value, the tighter the confidence intervals for a given record length. Typical values for the number of degrees of freedom are 16 and 32 for bandwidths of 8 and 16, respectively.

APPENDIX E

PROCEDURE FOR ANALYSIS OF WAVE DATA FROM 7-MINUTE PEN-AND-INK RECORDS (BASED ON A RAYLEIGH DISTRIBUTION FOR WAVE HEIGHT)

E-1. Run the period template (Figure E-1) along the 7-minute record until a group of fairly uniform waves is found which should contain some of the highest waves. A template can be fabricated on a clear overlay such as acetate.

E-2. Determine the appropriate period of the waves selected in step 1 by using the template according to instructions. When the wave period on the chart falls between two of the periods shown on the template, the analyzer may approximate what is considered to be neareast to the exact period; e.g., if the period is midway between the 5- and 6-second periods, it must be about 5.5 seconds.

E-3. Use Table E-1 to determine which wave should be measured in the full 7-minute record to get the approximate significant height for the waves. The wave number is determined by callling the highest wave in the full 7-minute record as wave number 1; the second highest wave is number 2, etc. Wave

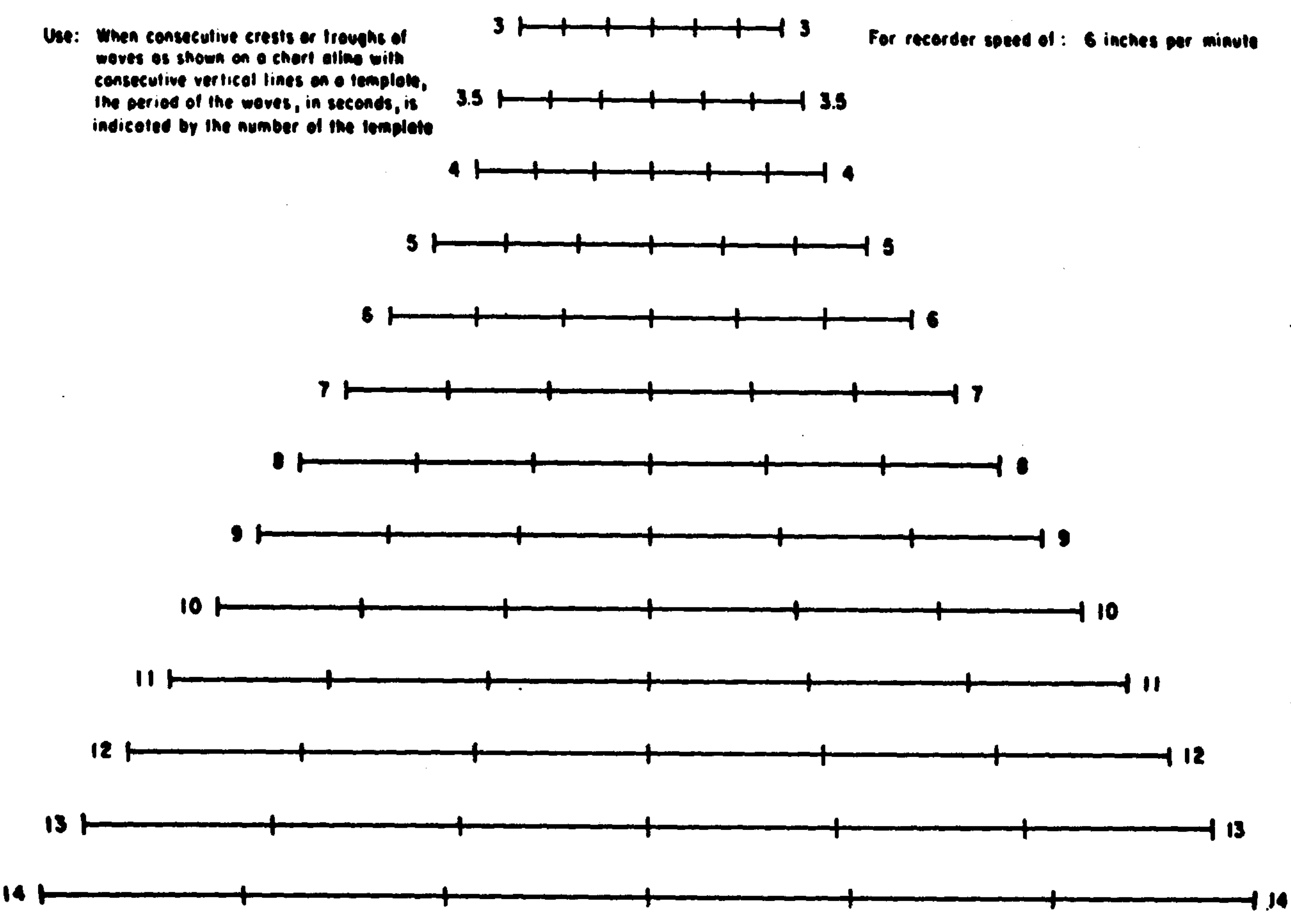

Figure E-1. Sample wave period template

Table E-1

Number of Waves to Measure for Manual Analysis of 7-Minute Pen-and-Ink Records

Wave period, s	Number of waves to measure
3.0	19
3.5	16
4.0	14
4.5	13
5.0	11
5.5	10
6.0	9
7.0	8
8.0	7
9.0	6
10.0	6
11.0	5
12.0	5
13.0	4
14.0	4
15.0	4
16.0	4

height is defined as the difference in elevation between a wave crest and the preceding trough.

E-4. Determine the height of the wave given by step 3 in terms of small divisions on the chart paper.

E-5. Using the appropriate relationship between chart paper divisions and actual elevations in feet or centimeters, convert the wave height determined in step 4 from chart divisions to feet or centimeters. Estimate to the nearest tenth of a foot or nearest centimeter.

APPENDIX F

NUMERICAL WAVE MODELS AVAILABLE IN THE CORPS OF ENGINEERS

F-1. SPM84.

a. Significant wave model.

b. Wave growth.

(1) Nomograms and equations.

(2) Deep water: based on JONSWAP spectrum with constant wind and no pre-existing waves.

(3) Shallow water: empirical, with constant depth and no pre-existing conditions.

(4) Hurricane: empirical, deep water.

c. Transformation in shallow water.

(1) Refraction/shoaling by orthogonal method (graphical) or nomograms (straight parallel contours).

(2) Diffraction (structure-induced) by diffraction diagram.

d. Input.

(1) Deep water: adjusted wind speed, fetch, duration.

(2) Shallow water: adjusted wind speed, fetch, duration, depth.

(3) Hurricane: radius of maximum wind, pressure difference, forward speed of hurricane.

e. Applications. Small, low-cost planning and engineering studies; quick estimates for various district activities. Orthogonal method for refraction analysis not recommended for routine use.

F-2. TMA Computational Model.

a. Parametric spectral wave model.

b. Transformation in shallow water (shoaling only).

c. Applicable to seas but not swell.

d. Input. Wind speed, peak spectral period, water depth (input varies with application).

F-3. GODAS.

a. Significant wave model.

b. Transformation in shallow water. Depth-induced wave breaking, shoaling.

c. Applicable to seas but not swell.

d. Provides estimate of significant, mean, rms, and maximum wave height in shallow water; also provides distribution of wave heights.

e. Code available in US Army Engineer Waterways Experiment Station (CEWES) computer program library and can be run on microcomputer.

f. Input. Deepwater wave height and period, beach slope.

g. Applications. Provides simple, quick estimate for distribution of wave heights, significant wave height, and other height parameters in shallow water.

F-4. TWAVE2.

a. Spectral wave model.

b. Transformation in shallow water.

(1) Refraction over straight, parallel bottom contours.

(2) Slopes less than 1:100.

c. Applicable to seas but not swell.

d. Available for IBM personal computer.

e. Input. Various options available for input.

(1) JONSWAP spectrum parameters and wave direction.

(2) Wind speed, direction, and fetch.

(3) Measured spectrum and direction.

(4) Shallow-water wave height, peak frequency, direction, and depth.

(5) Shallow-water wind speed, peak frequency, and depth.

f. Applications. Provides simple, quick estimates for changes in the energy-based significant wave height, directional spectrum, and mean wave angles between deep and shallow water and between various shallow-water depths.

F-5. SWWM.

a. Parametric spectral wave model.

b. Wave growth. Time dependent; includes wave-wave interaction, uniform wind over the water body for each time-step, and no pre-existing waves. Waves propagate in wind direction.

c. Transformation in shallow-water. Includes growth, white-capping and breaking, bottom friction, wave decay, and researching refraction processes.

d. Input. Time-history of winds, fetches, and depths at computational points.

e. Applications. Generation of long-term hindcasts or special events for confined, shallow-water areas.

F-6. WAVE.

a. Significant wave model.

b. Operates on a rectilinear grid.

c. Transformation in shallow-water; refraction and shoaling by rays.

d. Code available in CEWES computer program library.

e. Input. Gridded depths; wave height, period, and direction at seaward boundary.

f. Applications. If the bottom bathymetry is fairly regular, this may be an inexpensive, viable method, especially for some familiar with its application. More recent modeling techniques have helped to overcome or eliminate shortcomings of this type of technique.

F-7. RCPWAVE.

a. Significant wave model.

b. Operates on a rectilinear grid.

c. Transformation in shallow water. Propagation by interactive solution of finite difference approximations for the governing equations; includes bottom-induced refraction, shoaling, diffraction, and wave breaking.

d. Input. Gridded depths, deepwater wave height, period, and direction at seaward boundary.

e. Applications. Planning and engineering studies, with areas of interest which cover such a large extent that the use of more sophisticated, fully spectral models is not feasible and which contain very irregular bathymetry such that bottom induced diffractive effects become important.

F-8. WISS.

a. Spectral transformation wave modeling technique.

b. Transformation in shallow water. Refraction over straight and parallel bottom contours and wave shoaling; includes parametric form of wave-wave interactions, wave breaking, two-population wave system, and partial sheltering by shoreline.

c. Input. Time-history of wave height, period, and direction for a two-population wave system; shoreline geometry, water depth, and small-/large-scale sheltering information.

d. Applications. Generation of long-term wave hindcasts for finite water depth conditions along any open coastline; generation of shallow-water hindcasts for special storms or other events. An interactive mode is under development that will permit forecasting wave conditions given deepwater wave conditions.

F-9. WISD.

a. Discrete spectral wave model.

b. Operates on a spherical orthogonal grid and rectilinear grid.

c. Wave growth. Piecewise rays, wave-wave interaction, and swell wave decay mechanisms.

d. Input. Time-history of gridded wind field, constant over region or spatially variable. Includes wave input (two-dimensional discrete spectra) as well.

e. Applications. Generation of long-term wave hindcasts for deep water along US coasts; generation of deepwater hindcasts for special storms or other events; can model small, deepwater areas.

F-10. ESCUBED.

a. Spectral wave model.

b. Operates on a rectilinear grid.

c. Wave growth. Steady state, includes wave-wave interaction.

d. Transformation in shallow water. Refraction by piecewise rays, bottom friction, percolation, white capping, and breaking; bottom-induced diffraction being added.

e. Input. Gridded depths, directional wave spectra at seaward boundary, friction factor (default value), percolation factor (default value). This model has the flexibility to "turn on or off" all source mechanisms (wind, wave-wave interactions, friction, percolation, and high-frequency dissipation).

f. Applications. Planning and engineering studies.

F-11. SHALWV.

a. Discrete spectral wave model.

b. Operates on a square grid.

c. Wave growth. Time-dependent so that wave development under changing wind fields can be modeled; includes wave-wave interaction.

d. Propagation and decay. Piecewise rays , wave-wave interaction.

e. Transformation in shallow water. Refraction by piecewise rays, bottom friction, and percolation, includes growth.

f. Input. Time-history of gridded wind field, gridded depths.

g. Applications. Planning and engineering studies in which significant wave growth occurs in a variable depth, shallow-water environment.

F-12. HARBS.

a. Significant monochromatic wave model.

b. Operates on a finite element grid covering the near field and analytical solution covering the far field.

c. Steady state.

d. Calculates harbor resonance and wave scattering due to bathymetry and marine structures.

e. Obstacles may be floating or bottom-mounted.

f. Includes bottom friction and boundary absorption.

g. Input. Geometrical configuration, incident wave height and period, bottom friction coefficients, reflection coefficient of wall.

h. Output. Amplification factor for wave amplitude and/or pressure and phase difference relative to the incident wave, and wave forces (optional). Flow particle velocity will be added as an output in the near future.

i. Applications. Planning and engineering studies in which estimates of resonance and scattering effects on waves propagating in and through small, complicated constrictions are needed; studies in which hydrodynamic forces on large floating or bottom-mounted objects are needed.

U. S. GOVERNMENT PRINTING OFFICE 1989/624-702/10379